MS-DV- SE000 1486 R
C.01

MISSILE AND SPACE DIVISION

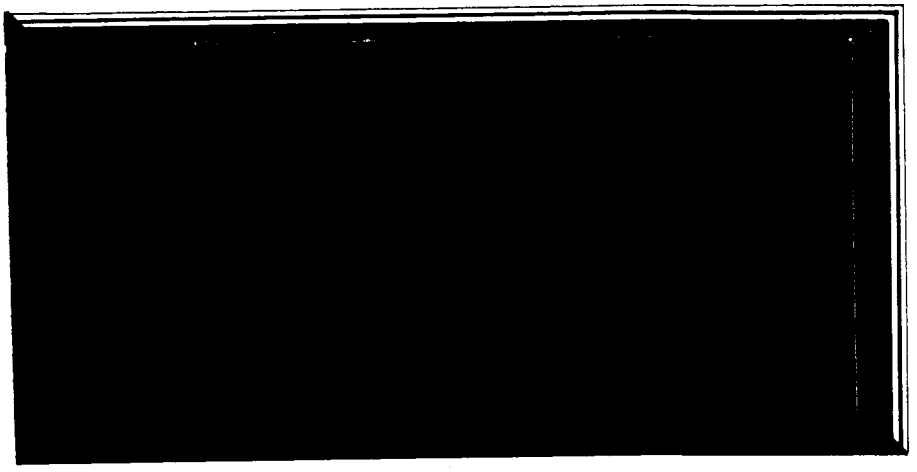

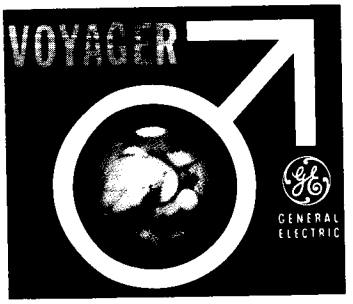

GPO PRICE $ _____

CFSTI PRICE(S) $ _____

Hard copy (HC) 3.00

Microfiche (MF) .65

ff 653 July 65

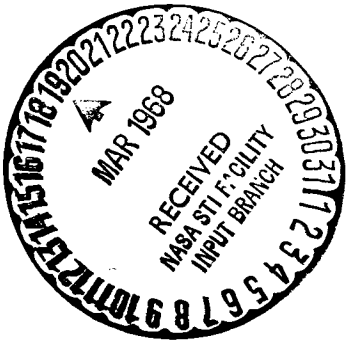

N68-19094

(ACCESSION NUMBER)		(THRU)
228 (PAGES)		1 (CODE)
CR-93551 (NASA CR OR TMX OR AD NUMBER)		14 (CATEGORY)

FACILITY FORM 602

GENERAL ELECTRIC

DIN 67SD4379
16 OCTOBER 1967

N68-19094

FINAL REPORT

VOYAGER SPACECRAFT

PHASE B, TASK D

VOLUME IV (BOOK 5 OF 5)

PHOTO-IMAGING

PREPARED FOR

GEORGE C. MARSHALL SPACE FLIGHT CENTER

UNDER MSFC CONTRACT No. NAS8-22603

GENERAL ELECTRIC

MISSILE AND SPACE DIVISION
Valley Forge Space Technology Center
P.O. Box 8555 • Philadelphia 1, Penna.

VOLUME SUMMARY

The Voyager Phase B, Task D Final Report is contained in four volumes. The volume numbers and titles are as follows:

Volume I	Summary
Volume II	System Description
Book 1	Guidelines and Study Approach, System Functional Description
Book 2	Telecommunication
Book 3	Guidance and Control Computer and Sequencer Power Subsystem Electrical System
Book 4	Engineering Mechanics Propulsion Planet Scan Platform
Book 5	Design Standards Operational Support Equipment Mission Dependent Equipment
Volume III	Implementation Plan
Volume IV	Engineering Tasks
Book 1	Effect of Capsule RTG's on Spacecraft
Book 2	Applicability of Apollo Checkout Equipment
Book 3	Central Computer
Book 4	Mars Atmosphere Definition
Book 5	Photo-Imaging

TABLE OF CONTENTS

TABLE OF CONTENTS (Continued

TABLE OF CONTENTS (Continued)

LIST OF ILLUSTRATIONS

LIST OF ILLUSTRATIONS (Continued)

LIST OF TABLES

SECTION 1

INTRODUCTION

1.1 OBJECTIVE

The broad objective of the Photo-imaging Study is to investigate alternate methods, such as the use of television sensors or photographic film, to perform photo-imaging experiments of the Martian surface from an orbiting spacecraft. In support of this, the following three specific objectives have been met. First, the scientific mission and the system requirements were determined. Second, several candidate photo-imaging systems have been defined. Third, the impact of each of these on the Voyager systems has been determined and compared.

1.2 MISSION AND SYSTEM REQUIREMENTS

This part of the study has provided a set of answers to the questions: "What do we want to find out about Mars? How fast can we obtain the data? How fast can we get the data back to Earth?"

The first question has required the evaluation of many of the desirable scientific missions to pinpoint the critical photo-imaging system performance requirements. Mapping missions such as topological, areological, meteorological, biological, and studies of the planet and its satellite's gross characteristics have been examined. For instance, one task is to find areas on the planet's surface that look promising for future biological exploration. The expected concentration of such areas between +10 and -40^{o} latitude, suggests that a 40^{o} inclined orbit would permit mapping most of them. Prospective soft lander sites should additionally be investigated at high spatial and intensity resolutions. Diurnal and seasonal variations, such as the advance of the wave of darkening, determine at what intervals the mapping of specific areas should be repeated. Similarly for each type of mission, design requirements for spatial and intensity resolution, solar illumination angles, optimum spectral bands, and multispectral and stereo operation have been determined.

The major results of the scientific mission study have been the selection of 100-meter and 10-meter spatial resolution requirements for the general mapping and spot reconnaissance missions, respectively. It is felt that topographic mapping will have to be performed under low-contrast conditions; i.e., intensity resolution of about 0.5 percent will be required. This is in agreement with Mariner IV results. The low contrast is partly due to the eroded surface condition, with its resultant small slopes, and scattering in the atmosphere, which tends to decrease contrast and make it less sensitive to solar illumination angle. Not unexpectedly, the spectral requirements for sensing are for longer wavelengths, towards the red.

Our studies of efficient mapping coverage by a photo-imaging system have compared the characteristics of the baseline orbit, selected primarily to meet requirements for lander separation and entry science, with orbits optimized for the photo-imaging mission alone. An example of this work is shown in Figure 1-1 which is a typical answer to the questions, "How fast can you map the Martian surface?" This curve shows the data-taking opportunity each candidate system has when placed in a nominal 1000 by 12000 kilometer orbit with a 40-degree inclination. This orbit permits mapping of about 32 percent of the total Martian surface in 1 month's time. However, this rate of mapping is dependent on the sensor field of view (10 degrees) and on the capability of the data handling system to transmit the equivalent amount of data at a rate fast enough for the spatial resolution desired.

Two data handling problems exist. The first is the limitation on the record rate of available and predicted tape recorders. This limits the field of view (width of the mapping strip) for a given resolution capability (or, conversely, the resolution for a given field of view) for those systems requiring auxiliary data storage. The second problem is the limitation on the data transmission rate that is set by the possible antenna size, power capability, and pointing accuracy. This limits the total area that each candidate photo-imaging system can map during one orbit.

An example of these problems is shown in Figure 1-2. This curve is drawn for a given rate of mapping (i.e., for the same mission as shown in Figure 1-1) and illustrates the

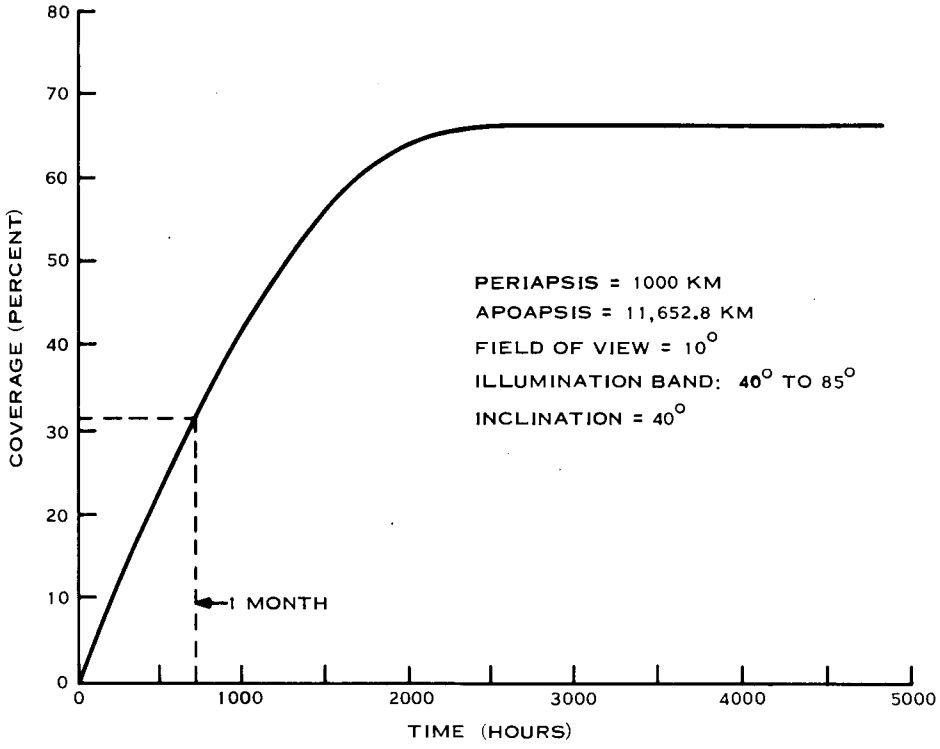

Figure 1-1. Mapping Coverage

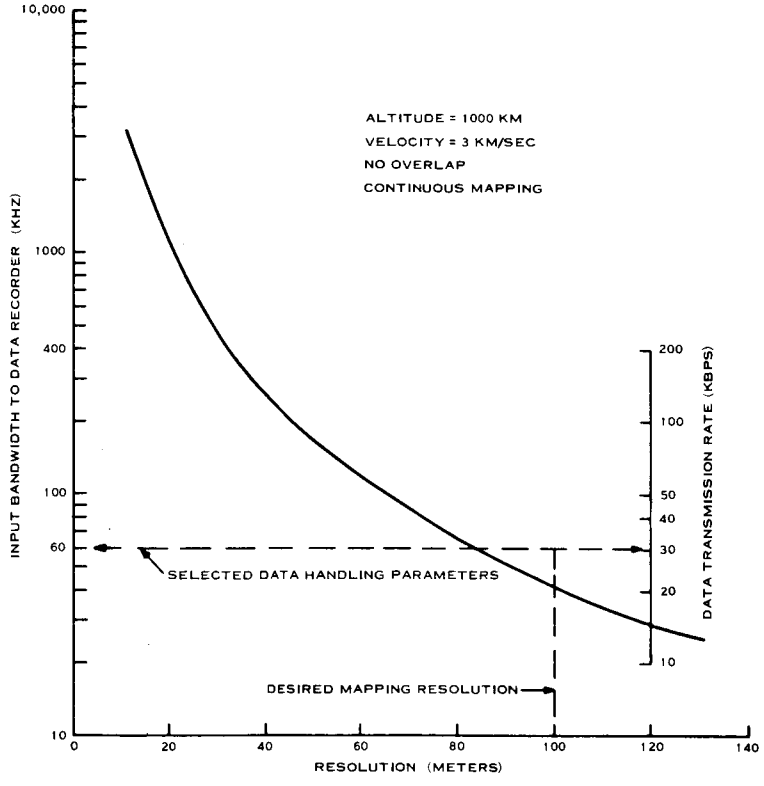

Figure 1-2. Data Handling Requirements for Mapping Coverage

constraint on resolution made by the record rate and the transmission rate. If it is desired to reduce the resolution by 30 percent from 100 to 30 meters, an order of magnitude increase in both data record rate (to 400 kilohertz) and in data transmission rate (to 200 kilobits per second) is required.

Our conclusion of a study of the data handling problem is that the 100-meter resolution requirement for mapping is in reasonable agreement with the data handling capability. We have selected for this study a transmission rate of 30 kilobits per second and a record rate of 60 kilohertz. Choosing these parameters permits, for the 100-meter resolution mission, a data collection period of up to 29 minutes per orbit for the baseline 8.2-hour period, 1000 by 12000 kilometer orbit. This is consistent with Figure 1-1. Data is transmitted to Earth for the remainder of the orbit period.

1.3 CANDIDATE PHOTO-IMAGING SYSTEMS

A television system, a photographic film system, and an optomechanical scan system have been selected for the candidate photo-imaging systems. The three systems were selected by eliminating many other attractive candidates because of state-of-the-art limitations and data storage and transmission rate constraints. Many of these may offer special advantages to Voyager once their development has progressed further. The selected systems are felt to be representative of many of the possible photo-imaging systems so that the comparison results will have general application.

Each candidate has been designed to meet the requirements specified above; that is, a 100-meter resolution capability for general mapping and a 10-meter resolution capability for spot-reconnaissance. Each candidate also has been designed to the same constraints imposed by a baseline 1000 by 12000 kilometer orbit, a maximum data transmission rate of 30 kilobits per second, and a data recorder input limitation of 60 kilohertz.

We have attempted to make each candidate system as similar as possible. For example, the effective field of view of each photo-imaging sensor has been made equal so that each can map the surface at the same rate. To accomplish this, three television sensors and

three optomechanical scanners are used, with their fields of view arranged as shown in Figure 1-3, to be equivalent to the single photographic camera whose larger image format permits a larger field of view for the same spatial resolution. Therefore, the three systems have equal resolutions and mapping coverage rate so that comparisons of their total weight, volume, and power can be made on a common basis.

a. Television. The television system consists of Vidicon sensors, camera optics, electronic controls, and a tape recorder. Three of the Vidicons are used for the 100-meter resolution mapping. The fourth Vidicon is used for the 10-meter-reconnaissance mission.

   The RCA Return Beam Vidicon has been selected for the television photo-imaging system because of its good sensitivity, unusually high spatial resolution, long storage capability, high signal-to-noise ratio, large signal output, and rugged construction. This tube has an ASOS (antimony sulphide oxysulphide) surface with characteristics similar to the Vidicon used on Mariner IV.

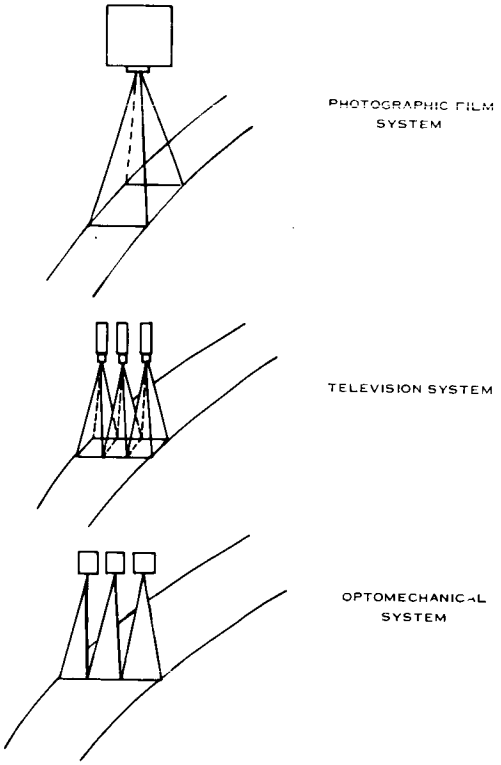

Figure 1-3. Equivalent Coverage of the Three Systems

An analog magnetic tape recorder has been selected for this photo-imaging system. Its design is based on a similar recorder, the RCA model QRA-2, which was flown on Nimbus.

b. Photographic Film. The photographic film system consists of cameras; high-definition silver halide film; a film processor; and a readout scanner. The selected film is Kodak SO-243, similar to that used on the Lunar Orbiter. It is a very fine grain aerial photography film that provides a large number of grains in each resolution cell. The film is fairly insensitive so that longer exposure times are needed. This feature, however, also reduces the fogging due to particle radiation. For the 1973 mission, only moderate shielding is required for film protection.

   Two lens systems are used for the single camera. One is used for the mapping mission; the other for spot-reconnaissance.

c. Optomechanical Scan. The optomechanical scan system consists of imaging optics, scanning wheel assemblies, photomultiplier detectors, electronics, and a tape recorder. In contrast to the other two systems, which take a series of adjacent photographs to form a total map, this concept produces the map line by line. The optical image is scanned in a direction perpendicular to the direction of ground travel, and the resultant signal variations are stored in the tape recorder. Each image line overlaps the preceding trace a small amount. The timing and size of these lines are adjusted to the spacecraft velocity so that a continuous map, with no gaps, results. This technique is analogous to the manner in which the electron beam or the flying spot scanner reads out the image formed by the Vidicon or the photograph.

1.4 PERFORMANCE COMPARISON

All three candidate photo-imaging systems meet the requirements for the 100-meter medium resolution mapping mission. Only the television system and the photographic film system can fully meet the 10-meter reconnaissance mission requirements. The optomechanical scan system can achieve a resolution of 10 meters but at the expense of a low signal-to-noise ratio such that a 4 percent contrast is required. It can achieve a 30-meter resolution at 2 percent contrast.

The spatial resolution performance as a function of contrast is also a major difference between film and television. Due to nonuniformities, film will have intensity distortions that limit the resolvable intensity differences it can sense. Also, particle radiation will tend to fog the film, again reducing the lowest contrast it can sense. Television will also

have tube surface nonuniformities. However, it is expected that these can be calibrated and will therefore not limit the resolvable intensity. Television also can be limited by the accuracy of the tape recorder. However, for a low-contrast scene, the technique of removing the average background level from the signal reduces this error source to a very small level. The indication at this time is that film will be limited to an intensity resolu- of 2 percent while television can achieve 1 percent or lower values. Additional work is required to demonstrate the feasibility of meeting the 0.5 percent intensity resolution requirement at the specified values of spatial resolution.

1.5 MAJOR IMPACT ON THE SPACECRAFT

The physical characteristics of each candidate system have been evaluated to determine their impact on the Voyager design and operation. A surprising number of impact areas are similarly affected by each candidate system, particularly data handling and in the orbit selection areas. Major differences exist in the complexity and long-life operating capability of each system, although it is not clear that any have a clear-cut advantage.

Several of these impacts are discussed briefly in the following sections.

1.5.1 OPERATION

For normal mapping or reconnaissance, the operation of each candidate system is similar. The baseline orbit provides adequate data collection time each orbit when the altitude and solar illumination conditions are suitable. Each system is activated during this period and stores its data on film or in the tape recorder. Data readout for transmission to Earth occurs during the remainder of the 8.2-hour orbit. Two exceptions to this operating procedure exist, both for the film system. The first is that substantial power must be supplied all the time for temperature control, film processing, and film readout. The second is an important advantage for film. Since the film provides permanent data storage, it can be read out again and again. This permits repeated data readout at different rates or conditions to reduce errors in transmission or readout.

1.5.2 RADIATION

Only film is sensitive to the radiation levels expected in the Voyager mission. Failure to protect against radiation can fog the film and further reduce its low contrast capability.

Although shielding can be included for the expected radiation levels, solar flares might constitute a potentially serious failure mechanism. In addition, significant impact upon spacecraft and lander design could result if radioisotope thermoelectric generator (RTG) power supplies are included anywhere in the spacecraft. Analysis indicates that the shielding weight required to protect photographic film during the 6-month interplanetary transit and up to 6 months in orbit is less than 25 pounds for the solar-array-powered spacecraft but is up to 130 pounds for the RTG-powered spacecraft.

1.5.3 TOTAL WEIGHT AND POWER

An estimate of the weight impact on the baseline spacecraft of the three 100-meter candidate systems when used with either 10-meter film or a TV system is shown in Table 1-1. The values shown are the increase in the baseline spacecraft weight, including the effects on structure, power, and propulsion as well as the actual weight of the candidate system.

The lightest system is the combination of optomechanical scan for 100-meter resolution and television for 10-meter resolution. The heaviest is television for 100-meter resolution and film for 10 meters. It is of interest that any combination of film and television is heavier by at least 100 pounds than the use of either for both resolution missions.

Table 1-1. Weight Impact of Each Candidate Photo-Imaging System (Pounds)

10-Meter Systems \ 100-Meter Systems	Television	Photographic Film	Optomechanical Scan
Television	428	611	189
Photographic Film	944	507	816

1.5.4 PLANET SCAN PLATFORM

Both the weight and volume of that part of the photo-imaging system mounted on the planet scan platform have a major effect on its design and performance. Added weight increases the structural weight, deployment, and actuator requirements and increases the difficulty

of maintaining a small center-of-mass tolerance for the entire spacecraft. Added volume increases the difficulty of locating and mounting the platform on the spacecraft and limits the fields of view of other spacecraft sensors. An analysis of these weights and volumes, shown in Table 1-2, indicates that the lightest is the combination of optomechanical scan and television and that the smallest is the all-television system. The 10-meter film system used with anything except itself for the 100-meter system produces a combination which is roughly 100 pounds heavier than an all-film system.

Table 1-2. Weight and Volume on the Planet Scan Platform

10-Meter Systems \ 100-Meter Systems	Television		Photographic Film		Optomechanical Scan	
	lb	cu ft	lb	cu ft	lb	cu ft
Television	200	8.8	222	15.2	150	17.4
Photographic Film	352	18.9	212	15	302	26

1.5.5 ATTITUDE CONTROL

The attitude control for the planet scan platform is reported in detail in Volume II, the Voyager system description. The design selected is a horizon sensor, direct drive control utilizing tachometer feedback for stability which is held to about 1 percent of the orbital rate of 1 milliradian per second at periapsis. A comparison of this performance with the requirements for the television and the film candidate systems has shown that no major difference exists in the attitude control for either.

The scan system presents a somewhat different problem, however, in that its equivalent frame time is several seconds. This means that the drift performance of the control of both the scan platform and the spacecraft may also affect performance. For example, the horizon sensor selected has an accuracy of 0.1 degree with a noise signal of 0.025 degrees. If it is desired to form an accurate map (as contrasted to a survey mission), the 0.1-degree error will distort the apparent distances measured with the scanning techniques. Smear will not be present, however, since the only error produced is that of distortion of the resulting map.

1.5.6 RELIABILITY

An indication of the system reliability is given by the complexity of the designs. Our evaluation of the three candidate systems indicates that image motion compensation (IMC) for the low-contrast Martian surface is perhaps the most complex and difficult development required. An attempt to increase the optics size, and therefore reduce the exposure time, to minimize the IMC indicates, for the 10-meter film system, that a weight penalty of nearly 300 pounds is needed to reduce the exposure by only one half. Other areas of complexity are the optomechanical scanning wheels for the scan system, the tape recorder for the television system, and the film processor.

An investigation of the candidate systems for critical failure modes has pinpointed two methods of improving reliability by using redundant elements or backup modes. One method is that the use of three television cameras and of three optomechanical scanners makes possible complete loss of one camera or scanner with only 33 percent reduction in the rate of mapping. This could mean almost full realization of mission objectives despite a major element failure.

A second method can provide a backup mode that protects against tape recorder failure. This method degrades the resolution capability of the television or the optomechanical scan system so that the data rate output is low enough for direct transmission to Earth. The degradation required is a factor of 4, i.e., a resulting resolution capability of 400 meters. The change can be made simply; for example, by reducing the line scan rate and increasing the scanning aperture of the optomechanical scan system, or by reducing the tube scan rate and the number of scan lines of the television system.

SECTION 2

PHOTO-IMAGING MISSION OBJECTIVES

2.1 INTRODUCTION

Generation of the photo-imaging strategy for the first orbital mission of the planet Mars is by no means a task that can easily be resolved in a study program lasting but a few months. What can be done, however, is to delineate a possible mission strategy based on what is desirable in a scientific sense and compare it with what is possible technologically in the time frame of interest.

Specifically, a possible mission strategy has been worked out and is presented in this section of the report. This strategy is based solely on what is desirable from a scientific viewpoint, but it is tempered somewhat by known technological constraints. How well even these objectives are met in this first iteration can be deduced from a comparison between the accompanying technological sections and this section of the report.

From a scientific point of view, it is desirable to plan a mission such that the data return serves the needs of as large a number of scientific specialists as possible. Thus, at the outset the mission must be diversified enough to be truly interdisciplinary in scope and content. It should not, however, be so diverse that its value to the discipline it is supposed to serve is compromised.

Therefore, we present in the following paragraphs the details of what appears, on balance, to be a scientifically attractive mission with full justification as to what it is that we wish to measure, and the requirements needed to adequately secure that data.

2.2 MAJOR SCIENTIFIC STUDY OBJECTIVES

2.2.1 INTRODUCTION

A photo-imaging mission is primarily concerned with providing a spatial reference in which it is possible to discern the presence or absence of specific features. Variation in scene

contrast (color and intensity) as well as the morphological properties of such features are used in this discernment.

Each scientific discipline has evolved an interpretation criteria about such features. These criteria can only be applied in a controlled observational framework, and it is this observational framework that the photo-imaging mission must supply. Such a framework is developed as follows.

2.2.2 MORPHOLOGY AND RELIEF OF THE MARTIAN SURFACE

When studying the morphology of a planetary surface, it is appropriate to speak of classes of features characterized primarily by their spatial extent. It is this characteristic which ultimately determines the scale of images or equivalently the scene resolution required: a parameter of singular importance in the photomapping of any surface.

In the case of Mars, it is desirable to map the surface in such a manner that all classes of features will be revealed, if present. This follows when we consider that our best terrestrial observations, resolution $\sim$ 80 km, are just capable of discerning the grossest features of the planet, canali and a few special cases excluded. Thus, we know of the existence of clouds, polar caps, and continental size markings but as yet have not detected the presence of mountain ranges or large craters. Therefore, unlike the moon, a reasonable reference frame does not exist before the first flight. In order to systematically explore the planet, such a system must be established as soon as possible on a continental scale, gradually working down to finer and finer values. (Note that Mariner IV photographs are of little value in this connection. Although they did detect craters, they were not able, by virtue of the coverage, which was less than 1 percent of the planet's surface, and resolution involved to place these craters within any but the crudest areographic reference frames.)

Consider therefore a systematic mission designed to observe classes of features with each step leading to more severe requirements on the image scale. These classes are identified below.

2.2.2.1 Classes of Morphological Features

2.2.2.1.1 Global Features

Observations of features such as the distortion of the figure of planet imposes minimal requirements on the image scale. The scale required is small, say $1:2x10^8$.

2.2.2.1.2 Gross Surface Features

A somewhat larger scale is needed if features such as continental masses and major basins (plateaus and vast depressions on Mars) are to be clearly recognized and provide the basic morphological framework for more localized study.

2.2.2.1.3 Continental Features

The next class of features encompasses major mountain ranges and smaller basins. Orbital photographic experience gained during the Gemini program is pertinent here. It clearly demonstrated that scales as small as $1:2x10^6$ or even smaller are geologically useful for the study of mountain chains, folding, faulting, coastal planes, and similar features.

2.2.2.1.4 Regional Features

A further increase in scale becomes necessary in studies of single mountains, volcanic complexes, lineations, and various statistical studies such as frequency distribution of crater diameters, etc. Note that the latter problem has a bearing on the age of the Martian surface, as determined by the survial rate of craters larger than a certain limiting diameter in the presence of erosion and filling due to wind action.

2.2.2.1.5 Local Features

Finally, the resolution required for the establishment of safe landing sites will impose the most stringent requirements on the images. Such images must yield information on objects whose size is comparable to that of the vehicle and detect rather shallow slopes.

Thus, the required scale depends on the areophysical and areological objectives which the images are intended to serve. Table 2-1 indicates slopes and elevations determined by

Table 2-1. Relative Elevation, Slopes, and Lateral Extent of Selected Martian Features

Feature	Relative Elevation	Slopes	Lateral Extent
Craters	150 - 1000 m	$\approx 10^{o}$	4 - 180 km
Mountains	10 - 12 km	$5\text{-}10^{o}$	100 - 250 km
Canals	3 - 6 km	$3\text{-}4^{o}$	100 - 250 km
Major Dark to Bright Areas	10 - 15 km	$1\text{-}2^{o}$	550 - 1700 km

terrestrial radar doppler spectroscopy and based on the work of Sagan and Pollack (1966) and from Mariner IV data. The probable error may be greater than 50 percent.

2.2.2.2 Morphological and Areological Setting

Earlier experience shows that interpretability of images depends both upon the image information content and prior knowledge of the imaged scene. Photographs of an area taken at vastly different resolutions and field coverage tend to yield geologically meaningless results since it is difficult, if not impossible, to relate high resolution small field of view images to the lower resolution image. The desirable resolution step appears to be 3:1, but under no circumstances must it exceed 10:1. Furthermore, images must be nested and preferably taken simultaneously under identical illumination conditions.

Note that in this respect the Mariner IV photographs, as opposed to Ranger photographs, represent a typical case of images taken out of "geological context." The Mariner IV photos covered too small an area of the planet at too high a resolution step in relation to the earth based observations to show either the variability of the Martian surface or to shed much light on the interpretation of such local features as canals, etc. The nested set of Ranger photographs on the other hand while still covering too small an area on the Moon did provide specific data about a particular locale that was interpretable.

2.2.2.3 Limitations Due to Atmospheric Effects

The smallest of morphological features detectable with a Mars orbiting system will be limited by the Martian atmosphere. Under cloudless conditions, the limiting mechanism will be scattering, both molecular and particulate. Its effects will lead to color distortion and contrast degradation with a subsequent loss of resolution. Consider Mariner IV photographs which reveal practically no small craters when the surface was viewed obliquely. This was true despite the fact that illumination conditions were more favorable than in vertical photographs. At the time of the flight, no clouds were in evidence. The loss of contrast occurred apparently due to a low lying obscuring layer. (Murray, private communication)

2.2.2.4 Relative Relief of the Martian Surface

The purpose of studying local features is to derive a detailed topographic map for landing purposes. The standard method of accomplishing this in aerial photography is to provide a pseudosteroscopic coverage by overlapping successive photographs by a considerable margin. The accuracy of stereoscopic height and slope determination is well known to be dependent upon the ratio of base line to altitude. Less known, but equally important is the presence of fine image detail accompanied by sufficient contrast, whatever its source. Without such contrast, stereoscopic work becomes ineffective.

The determination of topography by purely photometric means, used with considerable success for the Moon, is unlikely to yield useful results for Mars. For lunar surfaces, the reflected light is a strong function of the direction of illumination and reflection. The relation expressing this dependence, combined with the reflectivity of the surface, is known as the photometric function. The moon seems to have a very peculiar photometric function which is unlikely to be applicable to other kinds of surfaces. Certainly, the direction of illumination and reflection have very little effect upon the relative tones of extended terrestrial surfaces. In this regard the Mars surface is expected to resemble the Earth's surface to a much greater degree than that of the Moon and consequently topography will have to be deduced stereoscopically.

2.2.3 METEOROLOGICAL MAPPING

Martian atmospheric dynamics is of importance not only in a meteorological sense, but may also be used as an indirect indicator of possible biological activity on the planet's surface. One such indicator involves the possible biological regeneration of isolated dark areas on the planet after their apparent inundation by extensive dust storms. No meteorological phenomenon has been detected in this regenerative process. Of course any transport of water vapor in the Martian atmosphere, even though very slight, would be a key factor in the question of Martian biology. This transport, both global and local, is controlled by the atmospheric circulation in response to solar heating. Thus, a knowledge of the atmospheric circulation will allow a better understanding of broad-scale and local climate for a wide range of surface conditions. Also, the principal erosive process on the Martian surface is believed due to winds. The extent of this process has a major role in shaping the planet's surface features. Mariner IV was able to detect the cumulative effects of this process by recording the partial obliteration of craters in which the lateral redistribution of material by winds on Mars appears to be more rapid than the lateral redistribution in Lunar craters by meteoritic impact.

Extensive experience with earth meteorological satellites indicates their usefulness in determining atmospheric circulation by the detection and tracking of cloud patterns with on-board large-scale photo-imaging systems.

2.2.3.1 Atmospheric Circulation and Cloud Patterns

The existence of changing cloud masses on Mars clearly indicate that winds are present. Convective and wave processes seem to be indicated by the asymmetry in the cloud cover over the two hemispheres, by the occasional banding parallel to the equator, by the occurrence of so-called W-clouds, by the presence of polar anticyclones during the summer months, and by great dust storms resembling major cyclone systems. In most cases, attempts to interpret these phenomena failed in terms of earth meteorology. Reasons for this are not clear. However, one possibility is that cloud systems observable from the earth are simply not numerous or massive enough to serve as an adequate tracing mechanism of a possible large-scale planetary circulation.

Images of much greater resolution coupled with radiation-measuring instruments mounted on an orbiting vehicle will contribute much toward understanding Mars atmospheric dynamics.

2.2.3.2 Cloud Statistics

The study of the cloud cover distribution is also important in estimating the overall energy balance of the planet. For this purpose, photo-imaging observations on a global scale are of inestimable value.

Clouds observed visually are divided for convenience into two classes: white and yellow. An obscuring layer, known as the blue haze is not visually detectable. This color division is generally associated with a difference in composition. White or slightly yellowish clouds are generally associated with polar regions during autumn and winter. It is still a matter of debate whether these clouds are composed of water ice crystal, dry ice crystal or some other material. Suffice it to say that polarization measurements of these clouds resemble those of hoarfrost. Yellow clouds occur infrequently, covering only small areas of the planet. However, occasionally such clouds start in localized bright areas and eventually spread over extremely large regions. Such phenomena are ascribed to desert dust storms.

2.2.3.3 Obscuration in Blue Light

The blue haze as a rule obliterates all surface detail at wavelengths shorter than 4500 $\mathring{A}$. The transparency of this layer is variable both in time and longitude. Occasionally, the phenomenon vanishes entirely and one speaks of the blue clearing. It is interesting to note that the blue haze exhibits a banding pattern parallel to the planet's equator.

Theories advanced to explain the phenomenon of blue haze are too numerous to mention. Yet not one of them by itself accounts for the observations. The only plausible explanation is based on particles suspended in the atmosphere. These particles must be able to vanish very rapidly, and they must have a very low reflectivity. Finally, let us recall the problem encountered in counting craters on Mariner IV photographs. Oblique photographs, despite their more favorable lighting conditions, showed fewer small craters than the vertical

photographs. The cause of this loss of contrast is unknown. One hypothesis advanced to explain the effect postulates the existence of a sort of ground fog.

2.2.4 BIOLOGICAL ASPECTS OF MAPPING

Short of detecting animals, large plants, or unmistakable signs of activity of intelligent beings, an orbiting photo-imaging mission to Mars has no independent value as a life-detecting device. It is more likely that life, if any, will be of a microbiological nature. For its detection, one would employ a means other than photography.

An important preliminary to a life-detection mission, however, would be a study of the planet microenvironment, particularly its unusual aspects, detection of water in any of its phases, and search for the presence of organic compounds. Photography can make an indirect contribution to such studies by providing a reference frame for other instruments whose purpose will be to provide quantitative measurements of the surface properties related to environmental conditions. One expects to find unusual environmental changes in the areas of high reflectivity at the boundaries of polar caps, and particularly within the dark areas which exhibit seasonal changes in contrast.

2.2.4.1 Wave of Darkening

A particularly striking seasonal change observed on Mars is the progressive darkening of Martian dark areas occurring during spring and early summer. A brief description of this phenomenon is as follows. In the beginning of spring in the appropriate hemisphere when the polar cap begins to recede, various dark areas in high latitudes become darker. This change in contrast progressively affects areas at lower latitudes. The amplitude of the change decreases toward the equator. The front of this so-called wave of darkening travels 40 to 45 km per day. In the southern hemisphere, the wave may start at a latitude as high as 60 degrees at the end of winter, about mid-spring it crosses the equator, and eventually reaches north latitudes of 20 to 40 degrees. The total travel of 100 degrees in latitude takes about 130 days. For most areas, maximum darkening occurs at the time when the polar cap reaches its minimum extent. The numbers quoted are approximate. Furthermore, some areas, such as Tithonius Lacus, begin to darken earlier than others.

Others such as Depressio Hellespontica, reach their maximum darkening at the time of high local insolation rather than after the summer solstice.

Currently, there exist two interpretations for this phenomenon.

a. Wave of Darkening as a Biological Phenomenon. The standard biological interpretation of the wave of darkening invokes seasonal response of small organisms to the increased availability of water vapor.

b. Wave of Darkening as an Aeolian Phenomenon. An alternate hypothesis ascribes the phenomenon to the seasonal transport by winds of dust onto and off the dark areas. Crucial to this interpretation is the assumption that the bright areas are lowlands. Since the winds tend to be stronger in elevated regions, dust is removed from the dark areas during the spring and summer months when the temperature gradient between the summer pole and the equator is small. In winter, the stronger winds are capable of raising dust from both areas and some of it will be deposited on highlands.

A recent study by Pollack et. al. (Planet. Space Sci. 15, 817, 1967) indicates that at the present time no preference can be given to either model. Similar interpretations have been advanced for areas which exhibit secular changes. Among such areas we find Solis Lacus, Nepenthes Thoth, Trivium Charontis, Nodus Laocoontis, and others.

2.2.4.2 Duration of Martian Seasons

Seasonal phenomena associated with the wave of darkening are more pronounced in the southern hemisphere. Furthermore, the number of dark areas in the path of the wave is larger in this hemisphere. Consequently, observation of these phenomena in the southern hemisphere are expected to be more rewarding. Periods during which such observations could be conducted are indicated in Table 2-2 which summarizes the duration of Martian seasons during 1971 to 1975.

2.2.4.3 Polar Caps

Polar caps of Mars are perhaps the most prominent features which undergo seasonal changes. It is now well known that during the spring and summer the appropriate polar cap consists of a surface deposit, while during autumn and winter the cap is seen as an

Table 2-2. Duration of Martian Seasons

Hemisphere					
Heliocentric Longitude of Mars	Northern	Southern	Duration Earth Days	Approximate Interval (Earth Dates)	Opposition
267 - 357	Autumn	Spring	146	May 17, 1971 - Oct. 9, 1971	August 6, 1971 (34.9×10^6 miles)
357 - 87	Winter	Summer	160	October 9, 1971 - March 18, 1972	
87 - 177	Spring	Autumn	199	March 18, 1972 - Oct. 3, 1972	
177 - 267	Summer	Winter	182	October 3, 1972 - March 3, 1973	
267 - 357	Autumn	Spring	146	March 3, 1973 - July 27, 1973	
357 - 87	Winter	Summer	160	July 27, 1973 - January 4, 1974	October 21, 1973 (40.4×10^6 miles)
87 - 177	Spring	Autumn	199	January 4, 1974 - July 22, 1974	
177 - 267	Summer	Winter	182	July 22, 1974 - January 20, 1975	
267 - 357	Autumn	Spring	146	January 20, 1975 - June 15, 1975	December 15, 1975 (52.4×10^6 miles)

Note: Mars passes through its perihelion at $\eta = 335$ degrees which corresponds to August 28 in 1971.

extensive cloud cover. The cloud cover disappears rather abruptly at the beginning of spring. At the same time, a dark collar appears at the cap perimeter and as the cap recedes the band keeps pace with it. Observations show an irregularity in the structure of the caps indicated by rifts which appear during recession. These rifts appear as a rule in the same places. The receding cap leaves behind persistent bright areas which also occur at the same areographic coordinates. The best known of these areas, named the Mountains of Mitchel, are a part of the sourthern polar cap.

The vital role played by the caps in the seasonal changes observed in other areas is well established. However, to remove ambiguities in interpretations of these seasonal changes, it is necessary to establish the nature of the cap material. Arguments have been advanced that the material is water ice, dry ice, and even deposits of nitrogen tetroxide. In these hypotheses, the local topography plays an important role. For instance, temporary bright areas in the polar regions can be interpreted as elevated areas where water frost forms. However, an alternate interpretation suggests that regions such as the Mountains of Mitchel are deep depressions with sufficiently low nighttime temperatures to permit the formation of dry ice.

Clearly, a sufficiently detailed topographic map of these regions made during the summer months would greatly contribute toward an unambiguous interpretation of these problems.

2.2.5 WHOLE PLANET AND RELATED SUBJECTS

A number of useful studies can be performed as part of a Martian photo-imaging mission. A few typical possibilities are described below. Time allocation is unlikely to present difficulties since the proposed measurements can be done at the time when the principal mapping functions are inoperative.

2.2.5.1 Determination of the Planetary Radius

The major uncertainty in deriving the internal structure of the planet Mars arises from the uncertainty in values of the polar and equatorial radii of the solid surface. These uncertainties are equivalent to an uncertainty in the optical ellipticity of the planet's figure.

This parameter is, in turn, a measure of the balance between the gravitational and rotational forces acting upon a deformable planet.

The degree of improvement desired is indicated by the best presently available diameters of the planet. In yellow light these are

$$De = 6750 \pm 20 \text{ km}$$
$$Dp = 6700 \pm 20 \text{ km}$$

as recommended by de Vaucouleurs. The indicated uncertainty, as well as the differences between the above values of diameter and those derived by numerous other investigations, lead either to sufficiently different planetary models or to outright difficulties in constructing one. Prolonged tracking of the orbiter will lead to an improved knowledge of the planetary figure.

2.2.5.2 Major Continental Subdivisions

Interpretability of images taken at high resolution requires knowledge based on lower resolution images where the resolution of the two types of images does not exceed 10:1. The best available maps of Mars obtained from smoothed terrestrial observations presently show markings whose location accuracy is of the order of $\pm 1.0^{o}$ in longitude and $\pm 0.5^{o}$ in latitude in equatorial regions. These maps are on a self-consistent scale. Here, the errors involved are internal probable errors. Mariner IV photographs cannot be related to any features shown on such maps precisely because the step in resolution and coverage vastly exceeds the recommended step. It continues to be desirable, therefore, to acquire images of the whole planet, both during transit and at apoapse, in order to fill in the scale between the terrestrial maps and the high resolution maps which are to result from a photo-imaging mission.

2.2.5.3 Determination of the Radius of Phobos

The semimajor axis of Phobos, the inner satellite of Mars, is of the same order as the apoapse of the proposed orbiter. Consequently, under suitable astrodynamical conditions there exists the opportunity of acquiring images of this satellite. The value of this is in

the determination of its diameter which, although estimated at 15 to 20 km, is not really known. The present values are based on measurements which involve unjustified photometric assumptions.

Furthermore, detection of any surface markings would be of interest for, other than its orbital properties, little else is known about this moon.

2.3 SPECIFIC AREOGRAPHIC AREAS OF INTEREST

2.3.1 SURFACE FEATURES

The list of areas given in Table 2.3 is not exhaustive. However, the selection includes practically the entire range of seasonal and secular phenomena mentioned earlier. The areas are listed in the order of ascending longitudes. The coordinates are in most cases approximate. Coordinates for which higher precision is indicated are those recommended by de Vaucouleurs (Sky and Telescope, October 1965).

2.3.2 PERIODS FOR OPTIMUM VIEWING (Surface Features)

All dark areas subject to seasonal changes due to the wave of darkening ought to be observed during the spring and early summer in the appropriate hemisphere. It is preferable to observe the changes in a given location during the gathering wave of darkening, that is, between the beginning of the darkening and the time when the maximum is achieved. Changes during this time occur more rapidly and are more sharply defined than during the corresponding decline in contrast which follows the maximum.

It was pointed out by Pollack et al (Planet and Space Sci. 15, p. 817, 1967) that available observations of dark areas in the northern hemisphere are insufficient to produce a reasonably accurate timetable of changes due to the northern wave of darkening. In the southern hemisphere one can establish such a table and it is reproduced below as Table 2-4. This table lists, whenever available, the heliocentric longitudes (η) of the beginning, maximum, and end of darkening of the respective area as well as the numbers of days after the summer solstice (Δt) when the maximum darkening is achieved.

Table 2-3. Surface Features

Area	Coordinates		Reasons for Selection
	Longitude (degrees)	Latitude (degrees)	
Mare Acidalium	30	45	Infrared spectroscopy and polarimetry indicate the possibility of biological activity.
Southern Polar Cap	40	-82	Near minimum extent. Possibility of observing moisture and permafrost.
Aurorae Sinus			
Center	50	-15	Typical seasonal color changes
North point	48.0	-7.50	
Lunae Palus			
Center	64.8	18.4	In recent years the area has been exhibiting great changes in photometric contrast. Albedo shows a double cycle of changes.
Phrixi Regio	75	-45	One of the better-observed dark areas.
Tithonius Lacus	85	-5	One of the well-observed dark areas. Begins its darkening earlier than any other dark area.
Solis Lacus			
Center	86.2	-27.5	Has a history of remarkable secular changes.
Ceraunius	95	35	Site of classical canals. High radar reflectivity. Low visual albedo.
Nix Olympica	128	20	Bright area of standard coloration. Clouds tend to form at this location.
Mare Sirenum			
Center	160	-30	Marked seasonal color changes reported.
West point (at Atlantidum Sinus)	174.2	-24.5	
Mare Cimmerium			
Center	215	-25	Exhibits seasonal color changes. Darkening wave goes through a double peak.
East end	157.4	-37.3	

Table 2-3. Surface Features (Cont'd)

Area	Coordinates		Reasons for Selection
	Longitude (degrees)	Latitude (degrees)	
Propontis I	178.6	44	Region of typical canals of the earlier literature.
Trivium Charontis Center	198.9	15.4	Striking anomalous color changes have been reported. Secular changes have been observed.
North Polar Cap in Olympia-Lemuria region	210	70	Possibility of observing shadows of mountains; permafrost features. Observation of dark collar.
Elysium	210	25	A nearly circular bright region of pink coloration. Site of a canal system.
Nodus Laocoontis	245	22	Area of striking secular changes.
Nepenthes-Thoth	265	15	Site of unusual secular changes in 1940's. Former location of a so-called "canal" system.
Mountains of Mitchel	267 to 293	-73	Persistent regular feature of the southern polar cap.
Syrtis Major	290	10	It is the darkest of dark areas. Typical color changes have been reported. Polarimetry and IR spectroscopy indicate the possibility of biological activity. Wave of darkening exhibits a double peak.
Boreosyrtis	290	45	Dark area.
Hellas			
SE point of NW lobe (on Zea Lacus)	292.1	-41.8	Bright area of unusual yellowish color and high albedo.
North point NW lobe	295.9	-28.7	

Table 2-3. Surface Features (Cont'd)

Area	Coordinates		Reasons for Selection
	Longitude (degrees)	Latitude (degrees)	
Mare Serpentis	315	-30	Orifice of main Hellespontus channel of darkening wave.
Ismenius Lacus	332	40	Possibility of striking anomolous color changes.
Hellespontus	335	-48	Dark area connecting depression Hellespontica and Mare Serpentis.
Depressio-Hellespontica	350	-65	Maximum darkening does not occur after summer solstice, but at the time of maximum insolation. One of the better-observed dark areas.
Deuteronilus	340 to 350	40	Site of classical "canals." Very high radar reflectivity. Low visual albedo.

The corresponding calendar dates can be obtained from Table 2-2, which lists the correspondence between the heliocentric longitude limits of Martian seasons and calendar dates.

No corresponding recommendations can be made for areas exhibiting secular changes since these take place over a period of years. During the lifetime of an orbiter, such changes may or may not be sufficiently pronounced to be noticeable. Under such circumstances one can merely recommend that certain areas characterized by recent secular changes be observed regardless of the mission timing. Among such areas, Nepenthes-Thoth and Nodus Laocoontis should be mentioned. The first of these has a long history of secular changes going as far back as 1909. Recent changes occurred in 1952-1954. Nodus Laocoontis, an inconspicuous area to early observers, has recently developed into a major dark region. Those dark regions which show a "regenerative" property taking place in a few days will be regarded as targets of opportunity, since the phenomenon is connected with dust storms. There is basically no preferred times when bright areas are to be observed since their observed properties are essentially constant.

Table 2-4. Periods of Optimum Viewing

	Λ (degrees)	η begin (degrees)	η max (degrees)	η end (degrees)	Δt (days)
Depressio Hellespontica	-60	---	345	---	-25
Mare Chromium	-58	---	0	---	+ 4
Aonius Sinus	-45	---	0	50	+ 4
Phrixi Regio	-40	---	25	---	52
Mare Hadriacum	-40	310	10	80	23
Mare Sirenum	-30	---	5	---	13
Mare Serpentis	-30	330	20	120	42
Solis Lacus	-28	350	15	95	32
Pandorae Fretium	-25	---	5	105	13
Mare Erythraeum	-25	320	15	60	32
Mare Tyrrhenum	-20	350	32.5	85	66
Mare Cimmerium	-20	290	30	90	61
Iapigia	-20	320	5	---	13
Aurorae Sinus	-15	340	22.5	80	47
Margaritifer Sinus	-10	340	20	80	42
Sinus Sabaeus	- 8	330	30	80	61
Sinus Meridiani	- 5	360	35	90	71
Tithonius Lacus	- 5	280	0	80	4
Syrtis Major	+10	320	10	90	23
Lunae Palus	+15	350	20	70	42

The intervals indicated in Table 2-4 are also most suitable for observation in the polar regions since at this time the cap is receding.

A comment is in order with regard to the Mountains of Mitchel. They always appear on the same seasonal date, a Martian June 3rd, and persist for a few days but rarely as long as 1 week (about 5° of heliocentric longitude). Therefore, the opportunity for their observation is extremely limited.

2.3.3 CLOUD STUDIES

While it is impossible to state the exact position and time of occurrence of a cloud, it is possible to predict more probable locations and times where they might be found. Terrestrial observations (Robinson, J. C. - Icarus 5, 245-247, 1966) taken on blue and green plates indicate the existence of such preferential locales, some of which are recorded in Table 2-5.

Table 2-5. Regions of Clouds or Bright Haze (1965 Opposition)

Region	Approximate Area (sq km)	Center Coordinates	
		λ (degrees)	ϕ (degrees)
Phelegra	2×10^5	187	+42
Azania	1.2×10^3	185	+26
Elysium	1.2×10^5	215	+20
Atlantis	1.2×10^4	170	-29
Lumen	1×10^4	163	-20
Lubar	7×10^4	180	-18
Electris	7×10^5	180	-50

These regions repeatedly exhibit changes in brightness in a manner that could only be due to local obscuration, e. g., clouds, haze, fog, etc. These recurrences in the same region are strongly indicative of topographical influences. Not all the cloud regions display the same diurnal behavior. Clouds appear common to all regions in the morning hours, but Lubar, Azania, and Phelegia appear to be free of clouds in the afternoon. Thus a photoimaging mission designed to study cloud behavior on Mars should utilize such information in order to increase the probability of obtaining data on such unpredictable phenomena as clouds, haze, etc.

2.3.4 BLUE CLEARING

The phenomenon known as "blue clearing" has been observed on Mars for many years, but it is not always present. Figure 2-1 gives the averaged relative blue clearing per terrestrial observation as a function of heliocentric longitude. Thus any attempt to map the surface of the planet in blue light should be confined to the times of blue clearing as indicated.

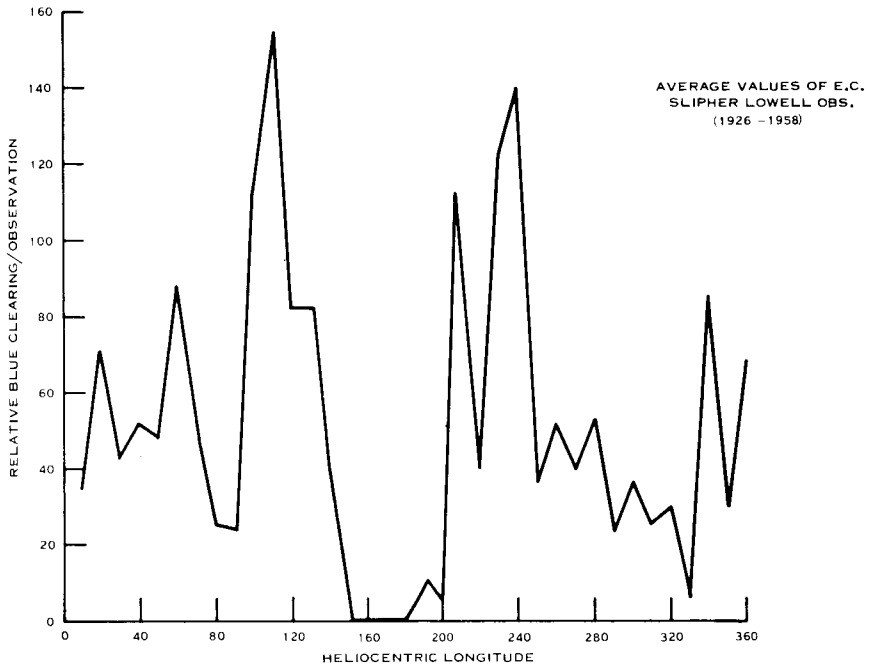

Figure 2-1. Relative Blue Clearing

2.4 MAPPING REQUIREMENTS

From the material presented in Sections 2.2 and 2.3 it is possible to set down in quantitative terms those parameters needed to completely identify the performance requirements for the entire photo-imaging mission. In order to do this we will define requirements and develop specifications for each. These 5 missions are easily identified with particular scientific objectives already discussed. They are:

a. Medium Resolution Mapping Mission (MRMM)

b. High Resolution Mapping Mission (HRMM)

c. Lander Site Survey Mission (LSSM)

d. Cloud Survey Mission (CSM)

e. Whole Planet Imaging Mission (WPIM)

2.4.1 SPATIAL AND INTENSITY RESOLUTION

Beginning with WPIM, we can immediately specify that the field of view must encompass the whole diameter of the planet (6800 kilometers) plus an additional 20 percent of that value. In order to establish the continental relief within such a frame and to accurately measure the planet's equatorial and polar radii, the resolution cell should provide a ground resolution on the order of 1/2000 of that value, or approximately 3 kilometers. Note that obtaining the radii of the planet to this accuracy will improve the best terrestrial values by an order of magnitude. For the CSM, fields of view on the order of 700 x 700 kilometers with a resolution cell of 500 meters are required. (See Table 2-5.) The MRMM, if we are to maintain a nested set of pictures, requires a field of view of 200 kilometers with a resolution in the 100 to 300 meter range. In Table 2-6 we note what geologic features can be identified as a function of the ground resolution.

Table 2-6. Resolution Necessary for Identification of Geologic Features

Feature	Minimum Ground Resolution (meters)
Relief	450
Major drainage (e.g., Rio Grande)	450
Tributary drainage (e.g., arroyos, streams)	150
Erosion and deposition surfaces (e.g., terraces, bajados, pediments)	200
Playas	1000
Large faults (e.g., San Andreas)	450
Smaller faults and fractures	100 to 150

(Modified from Merifield, P.M., NAS-5-3390 LR17666, February 1964)

Since it is impossible to predict the absolute sizes that similar features will take on Mars, the areophysical scale being smaller than the geophysical scale, we recommend that the 100-meter value be used. A relative scale that is independent of the planet being mapped is given in Table 2-7.

Table 2-7. Minimum Ground Resolution for Mapping

Feature	Minimum Acceptable Ground Resolution
Lithology	1/4 to 1/2 the width of the narrowest unit to be separately mapped.
Structure (folds)	1/16 to 1/8 the dimension of the structure being mapped.
Structure and landform patterns	About 1/2 to 1 times the "wavelength" of the pattern.
Structure (fractures)	No specific resolution-optimum when entire feature is in one frame.
Landforms, linear	1/4 to 1/2 times the width of objects.
Landforms, areal	1/8 times the size of objects
Vegetation boundaries	1/8 to 1 times the distance across the boundary; depends on contrast

(After Morrison, A. and Chown, M. C., NASA CR-126, December 1964

Coverage of as much of the planet's surface as possible should be obtained at this resolution since it will establish the basic areological domains on the planet and set the stage for more detailed observations of particularly interesting areas at higher resolutions. Assuming that regional image patterns have been established, then the HRMM can begin. Here a field of view, on the order of 10 kilometers and resolution on the order of 10 meters will be used to further define surface features. Of particular interest in this range will be the establishment of the homogeneity of the dark areas.

The LSSM is self-explanatory with regard to its objective. Here the field of view must contain the error of a predicted touchdown point for a lander, taken from previous lander studies as 87 kilometers square. The resolution required should be consistent with the dimensions of the landing gear, say 1 to 3 meters.

The intensity resolution is intimately associated with scene contrast. For surface mapping missions, the surface scene contrast is expected to be low. This expectation is based on terrestrial observations on a global scale and on Mariner IV on a kilometer resolution

scale. Essentially, the Martian surface has low contrast and, as far as Mariner IV was able to discern, shadowless. This matter is discussed in more detail in Section 2.4.2. Bruce Murray, loc. cit., indicated that intensity variations of from 2 to 3 percent were observed with the Mariner IV photographs. Thus in order to properly map the surface of Mars it appears that a photometric precision of 0.5 percent is required.

For clouds which exhibit more contrast when viewed against the planet's surface, a precision of 2 percent appears adequate.

2.4.2 SOLAR ILLUMINATION

It has already been mentioned in Section 2.2.2.4 that the photometric properties of the Martian surface will likely approach those of the Earth. Available observations are not sufficient to state this with certainty due to the fact that the resolution achievable is low and, besides, Mars never exhibits a phase angle greater than 47 degrees. However, should the photometric properties be as stated, then the implication is that the directions of illumination and reflection have little bearing on the relative tones on a photograph.

The contrasts which one would see under these circumstances would arise due to the total reflectivity differences. Both the earth-based observations and Mariner IV experience show that the Martian surface represents an intrinsically very low contrast scene. Topographic interpretation will, however, demand sufficient contrast. If the latter is to come from the existence of shadows, one would require that there exist local slopes which are illuminated at an angle greater than 90 degrees with respect to the surface normal. This implies that the Sun's elevation above the local horizontal is less than the angle which the slopes make with the horizontal. Table 2-1 shows that the expected large-scale slopes on Mars are less than 10 degrees. Consequently, for shadows to be observable when viewing the planet vertically, the Sun's zenith angle must be larger than 80 degrees. Unfortunately, this circumstance also corresponds to low illumination and, therefore, low scene brightness.

The photographs obtained by Mariner IV do not show clearly recognizable shadows for Sun zenith angles between 14 degrees and 88 degrees. However, frame number 16, taken at a

zenith angle of 69 degrees, shows a drastic decline of detail due to the decreasing level of signal. It appears then that to improve the chances of seeing shadows for zenith angles larger than 69 degrees, one needs greater system sensitivity than is available on Mariner IV. Failing to achieve this, one must employ a sensor of high intensity resolution capable of responding to slight differences in total reflectivity of the Martian surfaces. In fact, this was the approach employed on Mariner IV. What the Mariner IV flight did prove is that successful pictures can be taken for Sun zenith angles between 14 and 70 degrees.

2.4.3 SELECTION OF OPTIMUM SPECTRAL BAND

As has already been indicated, Mars, the red planet, exhibits the greatest surface spectral reflectances longward of 0.55 μ. This is believed to be a combined effect consisting of the natural reflectance property of the surface material, possibly a mixture of the iron oxides, e.g., hematite, limonite, geothite, etc., and a decrease in the optical thickness of the atmosphere as we progress to longer wavelengths.

A spectral reflectance curve is shown in Figure 2-2. Under 0.33 μ the reflectance is atmospheric, between 0.33 μ and 0.55 μ there exists a combined effect due to atmosphere and surface, and beyond 0.55 $\mu$the reflectance is due solely to the surface materials.

Thus in order to map the surface of Mars it is apparent that the spectral range should lie between 0.55 μ and the long wavelength cutoff of the detector. For blue haze and certain cloud studies, wavelengths in the blue and ultraviolet may be employed.

2.4.4 MULTISPECTRAL OPERATION

In recent years, attempts to distinguish objects that have the same photographic gray scale values on aerial panchromatic photographs resulted in an increased analytical use of photographs, and this in turn led to the development of multiband photography. The purpose of such an approach is to employ comparison of photographs taken in different spectral regions to yield information on observed objects which simply cannot be obtained by studying tonal values of single images. The technique has been developed to the point where such photographs are employed to create artificial color composites in which the information of no

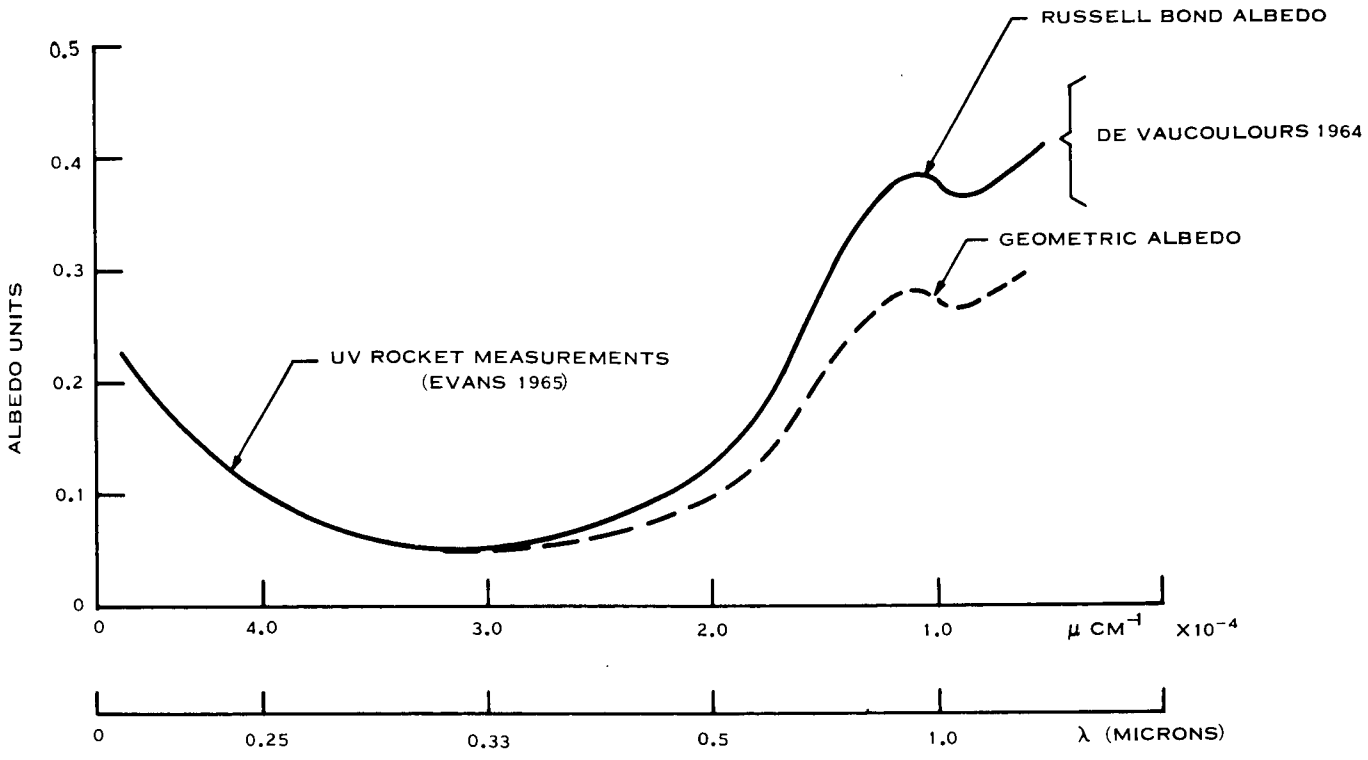

Figure 2-2. Spectral Reflectance of Mars

interest is suppressed and areas having slight tonal differences are greatly emphasized. Thus rocks which in single photographs may look the same, may exhibit significant differences when studied by multiband photography. These differences may be interpretable in geological and geochemical terms if comparison can be made with detailed results of similar studies of reference areas. The spectral resolution required is moderate (about 500 Å) and, generally, the larger the number of bands employed, the more effective the approach becomes.

For a photo-imaging mission to Mars the number of filters to be employed must of necessity be tempered by the technological limitations of the mission as a whole. If the multiband operation is to be attempted at all, a minimum of three filters is to be employed centered in the blue, yellow-green, and red regions of the visible spectrum. Tentatively the bandwidths (in Angstroms) could be selected as 4500 to 5000, 5000 to 5500, and 5900 to 6400. It must be realized that the use of other bands and/or narrower bands may eventually yield

more rewarding results. Thus it is well known that in the ultraviolet, certain geological features (e.g., limestone outcrops) on earth show noticeably greater contrast than in other spectral regions. However, the intervening atmosphere on Mars negates the use of filters shortward of 5500 Å, as we have already seen. Thus multispectral operation will be confined solely to the yellow-red portion of the spectrum. Such a limitation may make the use of this technique impractical for the 1973 mission. Laboratory studies, however, may show the value of such an approach for later missions.

2.4.5 SUMMARY

A photo-imaging mission for the first Martian orbiter has been generated in which a balanced scientific program is postulated and specific objectives delineated on the basis of known information and specified in a form suitable for specific technological design.

Based on this initial attempt, a summary of the orbiters first month's picture acquisition objectives is given in Table 2-8.

The field-of-view (FOV) requirement indicated for each objective can be met by frames having smaller instantaneous fields of view, if adjacent frames in the same ground trace and in adjacent ground traces overlap somewhat. For instance, the 20-degree FOV for medium-resolution mapping can be attained with a 10-degree FOV and some overlap between frames.

Table 2-8. First Month Mission
Summary of Data Rate Requirements and Pictures Accumulated

Objective	No. of Pictures	FOV (degrees)	Resolution	
			Spatial (meters)	Intensity (bits)
Medium-resolution map	965	20	100 300	8
High-resolution spot coverage	131	5	10 30	8
Lander site survey	1	5	1 3	8
Cloud survey	12	40	500 1000	6
Whole-planet photography	12	102 at periapse (1000 km)	1000 3000	6
Total number of pictures accumulated (first month)	1121			

SECTION 3

MAPPING COVERAGE

3.1 BASELINE ORBIT

The buildup of mapping coverage of a planet from an orbiting vehicle involves the capabilities of the photo-imaging sensor, the size of the orbit, the kinematics of the planet and orbiter, and the timing of the orbit.

The first step in a coverage analysis is to determine what conditions are desired by the sensor. Since resolution is directly proportional to altitude (unless special provisions are made), the sensor can be used only in a limited altitude range, such as the altitude range between periapsis (lowest point in the orbit) and two or three times periapse altitude. The sensor will operate best under certain illumination conditions. For example, long shadows (high sun angles) may be desirable, whereas low sun angles (satellite subpoint near solar subpoint) might not produce sufficient contrast. These sun angle considerations and altitude constraints are determined and expressed as a set of conditions favorable to photo-imaging. A typical set might be:

a. Minimum altitude = 1000 km (lowest point in orbit).

b. Maximum altitude = 3000 km (limit of resolution).

c. Minimum sun = 40 degrees. (Shadows produced below $\approx$ 40 degrees are too short to produce topographic data).

d. Maximum sun angle = 80 degrees (absolute illumination level too low to produce good images).

Once the sensor constraints are determined, the burden shifts to orbital mechanics to determine the orbit or class of orbits which are possible under a given set of booster capabilities, launch windows, trajectories, orbit-injection accuracies, and other mission contraints. It is beyond the scope of this discussion to examine the many interactions involved in the selection of the orbit and orbit-injection parameters. However, as an

example of the baseline orbit, i.e., one that is designed to satisfy both lander and orbiter objectives, a single set of orbit parameters is defined. These might be:

h_p = periapsis altitude = 1000 km

h_a = apoapsis altitude: 10,000 km

i = orbital inclination = 40 degrees
arrival date = 11 Mar 1974

Ω = longitude of ascending node = 242.6 degrees

The problem is to find out how well and how often the sensor constraints and conditions are satisfied by the selected orbit.

An analysis of sun angle and altitude is shown in Figures 3-1 through 3-3. These curves can be generated at different times into the mission; shown here are 0, 90, and 180 days from arrival. This analysis shows how the sun angle and the altitude varies for a given orbit at a specific date. From curves such as these, it is possible to determine if, and how often during the orbit, the sensor conditions are met.

This data is presented in a more graphical form in Figure 3-4, which shows the usable portion of the orbit as the mission progresses from arrival on for 6 months. The portion of the orbit, expressed as an arc of so many degrees of true anomaly, is a horizontal line at any given date. Thus, Figure 3-4 shows that under this set of sensor/orbital constraints, the sensors might operate continuously for part of each orbit during the early part of the mission; but as the mission progresses, they would have to be turned on and off twice each orbit to take maximum advantage of conditions. However, it also shows that later in the mission the first "on" time is relatively short and might be neglected if either the areas had been previously photographed or if the coverage during the first phase of continuous orbital surveillance was sufficient.

As the mission proceeds, the orbital mapping coverage builds up to the maximum allowed by the orbital inclination.

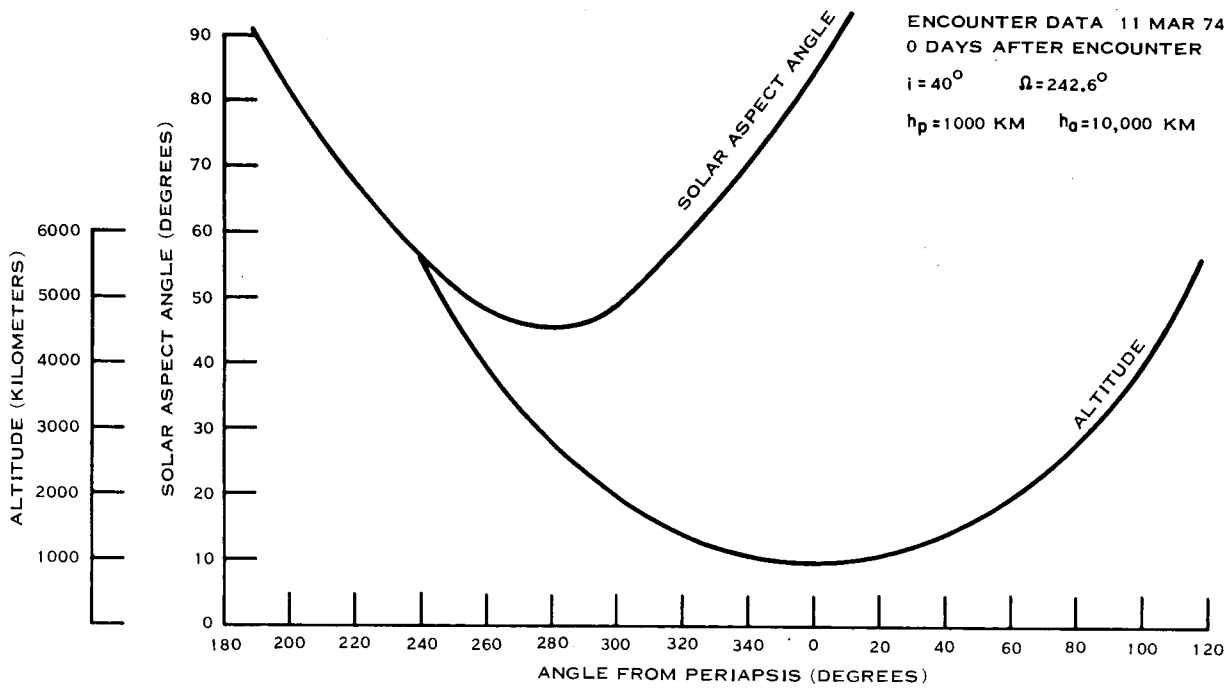

Figure 3-1. Sun and Altitude Conditions at Encounter

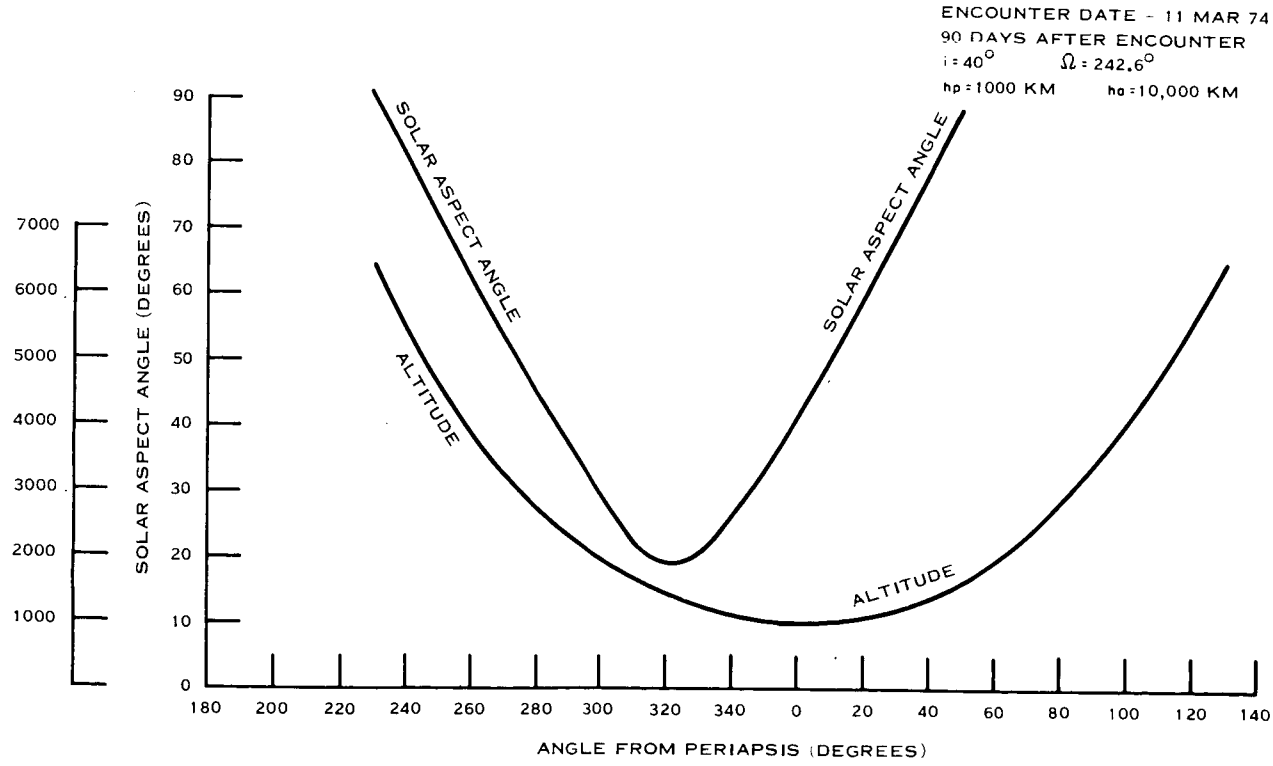

Figure 3-2. Sun and Altitude Conditions - 90 Days

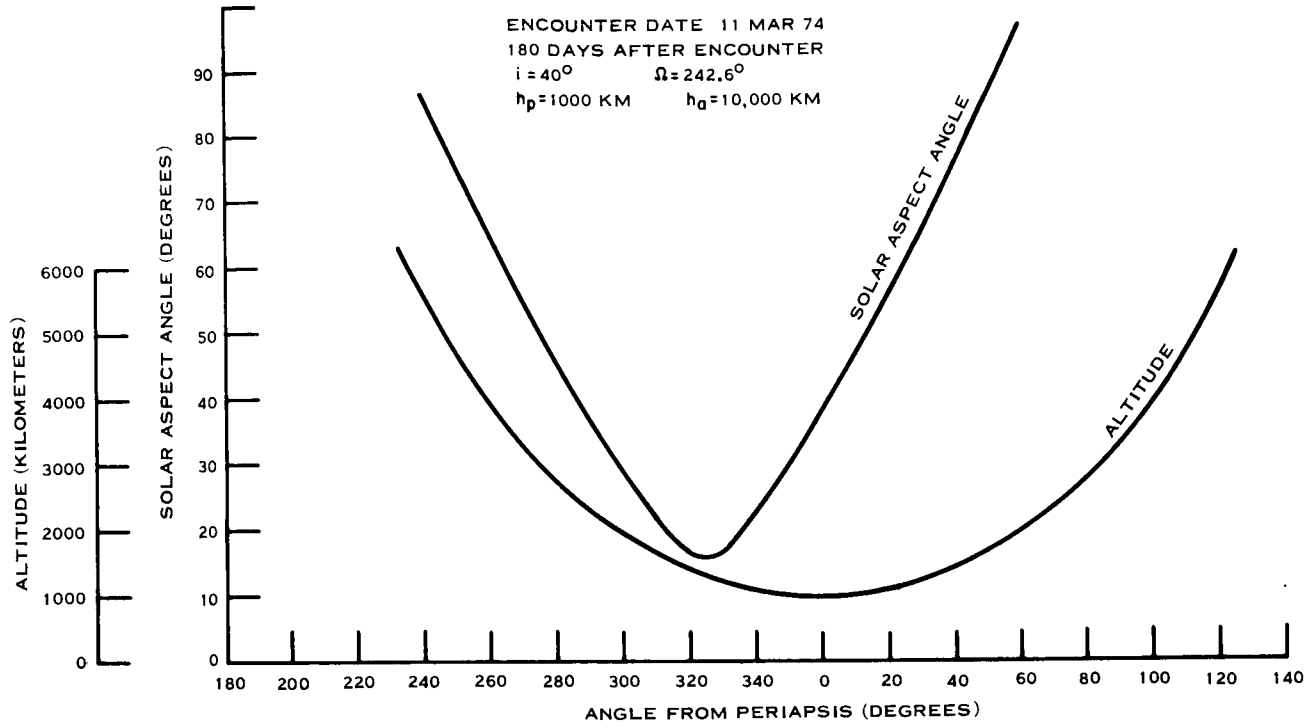

Figure 3-3. Sun and Altitude Conditions - 180 Days

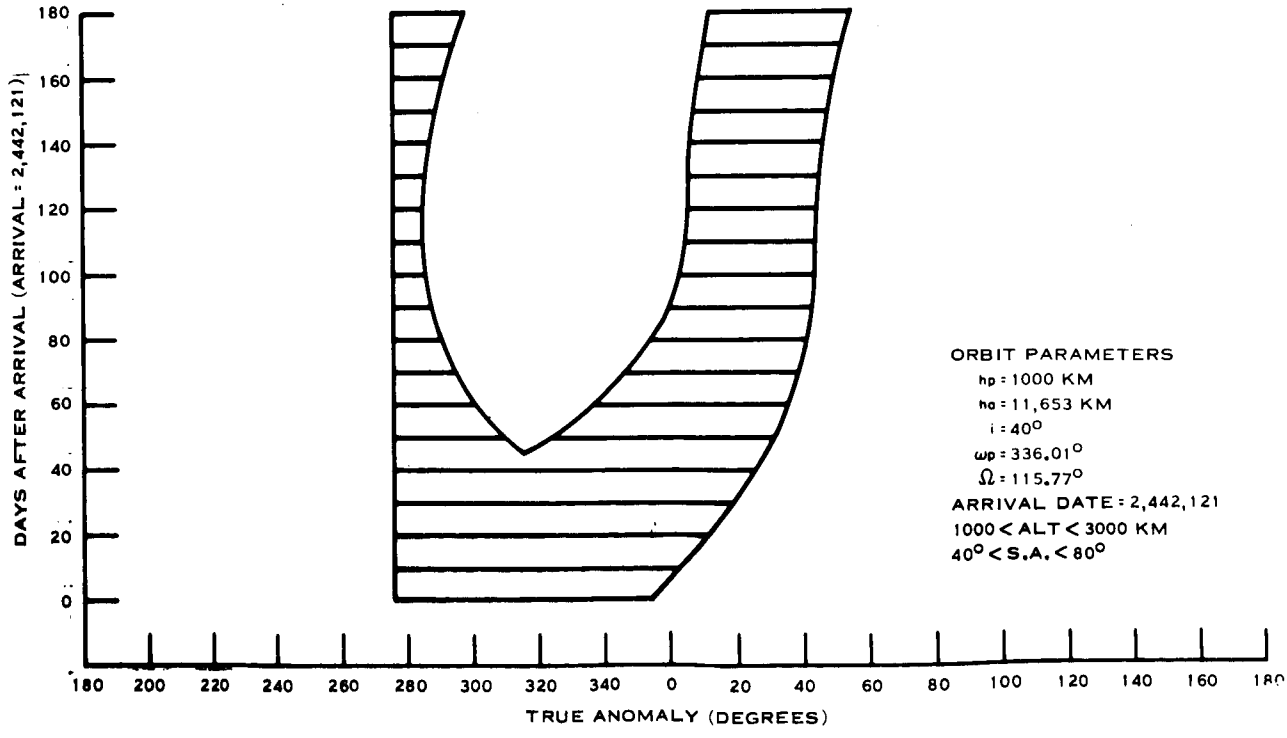

Figure 3-4. Usable Region of Orbit Versus Time in Orbit

Another interesting method of showing the mapping coverage is to plot the area covered on a map. Figure 3-5 is a Mercator projection of the Martian planetary surface as extracted from earth-based photography. Figures 3-6 through 3-10 repeat this map to show the portions of the planet that could be covered by the end of 10, 30, 60, 90, and 180 days into a typical mission. The shaded area is the area mapped from the beginning of the mission until the time indicated.

3.2 ORBIT TRADEOFFS

The tradeoffs that must be evaluated in order to select an orbit meeting the requirements of a photo-imaging mission range from the broad questions of conflicting missions to constraints of the spacecraft design and to the parameters directly affecting the mapping coverage. These tradeoffs are discussed in the following sections.

3.2.1. MISSION PRIORITIES

Mission priorities of the Voyager system are listed in 1973 Voyager Mission General Specification, January 1, 1967. Those priorities that affect the photo-imaging mission are:

a. Achievement of a Planetary Vehicle Mars orbit insertion.

b. Achievement of a flight capsule landing.

c. Performance of entry science experiments.

d. Performance of orbital science experiments.

e. Performance of landed science experiments.

Competing characteristics (b) and (c) place severe restrictions on the orbit from the photo-imaging standpoint. For example, these characteristics have evolved more than 18 orbit constraints designed to enhance capsule descent and landing conditions. Photo-imaging must then accept the resulting orbit, which may not be optimum for photo-imaging. If a lander is not carried or if the orbital science were to be considered a higher mission priority than flight capsule landing, the orbital parameters, discussed in Section 3.2.3, could be optimized for the photo-imaging requirements.

MERCATOR'S PROJECTION OF MARS

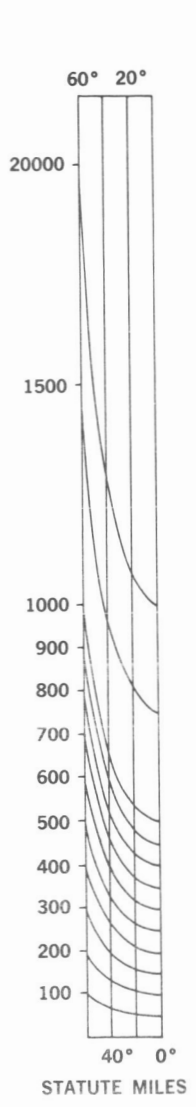

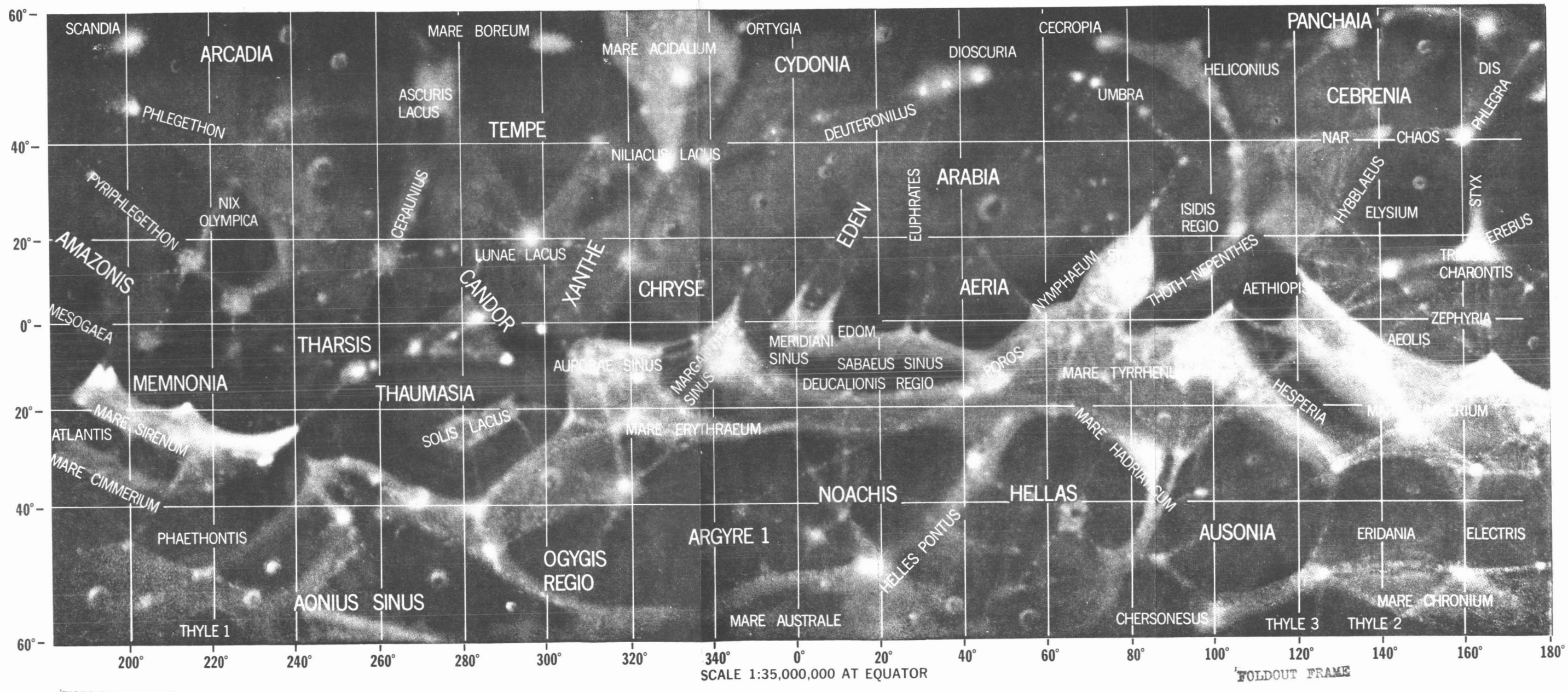

SCALE 1:35,000,000 AT EQUATOR

FOLDOUT FRAME

FOLDOUT FRAME

Figure 3-5. Mercator's Projection of Mars

3-6A

3-6B / 3-7/3-8

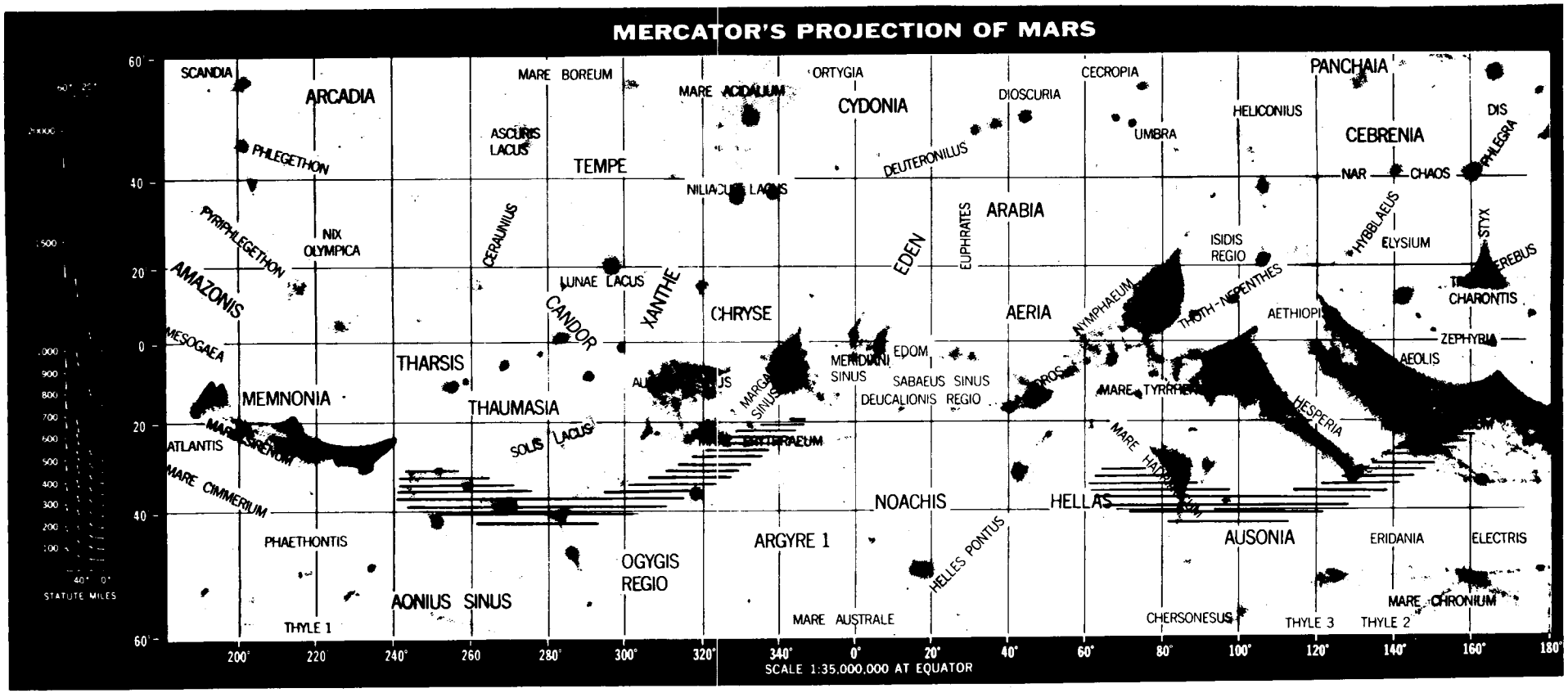

Figure 3-6. Coverage After 10 Days

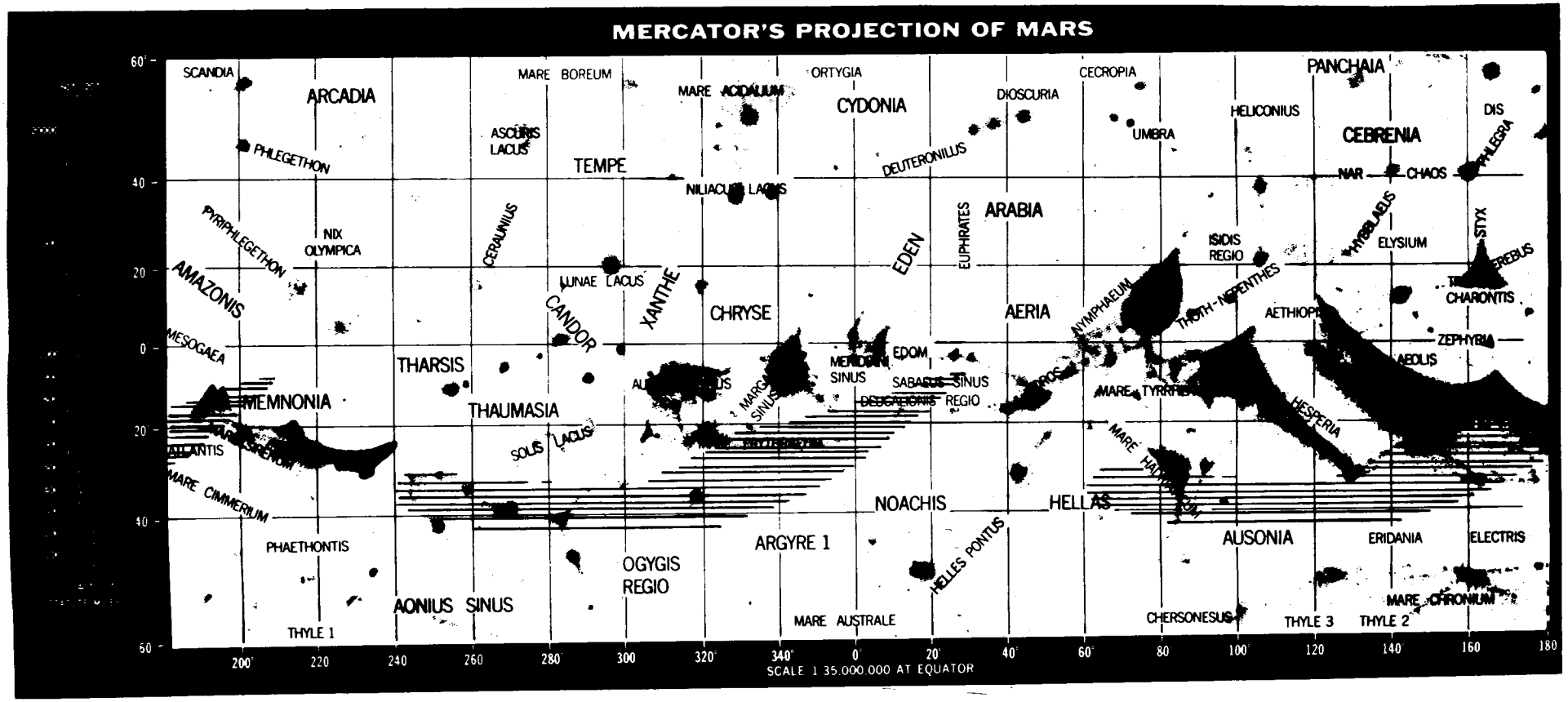

Figure 3-7. Coverage After 30 Days

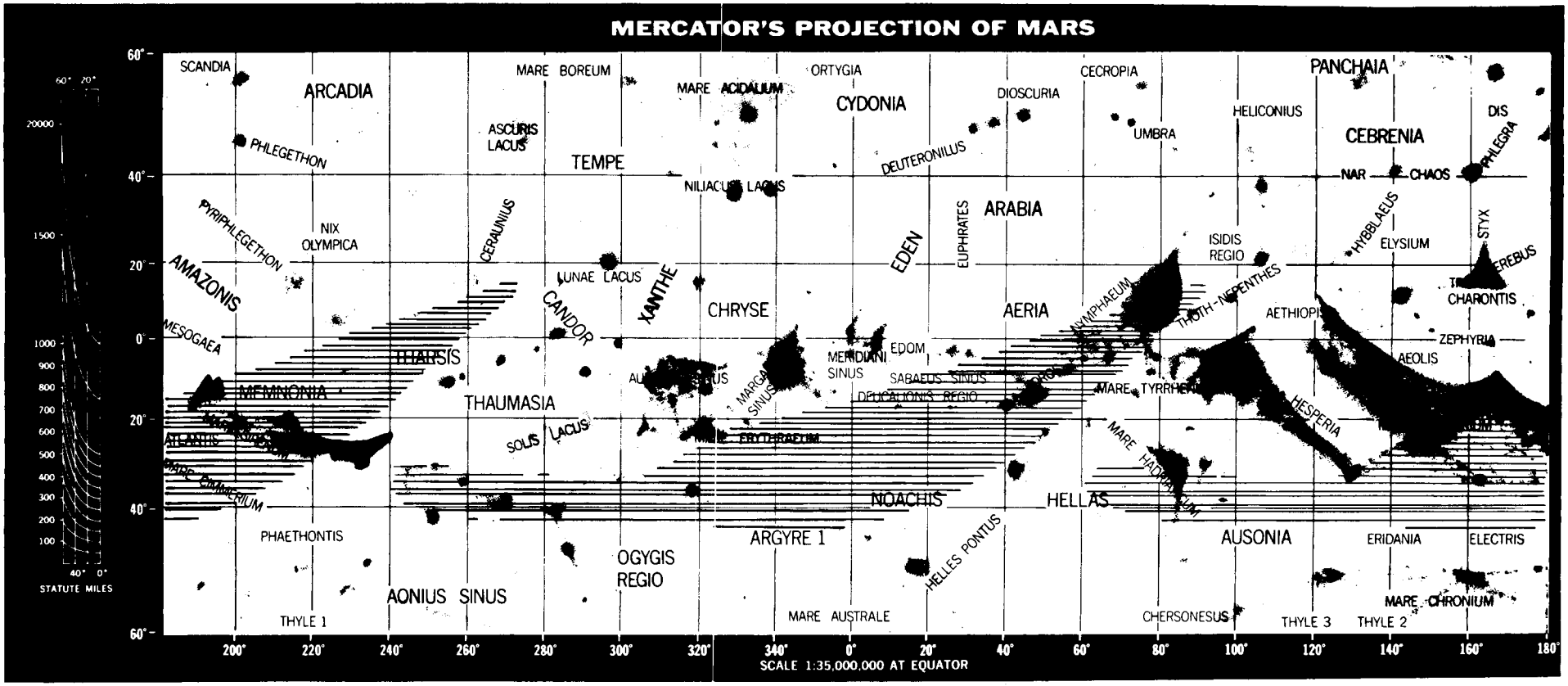

Figure 3-8. Coverage After 60 Days

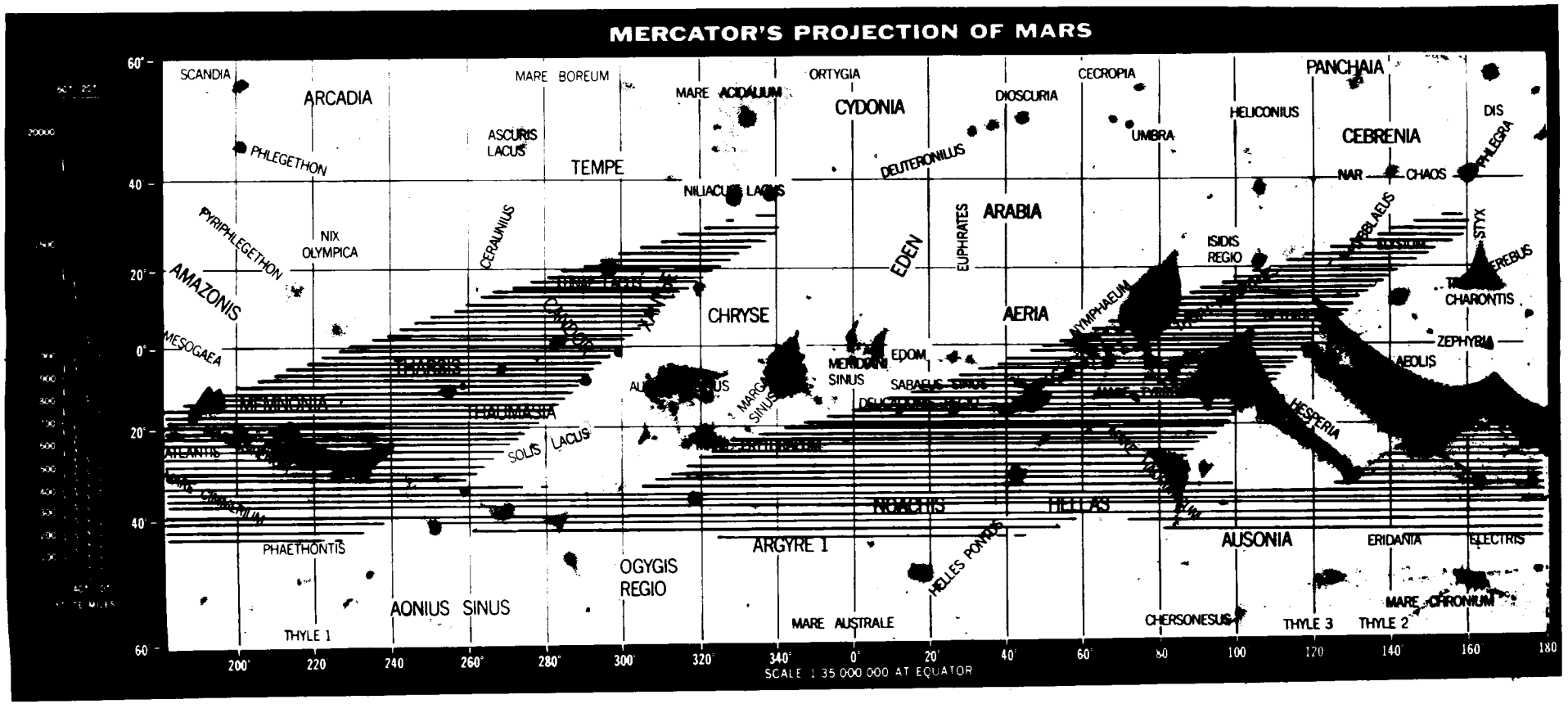

Figure 3-9. Coverage After 90 Days

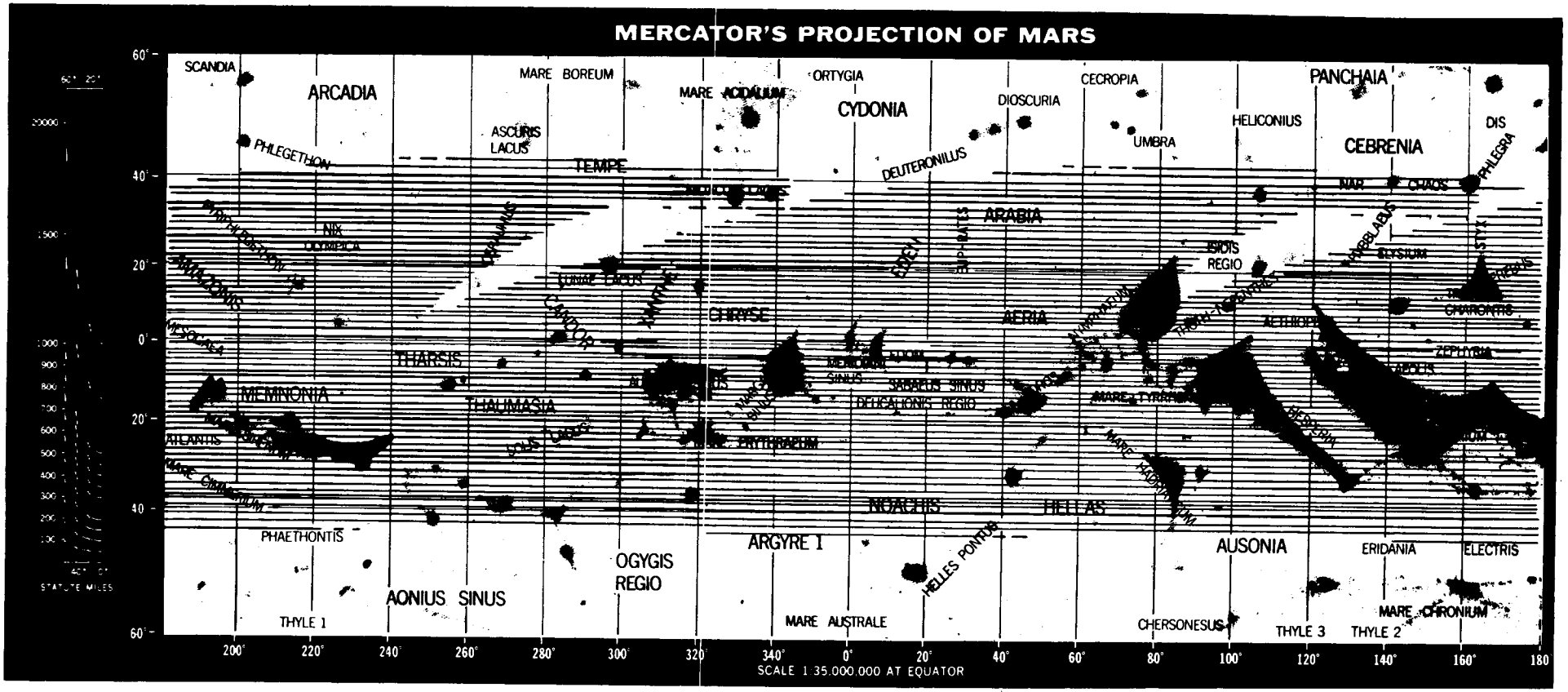

Figure 3-10. Coverage After 180 Days

3.2.2. ORBITAL CONSTRAINTS

The most obvious constraint on the orbit is one of energy available to choose a particular orbit. Unlimited booster, midcourse maneuver, and orbit trim energy is required to enter any conceivable Martian orbit and change that orbit at will. Since this is not the case, we are left with an envelope of possible orbit parameters. For instance, an example of an orbit that would not fall into such an envelope is one in which the orbit plane lies normal to the Voyager approach velocity vector to Mars. Such an orbit requires energies in excess of those available at Mars encounter. The envelope of physically realizable orbits is a function of:

a. The hyperbolic excess velocity.

b. ZAP angle (the included angle between the planetary approach assymtote and the Mars-Sun line).

c. The aiming point in the impact plane.

d. The energy available for orbit insertion.

e. The energy available for orbit trim.

To define such an envelope is considered to be a necessary study, but is beyond the scope of this task. However, such an envelope should be defined before the orbiting science system design is frozen at some later date.

Other constraints placed on the orbit are the duration and number of earth, solar, and Canopus occultations and the effects these have on the spacecraft design.

3.2.3 PARAMETERS AFFECTING COVERAGE

3.2.3.1 Orbit Inclination

In order to obtain coverage over the entire planetary surface it is necessary to use a near-polar orbit. However, since most areas of interest are at lower latitudes, as discussed in Section 2, a lower inclination angle may be acceptable. In general, effective coverage is bounded in scope by the orbit inclination such that areas north and south of the latitudes equal to the orbit inclination are not observable. This is somewhat ameliorated by the

altitude, h, of the vehicle and the sensor half angle field of view, $\gamma/2$. As these two parameters increase, there will be some additional observable area as Figure 3-11 shows.

3.2.3.2 Periapsis Location

Locating the periapsis at the time of orbit injection and modifying its position by means of an orbit trim maneuver is a very important consideration. Due to the Martian planetary oblateness, the periapsis point will move north or south in a predictable fashion during the mapping mission. Figure 3-12 shows the angular rate of travel of the periapsis point as a function of the orbit inclination and semimajor axis for a periapsis of 1000 km. Ideally, the movement of the periapsis should lie within the latitude band of maximum photo-imaging interest, which may be accomplished by judiciously picking the initial periapsis position. It may be seen from the curve that at inclinations of approximately 63 degrees and 117 degrees the periapsis point remains fixed. This means that for such inclinations the highest resolution pictures would all be constrained to the same Martian latitude. This, of course, may not be desirable. Notice that periapsis travel, $\Delta\omega_p$, is plotted for a single revolution of the spacecraft about Mars. Such a form is useful when considering a mission coverage pattern generated by n spacecraft revolutions about the planet. Thus, total periapse travel during the mission will be $n \cdot \Delta\omega_p$ degrees. Knowing this figure, the initial periapse location may be properly biased with respect to a Martian latitude to optimize resolution over the region of interest.

3.2.3.3 Eccentricity

If the orbit semimajor axis must be held to some minimum dimension, it is useful to consider eccentric orbits where the periapsis is located over the areas of interest during the mapping period. Since resolution is inversely proportional to the altitude, it becomes apparent that to achieve the best pictures, one has to get as close as possible to the surface. The quarantine restriction places a lower limit on the periapsis altitude and is considered to be 1000 km for this study. It might seem that an eccentric orbit would distort the symmetry of the equally spaced ground tracks of an optimum orbit. However, it turns out that this is not so, and regardless of the orbit eccentricity the longitudinal spacing between adjacent ground tracks, σ, remains constant if the orbit is optimum. The effect of eccentricity on coverage is that the varying altitude due to eccentricity produces a varying

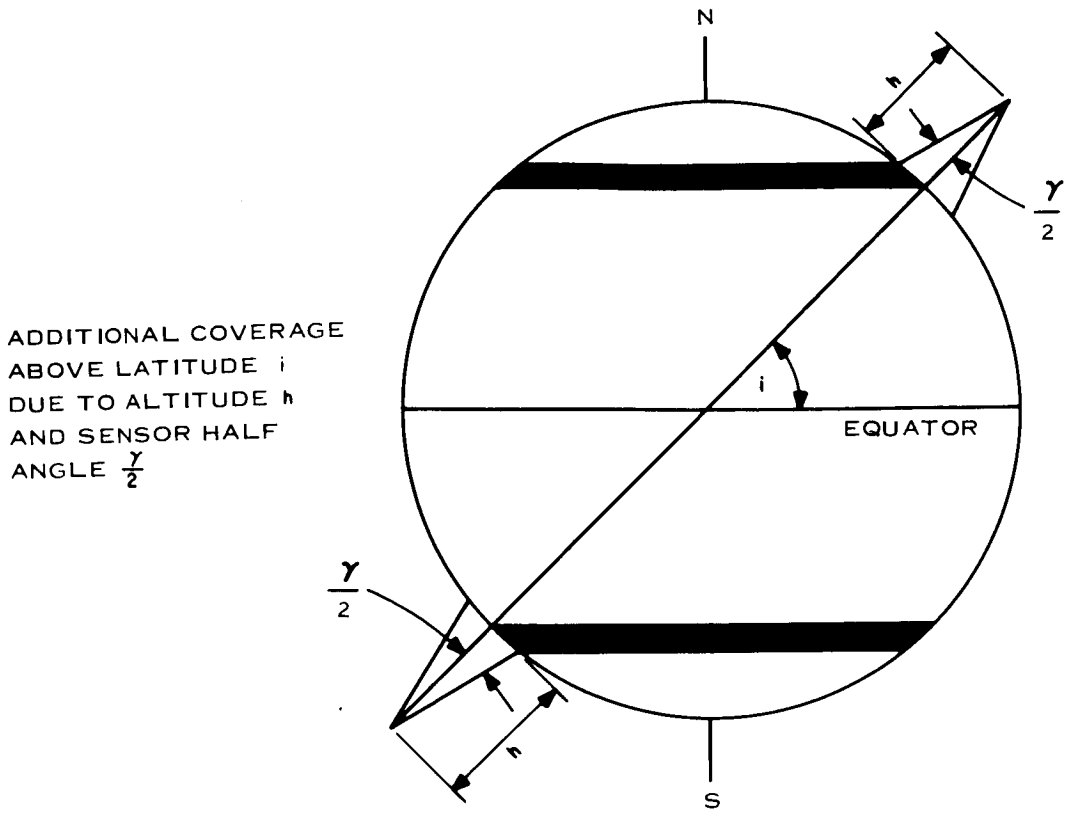

Figure 3-11. Surface Coverage

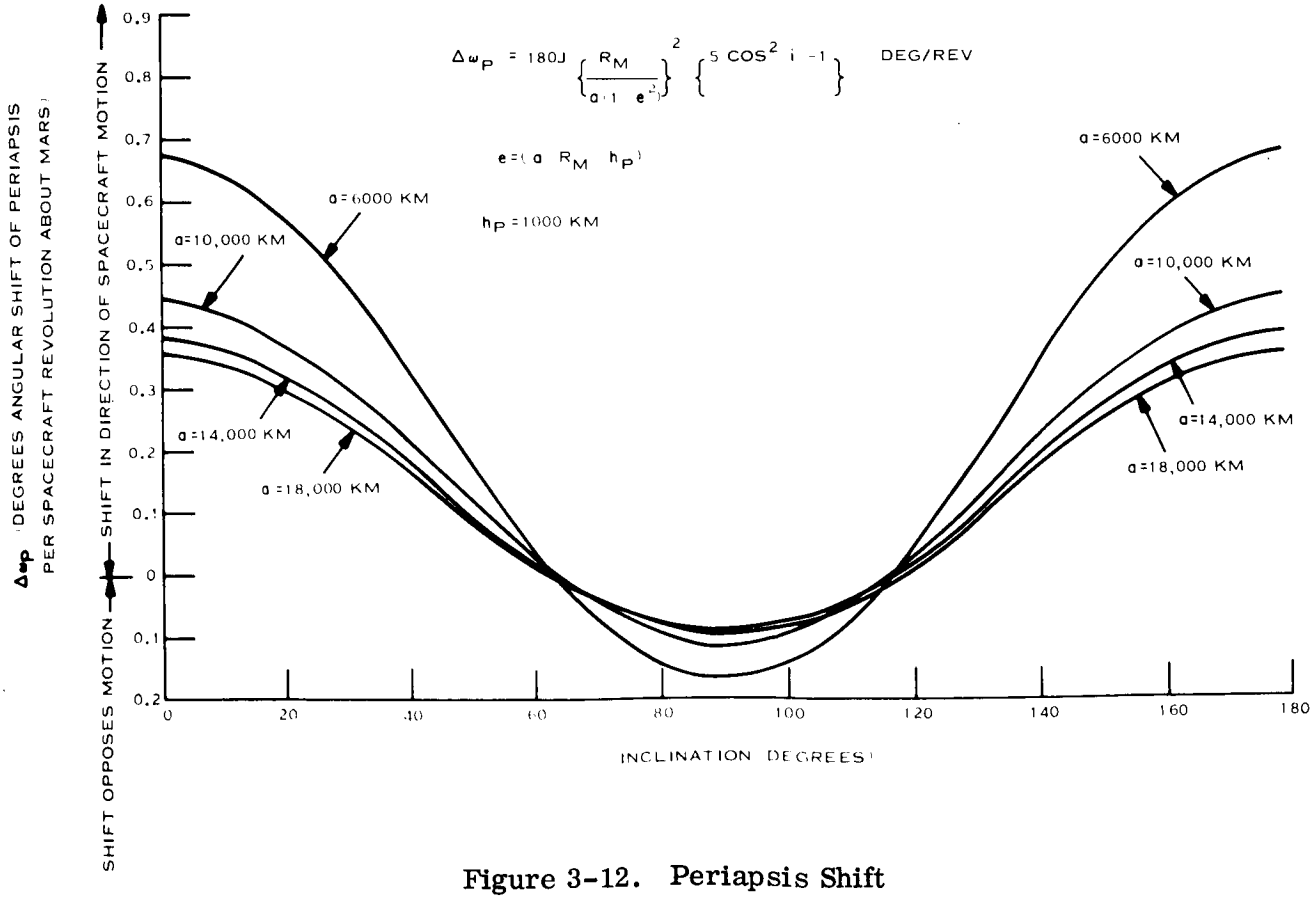

Figure 3-12. Periapsis Shift

ground swath width. It must be noted that the altitude and sensor field of view which produces the ground swath must be sized for altitude conditions at the planetary equator in order to ensure complete coverage over any specified time period.

3.2.3.4 Synchronism and Period Sensitivity

To ensure optimum coverage regardless of the orbit inclination chosen, it is necessary to generate a synchronous orbit, that is, one that repeats after n revolutions. Also, it should be noted that $360^{o}/n = \sigma$ must be less than or equal to the great circle arc width of the photo-imaging swath measured at the equator. If, due to orbit injection errors and trim errors, synchronism is accidently achieved for some $n' < n$, then a degraded coverage will ensue and certain Martian areas will be cyclically missed every N Martian days. As an example, in the extreme case of a purely synchronous orbit where the ground track repeats each orbital revolution, the mapping would be disastrously degraded.

As an example of the sensitivity of orbit period on mapping coverage, Figure 3-13 is shown. This curve shows what coverage will be achieved at 1000, 2000, and 4500 hours after arrival (40, 80, and 180 days). A constant periapse altitude is assumed, and apoapsis altitude (and, therefore, the orbit period) is varied to show that coverage buildup is relatively insensitive to apoapsis except in the area near where the orbit is trisynchronous, or exactly three revolutions/day.

3.2.3.5 Overlap Control

It is desirable to control the amount of overlap between adjacent frames in the same orbit trace and between ground traces of adjacent orbits for the following reasons:

a. Overlap will aid cartographers on Earth to fit the many pictures together into a complete map of the Martian surface. The pieces of this "jigsaw puzzle" will be difficult to match because the geometrical relationship, solar illumination angle, and resolution will change from frame to frame.

b. Stereoscopic information can be extracted from the overlapping portions of adjacent picture frames. As discussed in Section 2, this technique may be the chief way of obtaining topographic mapping data since Mars surface has a photometric function, like Earth's, that may prevent determination of topography by purely photometric means.

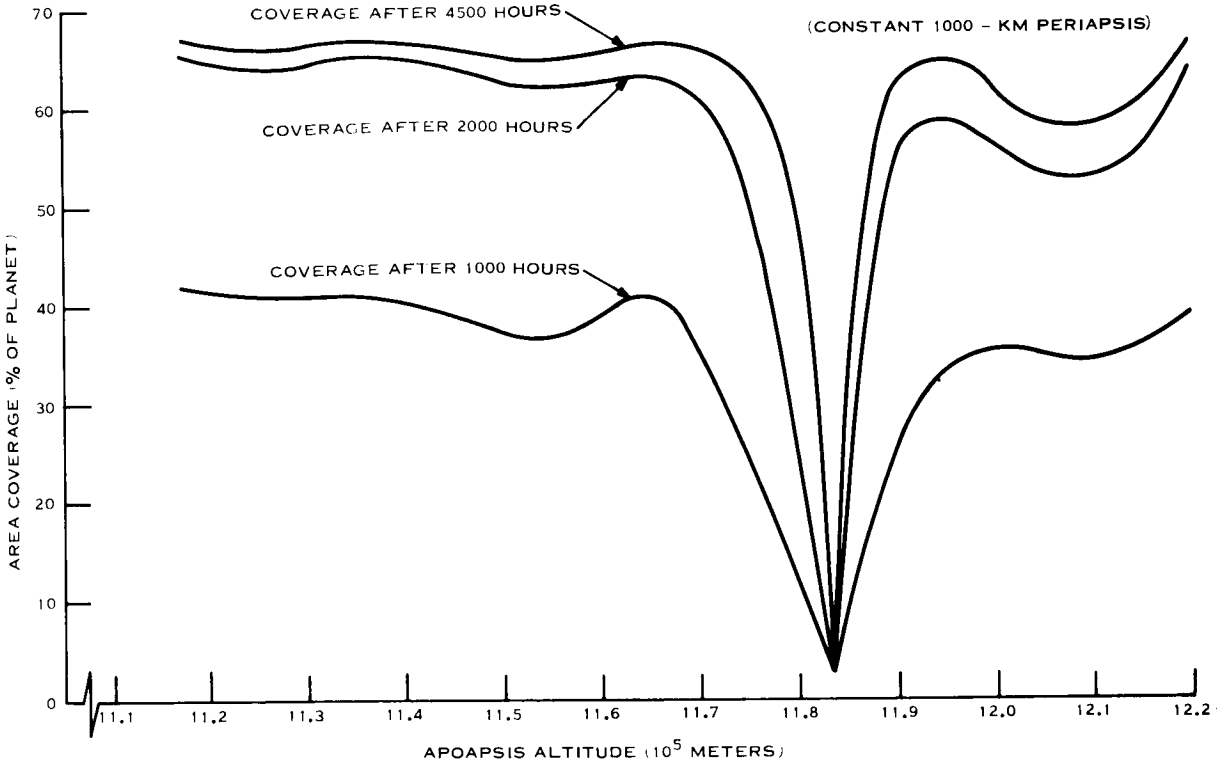

Figure 3-13. Coverage Buildup Versus Apoapsis Altitude

c. At high latitudes and altitudes or in near-synchronous orbits, the amount of overlap becomes excessive, and thus slows down the coverage buildup. To keep the overlap within reasonable limits, the field of view, time between frames, and the orbit period may have to be continually varied and adjusted.

One of the effects of controlling the overlap between ground traces of adjacent orbits is illustrated by Figures 3-14 and 3-15. These curves plot the percent coverage versus the time from the start of the orbiting mission. Both are for nominal 1000 by 1200 km orbits at 40 degrees inclination. Both have a photo-imaging sensor of 10 degree field of view which, at the 1000-km altitude, covers a swath width of 174 km. The difference in the two curves is the longitudinal spacing of the orbit ground tracks. Since they are near trisynchronous orbits, every third orbit returns nearly to the same ground track. The distance each third orbit is spaced apart is controlled by a slight variation in orbit period and is identified as the longitudinal spacing in kilometers per day (every three orbits). Figure 3-14 has a longitudinal spacing of 256 km/day, so that there is no overlapping of the 174-km

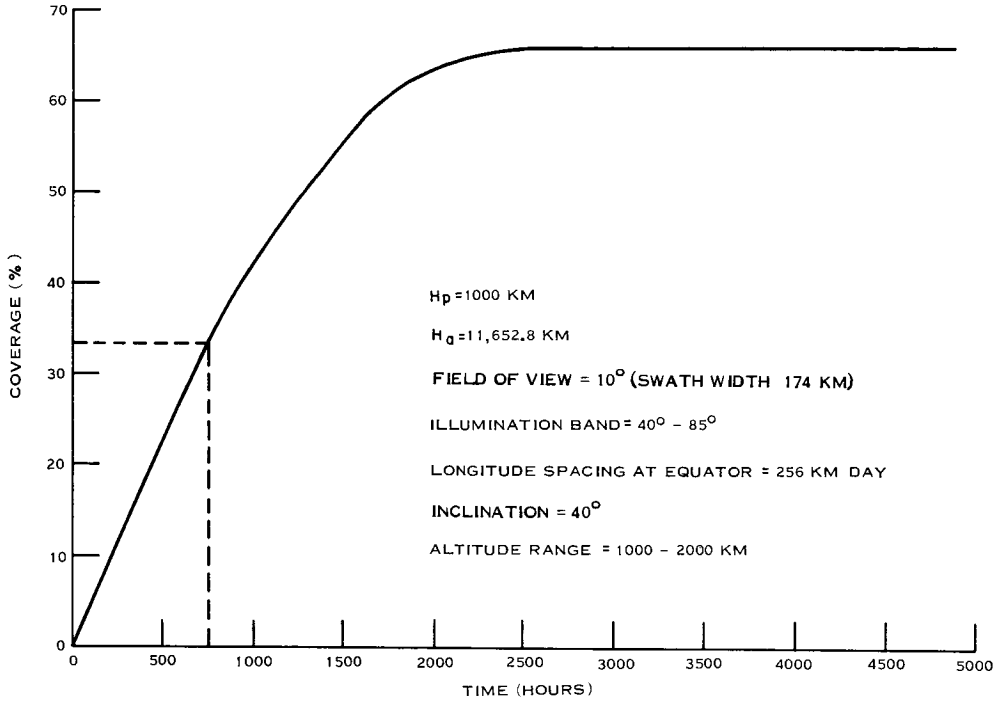

Figure 3-14. Rate of Coverage Without Overlap

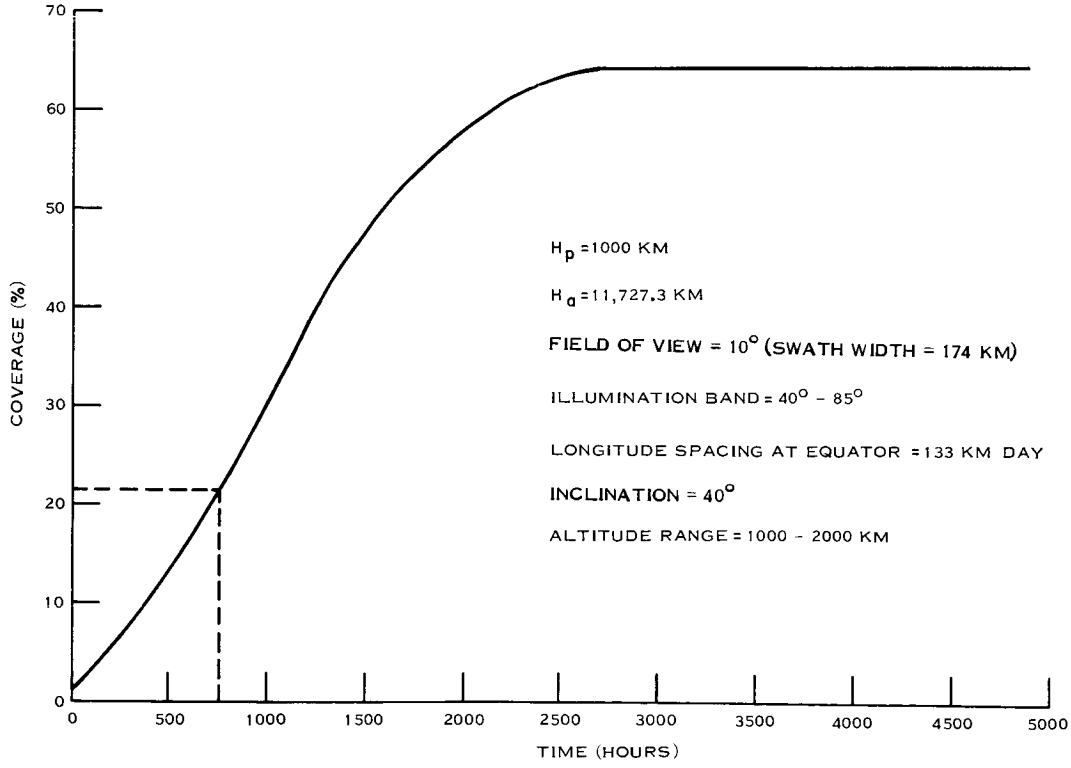

Figure 3-15. Rate of Coverage with Overlap

swath width on succeeding days. The coverage of the surface builds up rapidly to 32 percent at 1 month. Figure 3-15, however, has a smaller longitudinal spacing of 133 km/day, so that there is overlap. The coverage in this case builds up slower to only 21 percent at 1 month. On a total coverage basis, however, this initial rate does not continue; both the orbits shown in Figure 3-14 and 3-15 reach a maximum coverage in roughly the same time period.

3.2.3.6 Illumination Considerations

Lighting conditions that exist at time of encounter relative to the onboard sensors are dependent upon the orbit inclination and the right ascension of the ascending node with respect to the terminator. In general, when the right ascension is 90 degrees and the orbit inclination is 90 degrees, illumination will be maximum. There are definite favorable lighting conditions for the sensors which vary from minimum to maximum illumination conditions.

If it is desired to maintain constant illumination conditions on the planetary surface directly beneath the spacecraft, then it is necessary to enter a "Sun-synchronous" orbit. Such an orbit possesses a plane rotation (nodal regression) in inertial space that matches Mars' mean angular rotation about the Sun of 0.524 degrees per day. Figures 3-16 and 3-17 plot the relationships between inclination and semimajor axis which yield Sun synchronism for (a) orbits with a periapsis of 1000 km and for (b) circular orbits.

3.3 OPTIMUM COVERAGE ORBITS

An optimum orbit for the photo-imaging mission is not necessarily one that provides the maximum gross coverage of the surface in the shortest time but is one that provides an orderly progression of mapping such that overlap is known and controlled and total coverage is accomplished in the planned time. Such an optimum orbit can be defined with the assistance of Figure 3-18. This figure shows the relationship of two ground tracks (every third one for a trisynchronous orbit) of the spacecraft and the swath width of the photo-imaging sensor. An optimum orbit exists when the longitudinal spacing of the ground

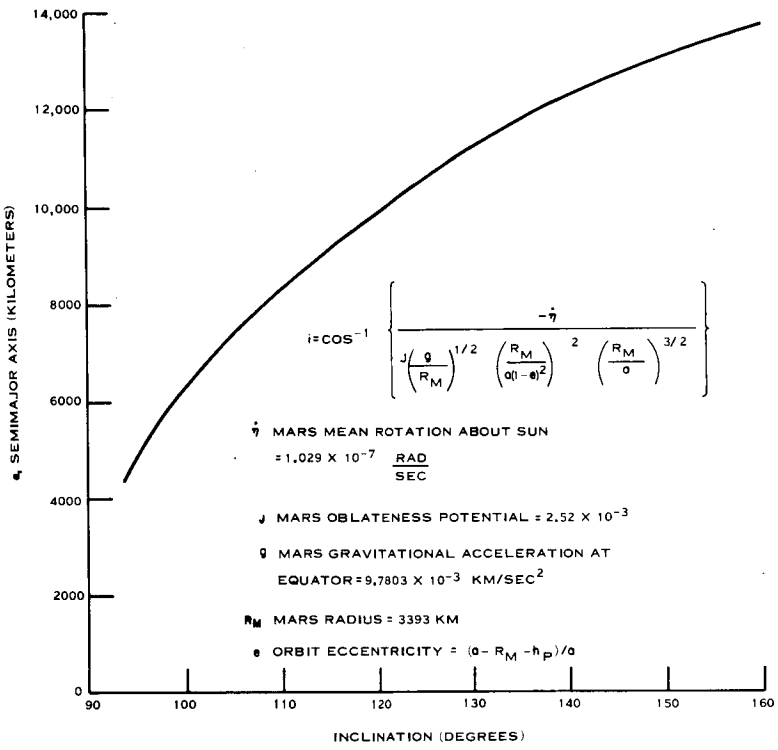

Figure 3-16. Sun-Synchronous Orbits - Periapsis 1000 km

tracks is less than the swath width (projected on the equator) by the specified amount of overlap. Further, the ground tracks repeat themselves after the specified total mapping period.

An analysis of such optimum orbits is described in Appendix A. A method is shown there that permits the selection of a set of orbit parameters and a sensor field of view that produces perfectly interlacing swaths about the planet's surface in some selected nominal time period.

An example of the results of this analysis is shown in Figure 3-19. This curve shows the set of orbits which yield uniform coverage over a 30.8-day period. The periapsis is constant at 1000 kilometers; apoapsis varies from 11,000 to 17,000 kilometers. Orbit inclinations are from 20 degrees to 160 degrees. Each line on the curve is

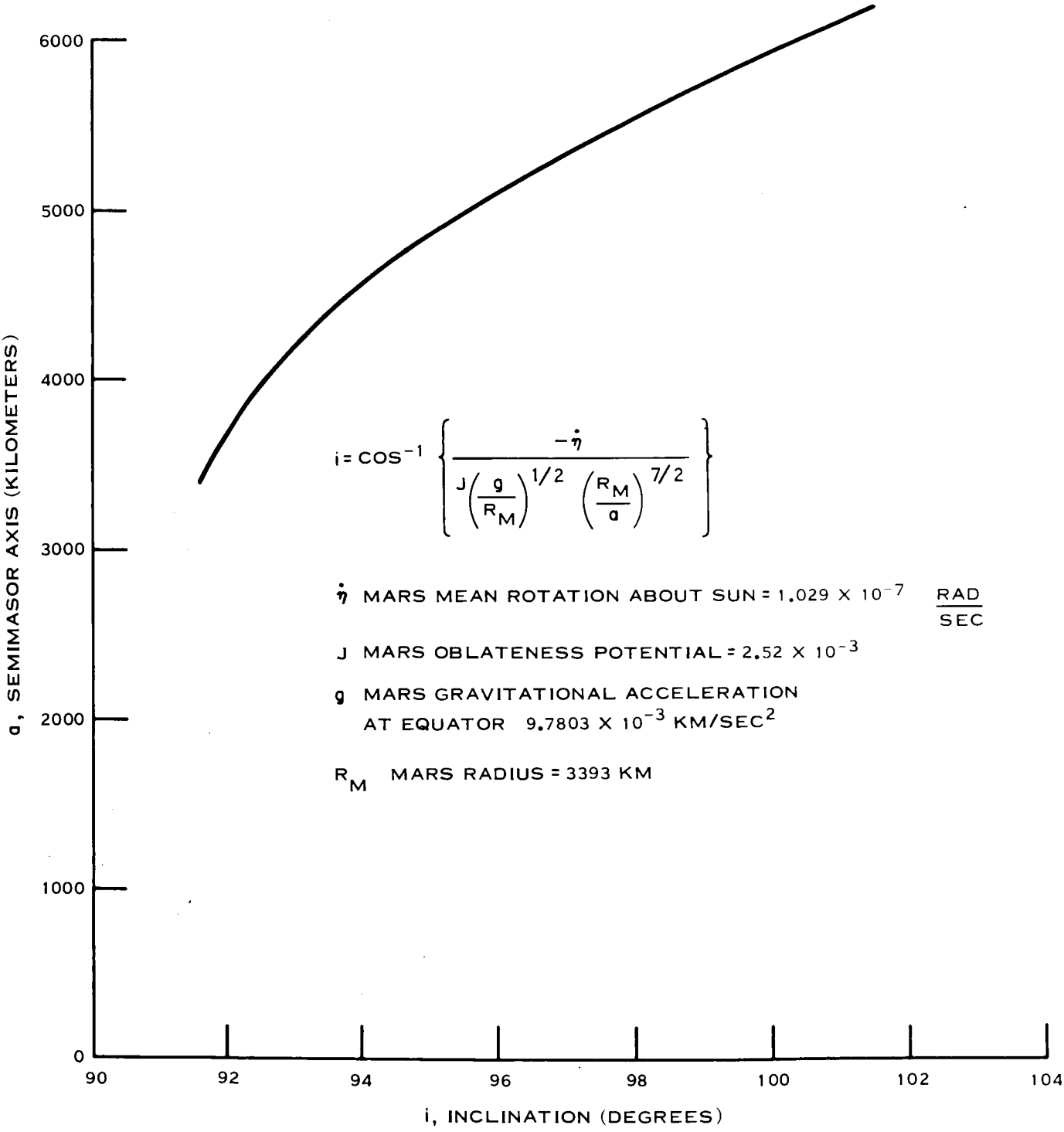

Figure 3-17. Sun-Synchronous Orbits - Circular

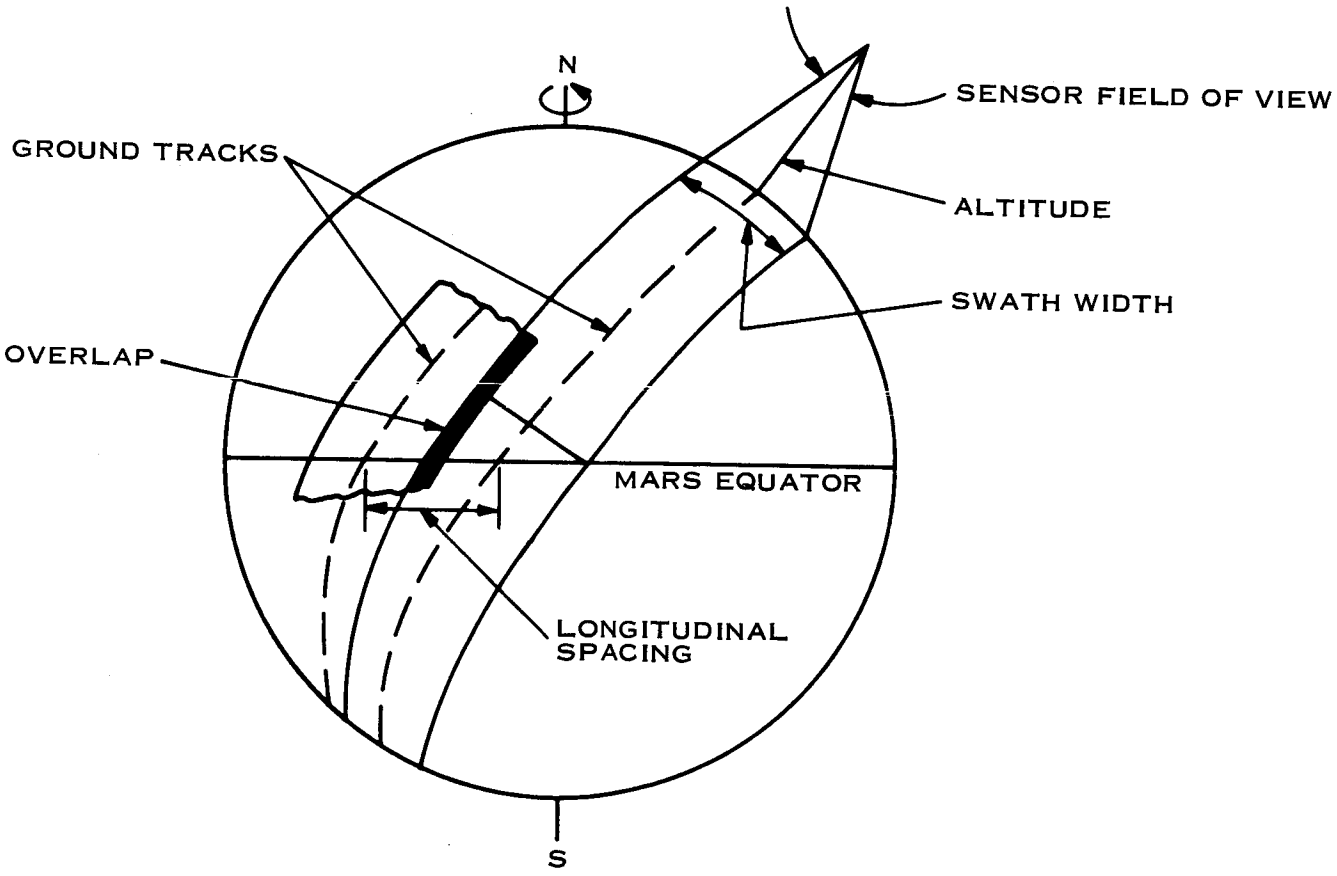

Figure 3-18. Optimum Orbit

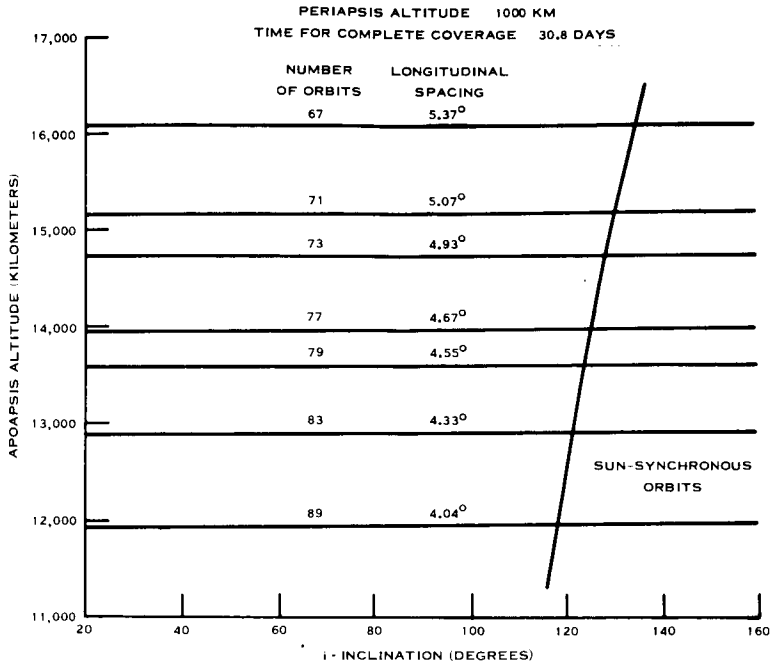

Figure 3-19. Optimum Orbit Parameters

a set of optimum orbits and is identified by the total number of orbits in the 30.8 days and the longitudinal spacing between ground tracks. In each figure there also appears a single curve representing the set of Sun-synchronous orbits for a periapsis of 1000 km. Where the curves intersect, the double constraint of uniform coverage and Sun synchronism is satisfied.

For a nominal orbit of the following parameters:

a. Inclination = 40 degrees

b. Periapsis altitude = 1000 km

c. Apoapsis altitude $\cong$ 12,000 km

d. Argument of periapsis = 336 degrees

Figure 3-19 shows that a 30.8-day uniform coverage may be achieved between 40 degrees south latitude and 40 degrees north latitude by selecting an apoapsis altitude of 11,950 km (89 orbits; 4.04 degree longitudinal spacing). The periapsis point of such an orbit will shift approximately 0.22 degrees/revolution (Figure 3-12). Since 89 revolutions of the spacecraft are required before the 30.8-day coverage is complete, the total angular travel of periapsis within the orbit plane is 19.6 degrees. Thus, only a relatively narrow Martian latitude band ($<$ 15 degrees) is observable at the periapsis altitude over the 30 days.

The swath width equivalent to the 4.04 degrees longitudinal spacing of this example is 155 kilometers. This can be provided with a 9-degree field of view sensor.

It must be emphasized that to ensure coverage, the field of view must be sized for the minimum altitude that will occur at the equator. As the periapsis location varies with time, the altitude at the equator is constantly changing also. For this example, it was assumed that the minimum altitude at the equator would be 1000 km.

SECTION 4

DESCRIPTION OF CANDIDATE PHOTO-IMAGING SYSTEMS

4.1 REQUIREMENTS AND PERFORMANCE SUMMARY

4.1.1 REQUIREMENTS

A Television System, a Photographic Film System, and an Optomechanical Scan System have been selected for the candidate photo-imaging systems. Each system has been designed to meet the requirements of a general mapping mission and a spot-reconnaissance mission. A low-contrast Martian surface has been specified, requiring a high degree of intensity resolution. The designs have been constrained to attainable data transmission rates and tape recorder input rates. The baseline 1000 by 12,000 kilometer orbit has been specified.

Specifically, these requirements are as follows:

a. Spatial resolution: 100 meters for mapping and 10 meters for reconnaissance

b. Intensity resolution: 0.5 percent

c. Field of view: 10 degrees for mapping (permits one third of Mars to be mapped in 1 month) and 1 degree or less for reconnaissance

d. Data Transmission rate: 30 kilobits per second maximum at 1.5 data compression ratio

e. Tape recorder input rate: 60 kilohertz maximum

In addition, although emphasis was placed on designs for single, black and white pictures, the capability for stereo and for multispectral or color pictures was considered.

The candidate systems presented in this section represent a wide range of designs. These are:

a. Television systems, such as those used on Mariner IV, Mariner '69, Ranger, Surveyor, and Nimbus. These systems store the effect of ground-radiated photons on an image tube storage medium; a scanning electron beam then recovers this information and places it on a separate tape recorder;

b. Photographic film systems, such as the silver halide film used on Lunar Orbiter. These systems store an image pattern directly on chemical film until used for real-time readout and transmission to Earth;

c. Optomechanical scanners, such as the Suomi scanner of the ATS-A and the Nimbus scanners. This class does not have intermediate storage on the sensing medium, but converts the scanned image to an electrical signal for storage on a separate tape recorder. The orbiting motion of the spacecraft itself develops an image strip.

All these systems have their own peculiar advantages and disadvantages. Selection of one system over another is not simple, since all three types appear capable of providing the information required for the 100-meter and 10-meter resolution missions. A final selection will depend on very careful weighing of the factors of information performance, reliability, and weight.

The three systems themselves were selected by eliminating many other attractive candidates because of state-of-the-art limitations and data storage and transmission rate constraints. Many of these may offer special advantages to Voyager once their development has progressed further. The selected systems are felt to be representative of many of the possible photo-imaging systems so that the comparison results will have general application.

4.1.2 OPERATION

The candidate photo-imaging systems are mounted on the planetary scan platform (PSP), which points the instruments as commanded; usually the PSP is responsible for keeping the sensors pointed towards the nadir. There are two candidate photo-imaging systems on the PSP: a 100-meter resolution camera and a 10-meter resolution camera. The 100-meter camera is responsible for mapping as much of the planet as the radio link will permit. The 10-meter camera is responsible for high resolution coverage. At first, this camera will be used to map particular regions that, for example, have been previously observed by Mariner IV, or to provide sampled coverage of the ground. After some 100-meter pictures have been returned and examined, experimeters will request that the 10-meter camera be used to photograph interesting areas that have been previously seen in a larger scale image.

After the first month, when the 100-meter camera has completed the bulk of its mapping, the 10-meter camera will be employed more often. The candidate photo-imaging systems will be controlled from Earth to carry out required actions. Every few orbits, the Computer and Sequencer will receive an agenda and instructions for taking pictures. Such instructions include:

a. Time of picture

b. Camera designation

c. PSP orientation

d. Spacecraft functional inhibits

e. Lens setting

f. Zoom lens setting (if used)

g. Exposure setting

h. Neutral density filter setting

i. IMC mode

j. Recorder speed

k. Recorder track and position

l. Recording modes

m. Downgraded mode instructions

n. Data tagging information

The three camera techniques provide similar coverages of at least 10 degrees by different techniques. Figure 4-1 shows how these coverages are developed. The film camera exposes one single frame of the whole field, and this is optically scanned later for transmission to Earth. The TV produces an array of three images which provide the same coverage. Similarly, the optomechanical scanner lays out three strips line by line. Figure 4-2 shows an overlay of these coverages for one complete picture.

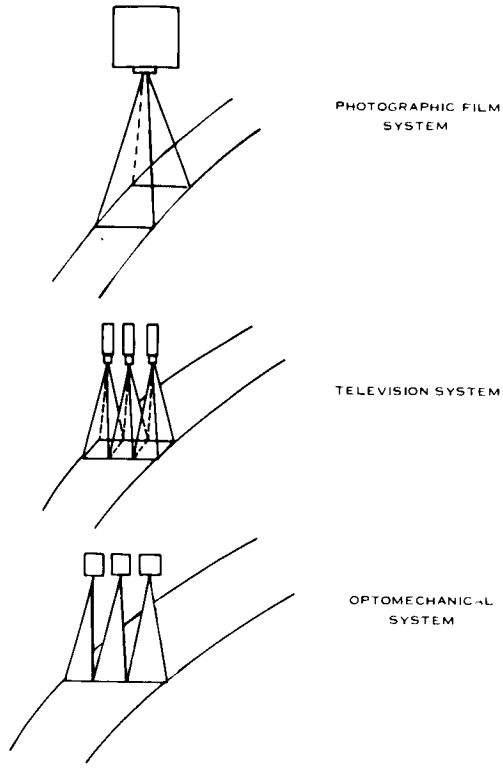

Figure 4-1. Equivalent Coverage of the Three Systems

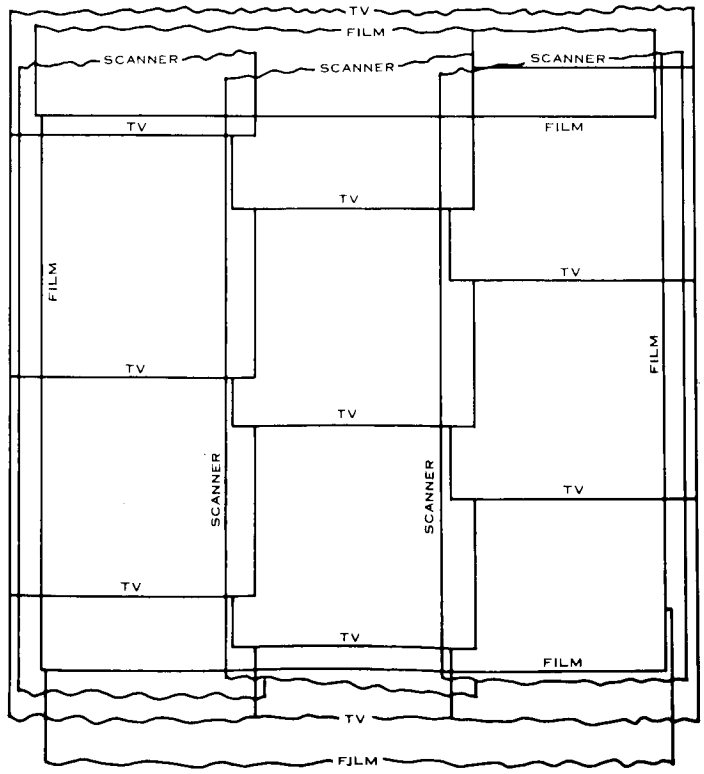

Figure 4-2. Photo-imaging Coverage Comparison

All three types of cameras ultimately scan the image to provide similar electrical signals. The film camera exposes its frame on a stored time command and then advances the film to the next frame which may be exposed a minute later. After one orbit's quantity of pictures has been exposed, the film is processed and run through the slow speed, light beam scanner; the signal is then converted to a digital level signal for instantaneous transmission back. Calibration, time and reference signals are also sent back with each frame.

The three TV cameras obtain the same coverage by taking nine pictures. Each camera shares one optical system by shifting a mirror; the field coverages are changed by moving a prism. On command, the optics expose the photoconductor for electron beam readout. While one of the three cameras is taking and recording its scanned image, the other two cameras are prepared for their next "shot". The scanned signal that contains the picture is preserved on a continuously moving magnetic recorder track. Later, the recorder reruns the tape, and the stored signal is converted to digital form and transmitted.

The optomechanical scanner continuously rotates a wheel of flat mirror surfaces to scan the ground image. The signal from the scanner appears similar to the signal from the TV, except that the recording channel is switched periodically between the three sensors before each scan line. Scan sync and calibration signals are automatically inserted by the scanner so that at the start of each scan, angular position and sensitivity is known accurately.

4.1.3 PERFORMANCE SUMMARY

A summary of the equipment descriptions for each candidate photo-imaging system is shown in Table 4-1. A summary of the key performance data is listed in Table 4-2.

There are two 10-meter photographic film systems to illustrate the tradeoffs in impacts. The first 10-meter system has a fast exposure so that IMC may be easier to implement, but its optics are very heavy. On the other hand, the second 10-meter system is lighter but requires a much lower IMC rate error.

Meeting the very low requirement for intensity resolution has been the most difficult design problem of this study. Because of the expected weight penalties and the data transmission rate limitation, it was elected to design each candidate system for a 2 percent intensity resolution (as listed in Table 4-2) and then to determine what problems each might have in attaining a lower value. For example, due to nonuniformities, film will have intensity distortions that limit the resolvable intensity differences it can sense. Also, particle radiation will tend to fog the film, again reducing the lowest contrast it can sense. Television will also have tube surface nonuniformities. However, it is expected that these can be calibrated and will therefore not limit the resolvable intensity. Television also can be limited by the accuracy of the tape recorder. However, for a low contrast scene, the technique of removing the average background level from the signal reduces this error source to a very small level. The indication at this time is that film will be limited to an intensity resolution of 2 percent, while television can achieve 1 percent or lower. The Optomechanical Scanner is limited by its signal-to-noise ratio to an intensity resolution of 4 percent for the 10-meter design and 1 percent for the 100-meter design. For all the systems, additional work is required to demonstrate feasibility of meeting the 0.5 percent intensity resolution at the specified spatial resolutions.

Each of these candidate photo-imaging systems are described in the following three sections of this report.

Table 4-1. Photo-Imaging Equipment Description

	Silver Halide Film System			TV Systems		Optomechanical Systems	
Optics	100-meter	10-meter(1)	10-meter(1)	100-meter	10-meter	100-meter	10-meter
Focal length	300 mm	3000 mm	3000 mm	363 mm	3630 mm	400 mm	4000 mm
Effective diameter	75 mm	750 mm	375 mm	171 mm	363 mm	400 mm	400 mm
f-number	f/4	f/4	f/8	f/2.12	f/10	f/1	f/10
Exposure time (sec)	0.01-0.1	0.01-0.1	0.04-0.5	0.01	0.22 sec	10^{-5}	$10^{-4}/70$
Sensor							
Number of sensors	1	1	1	3	1	3	3
Sensitive medium	Silver Halide	Silver Halide	Silver Halide	ASOS	ASOS	S-20	S-20
Sensor type	SO-243	SO-243	SO-243	Return Beam Vidicon	Return Beam Vidicon	Photomultiplier	Photomultiplier
IMC							
Angular velocity range	2-3mr/sec	2-3mr/sec	2-3mr/sec	Not needed	2-3mr/sec	Not needed	2-3mr/sec
Angular velocity accuracy	1/4mr/sec	1/40mr/sec	1/200mr/sec		1/80mr/sec		1/1000mr/sec
Control element	Platen	Platen	Platen		Flat or Mirror		Scanner wheel
Data Handling							
Medium	Film	Film	Film	Mag tape	Mag tape	Mag tape	Mag tape
Maximum input rate	---	---	---	60 kHz	60 kHz	60 kHz	6 kHz
Capacity	---	---	---	240 Frames	240 Frames	---	---
Compression ratio	3/2	3/2	3/2	3/2	3/2	3/2	3/2
Weight on PSP-pounds	170	575	220	150	50	100	75
Weight on S/C only pounds	---	---	---	100	50	50	50
Power taking 10 pictures (watt-hours)	20	20	20	20	10	10	10
Volume on PSP	10 ft^3	30 ft^3(1)	15 ft^3(1)	3 ft^3	6 ft^3	10 ft^3	10 ft^3
Volume on S/C only	---	---	---	2 ft^3	2 ft^3	2 ft^3	2 ft^3
Energy per orbit (watt-hours)	570	770(1)	690(1)	120	80	75	85

(1) Assumes a 100-meter system is already included.

Table 4-2. Photo-Imaging Information Description

	Silver Halide Film Systems		TV Systems		Optomechanical Systems	
	100-meter	10-meter	100-meter	10-meter	100-meter	10-meter
Pix cell ground resolution (meters)	100	10	100	10	100	10
Altitude of camera (km)	1000	1000	1000	1000	1000	1000
Ground extent (km x km)	174 x 174	17 x 17	70 x 196	7 x 7	196 km Wide	7 km x 7 km
Full F.O.V. (^{o} x ^{o})	10^o x 10^o	1^o x 1^o	4^o x 11^o	$.4^o$ x $.4^o$	11^o Wide	$.4^o$ x $.4^o$
Image extent (mm x mm)	60 x 60	60 x 60	25 x 25 Each	25 x 25	80 mm Wide	80 mm Wide
Pix cells per field	3.6×10^6	3.6×10^6	$.49 \times 10^6$	$.49 \times 10^6$	2100 x Strip	0.49×10^6
Intensity resolution (%)	2	2	2	2	1 to 5	4 to 20
Quantization levels (bits)	6	6	6	6	6	5
Readout time (sec)	20 min	20 min	7	7	10^{-5} Dwell	$10^{-4}/23$
Erase time	---	---	14	14	---	---
S/N at pix cell frequency 5 (percent constant)	5/1	5/1	5/1	5/1	10/1 to 2/1	2/1 to ---
Readout bandwidth (kcps)	---	---	60	60	60	60
Number of sensors	1	1	3	1	3	3

4.2 THE TELEVISION SYSTEM

4.2.1 DESCRIPTION OF MAJOR ELEMENTS

The Television System consists of Vidicon Sensors, Camera Electronics, Camera Programmers, and a Magnetic Tape Recorder.

Three Vidicons are mounted in a common assembly to view the adjacent areas on the ground, thus providing a nearly 4.0-by-11-degree field of view for the 100-meter medium resolution mapping mission. The second camera subsystem, with a 10-meter resolution capability, is a separate camera with its own optics.

The image motion compensation (IMC) is required for this camera only.

The TV-Camera subsystem for 100-meter and 10-meter resolution basically utilizes an identical TV-sensor for both applications. The only differences are the optics and the number of cameras used. The benefit of this approach is an identical video baseband output signal and therefore mutual compatibility.

The RCA Return Beam Vidicon has been selected for the Television Photo-imaging System because of its good sensitivity, unusually high spatial resolution, long storage capability, high signal-to-noise ratio, large signal output, and rugged construction. This tube has an ASOS (antimony sulphide oxysulphide) surface with characteristics similar to the Vidicon used on Mariner IV.

The camera operation can be described using Figure 4-3. Namely, the subsystem utilizes a functional split of modules, that is, the camera head, camera electronics and camera programmer.

4.2.1.1 Camera Head

The camera head contains the Return Beam Vidicon within the deflection yoke, which in turn is supplied by the focus current and alignment field regulators, as well by the vertical and horizontal sweeps.

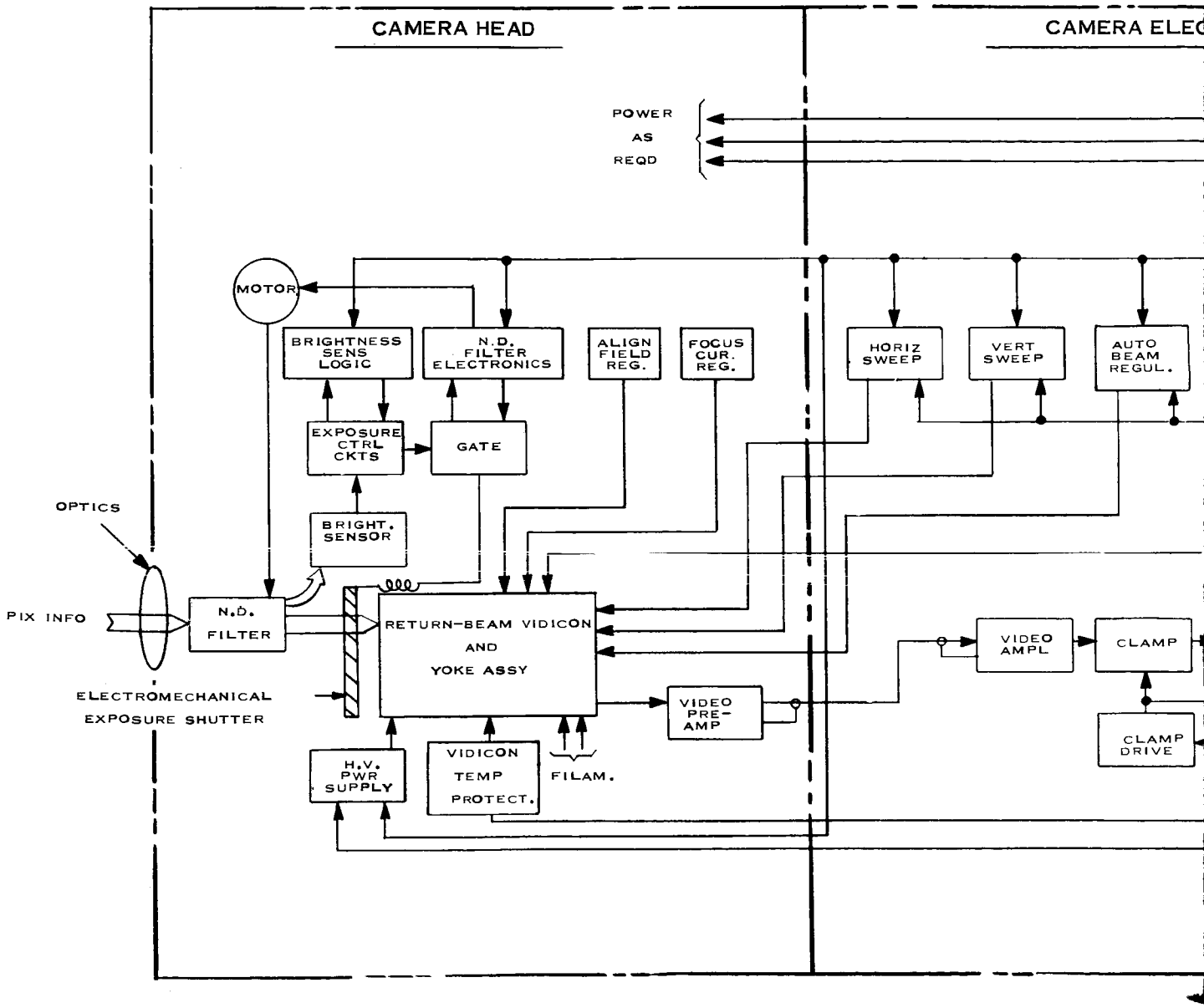

FOLDOUT FRAME

4-10A

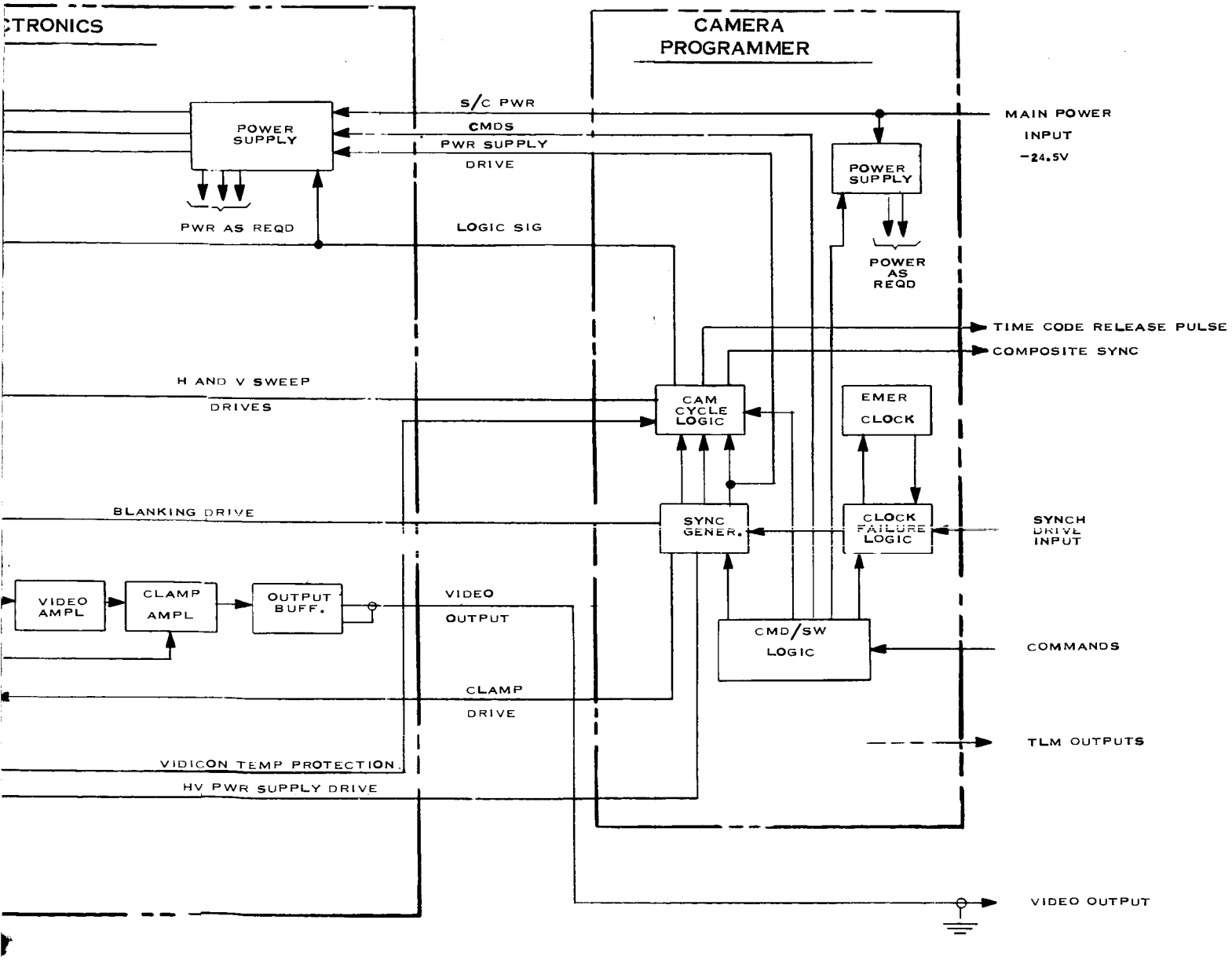

Figure 4-3. Return Beam Vidicon Camera, Elementary Block Diagram

FOLDOUT FRAME

4-10B/4-11/4-12

The pickup tube (the Return Beam Vidicon) supplies the output video signal, from the electron multiplier within itself, to the video preamplifier. The electromechanical exposure shutter, located in the focal plane of the RB-Vidicon, is driven by its own electronics circuitry but in synchronism with the programmer signal information. In addition, the shutter electronics actuates the neutral density filter drive electronics, which also utilizes as part of its logic the signal derived from the brightness sensor. An auxiliary circuitry is that of high-voltage power supply and vidicon temperature protection.

4.2.1.2 Camera Electronics

The Camera Electronics contains the video signal processing circuitry and the drivers for vertical and horizontal sweeps and the automatic Vidicon Beam Regulator. In addition, there is also the synchronously driven multivoltage power supply, with its outputs feeding not only the camera electronics but also the camera head. The camera electronics output signal is a triple base-band video, normally connected to the video recorder.

4.2.1.3 Camera Programmer

The camera programmer carries circuitry necessary for the generation of miscellaneous start-stop and synchronization signals. At its input, there is an emergency clock which is used in case the main spacecraft synchronization drive ceases. Further, the command/switching logic accomplishes the necessary correct camera sequence and switching functions. Being a common part for one or more cameras, it is provided with its own converter-type regulated power supply.

The camera assembly of the 100-meter resolution TV-subsystem (Figure 4-4) consists of three cameras mounted on the common optics housing. The assembly, viewed from the top, resembles a three-armed star (9) containing in each arm a mounted RB-Vidicon (1) and horizontal and vertical deflection yokes and a focusing yoke. At the base of the RB-Vidicon, there is an electronics compartment (8). The incoming rays corresponding to cameras 1, 2, and 3 are marked with (A), (B), and (C), respectively. On the other hand, ray steering is accomplished by an arrangement of diasperometer prisms (5), driven by a backlash-free

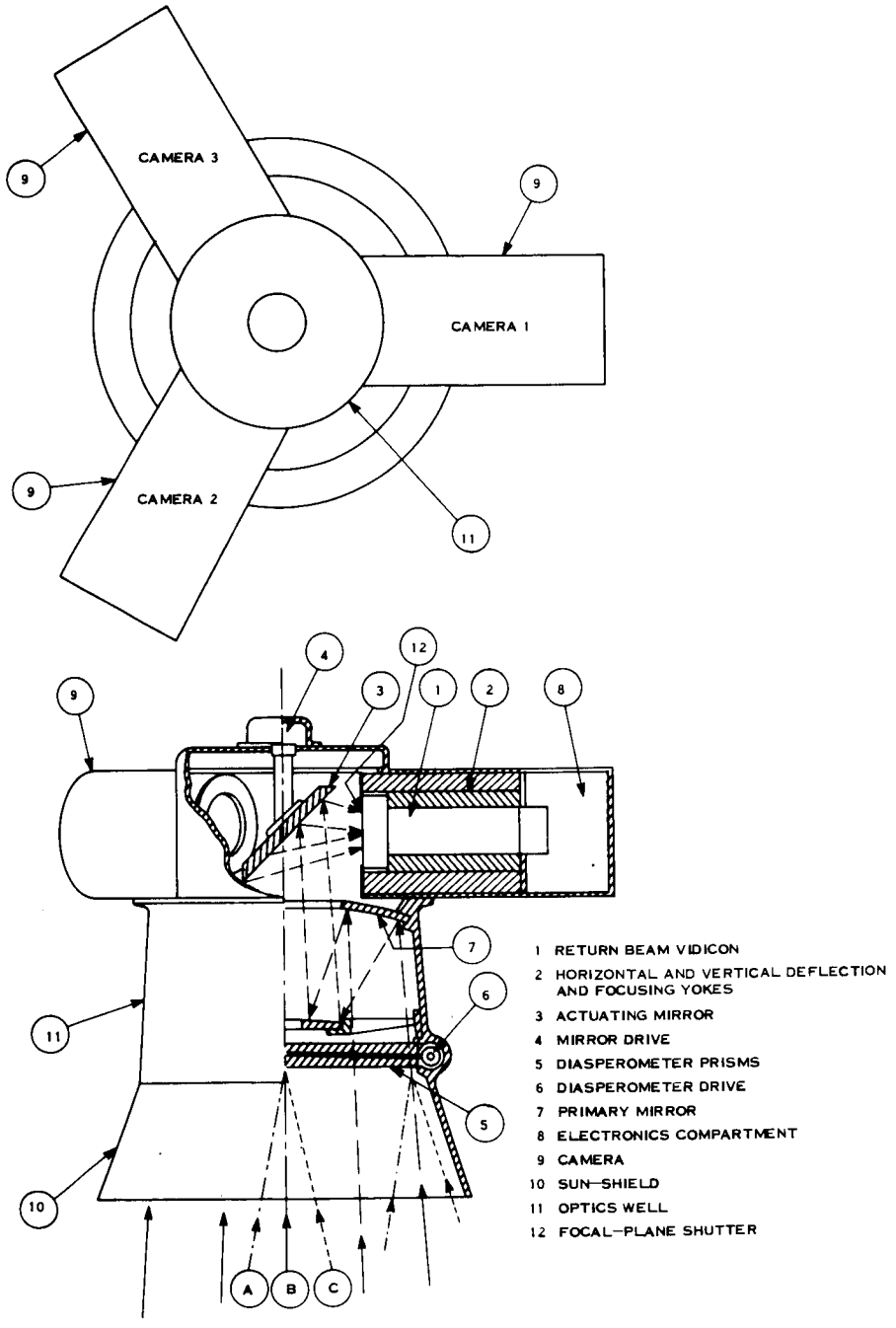

Figure 4-4. Assembly of 100-Meter TV Camera

drive (6), which is synchronized with the mirror drive (4) to actuate a front-side mirror (3), thus assuring proper sequencing of cameras.

The optics well (11) contains also a folded optics (Cassegrain or Bouwers-Maksutov systems) with its primary mirror (7). To avoid unwanted reflections during unfavorable sun illuminations, a sunshield (10) is provided.

The video output signal is switched in synchronism with the mirror (3) rotation and channeled to the tape recorder. The mirror must come to its proper position in a period smaller than 7 seconds to assure a motion-free exposure by a focal-plane shutter (12) arranged in front of each RB-Vidicon focal plane. The resultant picture geometry is shown as Figure 4-5. The system functional diagram is as shown in Figure 4-6. This approach

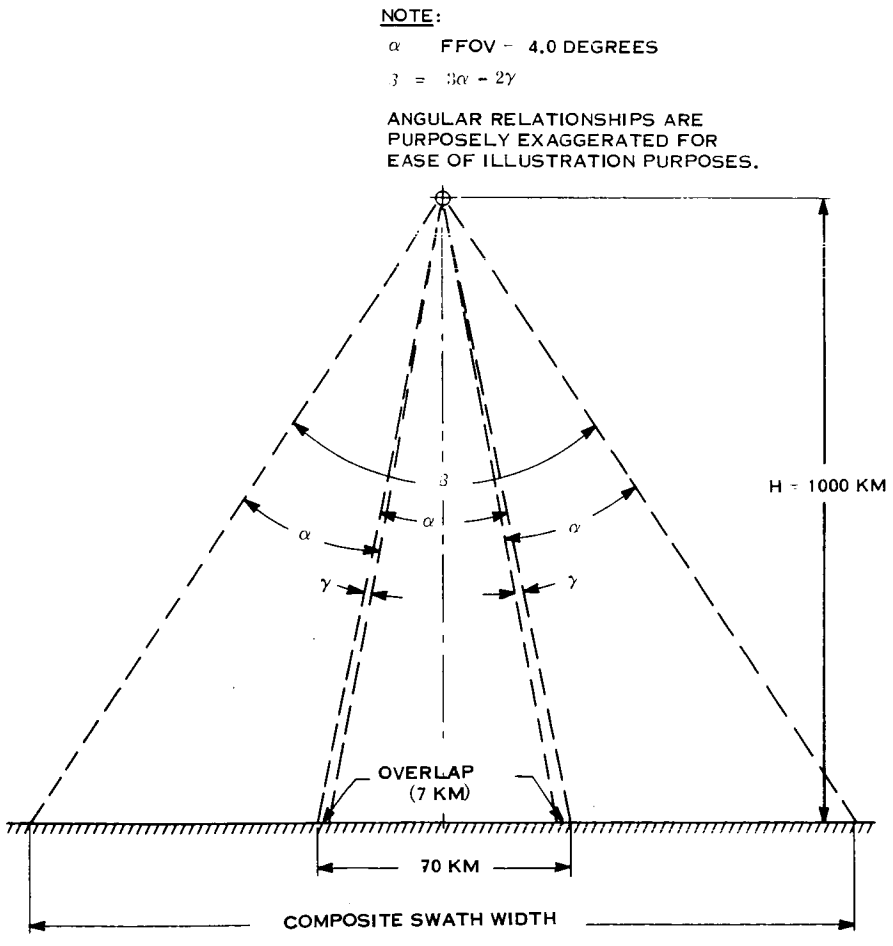

Figure 4-5. Trimetrogon Geometry of 100-Meter TV System

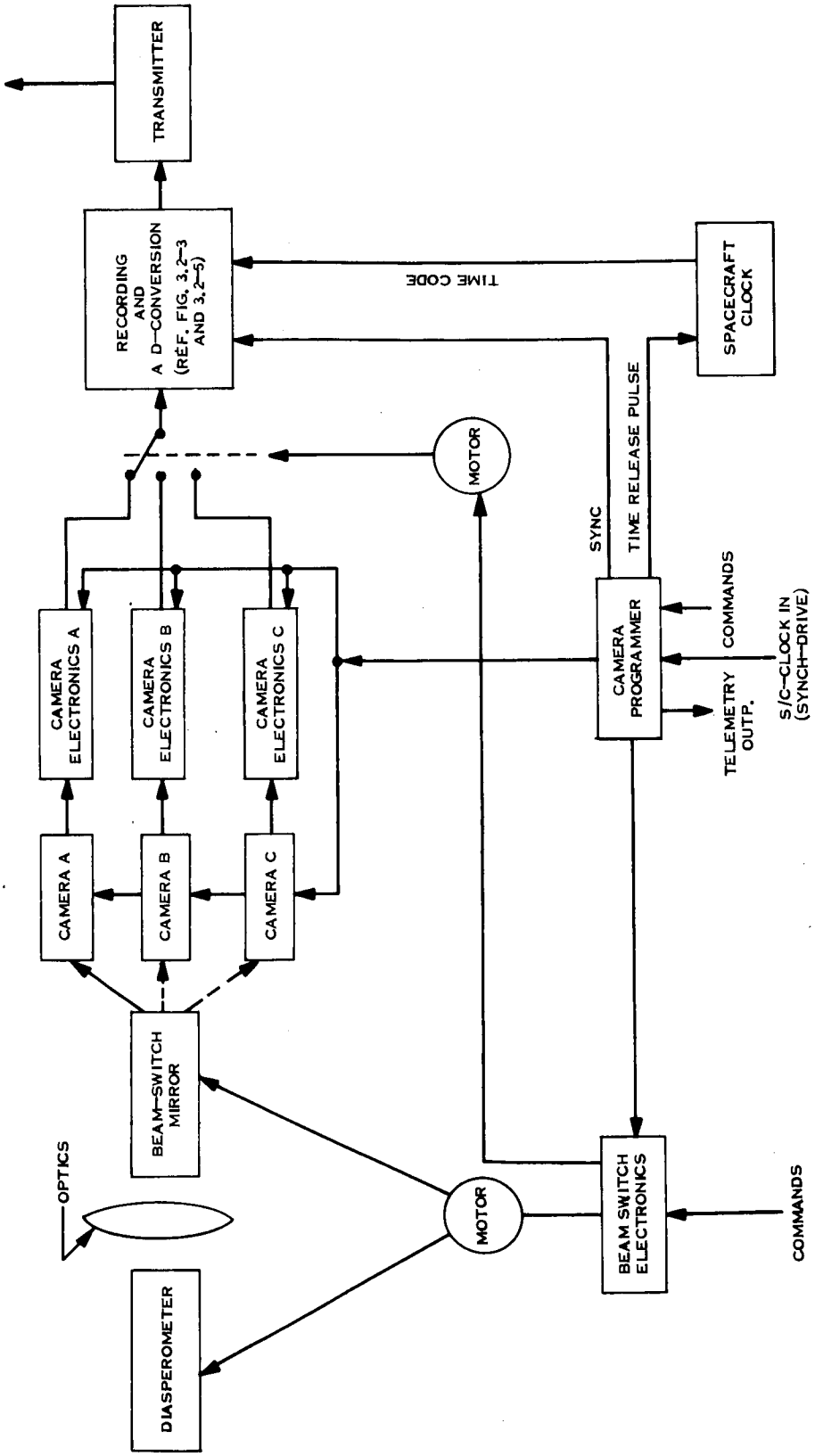

Figure 4-6. 100-Meter Resolution Camera System Functional Block Diagram

has the advantage of being applicable to the color picture-taking scheme as described in Section 4-7. On the other hand, very close similarity of the 100-meter and 10-meter TV-Subsystems permits a failure mode switching as shown in Figure 4-7. This approach will allow crosslinking of identical subcomponents, should a failure occur in one of them.

4.2.2 OPERATION FOR MAPPING AND RECONNAISSANCE

Mapping is accomplished by a sequential imaging of the surface with the three RBV-Cameras, utilizing common optics. The composite viewangle (trimetrogon) becomes 4 by 11.3 degrees and results in a continuous flow of data to the recorder.

The reconnaissance, at 10-meter resolution, is accomplished with a single camera and its own optics.

The requirements for a mapping mission usually specify a continuous coverage of the investigated surface. The covered area in such cases has to be rather large. This usually represents a problem for a coverage with a single camera. The most usual solution is to combine few camera view angles into a composite one with overlaps between cameras and contiguity being assured by an adequate timing interval of the camera shutters. Unfortunately, this approach results in an interrupted data flow, due to usual requirements for erase cycle of the pickup device, the Vidicon.

The pickup device in the case of 100-meter and 10-meter resolution camera, is a Return Beam Vidicon which has erase cycle specified as twice of the read duration. This fact allows a rather convenient arrangement of staggering the exposure and read and erase cycles, resulting in a continuous video signal flow to the recorder. The approach can be readily seen from Figure 4-8.

Assuming a warmed-up camera subsystem, the acquisition cycle is commanded at time T_0, when the camera 1 exposure shutter is triggered and Vidicon exposed, thus recording the detail within the shaded area as picture 1_{n+0}.

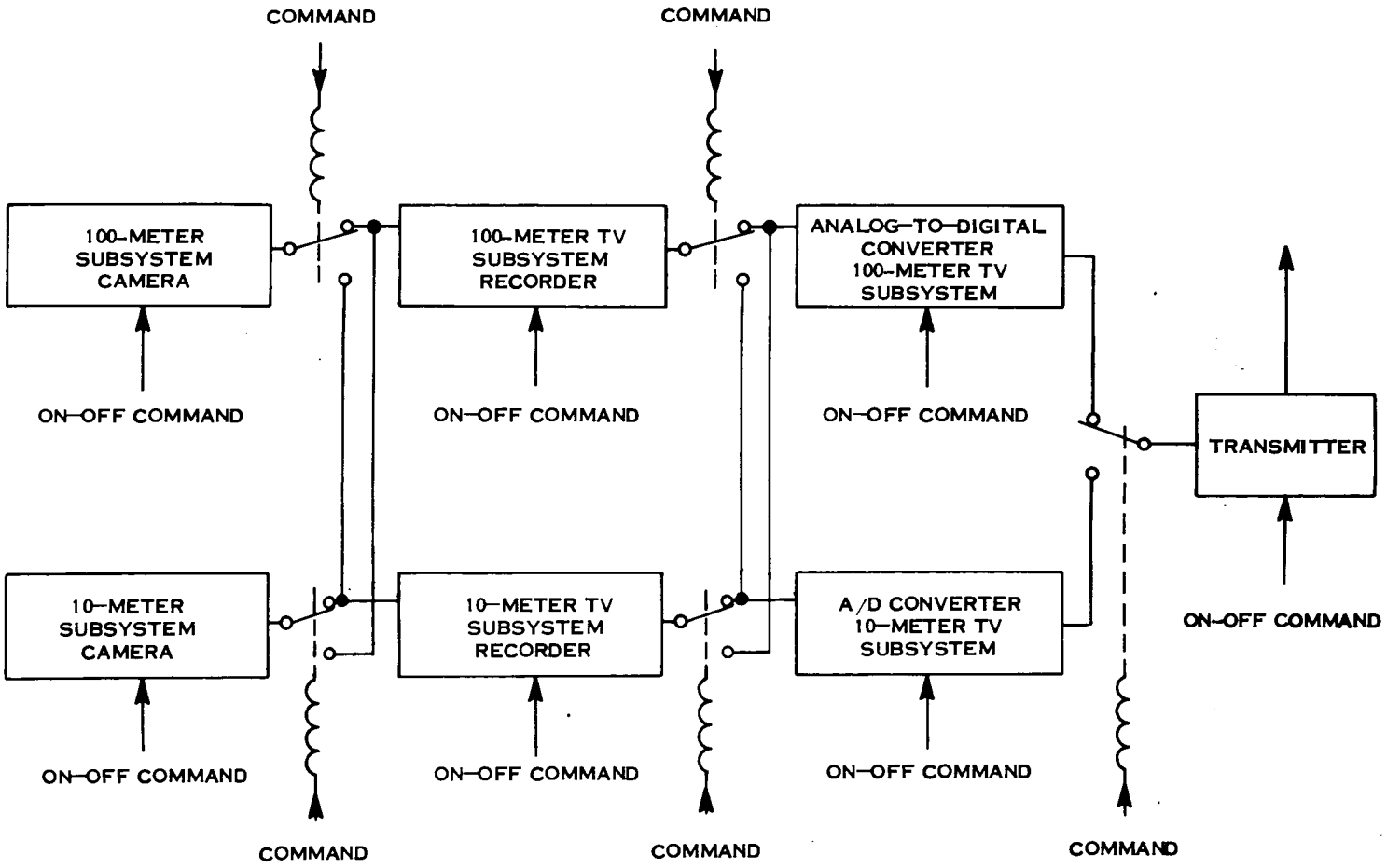

Figure 4-7. TV Systems Failure Mode Switching

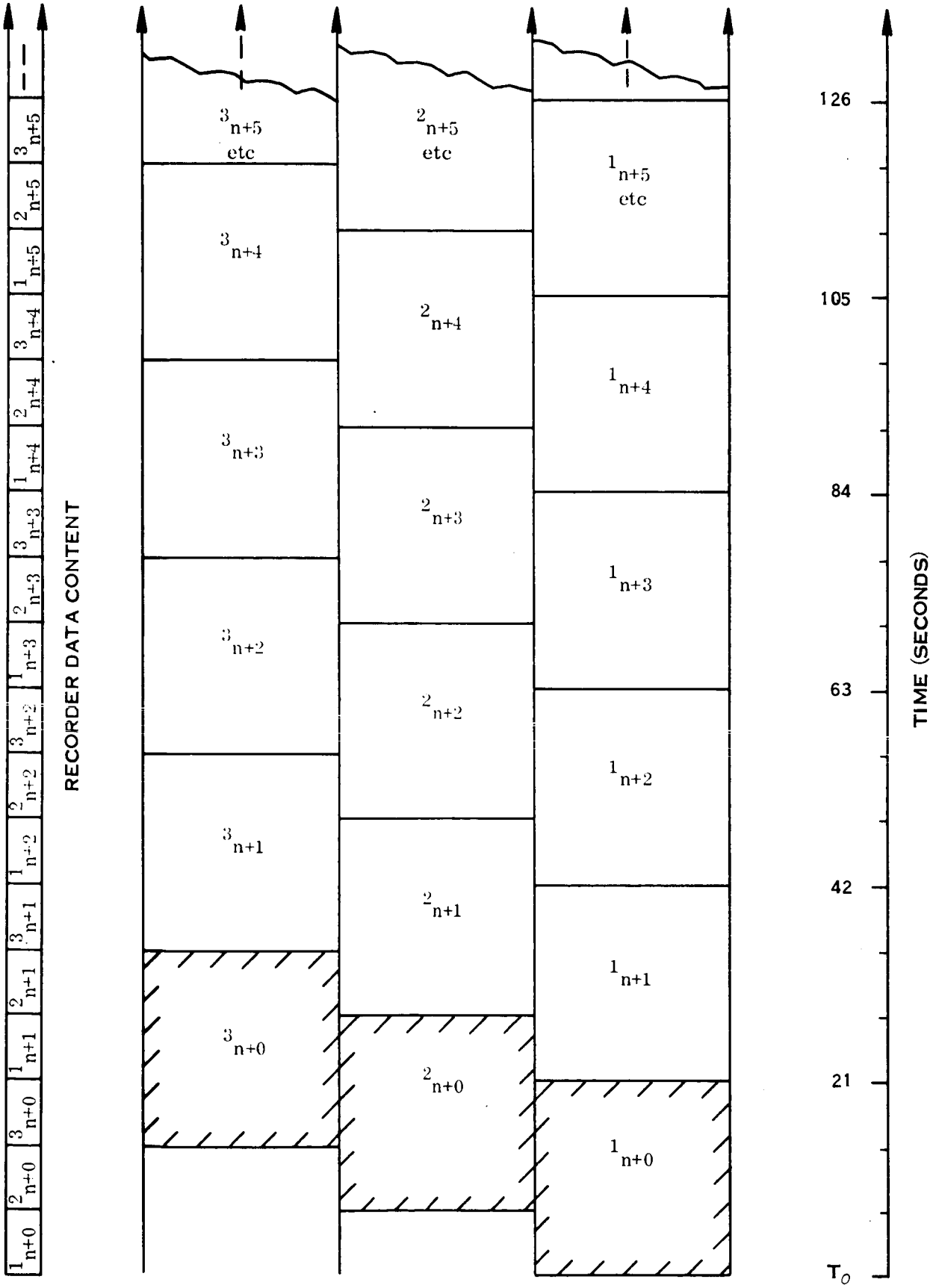

Figure 4-8. Ground Track Frame Layout and Timing

Immediately after exposure, the readout cycle starts and is completed within the nominal 7 seconds. The completion of readout initiates not only the erase cycle of camera 1 Vidicon, but also enables the shutter of camera 2 on time base indicated as T_{0+7} seconds.

Utilizing the same logic and sequencing, one can see the data signal flow is indeed continuous, each recorded picture consuming the nominal 7 seconds and following the sequence camera 1, camera 2, camera 3, camera 1, camera 2, and so on.

The recorded data being continuous is recorded as information 1_{n+0}, 2_{n+0}, 3_{n+0}, 1_{n+1}, 2_{n+1}, 3_{n+1}, 1_{n+2}, 2_{n+2} and so on. Diagrammatically it appears on the left hand side of Figure 4-8 as "Recorder Data Content."

The reconnaissance, 10-meter resolution camera does not utilize this approach since continuous mapping is not required. When commanded "ON", the video signal flow will last for 7 seconds and if not recommanded, will cease. Operation of the recorder, therefore, will be step-wise.

4.2.3 DATA HANDLING AND STORAGE

The block diagram of the data handling and storage scheme is shown in Figure 4-9. The data handling and storage equipment will receive a number of signals from the imaging device, including the video signal, synchronization signal, and various control and status signals. The video signals can be represented as being comprised of two components: the background level and the contrast signal. It is expected that the background level will occupy in excess of 75 percent of total output voltage. The background level is essentially a dc component, and, therefore, it is not desirable to transmit this information as often as the contrast signal. Also considering the errors introduced by the data processing and data storage elements, it is desirable to remove the dc component so that the contrast signal can occupy the complete dynamic range of the data processing and data storage elements. In this way, the errors that occur will be with respect to just the contrast signal instead of the background level and contrast signal. A number of schemes are possible for determining and removing the background level. The most obvious scheme is to average the signal over

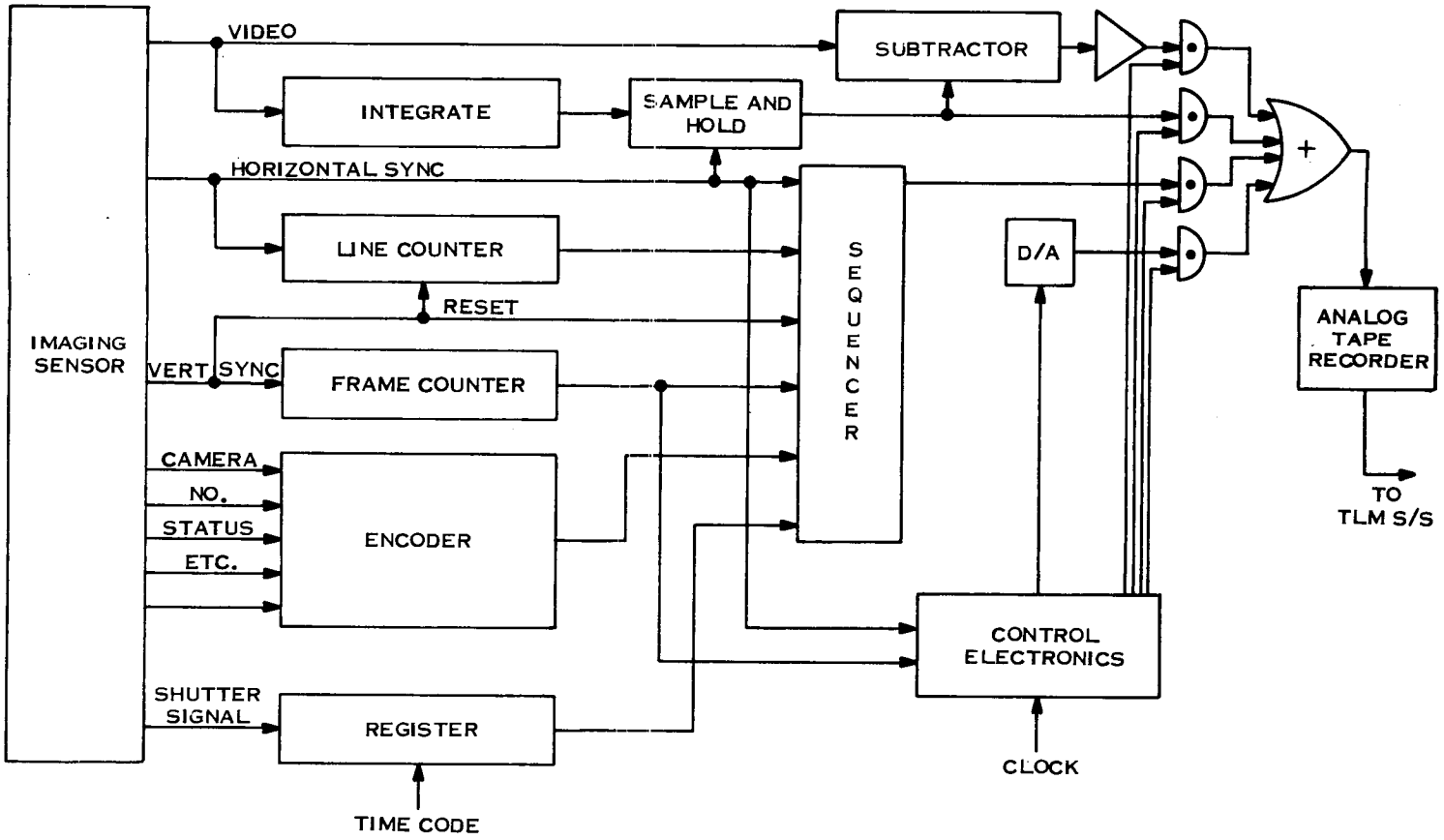

Figure 4-9. Data Handling and Storage

a line and use the average value found to remove the background level for the next line. This scheme is shown in Figure 4-9. The background level can be inserted in the data stream during retrace time.

In order to further reduce the error caused by the data storage elements, it is desirable to include a calibration signal in the video signal. One way of accomplishing this is to introduce a staircase signal during the vertical sync time. The signal will be generated by using a four-bit digital-to-analog converter to define 16 video levels which will be used by the ground equipment to correct for any nonlinearities introduced by the data storage equipment.

The various control and status signals from the sensor will be used to generate an identification number for each frame as follows:

a. The shutter trip signal will be used to strobe the spacecraft time into a register to indicate when the picture was taken.

b. The vertical sync signal will be used to generate a frame number.

c. The horizontal sync signal will be used to generate a line number. This number will be reset to zero at the beginning of each frame by the vertical sync signal.

d. The discrete signals indicating which camera is being used, the filter used, etc., will be encoded to provide a digital number.

The data thus generated will be combined with the video background level and added to the video signal during the horizontal retrace time between scan lines.

The composite signal representing one complete picture is generated in 7 seconds and can be divided into approximately 7-millisecond segments, each of which represents one line of data. During the first three lines, which represent the vertical sync time, the calibrate signal will be recorded. During each line of the remainder of the picture, the following

will be recorded: approximately 7 milliseconds of video and 700 microseconds of identification data including:

PN code	31 bits
Camera No.	2 bits
Frame count	7 bits
Time code	26 bits
Line No.	11 bits
Status	4 bits
Background level	Analog

The signals from each of the three cameras will be processed sequentially so that the tape recorder will record Camera 1 signal for 7 seconds, Camera 2 for 7 seconds, Camera 3 for 7 seconds, Camera 1 for 7 seconds, etc. In this way, the recorder will be able to run continuously during the entire picture-taking sequence.

The video analog signal from the camera can be stored directly or converted to a digital signal and then recorded. A discussion of the analog-versus-digital tape recorders is given in Appendix C.

The analog tape recorder was selected, and its characteristics are presented in Table 4-3. The specifications in this table are based on a similar recorder, RCA Model QRA-2, which was successfully flown on Nimbus.

Assuming a 30-kilobit per second transmission rate (see Appendix C) as a minimum and a compression ratio of 1.5, two samples per cycle, and six bits per sample, the maximum input frequency to the analog-to-digital converter from the analog tape recorder is 3.75 kHz. This results in a recorder output speed of 30 ips x 3.75 kHz/60 kHz = 1.875 ips. Additional playback speeds at 0.937 and 0.468 ips are provided to match the transmission capability as the range increases.

Table 4-3. Analog Tape Recorder Characteristics

Characteristic	Specification
Data bandwidth	DC to 60 kilohertz
Modulation	FM
Signal-to-noise ratio	35 decibels
Number of tracks	4
Tape length	1200 feet
Speeds	
Record	30 inches per second (ips)
Playback	1.875/0.937/0.468 inches per second
Dimensions	14-inch diameter by 7.5-inch height
Weight	16 pounds
Power	20 watts

The total data collection time as constrained by the transmission capability is

$$Tc = \frac{R_D \cdot C \cdot T_O}{KB_i + R_D \cdot C} = 29 \text{ minutes}$$

where:

R_D = transmission rate

Cq = compression rate

K = conversion from bits/sec to hertz = 12

T_O = orbit period

B_i = input bandwidth

The required effective tape length is then 30 ips x 29 min = 4350 ft. Forty-eight hundred feet is provided to allow for acceleration and deceleration during track switching.

4.2.4 MAJOR PERFORMANCE CAPABILITIES AND LIMITATIONS

The TV Systems utilize a Return Beam Vidicon as a sensor element. Like all Vidicons, its sensitivity is mainly in the visible range of the electromagnetic spectrum. Due to haze present in the Mars atmosphere and its detrimental effects on contrast which already is low,

a haze cutoff filter must be utilized, thus determining the spectral response from 0.47 to 0.86 microns.

At contrast levels of about 5 percent, intensity resolution is in the order of 100 grey levels over a dynamic range of 0.8×10^{-3} foot-candle-seconds.

The spatial resolution under the same conditions is in the order of 16 line pairs per millimeter.

4.2.4.1 Spectral Characteristics

The radiant-compensated spectrum of Mars in terms of albedo is given in Figure 4-10. From this figure, it is obvious the most preferable part of the spectrum to be sensed is from 0.6 to about 1.2 microns. Unfortunately, the sensors in this range are not readily available if a high resolution is also required. Therefore, the selection must be along a compromise between a high resolution and spectral sensitivity. Such a compromise selection is the Return Beam Vidicon tube.

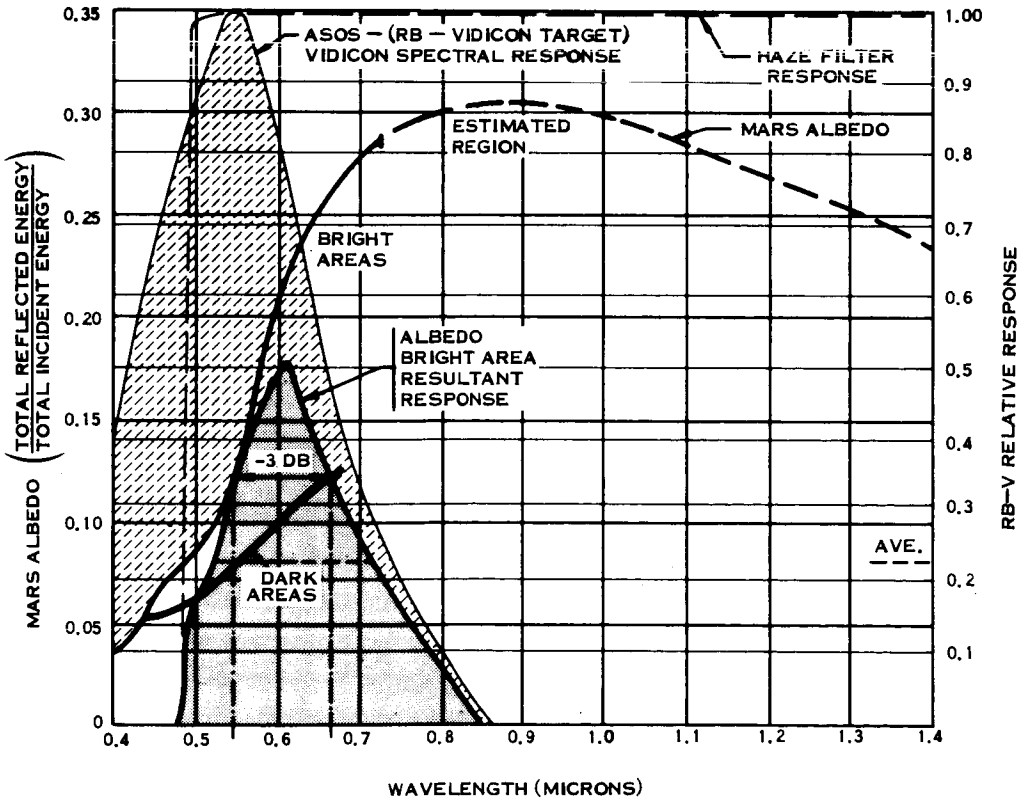

Figure 4-10. Spectral Characteristics

Evaluation of the combined characteristics corrected for the required haze filter produces passband limits from 0.47 to 0.87 microns.

Recalculations, considering the influence of sun and latitude of areas of interest on Mars, determine the maximum and minimum camera lens illuminance as 545 and 21.2 foot-lamberts, respectively, which also defines the selection of the lens system, exposure, and general camera design.

4.2.4.2 Effect of Contrast on Resolution

The considerations of this subject are mainly concentrated around a fact common to all pickup devices, namely, the degradation of resolution with dropping contrast value.

Normally, pickup devices are intended for operation at high contrast levels and therefore all performance specifications are given for the 100 percent contrast. By utilizing crossplotting techniques and modulation transfer functions to determine resolution for a range of contrast values, the contrast performance characteristics shown in Figure 4-11 are obtained. The effects of noise are assumed as nonlimiting, so that for a maximum recognition capability of brightness changes (i.e., "gray scales"), the inherent noise signal must be minimized or a distinct "gray" transition cannot be assured without inducing ambiguity. The curves show a drastic loss of resolution capability under very low contrast conditions. A resolution of about 700 TV-lines is possible at a contrast of 5 percent and face plate illumination of 1×10^{-2} foot-candle-seconds. This value limits the frame width to 70 km per camera for the 25 mm image size of the RB-Vidicon.

4.2.5 INTERFACE REQUIREMENTS

The interface requirements of the TV System must be carefully considered in order to assess the impact on the spacecraft. These requirements are presented in Figures 4-12 through 4-15, and Tables 4-4 and 4-5.

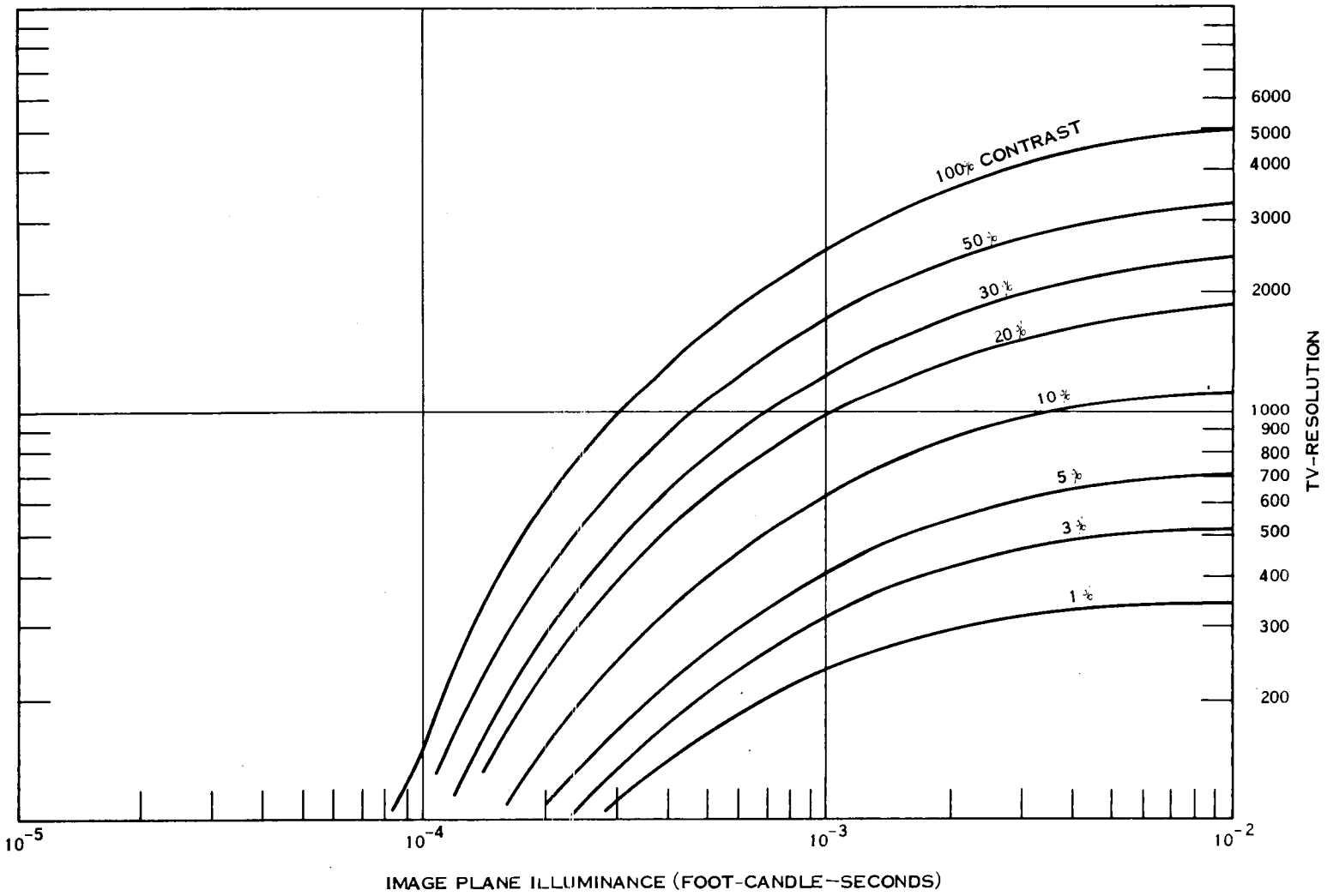

Figure 4-11. Return Beam Vidicon Contrast Characteristics (Computed)

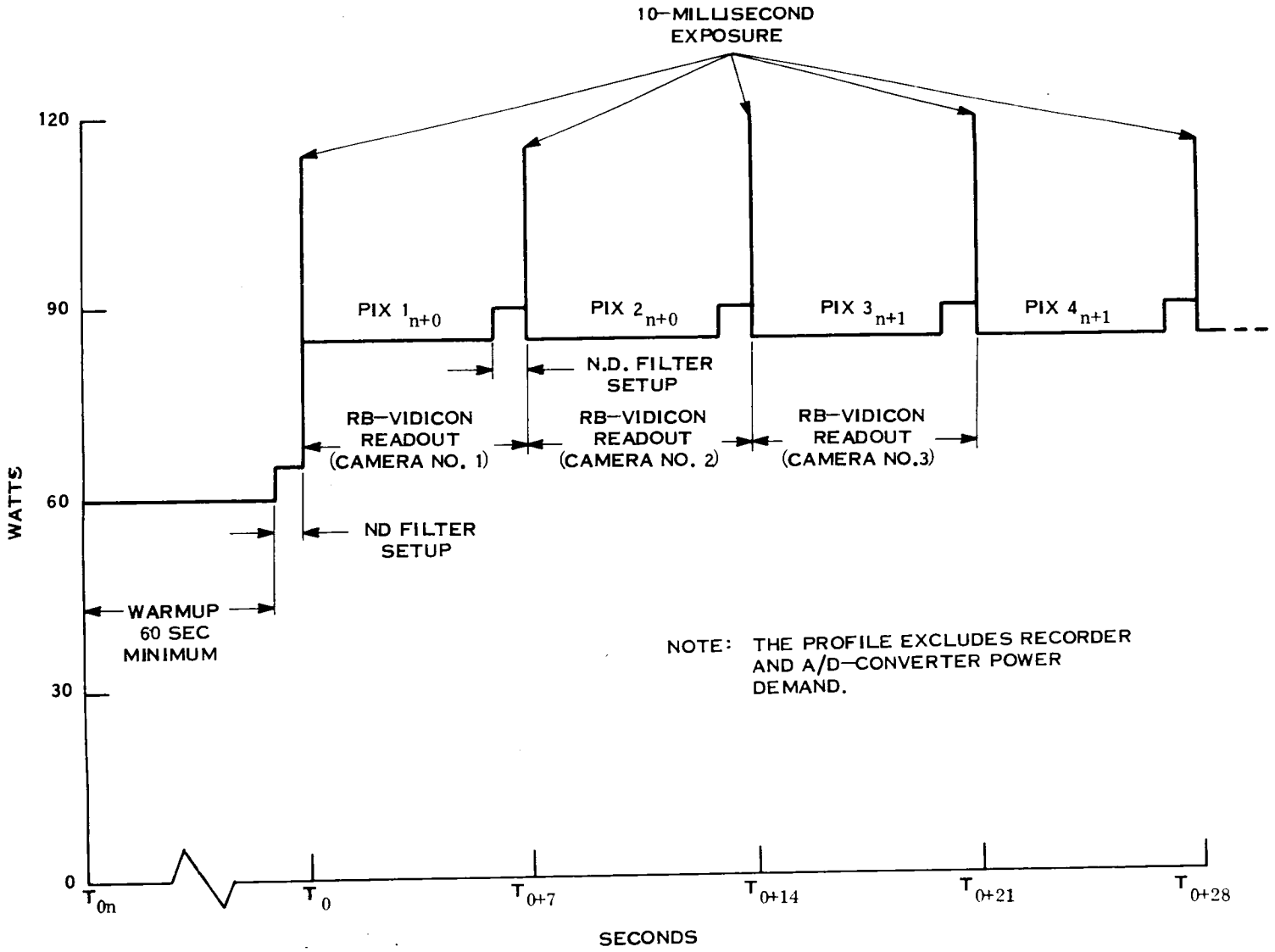

Figure 4-12. Composite Power Demand Profile for 100-Meter TV Camera

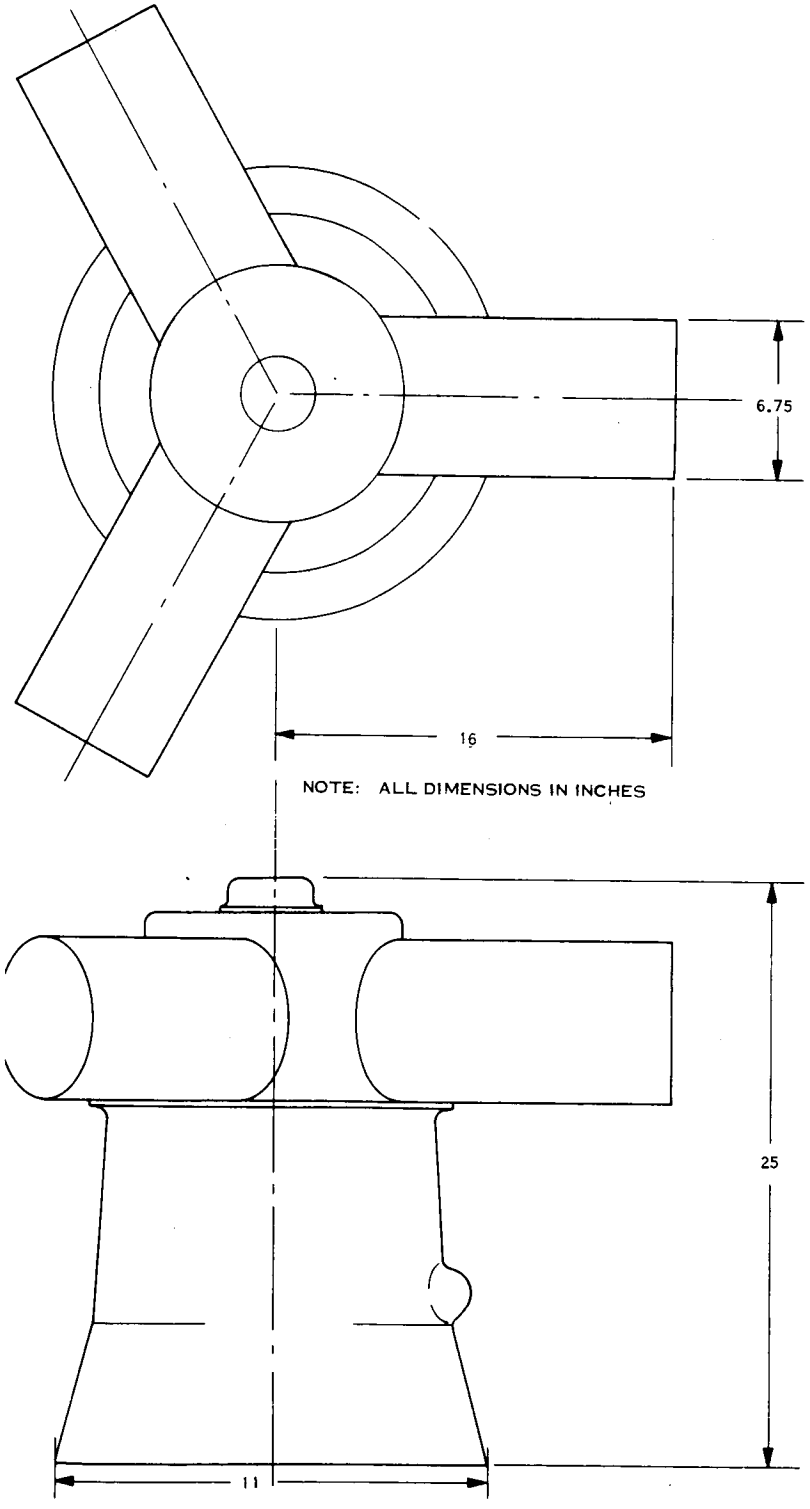

Figure 4-13. 100-Meter TV Camera Dimensional Outline

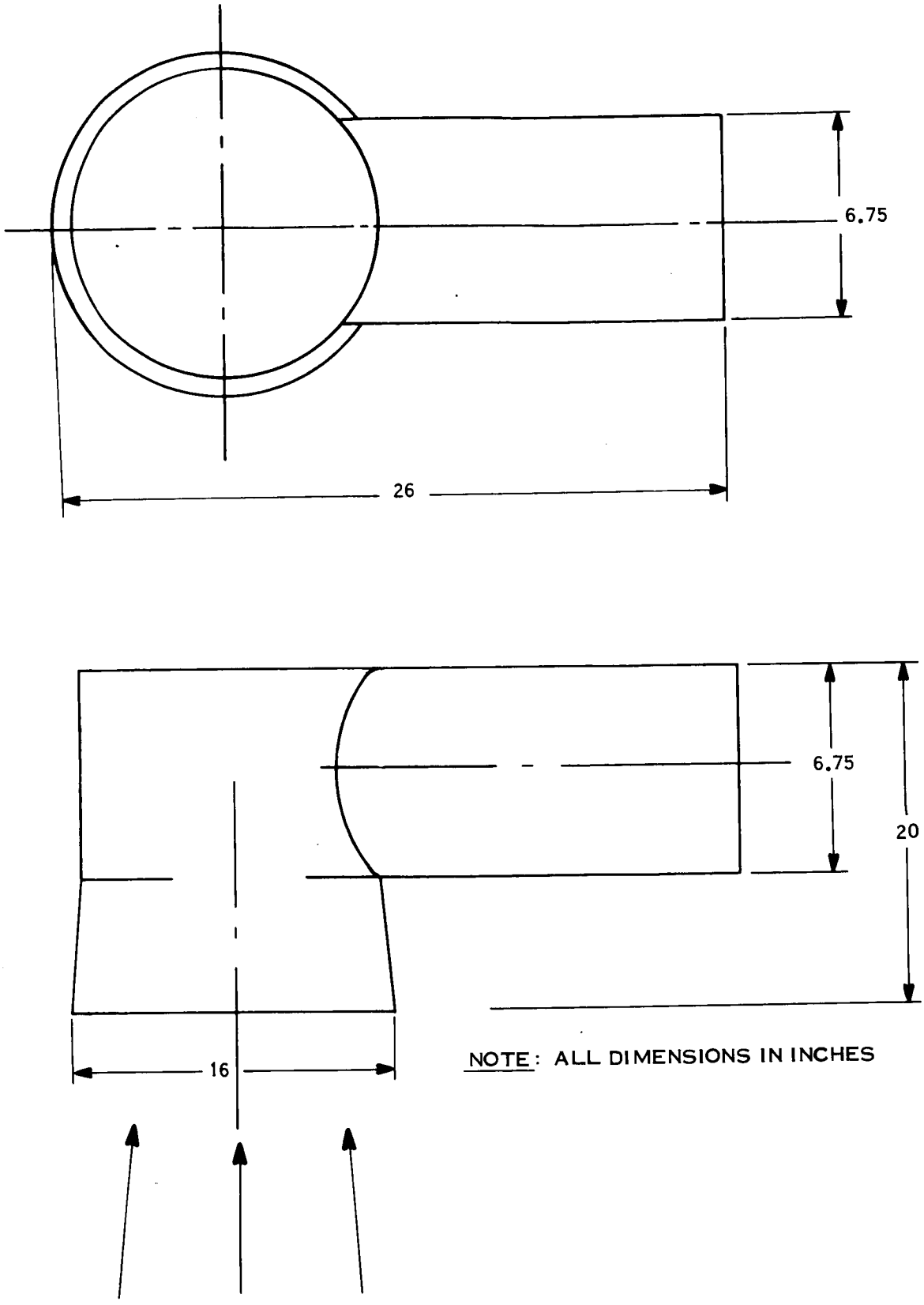

Figure 4-14. 10-Meter TV Camera Dimensional Outline

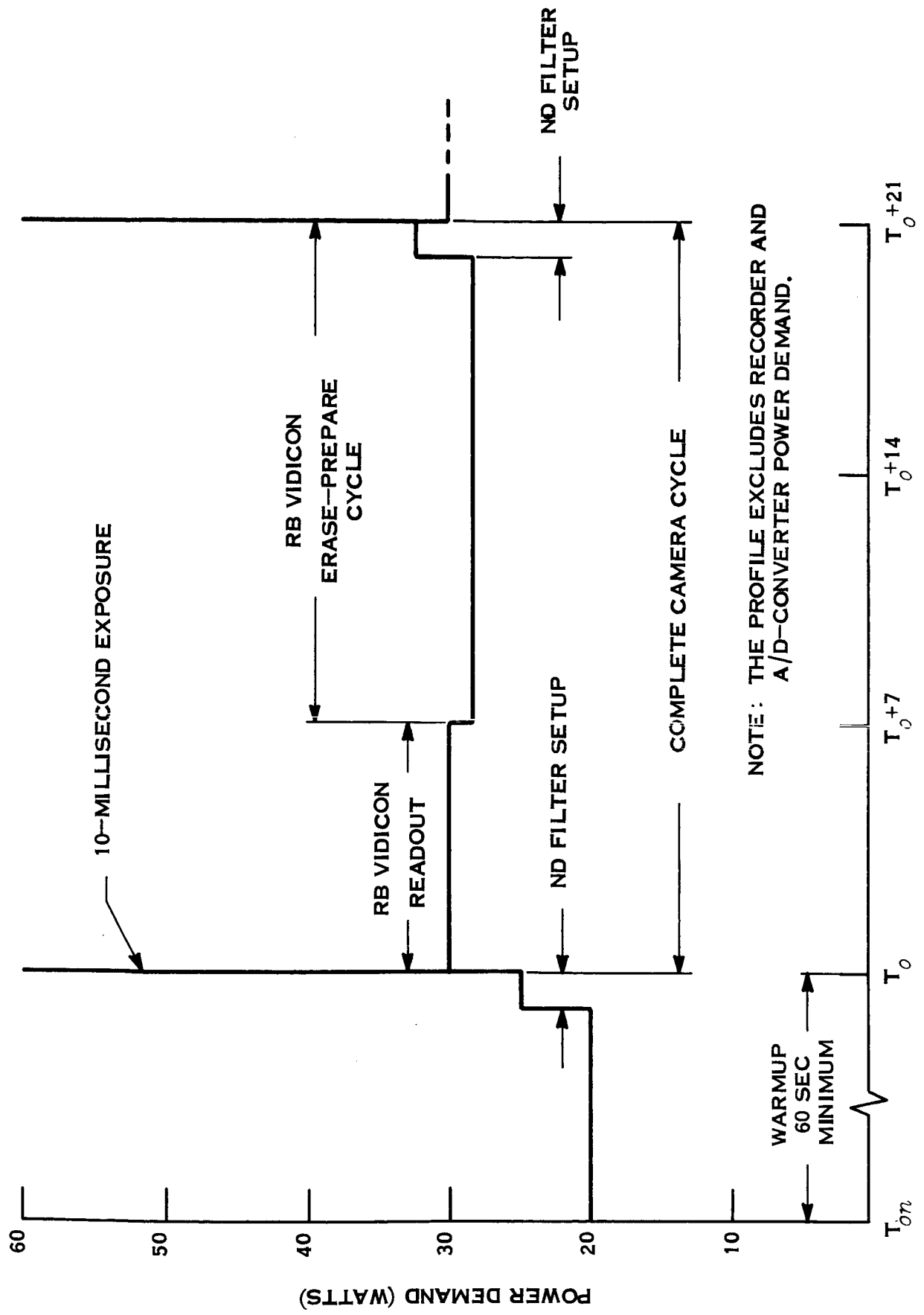

Figure 4-15. 10-Meter TV Camera Power Demand Profile

Table 4-4. Interface Details Estimate, 100-Meter Resolution TV-Camera

Component	No. of Units	Size (in.)	Weight (lb)	Power (watts)	Signal Inputs	Signal Outputs	Remarks
3-Camera Head	1	Figure 4-12	150 max.	Figure 4-11	Drive waveforms Power (dc) Commands	Video signal Telemetry Temperature protection	1. Power for total System less Recorder and A/D Converter. 2. Includes optics 3. Refer to Figures 4-4, 4-12, and 4-3.
Electronics	3	12 x 6 x 6	13	Figure 4-11	S/C power (dc) Drive logic Drive waveforms Commands	Video signal Telemetry	1. Refer to Figures 4-3 and 4-6.
Programmer	1	12 x 6 x 6	13	Figure 4-11	S/C power (dc) Sync-drive Commands Telemetry	Drive waveforms Commands S/C Power (dc telemetry) Special signals	1. Refer to Figures 4-3 and 4-6.
Recorder	1	14 Dia x 7.5H	16	20	Video signal S/C power Drive signal Commands	Video FM-analog Telemetry	1. Refer to Figure 4-6.
A/D-Converter	1	2 x 6 x 1	2	1	Video FM-analog S/C power (Commands)	Digital signal Telemetry	1. Refer to Figures 4-6 and 4-8.

Table 4-5. Interface Details Estimate,10-Meter Resolution Camera

Component	No. of Units	Size (in.)	Weight (lb)	Power (watts)	Signal Inputs	Signal Outputs	Remarks
Camera Head	1	Figure 4-13	50		Drive waveforms Power (dc) Commands	Video signal Telemetry Temperature protection	1. Subsystem Power less Recorder and A/D Converter. 2. Includes optics. 3. Refer to Figure 4-3.
Electronics	1	12 x 6 x 6	13	Figure 4.2-13	S/C power (dc) Sync drive Commands Telemetry	Video signal Telemetry	Refer to Figure 4-3.
Programmer	1	12 x 6 x 6	13		S/C power (dc) Sync drive Commands Telemetry	Drive waveforms Commands S/C power (dc) Telemetry Special signals	Refer to Figure 4-3.
Recorder	1	14 Dia x 7.5H	16	20	Video signal S/C power drive signal Commands	Video FM-analog Telemetry	Refer to Figure 4-7.
A/D-Converter	1	2 x 6 x 1	2	1	Video FM-analog S/C power (Commands)	Digital signal Telemetry	Refer to Figure 4-7.

4.2.6 IMPACT OF COLOR ON TELEVISION SYSTEM DESIGN

Color imaging is feasible, but only by sacrificing the swath width and low-light-level performance.

In order to be able to transmit a color information to a distant point, utilizing television cameras, a modification of the TV System is necessary. Namely, based on the fundamental principles of optics, one must transmit correct amounts of analog information corresponding to the red, blue, and green components.

According to these principles and standardized by the "Commission Internationale de l'Eclairage," any single wavelength color (C_λ) can be described by the following expression:

$$C_\lambda = \bar{x}\,X + \bar{y}\,Y + \bar{z}\,Z$$

where:

$\bar{x}$, $\bar{y}$, $\bar{z}$ = intensities of primary colors

X, Y, Z = primary colors by the CIE definition.

The proper intensities and matching of the RB-Vidicon (or similar sensor) are accomplished by means of suitable filters, transmission characteristics of which are computed from equation:

$$T_\lambda = \frac{R_\lambda}{S_\lambda}$$

where:

T_λ = required filter response (Figure 4-16)

R_λ = required response according to CIR standard (Figure 4-17)

S_λ = RB-Vidicon response (from Figure 4-10)

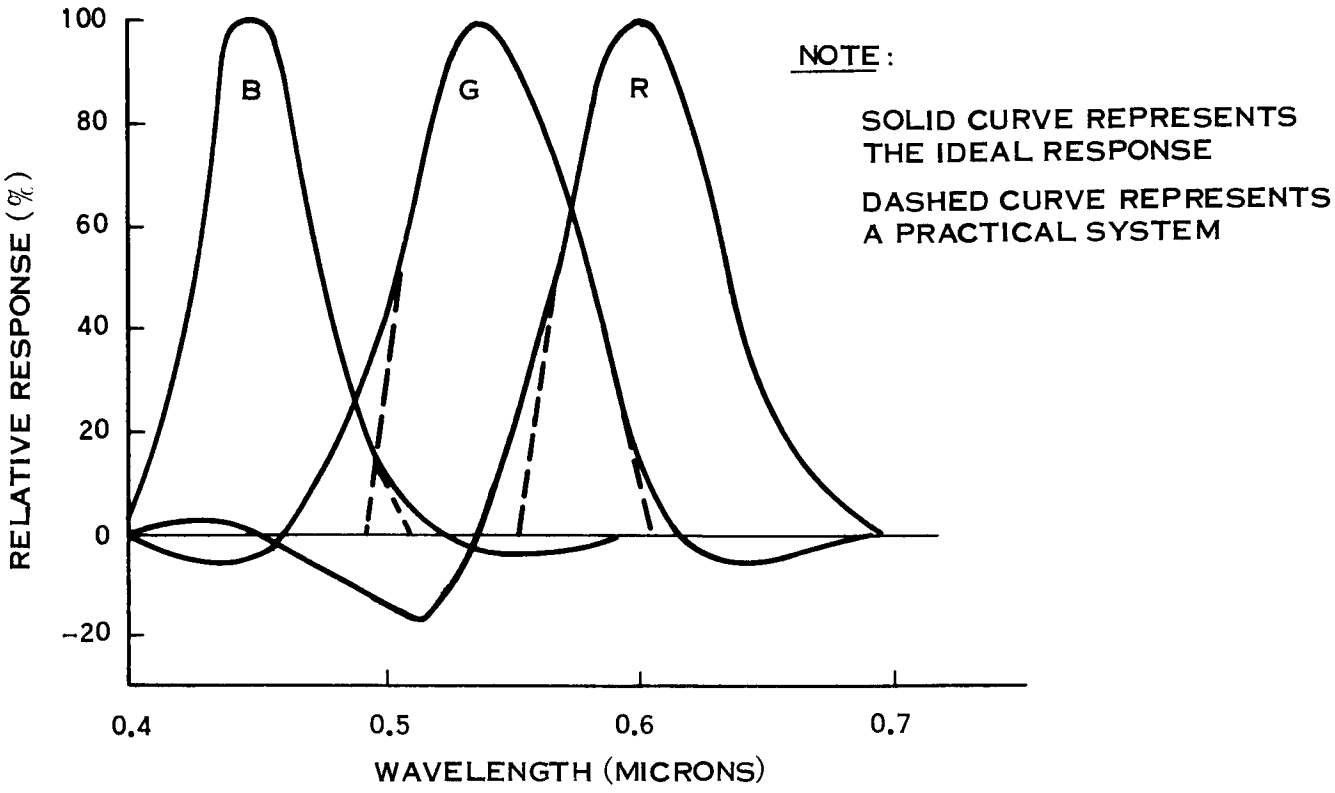

Figure 4-16. Required R-, G-, and B-Filter Responses

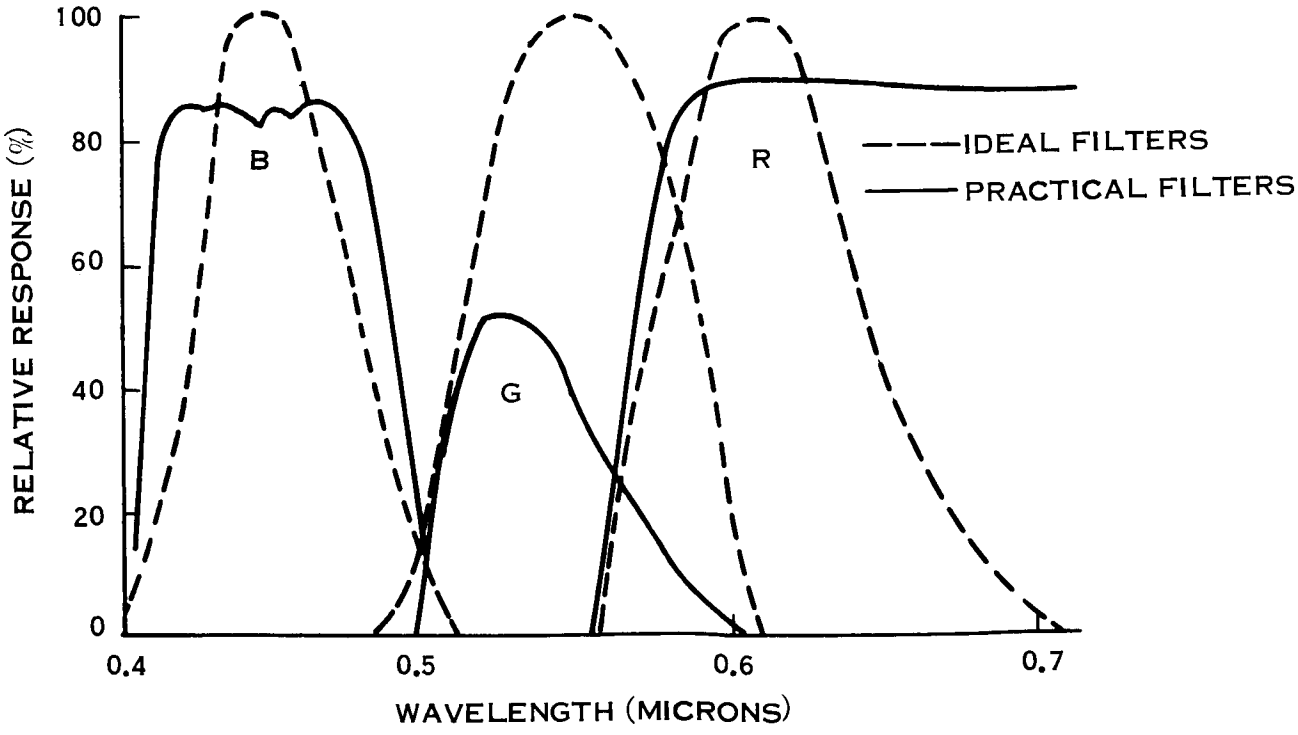

Figure 4-17. Transmission Characteristics of Camera Filters

Physically, the R, G, and B filters can be arranged in the optical path of each of the three cameras in the 100-meter TV Subsystem. The color superposition may be accomplished by commanding the diasperometer to "left," "center," or "right" position but retaining the previously described camera cycle. The result will be a color picture sequence as shown diagrammatically by Figure 4-18. The penalty paid for this approach will be a 4-degree square field of view only, but commandable to the "left," "center," or "right" position if desired.

Another limitation is low-light-level imaging capability, which is shifted upwards due to smaller amount of energy available for each of the TV cameras.

The recording and digitizing techniques do not change, nor does the video baseband, and therefore resolution is not affected.

Changes of the overall power consumption and weight of the subsystem are within the estimating tolerances and therefore can be safely disregarded.

The color adaptation of the 10-meter TV-camera subsystem is not readily accomplished, unless the data readout timing is considerably changed.

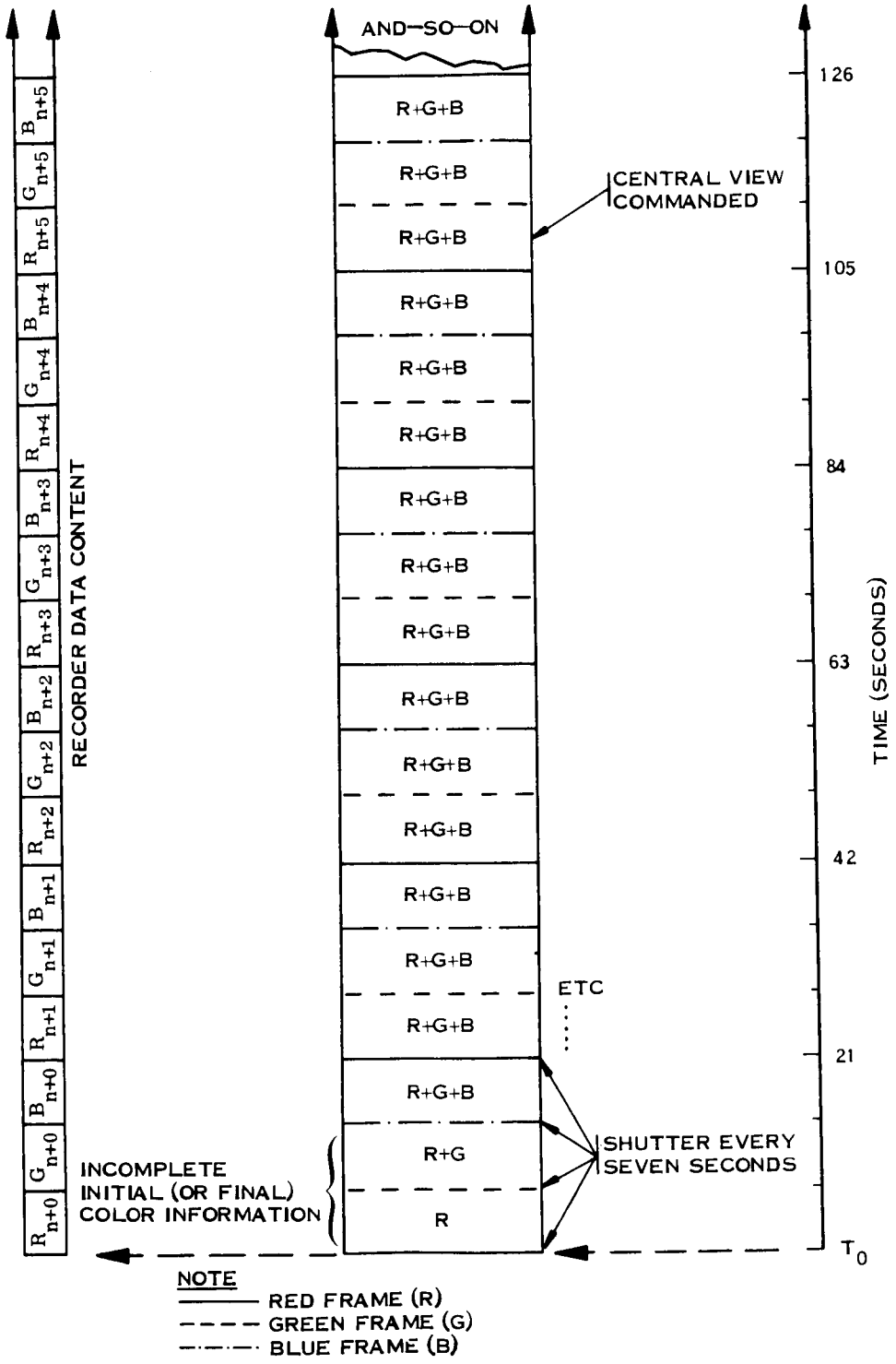

Figure 4-18. Color Adaptation of 100-Meter Camera Subsystem, Ground Track Layout

4.3 PHOTOGRAPHIC FILM SYSTEM

4.3.1 DESCRIPTION OF MAJOR ELEMENTS

The Photographic Film System consists of cameras, high-definition silver halide film, a film processor, and a readout scanner.

A schematic of the Film System is shown in Figure 4-19. It is a dual lens system, modeled after the Lunar Orbiter camera. The wide-angle lens is 3 inches in diameter with a 12-inch focal length; it is used for the 100-meter mapping mission. The map is formed from the sequential pictures taken with this lens. After exposure, the film is developed in the film processor, passes through the readout film scanner, and is stored on the take-up reel. Readout of the data can occur during this first run through of the film scanner and also after all the film is exposed and rerun through the scanner.

Reconnaissance photographs are taken with the narrow angle lens. This is a long-focal-length, 15-inch-diameter lens. The exposure is quite long, requiring precise image motion compensation and attitude stabilization.

4.3.1.1 Camera

The camera equipment includes supply and take-up reels, supply and camera loopers, two platens, and the film transport. The camera is of the frame type. This was chosen over the slit camera because it permits better mapping and photometric fidelity.

One platen is for the internally mounted 12-inch-focal-length lens; the other is for the 120-inch-focal-length lens, which is external to the pressure vessel. The film is held flat against the platen by means of an air pressure differential and is mechanically clamped. The clamp is desirable to maintain relative position when the platen is moved to compensate for image motion. The platen associated with the 12-inch lens moves at a rate of 0.036 inch per second for the time that the shutter is opened. This lens will use a between-the-lens shutter, and, therefore, the shutter opening time is the same as the exposure time.

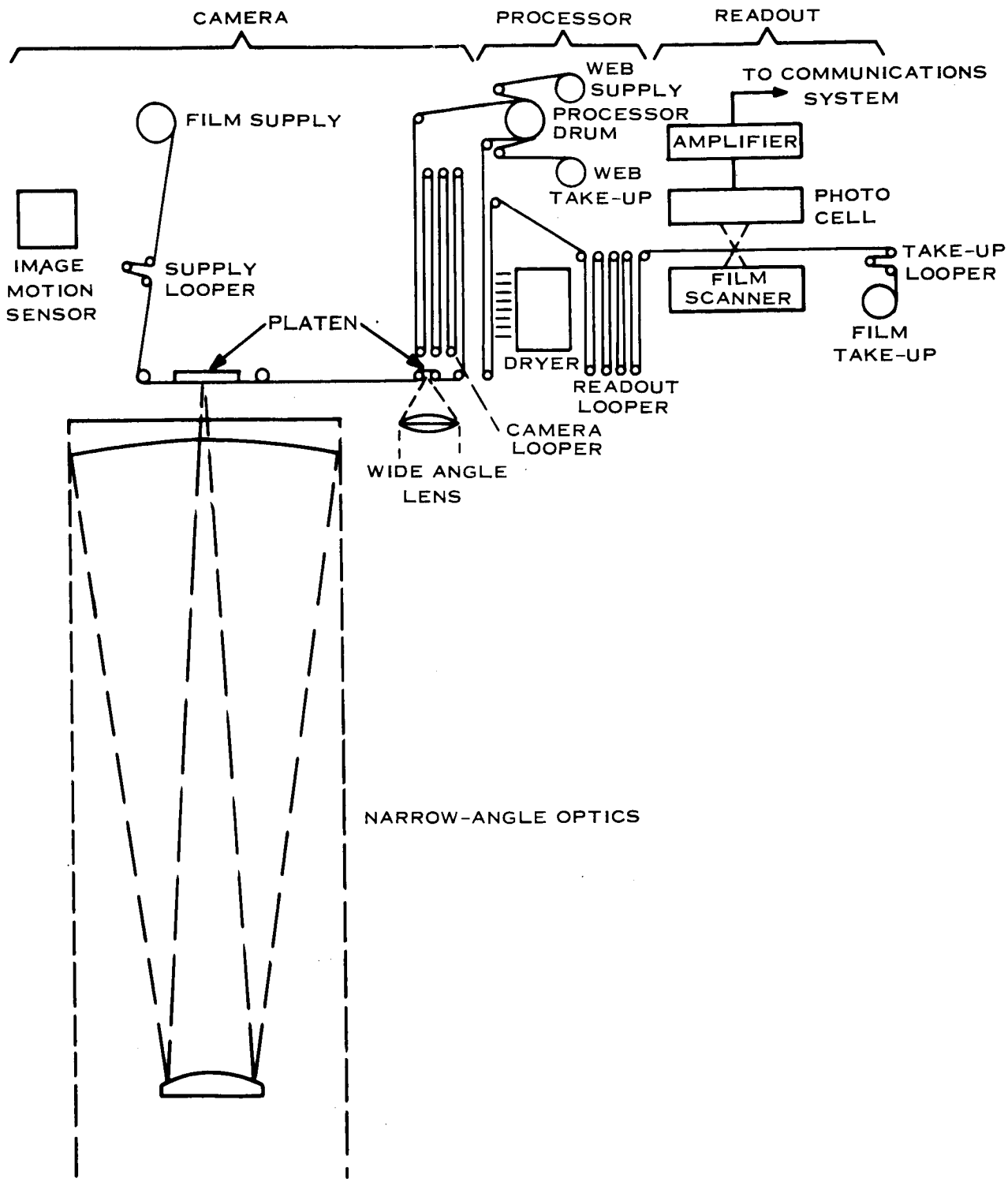

Figure 4-19. Dual Lens Camera System

The other platen moves at 0.36 inch per second, and, since a focal plane shutter is used, the platen will move for a time which is significantly longer than the exposure time.

Attached to the platen will be a system to place data on the film. This data will include resolving-power targets, gray scales, frame number, time of exposure, vehicle or scan platform attitude, altitude, and fiducial marks. The purpose of these data is to locate the principal point, to relate this point to the ephemeris and a point on the planet, and to permit the control and evaluation of the readout and data encoding/decoding equipment. A Reseau grid will be pre-exposed on the film.

The film is taken from the supply reel through a supply looper to the platen. The supply looper will hold about 2 feet of film, and its purpose is to allow the supply reel and platen motions to be independent of each other and to keep a relatively constant tension on the film. From the platen, the film is transported to the camera loopers which are sized to hold 24 feet of film.

4.3.1.2 Optics

There are several lenses available that approximate the 12-inch lens used for the 100-meter mapping. For example, the Itek Corporation has a fine quality of 13-inch f/3.5 lens which can cover a 70-millimeter field and gives about 250 line pairs per millimeter resolution on 3404 film (similar to SO-243) at high contrast. At 2:1 contrast, the resolution is 150 line pairs per millimeter. The lens is of the Petzval type and is estimated to weigh 10 pounds. At 1.02:1 contrast, this lens will give resolution exceeding the required 16 line pairs per millimeter. Although the focal length is 13 inches, it can fill the requirement of the 12-inch lens while providing slightly better ground resolution. The field of view of this lens on 70 millimeter film is 10.3 degrees full field.

Figure 4-20 is a sketch of a cassegrainian optical system which is a candidate for the 120-inch, f/8 system to obtain 20-meter resolution. The initial estimate of the weight of the optics is 50 pounds. Since this assembly is external to the pressure vessel, it must have its own thermal controls, insulation, thermal door, and sun shield. Using 70 millimeter film and a square format, the required field of view is about 1.1 degrees full field. This is within the capability of the system. These optics would have to be developed.

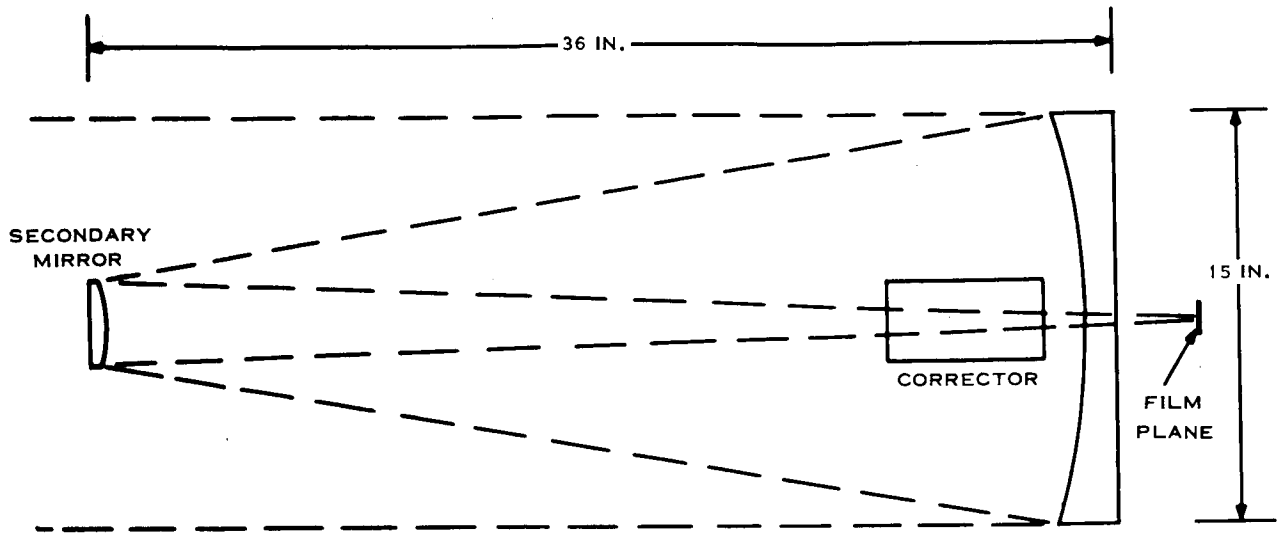

Figure 4-20. Sketch of 120-inch f/8 Wynne-Rosin Cassegrain

4.3.1.3 Image Motion Sensor

Image motion sensors share the light with the main optical system. In the case of a dual lens system, the IMC sensor is associated with the fine-resolution lens system and receives light either through a hole in the diagonal mirror behind the fine-resolution lens (see Figure 4-19) or by means of a dichroic mirrors. The image motion sensor is a correlation device which looks at an area on the planet at two points in time and measures the displacement of the image. The output of a correlation sensor is the rate at which the film should be moved. The output of a sensor behind a lens is the required platen linear rate, since the optics in effect converts angular motion to linear motion. This is the control signal for the platen drive. Alternately, the output of an image motion sensor can be used to drive a plane mirror at half the line-of-sight rate.

4.3.1.4 Film Description

The nominal film is High Definition Aerial Film Type S0-243. This film is described by the Kodak data sheets included in our earlier Milestone Report VOY-D5-TM19. Other characteristics of the S0-243 film are:

Weight: 0.037 lb/sq ft or 8.49 lb/1000 ft of length

Width: 70 millimeter = 2.754 inch $\pm$ 0.002 inch

Thickness: 5.49 mils

Core Diameter: 4.251 inches - 0.002 inch

Typical core or roller width: 2.768 inches - 0.002 inch

To cover Mars within ± 40 degrees latitude with 10 percent overlap and sidelap at 100-meter resolution requires 2360 frames of 70 millimeter film. This is a film length of 540 feet. Using a 4.25-inch core, the reel diameter is about 8 inches. The film weighs 4.5 pounds.

A shielding thickness of 1.3 inches of aluminum will keep the dose below 50 rads. This is a conservative estimate using the more severe 1972 environment. The shield weighs 23 pounds.

4.3.1.5 Processor/Dryer

Bimat processing material was successfully used in the Lunar Orbiter; however, its shelf life/temperature characteristics do not allow it to be used directly on the Voyager Program. The Eastman-Kodak Co. is confident that a modified Bimat-type processing system can be developed in time. Fairchild's Poromat, already developed, has a longer shelf life and is a candidate for Voyager applications. The Itek Corporation has recently developed a "dry processing" system which should be evaluated to determine its applicability to Voyager.

As stated above, there are three potential candidate processing systems for Voyager. The Bimat system is described here because operational experience has been had with it.

The processing film is kept in contact with the S0-243 film for 3 to 5 minutes, depending upon the processing film type used. Longer contact will not cause overdevelopment, but the two films could stick together if not separated within about 12 hours. The film moves through the processor at the rate of about 2.5 feet per minute. To estimate the processing time, a capability of 60 frames per orbit will be used.

Sixty frames, each 66 millimeters long, represent 12 feet of film. This quantity of film could move through the processor in 4.8 minutes. Allowing 5 minutes development time, the entire processing operation would take about 10 minutes. To simplify the programming and eliminate possibility of power peaks coinciding, it may be desirable to process at the end of the photography for the orbit.

4.3.1.6 Readout

A readout system of the type developed by Eastman-Kodak for the Lunar Orbiter is adequate for the 100 and 10-meter resolution systems and will be described here. But to take advantage of the higher resolution which is obtainable at higher contrasts, a readout system having finer resolution and slower scan rates than the nominal system described here is desired. The readout scan rate would be about 1/25 of the rate for the system described here. A cathode-ray tube system may not be the best method to obtain these characteristics, and another approach may be more optimum for a high-resolution system with a narrow allowable bandwidth.

The basic technique used by the readout for the conversion process consists of scanning the lunar images with a very small, high intensity light source, (Figure 4-21). The source of light is a cathode-ray tube similar to the Line Scan Tube developed by CBS Laboratories. This has a P-16 phosphor deposited on a cylindrical anode which is rotated during operation. The P-16 phosphor light output peaks near 4000 Angstroms and is detected using an S-11 photocathode.

As the spot scans across the varying densities of the film image, the modulated light beam emerges from the other side of the film and is focused on the face of the photomultiplier tube whose electrical output is then a time varying signal directly proportional to the film transmittance. The high-speed electrical scanning by the cathode-ray tube spot motion is combined with an orthogonal, slow mechanical scan to produce framelets which are the basic unit for ground photo reassembly. Table 4-6 summarizes the performance and characteristics of the readout system.

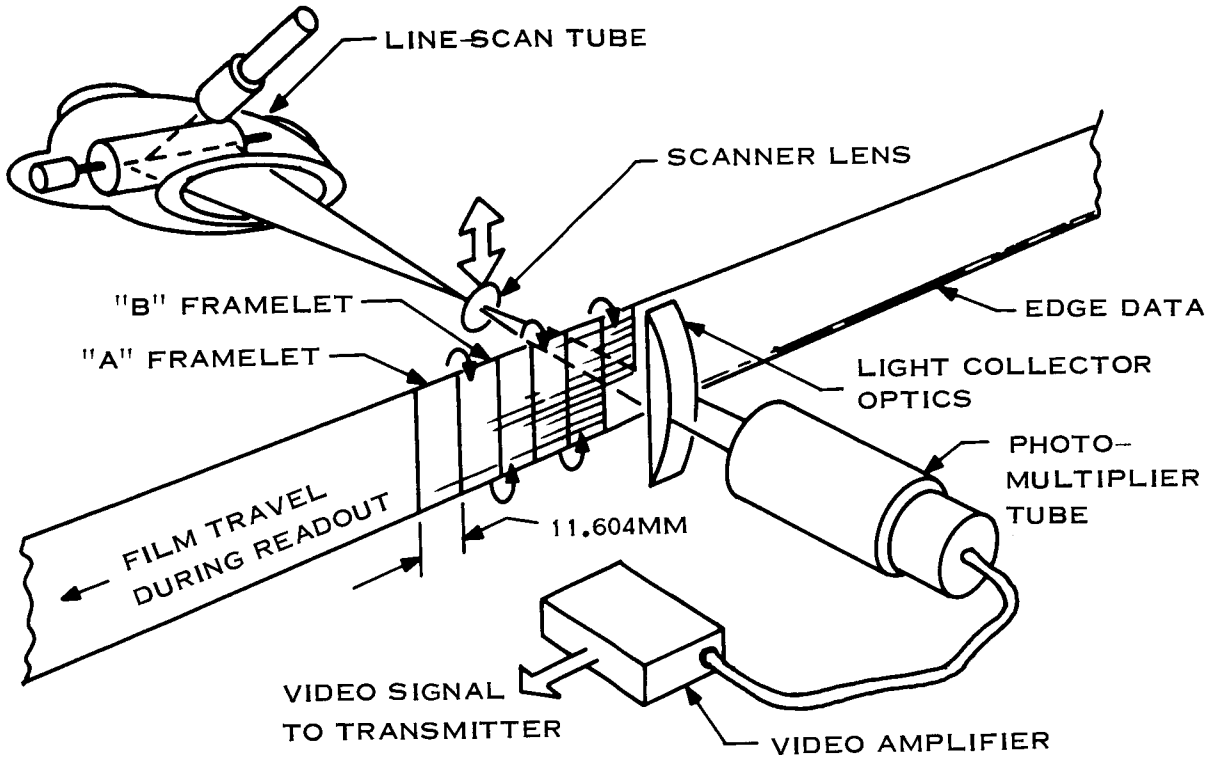

Figure 4-21. Line Scan Tube Readout Scanner

The impact of the Ground Reconstruction Equipment was considered when the Lunar Orbiter scan parameters were modified. The length of the scan line on the film was increased inversely proportional to the decrease in resolution so that there are the same number of elements across both the Lunar Orbiter and Voyager framelets. Therefore, the present technique of ground recording on 35 millimeter film can be maintained.

The readout rate is 0.01125 foot per minute as limited by the transmission capability of 30×10^3 bits per second and a 1.5:1 compression ratio. This film is stored in a readout looper until it can be read out.

Table 4-6. Characteristics of the Readout System

Rate of readout	16.92 minutes per frame
Size of frame	
a. Across film	62 millimeters
b. Along film	58 millimeters
Number of framelets per frame	5
Size of framelet	
a. Across film	62 millimeters
b. Along film	11.604 millimeters
Time to read out framelet	2.82 minutes
Number of lines across frame	2852
Scan time per line within framelet	59.32 milliseconds
Retrace time per line	4.287 milliseconds
Line length on scan tube	60.2 millimeters
Demagnification from tube to film	5.186

Unlike Lunar Orbiter, which reads out only selected frames during the 2 weeks of photography, the film will be read out on the same orbit as it is exposed.

4.3.1.7 Environment Control

The general atmosphere of photographic system payload environment consists of nitrogen environmental gas having 1 percent volume oxygen content. This low oxygen level avoids any oxidation effects within the processing material. An absolute pressure control system which operates within the range of 1.0 psia to 2.0 psia and has provision for making up gas leakage from a high-pressure nitrogen supply tank initially at 2100 psia. The photo system pressure is thus maintained, at all times, above the vapor pressure of water for the highest expected payload design temperature levels. A saturated potassium thiocyanate (KCNS) chemical salt solution passively controls relative humidity and maintains a 50 percent nominal relative humidity at 60°F. The processed negative material must be dried. The amount of moisture to be removed from the negative is 2 grams per square foot or less. This is about 460 grams of moisture for the total film load.

Both ends of the dryer drum are enclosed with aluminized mylar to reduce radiation heat transfer losses. During processor-dryer operation, the drum temperature is maintained at $95^{o}F \pm 2^{o}F$, by means of the motor heat and the controlled tape heaters, which can remove 3.3 grams per hour of water from the film.

The photographic payload temperature control system should maintain the processing film at about $60^{o}F$ at all times prior to and during the film processing phase of the mission and control the processor drum at $85^{o}F \pm 2^{o}F$ during processing. The dryer drum is held at $95^{o}F \pm 2^{o}F$, during processing. The primary film is rather tolerant of temperatures as long as it does not exceed $125^{o}F$.

The camera assembly during its operational period is held at a temperature of $70^{o}F \pm 5^{o}F$. The 12-inch focal-length optics has a tighter temperature requirement, and the lens is placed within a thermal shield of thin reflective aluminum. This shield and heaters maintain the temperature at $70^{o}F \pm 2^{o}F$.

The lens is further thermally isolated by a thermal door which is closed except during the actual photography. A heater on the inside of this door maintains its temperature at $70^{o}F \pm 2^{o}F$.

The 120-inch-focal-length optics is outside the pressure vessel and has its own thermal control system. The optical system consists of two concentric barrels which are thermally isolated from each other. About 1 inch of aluminized mylar superinsulation will be between the two barrels. The inner barrel will also be mechanically decoupled from the outer barrel so that flexure of the outer barrel due to differential solar heating will not distort the optics.

A thermal door is closed except during photography to maintain the inner environment. The local ambient within the barrel is $70^{o}F \pm 5^{o}F$, with 10 degrees being the allowable gradient from one end of the barrel to the other. The radial gradient for the primary and secondary mirrors is 5 degrees. The maximum circumferential gradient of the inner

barrel has the same maximum value. Heaters will be placed on the inside of the thermal door and distributed within the inner barrel to maintain the environment.

A sun shade will be required in front of the optics. This consists of a lightweight tube extending in front of the optics. This will weigh 10 pounds and will be held in a retracted position until orbit is achieved.

4.3.2 OPERATION FOR MAPPING AND RECONNAISSANCE

The wide-angle lens covers 174 km on the surface from an altitude of 1000 km. For stereo coverage, this system can take a photograph every 27 seconds, giving 60 percent overlap. Between exposures, the vehicle travels 81 km. If stereo is not desired, an exposure will be taken 53 seconds apart, giving 10 percent overlap. Between these exposures, the vehicle travels 157 km. The orbit tracks will be laid down to give 10 percent sidelap if optimum mapping orbits are selected. Figure 4-22 shows the coverage of the wide angle system on the planet's surface.

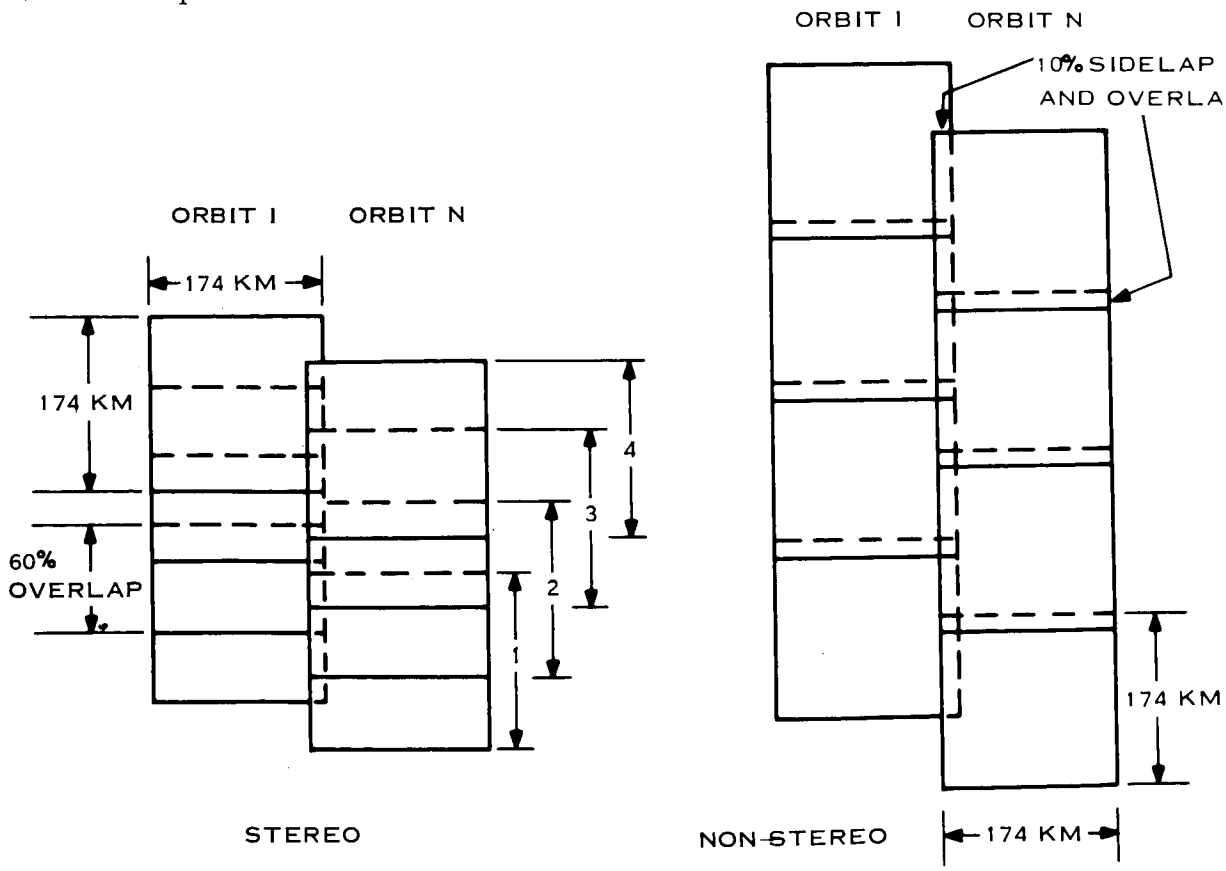

Figure 4-22. Wide Angle Coverage on Planet

The wide-angle system will be used independent of or in conjunction with the narrow-angle system. But the narrow-angle system will not be used independently of the wide-angle system. Every time a narrow-angle shot is taken, at least one wide-angle shot will be taken. The reason for this is that an area 10:1 different in dimensions and resolution is difficult to find and evaluate unless it is referenced to a larger area photographed at the same time.

The narrow-angle lens covers 17 km on the surface. This system will be used for selective reconnaissance coverage, and mapping is not its primary objective. Stereo can be obtained by taking photographs 2.7 seconds apart, but stereo is not a requirement for this system and is not considered in the planning of the operation. The normal operation of this system is to take single frames or a photograph every 5 seconds obtaining 10 percent overlap over selected areas. The vehicle travels 15 km during this time. Figure 4-23 shows examples of the operation of the narrow-angle system and shows how its coverage is related to the wide-angle coverage.

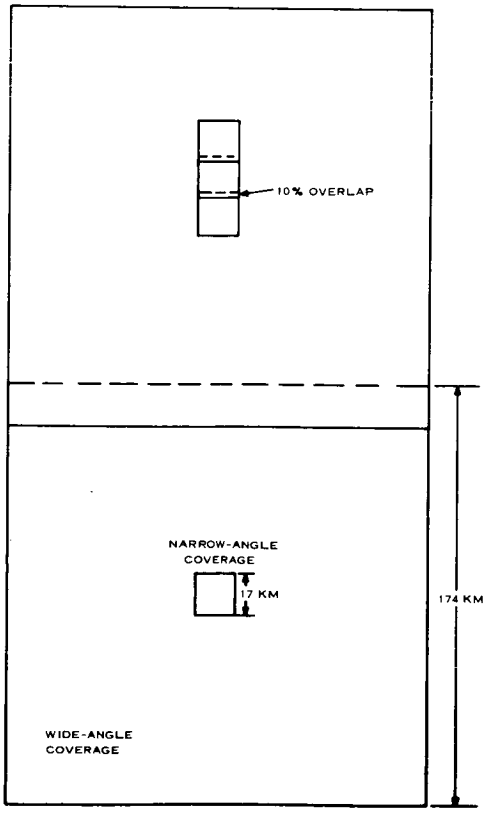

Figure 4-23. Examples of Narrow-Angle System Operation

4.3.3 DATA HANDLING

The data handling equipment will receive signals from the film scanning equipment, including a video signal, synchronization signals, and various control and status signals. The background removal scheme as discussed in Appendix C is shown in Figure 4-24. The background level can be inserted in the data stream during line retrace time. For the film system, the background level is removed to reduce redundancy and not to minimize the effect of the system errors on the signal. The video signal has edge data included in it. The edge data includes the shutter time and calibration data. The background level determination circuitry is gated off during edge data transmission so that the averaging and signal subtraction does not degrade the edge data.

The various control and status signals from the scanner will be used to generate an identification number for the data as follows:

a. The horizontal sync pulse of period = 59.3 msec and duration of 4.29 msec is used to generate a line number (2852 per framelette). This number is reset to zero at the start of each framelette.

b. The vertical sync pulse (film stepped 11.6 mm) is used to generate a framelette number. This number is reset to zero at the start of each frame.

The data thus generated will be combined with the video background signal and added to the video signal during horizontal and vertical sync times.

A block diagram of the complete data handling equipment is shown in Figure 4-24.

The composite video signal will include the following:

a. Video information (image sensor data, time code, calibration data, etc.)

b. Background level

c. PN code for horizontal sync — 31 bits

d. Line number — 12 bits

e. Framelette number (5 framelette/frame) — 3 bits

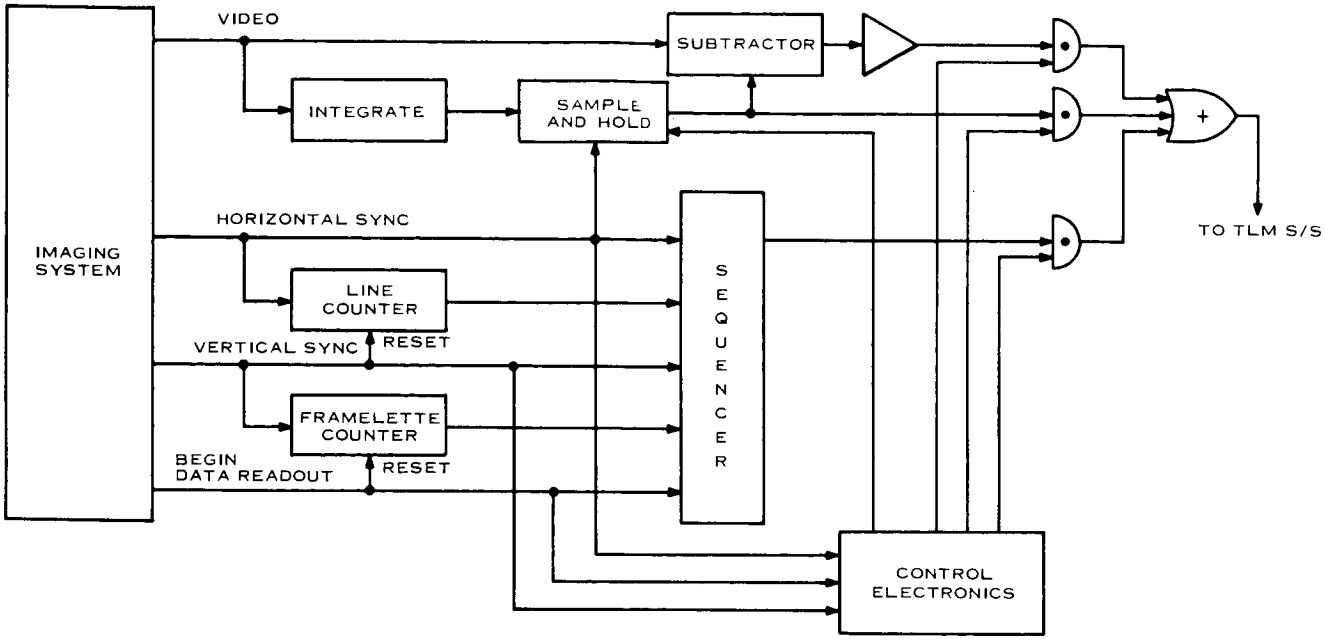

Figure 4-24. Data Handling

Assuming a 30-kilobit per second transmission rate as a minimum, 3:2 data compression, six bits per sample, and two samples per cycle, the maximum input rate to the analog-to-digital converter from the film scanner is 3.75 kHz.

The analog signal is converted to digital and outputted to the telemetry subsystem. As the transmission range increases, reduced scan rates provide input signal bandwidths of 1.875 kHz and 0.937 kHz to match the transmission data rates.

4.3.4 MAJOR PERFORMANCE CAPABILITIES AND LIMITATIONS

4.3.4.1 Effect of Contrast on Resolution

Modulation transfer functions have been used to obtain the resolution as a function of contrast down to a contrast ratio of 1.005:1. The contrast ratio is defined as the ratio of target luminance; e.g., ratio of 1.05:1 could indicate a 5 percent change in reflectivity

between the target and background. The effect of contrast on resolution attainable with various focal lengths for an f/4 system is shown in Figure 4-25.

The resolution obtainable with an f/4 system is almost equal to that with an f/8 optics at the lower contrasts. The two systems are compared in Table 4-7 using an 120-inch focal length.

4.3.4.2 Rates of Film Operation within Camera System

The principal operations in the camera system are photography, processing, and readout. The rates for these are different and, consequently, film loopers are required as buffers between the subsystems.

The camera rate is determined by the rate at which photos are required to be taken. This is determined by the ground coverage, the orbital velocity, and the desired overlap. The camera mechanics are not limiting; pictures can be taken every second if required.

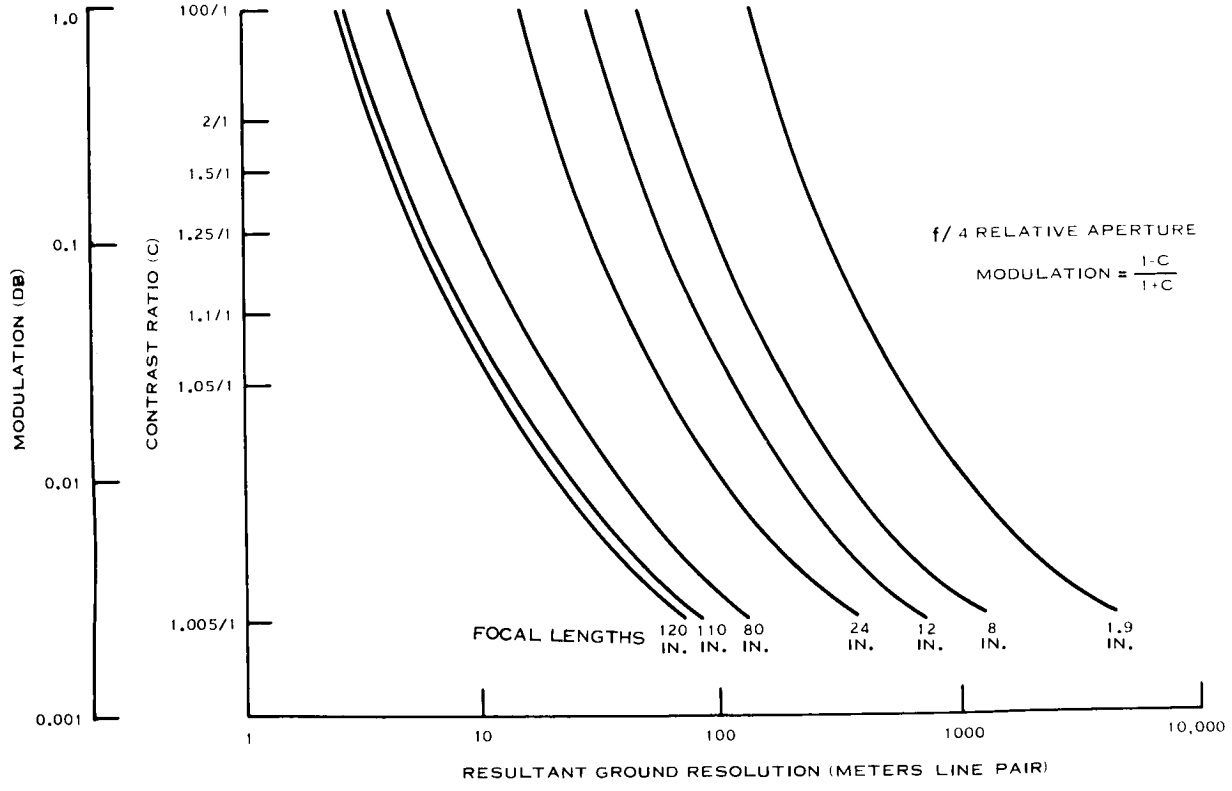

Figure 4-25. Effect of Contrast on Resolution and Focal Length

Table 4-7. Comparison of Resolution with f/4 and f/8 Optics

Contrast Ratio	Resolution (meter/line pair)	
	f/4	f/8
1.02	19	21
1.05	11	12
1.1	7	8
1.25	4	5
1.5	3	4
2	2	3

Table 4-8 gives the time interval between photographs taken from 1000 km altitude. The fine resolution system will probably not be used for stereo and, therefore, no time is entered for 60 percent overlap.

Each frame is 58 millimeters long including data annotation, and, using the photography time intervals, a rate can be determined in feet per minute. This data is also included in the table. A photography rate in feet per minute doesn't indicate constant velocity film movement or continuous photography.

Table 4-8. Rate of Photography

Resolution Ground Coverage	100 m 174 km		10 m 17 km	
	Time (seconds)	Rate (ft/min)	Time (seconds)	Rate (ft/min)
No Overlap	58	0.20	5.8	2.0
10% Overlap	53	0.22	5	2.2
60% Overlap	23	0.48	-	-

The processing rate is determined by, among other factors, the size of processing and drying drums and the development time. These are a function of the particular technique, and a reasonable estimate of the rate is 2.5 feet/minute and the time in minutes is $\frac{L}{2.5 \text{ ft/m}} + 5$ where L is the film length and the developing time is 5 minutes.

The readout rate is limited by the data transmission capability. A transmission rate of 30 kbs, 1.5 compression ratio, and six-bit encoding limit the readout rate to 0.01125 feet/minute.

4.3.5 INTERFACE REQUIREMENTS

4.3.5.1 Size

The camera system has two connected volumes. One is the pressure vessel containing the wide-angle optics, processor, and readout. The narrow-angle optics is outside the pressure vessel, connected to it to maintain optical alignment, and imaging on film within the pressure vessel through an optically flat window. The pressure vessel is 26 inches by 22 inches by 32 inches and is egg-shaped.

The overall dimensions of the narrow-angle optics are a diameter of 15 inches and a length of 36 inches. A thermal shield extending in front of these optics will be required. This is a lightweight assembly extended after orbit is achieved. Its length has not been determined, but it should be no longer than 36 inches.

4.3.5.2 Weight

The pressure vessel and its components weighs 160 pounds, including film, processing material, and shielding. The narrow-angle optics, with its thermal controls, insulation, thermal door, and thermal shield (sun shield), weighs an additional 50 pounds. The total weight of the dual lens camera system is then 210 pounds.

4.3.5.3 Electrical Power

Table 4-9 presents the electrical power requirements, indicating the major consumers and the duty cycles. To satisfy these requirements, the average input to the camera system will be 80 watts.

Table 4-9. Electrical Power

Item	Power Watts	Duty Cycle Percent
1) Narrow-angle optics thermal control	15	100
2) Image motion compensation	10	6
3) Pressure vessel thermal control	15	100
4) Processor/dryer	30	2
5) Readout	40	100
6) Camera Control & Programmer	10	100
7) Film Transport	50	~0

4.3.5.4 Thermal

The elements of the camera system have their own active and passive thermal controls. The scan platform will be used as a cold plate, and its temperature should be within the range of 25°F to 90°F.

4.3.5.5 Data Rate

Data from the readout system is encoded in digital form using six-bit encoding and is at the rate of 30 kilobits per second.

4.3.5.6 Attitude Control

The attitude control and stabilization requirements (shown in Table 4-10) are based upon limitations imposed by resolution requirements. Maximum allowable values are given in the title.

Table 4-10. Attitude Control and Stabilization Requirements

	12-inch, f/4	120-inch, f/8
1) Yaw angle	45^{o}	2^{o}
2) Yaw drift rate	3 mr/sec	0.75 mr/sec
3) Amplitude of high-frequency yaw rate (peak-to-peak)	233 Micro rad	47 Micro rad
4) Pitch and roll drift rates	0.42 mr/sec	0.105 mr/sec
5) Amplitudes of high-frequency pitch or roll rates (peak-to-peak)	33 Micro rad	6.6 Micro rad

Yaw is about the local vertical, and the roll axis is parallel to the ground track.

These requirements are for the nominal exposure times. To have the same photography performance at longer exposure times, certain of the allowable errors, items 1, 2, and 4, should be multiplied by $\frac{1/50}{t}$ for the f/4 system and $\frac{1/10}{t}$ for the f/8 system, where t is the new exposure time.

The vehicle will probably have disturbances of the type indicated by item 2 or 3 and not both. This comment also applies to items 4 and 5. A high-frequency rate is one which goes through a number of cycles in the exposure time.

4.4 OPTOMECHANICAL SCAN SYSTEM

4.4.1 DESCRIPTION OF MAJOR ELEMENTS

The Optomechanical Scan System consists of imaging optics, scanner assemblies, point detectors with electronics, and a magnetic tape recorder. The concept is shown in Figure 4-26. The optical image is scanned line by line in a direction perpendicular to the direction of ground travel by the rotation of a scanning wheel carrying a set of flat mirrors, and

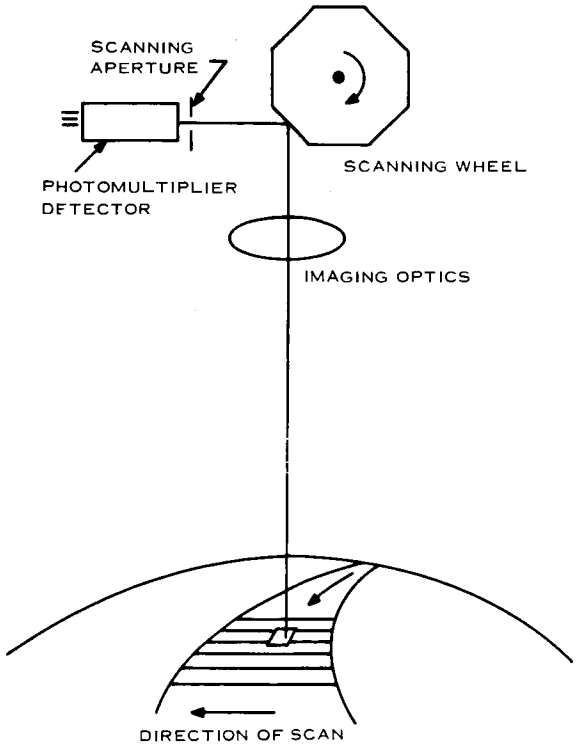

Figure 4-26. Optomechanical Scanner Schematic

the resultant photomultiplier signal variations are stored in the tape recorder. The next image line formed by the succeeding mirror face of the wheel overlaps this trace a small amount. The timing and size of these lines is adjusted to the spacecraft velocity so that a continuous map, with no gaps, results. This technique is analogous to the manner in which the electron beam or the flying spot scanner reads out the image formed by the vidicon or or the photograph.

A very lightweight system for 400-meter resolution can be included, which allows direct data transmission without intermediate recording media.

4.4.1.1 Optics

The main characteristics for the 100 meter and 10 meter optics are shown in Table 4-11.

Table 4-11. Main Characteristics for 100-Meter and 10-Meter Optics

Characteristics	100 meter system	10 meter system
Ground resolution	100 meter	10 meter
Angular resolution	0.1 milliradian	0.01 milliradian
Aperture	0.4 meter	0.4 meter
Equivalent focal length	0.4 meter	4.0 meters
Optical speed	f/1.0	f/10
Field of view (scanned)	12 degrees	0.4 degrees
Image flatness	Not needed	Not needed
Transmission	60%	60%
Passband	0.60-0.75 microns	0.60-0.75 microns
Length	1 meter	1 meter
Diameter	0.5 meter	0.5 meter
Weight	60 pounds	60 pounds
Type of design	concentric catadioptric	concentric catadioptric with relay lens

A short outline of the considerations underlying these specifications follows:

4.4.1.1.1 Aperture

As discussed in Section 4.4.1.3, the performance of this optomechanical system is limited mainly by the number of photons received at optics aperture. An aperture of 0.4 meter has been set as a practical upper limit, in view of the limitations on volume and weight. With such an aperture, it is possible to carry out the 100-meter mission and a degraded version of the 10-meter mission.

4.4.1.1.2 Focal Length

This is set primarily by the maximum image size that the line scanner can accept, and not by the detector resolution, because its spatial resolution can be given any value by choosing the proper scanning aperture diameter.

In an earlier Milestone Report, VOY-D5-TM19, pages 4-5, a wheel type of line scanner is analyzed. It consists of a set of plane mirrors, mounted at the perimeter of a continuously rotating "mirror wheel" as shown in Figure 4-26. In order to keep the diameter of this wheel down to 10-20 cm, the size of the scanned image cannot be much larger than 2-3 cm. Also, this type of scanner introduces defocusing problems because the ends of each line scan have to be compensated for by dynamic focusing (driving the scanning aperture in order to maintain coincidence with the image plane). This also limits the size of the scanned image to some 3 cm or less.

If a mirror wheel scanner is used, the image to be scanned cannot be larger than about 8 cm, which requires the use of three scanners in parallel. This means a maximum focal length of 0.4 meter for the 10-meter optics and 12 meters for the 10-meter optics. The optical speeds become respectively F/1 and F/30.

For the present purpose, the focal lengths have been set at 0.4 meter and 4.0 meter allowing the use of three mirror wheel scanners for the 100 meter system. This choice is somewhat arbitrary, and is made for feasibility use only.

4.4.1.1.3 Type of Design

4.4.1.1.3.1 100-Meter System. This employs optics of 12 degrees field of view (FOV), 0.1 mr resolution, and speed down to f/1. Such a combination can be handled very well by the concentric meniscus system of Bouwers and Maksutov (Figure 4-27). Although theoretically a heavy and large system, its weight and size are in the present case reasonable due to the small focal length.

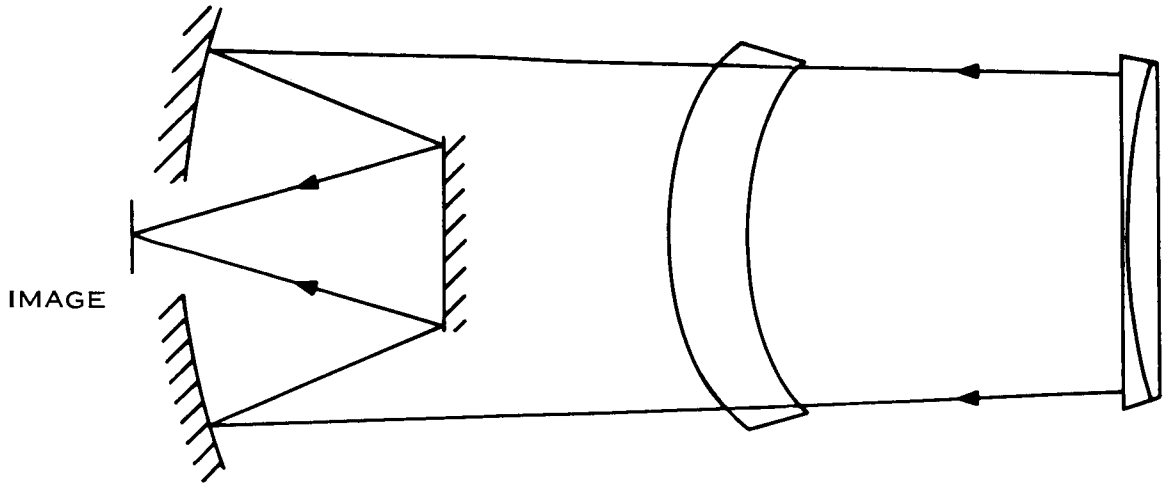

Figure 4-27. Bouwers/Maksutov System

4.4.1.1.3.2 10-Meter System. The scanned FOV is 0.4 degrees, but this FOV is looked at for an appreciable amount of time. This is in order to increase elementary viewing times, build up signal levels, and improve signal to noise (S/N) ratios to useful levels. During this viewing, the scene drifts by due to motion of the spacecraft, and its angular displacement is up to 12 degrees. This motion could be compensated for by a flat mirror in front of the optics, but this would be very large and heavy and exposed to thermal and other influences that tend to degrade its flatness and reflectivity.

A better way to compensate for the scene drift is by adjusting a flat mirror in the converging light beam. This mirror is smaller and is protected. But now the optics has to provide 10-meter resolution over about 12 degrees FOV instead of over only 0.4 degrees. This precludes the use of a folded two-mirror system, like an image-corrected Cassegrain.

The adopted optical system is a corrected concentric meniscus system of speed f/1 to f/1.5, which has ample optical performance for our purpose. A 0.4-degree part of the main image is enlarged by a relay lens and sent to the scanner. The drift in the main image plane can be compensated by a driven plane mirror, which is in our case the flat secondary of the meniscus optics. This compensation is not a complete one, permitting

a small and constant residual motion of the 0.4 degree area to remain, and allowing a line scan of this area by the scanner.

The rotation of the flat secondary mirror causes some defocusing, which can be optically or mechanically compensated.

4.4.1.2 Scanner

The scanning wheel type of optomechanical scanner, shown in Figure 4-26, is one method of implementing the scan requirements for the Optomechanical Scan System. It was realized that this particular scanner may not be the best one for this mission, and, in fact, a new type has been conceived and is under consideration for development. It allows the use of only one scanner and one detector in the 100-meter system, and it eliminates dynamic focusing. For illustration purposes, however, the scanning wheel concept is used in this report, realizing that its particular limitations are not basic ones.

Any scanner for this large aperture optical system should operate close to the image plane instead of in front of the optics, because the latter would require large size mirrors or prisms.

The scanner works as follows. The converging light beam is reflected by a rotating mirror prior to image forming, and the image is thus swept over a stationary scanning aperture. This aperture scans a line of the optical image and permits light to illuminate the sensor. The sensor output is representative of one line in the optical image. When this process is repeated, the spacecraft will have moved in its orbit path, and an adjacent line element of the image is swept over the aperture. In this way, a continuous strip of ground scene can be scanned out and converted into electrical signals.

In order to reduce the rotational speed of the mirror and decrease the dead time between scans, several mirrors are mounted in a wheel and used in succession. The scanning efficiency then goes up to about 0.3-0.4. The values for wheel size, wheel speed, and

mirror size are given in Table 4-12. For the 100-meter system, three such scanners operate in parallel. When properly phased, the dead time between scans is zero.

Table 4-12. Scanner Data for the 100-Meter and 10-Meter Systems

	100-Meter System	10-Meter System
Mirror wheel diameters	0.22 m	0.10 m
Mirror wheel location (distance to image plane)	0.04 m	0.04 m
Wheel speed	8 rps	8 rps
Number of mirrors	5	5

This method of scanning results in an appreciable defocusing at the ends of each scanned line element, especially in the 100-meter system. It also introduces image distortion (nonlinearity). The distortion is identical for each line scan and can be calibrated out, but the defocusing has to be corrected. A possible solution is to let the scanning aperture oscillate in such a fashion that its location at all times coincides with that of the picture element under scan. The oscillation frequency is N times the scanning wheel speed, with N being the number of mirrors on the wheel. The phase difference between the mirror drive and the aperture drive must be maintained accurately; therefore, the two drives could be combined into one. Another possibility is to use a low-power tuning-fork-type of drive for the scanner aperture (because its required motion can be nearly sinusoidal) and a synchronous motor for the wheel drive. The motor can be kept "in step" by sync pulses supplied by the tuning fork.

In order to reduce the size of the scanner and the defocusing effects, the scanner for the 100-meter system has a FOV of 4 degrees, which is one-third of the total FOV. Three such scanners are used in parallel, with their mirror wheels running at the same speed and properly phased. These wheels can, therefore, be mounted in a common shaft.

4.4.1.3 Detectors

4.4.1.3.1 Detector Choice

The Point Detector Scanning System looks at an image one resolution element at a time. In order to cover an extended area within a reasonable time span, the viewing times per element are very short, on the order of 10 to 100 microseconds. In such a small time, the number of collected photons is not very large, and the number of photo electrons created in the detector is smaller still. The natural statistical fluctuations in this photo current set an upper limit to the S/N ratio of the complete system. This limit is further degraded by the preamplifier unless the input signal is at a fairly high level, on the order of 10^{-7} Amp. Such levels cannot be produced by purely photoconductive devices, although their quantum efficiency and also their spectral response can be very favorable. Detectors employing electron multipliers are, therefore, required. Examples are the photomultiplier and the Channeltron. The latter is a relatively new device. It contains a small photoemitter surface (of the order of 1 mm^2 as compared to a 1-to-5 cm^2 in ordinary photomultipliers) and a very compact electron multiplier system. Basically the two detectors have the same sensitivity, but the much smaller photocathode of the Channeltron results in an accordingly smaller dark current.

In the bandwidth of interest (0.6-0.75 microns), the best photo emissive surface is S-20, with a quantum efficiency of about 3-6 percent. The constant dark current of an S-20 photomultiplier is low enough that no cooling of the photo-cathode will be needed for the 100 meter system. For 10 meter it will be, unless the Channeltron with its 100 x smaller cathode area is used.

4.4.1.3.2 100 Meter System

The elementary viewing times are 10 microseconds, in which 320,000 (maximum) and 12,700 (minimum) photons are received. These are converted into 12,500 (maximum) and 500 (minimum) photoelectrons. Their statistical fluctuations give rise to signal-to-rms noise values 110 (maximum) and 22 (minimum). Further degradation by the electron multiplier and the detector electrons is very small due to the large signal levels after multiplication.

4.4.1.3.3 10-Meter System

Due to the small size of the area scanned by this sensor, the S/N of the 10-meter resolution scanner is inherently much lower than for the 100-meter resolution. The scanning wheel is, therefore, slowed down and a form of motion compensation used to cause succeeding lines of scan to be adjacent to each other and to create a frame of ground coverage. For a frame time of about 70 seconds and a 70 km distance between the scanned 7 X 7 km areas, the S/N values, again limited by the photoelectrons, are equal to 11 (maximum) and 2 (minimum).

It is clear that the 10-meter system falls far short in the detection of weak contrast. Its only value is in the sensing of small ground details that on the average might have higher contrasts than the 100-meter resolution elements.

4.4.1.4 Motion Compensation

A form of motion compensation is required for the 10-meter system. The scanning rate in this system is slowed down so that the dwell time on the smaller resolution element is large enough to produce an adequate signal. However, this means that a continuous map cannot be formed; each line is separated too far from succeeding ones due to the spacecraft velocity. Therefore, the scanning FOV is rotated about an axis normal to the orbit plane at a rate sufficient to lay down adjacent lines.

The total rotation required is 12 degrees. This can be accomplished by programmed tilting of the flat secondary mirror in the 10-meter optical system.

This is not image motion compensation in the usual sense, since image smear is not a problem with a scanning system when the electronics provides sufficient bandwidth. This motion compensation is a technique to avoid gaps in the picture at the required slower scan rates.

4.4.2 OPERATION FOR MAPPING AND RECONNAISSANCE

In contrast to the other two systems, which take a series of adjacent pictures to form a total map, the Optomechanical Scanning System produces the map line by line. A small sampling area is swept over each elementary strip of this map, perpendicular to the direction of ground travel. This is similar to the way in which the photographic image, or the electrical image in the TV tube, is read out. One or three such scans are used for medium-resolution mapping, and one for high-resolution reconnaissance.

The scan pattern for the 100-meter medium resolution mapping is shown in Figure 4-28. The total swathwidth of 196 meters is covered by 3 overlapping scans, each 70 meters wide. The scan width is 70 meters in order to produce the 100 meter resolution.

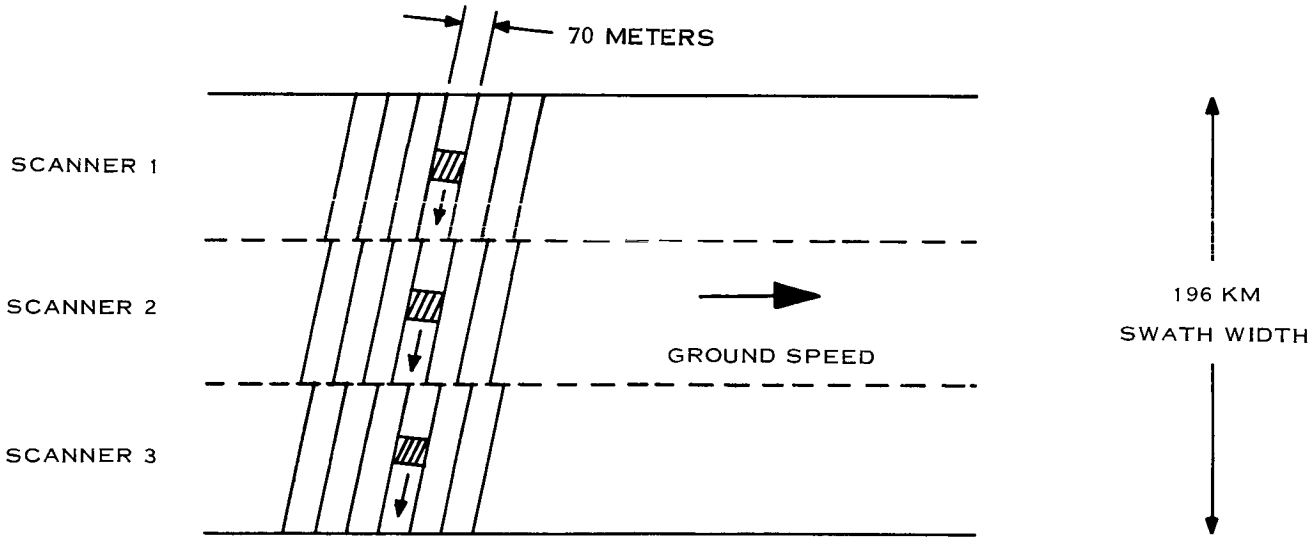

Figure 4-28. Medium-Resolution Mapping Diagram

The scan pattern for the high-resolution reconnaissance is shown in Figure 4-29. This is shown for a 30-meter resolution rather than 10 meters in order to increase the S/N as discussed later in section 4.4.4. The line scans, therefore, are 7 km long and 20 meters wide. The complete scanned frame area is 7 by 7 km. The distance between each frame is 210 km.

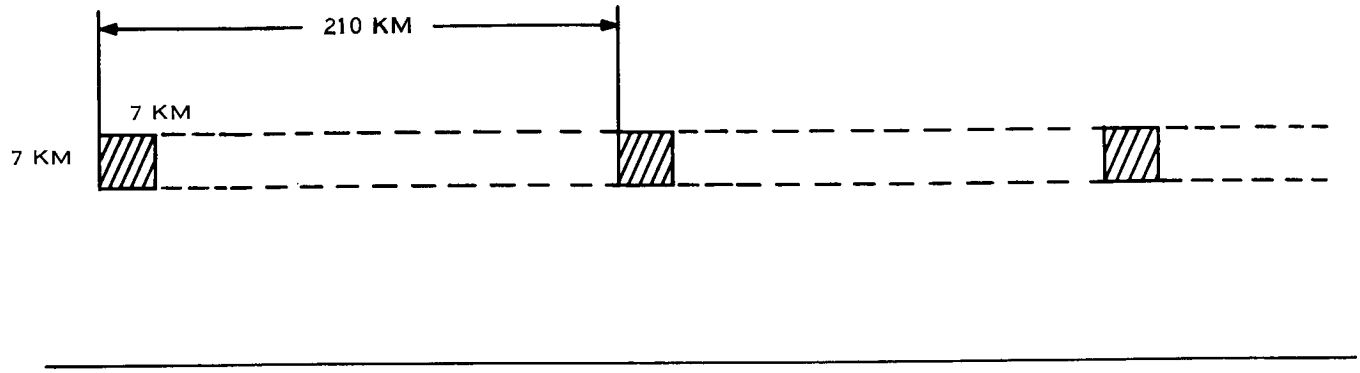

Figure 4-29. High-Resolution Mapping Diagram

4.4.3 DATA HANDLING AND STORAGE

Figure 4-30 shows the data handling and storage for the optomechanical scanner scheme. The data handling and storage equipment will receive a number of signals from the three scanners, including three video signals, synchronization signals, and various control and status signals. The video signal can be represented as being composed of two components: the background level, and the contrast signal. The removal of the background level is discussed in Appendix C. The most obvious scheme is to average the signal over a line and use the average value found to remove the background level for the next line. This is the method shown in Figure 4-30. The background level can be inserted in the data stream during retrace time.

Since the video consists of three signals, one from each sensor, which must be time multiplexed on a line by line basis, it is necessary to have three circuits to determine and remove the background level. Each circuit integrates the signal from one sensor during its scan. At the end of the scan, the average value is stored in the sample and hold circuit, where it is held until that same sensor produces its video for the next scan line. At that time, the stored signal is subtracted from the video signal. It follows that there are three background signals to be transmitted with the video signal.

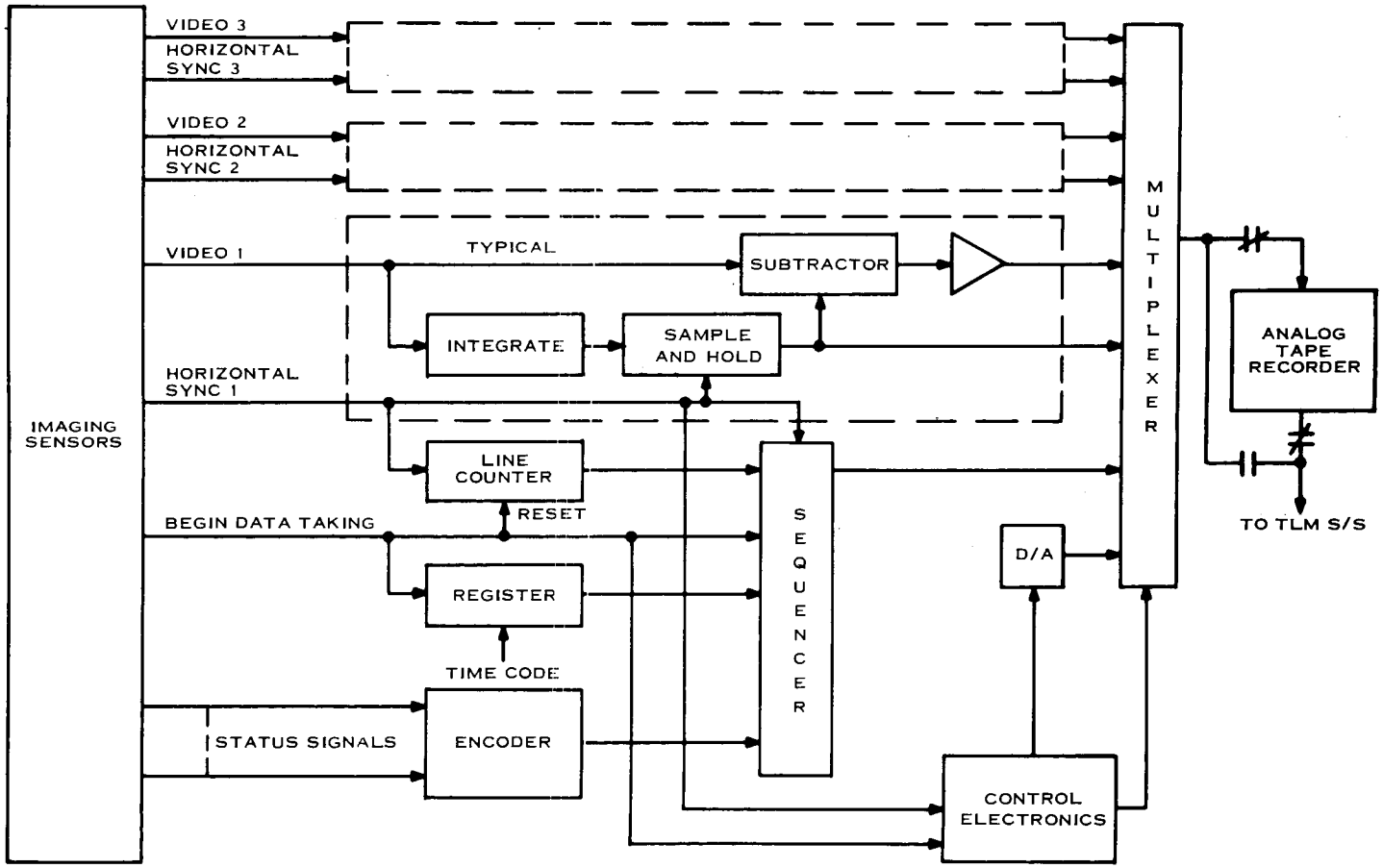

Figure 4-30. Data Handling and Storage for the Optomechanical Scanner Scheme

In order to further reduce the error caused by the data storage elements, it is desirable to include a calibration signal in the video signal. This is accomplished by introducing a staircase signal during the horizontal sync time. This signal is generated by a four-bit digital-to-analog converter to define 16 video levels which will be used by the ground equipment to correct for any nonlinearities introduced by the data storage equipment.

The various control and status signals from the sensors are used to generate an identification number for the data as follows:

a. The start of scan signal is used to strobe the spacecraft time into a register to indicate when the scan was started.

b. The horizontal sync signal is used to generate a line number. This number is reset to zero at the start of the picture-taking sequence.

c. The discrete signals from the sensor indicating which sensor is in use and other data relative to the system status are encoded for insertion into the data stream.

The data thus generated is combined with the video background level signals and added to the video signals during the horizontal sync times.

The composite video signal contain the following data:

a. Video Signal 1

b. Background Signal 1

c. Video Signal 2

d. Background Signal 2

e. Video Signal 3

f. Background Signal 3

g. PN Code for Horizontal Sync — 31 bits

h. Line No. — 11 bits

i. Sensor No. — 2 bits

j.	Time Code (better than 0.1 sec. resolution 30 minutes)	15 bits
k.	Lens No.	2 bits
l.	Status Signals	4 bits

The analog data readout from the cameras has a 50-kilohertz bandwidth, which can be recorded directly or converted to a digital data stream. A discussion of analog-versus-digital tape recording is given in Appendix C.

The analog tape recorder was selected, and its characteristics are presented in Table 4-3. The estimates in this table are based on a similar recorder, RCA Model QRA-2, which was flown on Nimbus.

Assuming a 30-kilobit-per-second transmission rate as a minimum, 3:2 data compression two samples per cycle, and six bits per sample, the maximum input frequency to the analog-to-digital converter from the analog tape recorder is 3.75 kHz. This results in a recorder output speed of 30 ips X 3.75 kHz/60 kHz = 1.875 ips, which should allow a sufficient signal-to-noise ratio for playback. The recorder will be provided with multiple playback speeds to allow a reduction in transmission rate as the planetary distance increases. On the basis of an 8.2 hours orbit and the record and playback rates developed, the record period is 29 minutes, which corresponds to picture-taking from approximately 1000 km to 3000 km in altitude. Using a record speed of 30 inches per second results in a tape length of 4350 feet, which can be provided by using 1200 feet and a four-track recorder.

4.4.4 MAJOR PERFORMANCE CAPABILITIES

For 2 percent intensity resolution, the system S/N ratio should be at least 100. The expected ratios for 100-meter medium resolution mapping are 110 (maximum illumination) and 22 (minimum illumination). The expected ratios for the 10-meter reconnaissance are too low to expect satisfactory operation at 2 percent contrast. This system can be used at higher contrasts or, as discussed below, at coarser resolutions.

The particular characteristics of the optomechanical scanner lead to an interesting tradeoff between spatial resolution and intensity resolution.

If one increases the scanning aperture and slows the scanner down accordingly in order to maintain scanning without overlap between lines, the signal level goes up with the fourth power of the resolution degradation factor. The reasons for this are: increased scanning aperture area (gain = 2 powers), longer specific dwell time on any one ground object due to larger linear size of the back-projected scanning aperture moving over the ground (1 power), and slower scan in order to cover the same swath width (1 power).

In other words, degrading the ground resolution by a factor n produces a gain in photoelectron limited S/N by a factor n^2.

Following this concept, a 140-meter system will, in principle, produce S/N values 220 (maximum) and 44 (minimum), while a 30-meter system operated at 50 seconds frame time has S/N = 100 (maximum) and 18 (minimum).

It is, therefore, suggested that:

a. The aperture size of the 100-meter system be adapted to changing ground illuminations and thereby contrast resolution be conserved at some expense of spatial resolution.

b. The 10-meter system be degraded to about 30 meters when operated at about 70 seconds frame time.

Another modification of the optomechanical scanner that provides an attractive system backup mode is to reduce the resolution ability to a value that permits operation without the magnetic tape recorder. This can be done by reducing the scanner speed and increasing the scanning aperture size, each by a factor of 4. This reduces the resolution to 400 meters and also reduces the data output rate by a factor of 16, which is then sufficiently slow that the tape recorder can be by-passed and the data sent out in realtime at 30 kilobits per second.

SECTION 5

IMPACT UPON SPACECRAFT

5.1 INTRODUCTION

This section describes the relative impacts of the candidate photo-imaging systems upon the Voyager spacecraft. Each of the systems is analyzed with respect to weight, power, volume, complexity, ability to perform a mission, necessary propulsion, and spacecraft design constraints. The results are then presented in such a way as to facilitate comparison between the several systems with respect to these significant parameters. Specific areas of strength or weakness for each system are identified and discussed.

5.1.1 CANDIDATE SYSTEMS CONSIDERED

The candidate systems examined are those described in Section 4 and in an earlier Milestone Report.* There are three systems for the 100-meter resolution mission: a television system, an optomechanical scanner, and a photographic film system. There are four candidates for the 10-meter reconnaissance mission: a television system, an optomechanical scanner, and two photographic film systems. These seven candidate systems define a total of 12 combination systems which might be considered for a Voyager-type spacecraft having both a medium resolution mapping mission and a high resolution spot-reconnaissance mission. In this section, the three medium resolution systems are compared first; then the four high resolution systems are compared. Next, the characteristics of the 12 possible combinations are examined. Finally, an evaluation of the effect that each of the 12 combinations of candidate systems has on the total planetary vehicle weight is given. The planetary vehicle as defined in the General Electric Task D system update study was used as a baseline for this final section.

*"Selection and Design of Candidate Photo-Imaging Systems," VOY-D5-TM-19, 11 September 1967.

5.1.2 SPACECRAFT SUBSYSTEMS CONSIDERED

For this report, the spacecraft is considered to be composed of 18 subsystems as detailed below:

a. Attitude Control
b. Command
c. Computer/Sequencer
d. Data Storage
e. Ground Support
f. Harness/Cabling
g. Lander
h. Meteoroid Protection
i. Power
j. Primary Structure
k. Radio
l. Scan Platform
m. Propulsion
n. Pyrotechnics
o. Science
p. Solar Array
q. Telemetry
r. Thermal Control

It was immediately obvious that there are some subsystems which are not significantly altered by any of the candidate systems. Such areas as Ground Support Equipment might require slight changes as a function of system choice, but these changes would be negligible when viewed from an overall program or system point of view. For such reasons attention is focused primarily upon the following subsystems:

a. Attitude control subsystem of spacecraft
b. Data storage subsystem
c. Lander and Lander interfaces
d. Power subsystem
e. Propulsion subsystem
f. Science subsystem
g. Planetary scan platform

5.1.3 REQUIREMENTS

The requirements used in the design and definition of the candidate photo-imaging systems are followed in the comparison and impact study.

A nominal orbit of 1000 km periapsis altitude, 11,700 km apoapsis altitude, 40^{o} inclination, with an arrival date in the first quarter of 1974, is used. The interaction of scientific mission and orbit choice is discussed in Sections 2 and 3 of this report.

The instruments are designed to operate while pointing along the local vertical toward the center of the planet. It is assumed that they are mounted on a fairly stable scan platform so that image smear or blur due to high frequency vibration or "jitter" is negligible. This assumption itself has an impact on the design of the scan platform. Image smear due to other effects (such as long exposure times, drift rates, and control errors) is not neglected.

Image motion compensation, if necessary, is to be included in the candidate photo-imaging system design.

It is assumed that the power supplied by the spacecraft will be compatible in form (ac, dc, voltage, frequency, etc.) with the bus power requirement of the instrument. All voltages other than bus voltage will be produced in the subsystem.

Broad thermal control is considered to be performed by the scan platform on which the instruments will be mounted. Unusually close temperature control or unusual environmental requirements are satisfied within the instrument package.

5.1.4 SYSTEM COMPLEXITY FACTOR

As the impact study progressed, it became apparent that there was a requirement for some means of comparing the reliability or complexity of the candidate systems. A "system complexity factor" was used for this comparison. This factor is computed for any combination mapping/reconnaissance mission as the sum of six numbers:

$$SCF = C_{pm} + C_{im} + C_{am} + C_{pr} + C_{ir} + C_{ar}$$

where:

- SCF = System Complexity Factor
- C_{pm} = Complexity of photo-imaging sensor, equal to sum of number of "prime-mover" moving parts (motors, etc.) plus number of critical, life-limited components (tubes, chemicals, etc.) contained in sensor for mapping mission
- C_{pr} = Same as above for reconnaissance mission
- C_{im} = Complexity of image motion compensation for the mapping mission

$$= 4 - \log R + \log t$$

where:

R = linear ground resolution (meters)

t = frame exposure time (seconds)

- C_{ir} = Same as above for reconnaissance mission

NOTE:
C_{im} and $C_{ir} = 0$ if no image motion compensation is required.

C_{am} = Complexity of ancillary equipment for the mapping mission. Computed in the same manner as C_{pm} or C_{pr} but applying to such equipment as data storage or film developing and readout.

C_{ar} = Same as above for reconnaissance mission.

This technique is an indication of the relative complexity of implementation for a given photo-imaging system.

The computations for one system are indicated below, while the results of similar analyses on the other systems are tabulated in Table 5.1. The system to be used in the example below consists of an optomechanical scanner for the 100-meter mapping mission and a television system for the 10-meter reconnaissance mission.

C_{pm}:	Beam-steering drive	= 1	C_{pm} = 5
	Photomultiplier tubes	= 3	
	Dynamic focusing drive	= 1	
C_{im}:	None required		C_{im} = 0
C_{am}:	Tape recorder drive	= 1	C_{am} = 1
C_{pr}:	Return-beam vidicon	= 1	C_{pr} = 3
	filter drive	= 1	
	shutter drive	= 1	
C_{ir}:	R = 10 t = 1/4		C_{ir} = 2.4
	4 - 1 - .6 = 3.4		
C_{ar}:	Tape recorder drive		C_{ar} = 1

$C_s = 5 + 0 + 1 + 3 + 2.4 + 1 = 12.4$

Table 5-1. System Complexity Factors

10-METER SYSTEMS \ 100-METER SYSTEMS	Television	Photographic Film	Opto-mechanical Scan
Television	12.4	14.4	12.4
Photographic Film (f/8, light)	15.7	11.7	15.7
Photographic Film (f/4, heavy)	15.0	11.0	15.0
Optomechanical Scan	14.4	14.4	14.4

5.2 100-METER RESOLUTION MAPPING SYSTEMS

Table 5-2 is a matrix showing a comparison of the pertinent characteristics of the 100-meter medium-resolution candidate systems. This section discusses various aspects of the comparison

5.2.1 TELEVISION SYSTEM

The outstanding characteristic of television systems in general is their high sensitivity, which allows short image integration time and thus short exposure times. This in turn reduces the need for image motion compensation, since smear is limited to less than 1/3 of a resolution cell in 10 milliseconds. Another advantage is the ability to use a constant exposure time over the entire illumination level range. Because the camera is sensitive enough at the low light levels, operation at high light levels is achieved by neutral density filters instead of varying exposure or aperture. Since the high sensitivity is achieved simultaneously with a fairly small imaging surface or format, the optics can in general be made more compact.

The major shortcoming of the television system is the relatively high total system weight which is due primarily to two factors. First, the television system has insufficient image storage time to permit real-time data readout with present communication bit rates.

This necessitates an intermediate storage system using magnetic tape. The image is read in at a high rate, stored, and then read out slowly to the RF system at a compatible rate. Tape recorders are fairly heavy and thus add significantly to total system weight. The second weight factor is the trimetragon geometry of the system to achieve the required field of view. Since the nominal field-of-view of a single 100-meter resolution camera is 4 degrees, a combination of three cameras is used to achieve the required 10-degree field of view. The beam-steering requirements to three cameras, coupled with the necessity to fold the optics, result in the fairly heavy and complex optical system described in the television section. In addition, the television system requires fairly sophisticated control electronics, a multiple output power supply, and significant other electronics. Although the latter items can be mounted on the spacecraft body with little or no structural weight penalty, they do increase the overall system weight.

The considerable "folding" of the optics and the volume-efficient trimetragon geometry mentioned earlier allow the television subsystem to be "compacted" into the smallest volume of any system.

The short and constant exposure time and the all-electronic aspects of the control system (except for image steering and filter control) are the main reasons for the relative simplicity as shown by the system complexity factor. This subjective and qualitative assessment of system complexity is described briefly elsewhere.

Power requirements for the television subsystem are moderately high due to the complex internal power supply with its attendant conversion efficiency. This supply must power all three vidicons during "picture-taking" time despite the fact that only one is being read out or exposed at a given instant. The control electronics, although efficiently designed, do consume significant amounts of power.

Radiation effects upon the television system can be assumed to be negligible. In fact, radiation levels up to 10 times greater than expected would not cause significant degradation of the system operation.

Table 5-2. Photo-Imaging Candidate Systems for a 100-Meter Resolution Mapping Mission

Parameter For Comparison \ Candidate Systems	Television	Photographic Film	Optomechanical Scanner	Units
Weight on Scan Platform	150	172	100	lb
Weight on Spacecraft	100	None Req'd	50	lb
Weight on Required Data Storage	Incl. Above	None Req'd	Incl. Above	lb
Total System Weight	250	172	150	lb
Volume on Scan Platform	2.1	8.7	11.0	ft^3
Volume on Spacecraft	1.2	None Req'd	1.2	ft^3
Volume of Required Data Storage	Incl. Above	None Req'd	Incl. Above	ft^3
Total System Volume	3.3	8.7	12.2	ft^3
Power on Scan Platform	50	122	6	watts
Power on Spacecraft	40	None Req'd	40	watts
Power for Data Storage	Incl. Above	None Req'd	Incl. Above	watts
Power Required 100% Duty Cycle	$\approx$ 0	90	$\approx$ 0	watts
Total Average System Power	90	122	46	watts
System Complexity Factor	6	8	6	
Background Radiation Immunity	High	High	High	
Flare Radiation Immunity	High	Medium	High	
RTG Radiation Immunity	High	Low	High	
Overall Radiation Immunity	High	Low	High	
Resolution Cell Exposure Time	1/100	1/10	10^{-5}	sec
Frame Exposure Time	1/100	1/10	10	sec
Required Image Motion Compensation	None	30	None	%
Nonoperating Temperature	25 $\pm$ 5	15 $\pm$ 20	0 $\pm$ 50	^oC
Operating Temperature Range	25 $\pm$ 5	15 $\pm$ 20	0 $\pm$ 20	^oC

5.2.2 PHOTOGRAPHIC (SILVER-HALIDE) FILM SYSTEM

The photographic film system is somewhat difficult to evaluate because its operation is in many respects unique. For example, while the system is moderately heavy on the scan platform and requires considerable power, there is no need for an intermediate data storage subsystem. The image is permanently recorded on film and can be read out on command at the desired data rate. In addition, the film can be read out as often as required (or allowed) since the record is permanent. This allows for quick-look data examination prior to lengthy full-resolution scan. As is usually the case, the price paid for these additional capabilities is system complexity and high power drain. The volume of the unit is only moderate and lends itself somewhat to shaping.

A reason for the high system complexity factor shown in Table 5-2 is the low sensitivity of the sensor (SO-243 film, ASA 1.6). Just as the high sensitivity of the television system allowed a single, short exposure time, the lower sensitivity of the film forces longer exposure times (up to 10 times longer) and thus requires some type of image motion compensation system. The film system is the only candidate for the 100-meter mapping mission that requires image motion compensation.

Although the power consumption during operation of the photographic film system is the highest of the candidate systems, the actual energy would not be much greater if the load occurred only in the region around periapsis, as with the other systems. Unfortunately, a large portion of the power is required throughout the whole orbit. Thus, the total energy required is much greater and will have a decided impact upon the power subsystem of the spacecraft. Use of a film system, then, significantly increases the requirements on the power subsystem. The high energy requirement results from three factors. First, in order to provide very precise thermal control at different temperatures and at several locations, a separate environmental control system is required within the package. This must operate at all times with a power level of about 15 watts. Second, there will be a developing cycle after the picture-taking period. The developing takes place within the processor/dryer unit and requires about 30 watts. Third, the readout phase, which can be as long as the entire orbit, requires 45 watts.

Depending upon the thermal design, the relatively high power dissipations discussed above could help or hinder the scan platform thermal control subsystem; however, the fairly wide temperature ranges allowed might simplify thermal design of the scan platform. It should be kept in mind that the relaxed thermal control for the entire package is at the expense of an independent thermal control system within the candidate film system.

The photographic film system has other environmental requirements. The entire film subsystem is contained in a pressurized container. No external pressurization or atmospheric control is required; however, such a system may have a catastrophic failure mode if the container is punctured or leaks. Protection against such a failure mode might involve more micrometeorite shielding of the scan platform, and/or continuous pressurization and atmospheric control of either the entire scan platform or the film system package.

Any photographic film system has low radiation immunity. Although shielding can be included for normal radiation levels, solar flares might constitute a potentially serious failure mechanism. A significant impact upon spacecraft and lander design could result if RTG (radioisotope thermionic generators) power supplies are included anywhere in the spacecraft. Preliminary analysis indicates that the required shielding weight required to protect photographic film during the 6-month interplanetary transit and for up to 6 months in orbit could easily negate any weight advantages offered by RTG power supplies.

5.2.3 OPTOMECHANICAL SCANNER

Two characteristics become significant when examining the optomechanical scanner system. The first, as shown in Table 5-2, is that the power requirements on the PSP are very low. The problems of scan platform thermal control and perhaps transfer of power across slip rings (is used) might make this feature desirable. The second characteristic is that the medium resolution optomechanical scanner is simple in design and implementation. The scanner does not require image motion compensation. It has a simple scanning system, optics which do not require a flat image plane, and uses well-understood state-of-the-art photomultiplier tubes as sensors. The equipment on the spacecraft is almost exactly the same as that for the television system with regard to data storage, but the associated electronics is much simpler.

Again depending upon thermal design, the low power consumption of the optomechanical scanner aboard the scan platform could be desirable or undesirable from the standpoint of thermal control; however, the extremely wide operating temperature ranges could simplify the thermal design. Within certain broad constraints, the scanner can be designed for almost any temperature range, although there might be a slight improvement in signal-to-noise ratio below $0^{o}C$ and a gradual degration above $25^{o}C$.

The volume of 11 cubic feet on the scan platform is considered to be a conservative estimate of volume for this candidate system. As can be seen from Table 5-2, the optomechanical scanner is the lightest system despite the large volume.

The optomechanical scan system, like the television system, is highly resistant to radiation. Either system could probably operate with little or no degradation in an RTG environment. The optomechanical scanner is perhaps even more resistant than the television system because of the small sensitive area of the photocathode and the lack of an integration mechanism.

5.3 10-METER RESOLUTION SPOT RECONNAISSANCE SYSTEMS

Table 5-3 is a matrix that compares the four 10-meter high-resolution candidate systems. This section discusses various aspects of the comparison.

5.3.1 POINTING STABILITY

A characteristic common to each of the four candidates is stringent pointing requirements. These requirements have an impact upon the spacecraft attitude control subsystem, the scan platform attitude control subsystem, the image-motion-compensation system, and the mechanical and structural design. The design value for the pointing stability requirement is set by its contribution to image smear. If the contribution is held to less than 1/3 of a resolution element, the pointing deviation during the photo-imaging sensor exposure time must be less than 3×10^{-6} radians. Pointing stability, then, is specified by this angle and the exposure time.

Table 5-3. Photo-Imaging Candidate Systems for a 10-Meter Resolution Spot-Reconnaissance Mission

Parameter For Comparison \ Candidate Systems	Television	Photographic Film (light) Note 1	Photographic Film (heavy) Note 1	Optomechanical Scan	Units
Weight on Scan Platform	50	202	562	75	lbs
Weight on Spacecraft Body	50	Negligible	Negligible	50	lbs
Weight of Required Data Storage	Incl. Above	None Req'd	None Req'd	Incl. Above	lbs
Total System Weight	100	202	562	125	lbs
Volume on Scan Platform	6.7	15	33.9	11.0	ft^3
Volume on Spacecraft Body	1.2	Negligible	Negligible	1.2	ft^3
Volume of Required Data Storage	Incl. Above	None Req'd	None Req'd	Incl. Above	ft^3
Total System Volume	7.9	15.0	33.9	12.2	ft^3
Power on Scan platform	15	122	132	3	watts
Power on Spacecraft Body	35	Negligible	Negligible	35	watts
Power of Data Storage	Incl. Above	None Req'd	None Req'd	Incl. Above	watts
Power Required Continuously	Negligible	90	100	Negligible	watts
Total System Power	50	122	132	38	watts
System Complexity Factor	6.4	9.7	9.0	8.4	
Background Radiation Immunity	High	High	High	High	
Flare Radiation Immunity	High	Medium	Medium	High	
RTG Radiation Immunity	High	Low	Low	High	
Overall Radiation Immunity	High	Low	Low	High	
Resolution Cell Exposure Time	1/4	1/2	1/10	10^{-4}	sec.
Frame Exposure Time	1/4	1/2	1/10	$\approx$ 200	sec.
Break Frequency	1.0	.5	2.5	3.75	Hz.
Max. P-P Angular Hi-freq. Jitter	10^{-6}	10^{-6}	10^{-6}	10^{-6}	Rad.
Max. Lo-freq. Angular Drift Rate	10×10^{-6}	5×16^{-6}	25×10^{-6}	37.5×10^{-6}	Rad/Sec.
Required Image Motion Compensation	95	99	90	90	%
Non-Operating Temperatures	25 $\pm$ 10	15 $\pm$ 20	15 $\pm$ 20	0 $\pm$ 50	°C
Operating Temperature Range	25 $\pm$ 5	15 $\pm$ 20	15 $\pm$ 20	0 $\pm$ 20	°C

NOTE 1. Assumes no 100-meter film system.

The magnitude of the problem can be described by three specifications:

a. Maximum peak-to-peak magnitude of high-frequency angular motion (jitter) of the instrument view axis. (Measured in radians.)

b. Maximum rate of low-frequency drift or angular motion of instrument view axis. (Measured in radians/second.)

c. Break frequency between high and low frequency mentioned above. (Measured in Hertz.)

The major impact of these requirements is on the vibration design of the spacecraft and on the attitude control of the Planet Scan Platform (PSP).

The main sources of vibrational excitation (fuel movement and attitude control limit cycle activation) would provide vibrations of very low frequencies. Moving parts (e.g., tape recorders) on the Planetary Vehicle proper would produce some vibration, but this will be isolated from the PSP proper. The system can be visualized as comprising an extremely large rigid mass (Planetary Vehicle) and a small rigid mass (PSP) interconnected by an elastic beam PSP support structure. Any excitations imposed on the large mass in this free-free system thus produce a rigid body PSP motion but very little PSP elastic body response. The three tape recorders, for example, produce a PSP vibration of 7.5 (10^{-9}) radians. Hence, vibration or jitter during planetary photographic exploration should not pose any problems.

The attitude control for the Planet Scan Platform is reported in detail in Volume 2, the System Update Report. The design selected is a horizon sensor with direct drive control utilizing tachometer feedback for stability which is held to about 1 percent of the orbital rate of 1 milliradian per second at periapsis. Through a comparison of this performance with the requirements for the television and the film candidate systems, it has been concluded that no major difference exists in the attitude control for either.

The scan system presents a somewhat different problem, however, in that its equivalent frame time is several seconds. This means that the drift performance of the control of

both the scan platform and the spacecraft may also affect performance. For example, the horizon sensor selected has an accuracy of 0.1 degree with 0.025 degree noise signal. If it is desired to form an accurate map (as contrasted to a survey mission), the 0.1 degree error will distort the apparent distances measured with the scanning techniques. Smear will not be present, however, since the only error produced is that of distortion of the resulting map.

5.3.2 TELEVISION SYSTEM

The television system is the smallest and lightest of the 10-meter resolution systems considered. Again the credit for these advantages goes to the inherent high sensitivity of the Return Beam Vidicon sensor. The use of a single tube permits higher packaging efficiency on the scan platform as well as less electronics for control and power. A simpler optical system permits a wider nonoperating or storage temperature range. Operating temperature ranges are the same as for the medium-resolution television system. As discussed in the medium-resolution system section, a spin-off advantage of high sensor sensitivity is the constant exposure time for different light levels. Constant exposure times are also reflected in a low system complexity factor.

The data storage for the high-resolution television system is basically the same as that used for the high-resolution optomechanical scanner as well as the television and optomechanical scanners for 100-meter medium resolution. The similarity allows a degraded mode of operation in which one tape recorder is used to provide data storage for both high- and medium-resolution systems.

As in the medium-resolution system, the power requirements are only moderate and are significant only in the region around periapsis. Therefore, the impact upon the spacecraft power subsystem is minimal from a total energy point of view.

The high-resolution television system enjoys the same immunity to radiation damage (from both internal and external sources of radiation) as the medium-resolution system. As such, it can operate at radiation levels more than 10 times higher than expected, with little or no degradation.

5.3.3 PHOTOGRAPHIC FILM SYSTEMS

There are two candidate high-resolution photographic film systems. The two differ in optics (f/4 vs f/8) and in weight, and are drastically different in impact upon a spacecraft. For that reason they will be discussed separately. The "light" f/8 system, will be discussed first.

5.3.3.1 f/8 Photographic Film System

The f/8 photographic film system for 10-meter resolution is heavier than either of the two nonphotographic systems and has a larger volume, primarily because of the fairly large optical system and the all-in-one nature of the design. Essentially the whole system (sensor, data-storage, and read-out) is contained in one pressurized package mounted on the scan platform. The high-resolution optics are mounted in another package rigidly connected to the first. The f/4 system is even heavier, of course, because of larger and more massive optics. The f/8 system does not require these extremely large optics because it uses a longer exposure time. The penalty of such a trade, of course, is the very high accuracy image motion compensation required. For this f/8 system, 99 percent of all image motion must be taken out or compensated for to achieve 10-meter resolution with low smear. This is the most severe IMC requirement of any of the systems.

The candidate design incorporates a variable exposure-time system to compensate for varying illumination levels. Such systems have yielded very good flight performance data, but they cause an extra design complexity that some of the simpler designs do not require.

The processor/dryer and separate readout system and the tight internal thermal control requirements all contribute to the high system complexity factor. Both the pressurized camera package and the external optics require tight temperature control. This control is provided by heaters and presents a significant energy increase to the power subsystem. The full-time power needed for the processor/dryer and readout system also places a moderately high energy requirement upon the power subsystem.

The internal pressurization is maintained by complete positive sealing, and no requirement is placed upon the spacecraft. The pressurization suggests the possibility of a leakage failure mode. Increased micrometeorite protection (a possible weight penalty) should also be considered.

The radiation sensitivity of the ASA 1.6 film used presents another failure mechanism. Although the film is provided with a moderate amount of shielding against radiation, the year-long mission design goal presents a significant problem, as discussed in Appendix D. The radiation sensitivity of film also might influence the power subsystem design if an RTG power source were to be included either on the spacecraft or lander. The additional shielding weight required on the scan platform might quickly nullify any efficiency, weight, and size advantages of radioisotope power sources

The 10-meter photographic film system can provide a backup mode at a small cost in added weight. If a photographic film system is chosen for the high resolution mission, the complete medium resolution capability at 100 meters can be included by the addition of relatively small and light optics which would be contained inside the pressurized container. This backup system does not require magnetic tape storage, so it could be switched in for an alternate mapping capability if either the high resolution sensor or its tape recorder failed or was degraded.

5.3.3.2 F/4 Photographic Film System

The second photographic film high-resolution system would probably be considered only if the spacecraft is not particularly weight-limited, or if subsequent analysis indicates that the image-motion-compensation system cannot provide the over 90 percent correction required for at least two of the other candidate high-resolution systems. The reduced IMC requirement (and therefore, slightly reduced system complexity factor) of this "heavy" f/4 system is accomplished by a moderately fast exposure-time capability. This capability is bought only at a very significant weight and volume increases and a slight increase in power drain.

This system, with the above exception, is basically similar to the "light" f/8 system.

5.3.4 OPTOMECHANICAL SCANNER

Design of the high-resolution point scanner is very similar to the medium-resolution design. In both cases, a single photomultiplier tube is not sufficient to obtain the required angular field of view, so that three tubes must be used. The same rotating mirror used for scanning can perform beam-steering simultaneously, again resulting in a fairly simple system to implement. The dynamic focusing mechanism is not as critical as that for the 100-meter design. This might allow a more efficient packaging scheme. Overall volume will probably not change significantly with optics and configuration design. In any case, volume will never be less than the volume for the medium-resolution optomechanical system. The weight of the beam-steering mechanism is the main factor preventing the high-resolution optomechanical from being the lightest and smallest of the 10-meter candidates.

Despite the moderately high weights and volumes of the scanner system, its power consumption is very low. The electronics on the spacecraft body and the data storage tape recorder are very similar to those for the television systems; the difference in power results from the minimal power required for the photomultipliers and from the lightweight, simple drive system on the scan platform. The similarity between the data storage tape recorders used for both of the optomechanical scanners and those used for the television system implies a redundancy technique. It appears quite possible that in the event of the failure of the medium-resolution tape recorder, a degraded mode of operation could result if the high-resolution recorder could serve as data storage for both systems.

The low power dissipation of the optomechanical scanner on the scan platform may or may not have an impact upon the thermal control of the scan platform, depending upon thermal design philosophy. It seems certain, however, that the broad ranges specified for operating temperature will ease the thermal design somewhat. It is important to point out that, within certain broad constraints, the photomultiplier system can be designed to almost any temperature range. There might be slight improvements to the signal-noise-ratio if the temperature could be held below $0^{o}C$, and some degradation above $25^{o}C$. As in the case of the 100-meter optomechanical scanner, the storage or nonoperating temperature specifications are relaxed considerably from the other systems.

The optomechanical scanner probably has the highest radiation resistance of any class of candidate systems. In either the high- or medium-resolution configuration, radiation levels greater than ten times higher than expected will cause no significant degradation.

A potentially serious shortcoming of the 10-meter photomultiplier system is its inability to perform with an adequate signal-to-noise ratio at the very low contrast levels expected. It is not foreseen that this condition can be improved without extremely large, heavy optics, or a break-through in photomultiplier efficiency. The basic lack of an integrating mechanism in a photomultiplier causes a "photon-starved" condition at high resolutions, despite the inherent high gain.

The optomechanical scanner can provide two important backup modes of operation. The first of these it shares with the television system: that is, since there are 3 scanners, if one fails 2/3 of the coverage can still be provided. The second backup mode can protect against a tape recorder failure. If the scan wheel is showed to 1/4 or less of its normal speed, and the scanning aperture is increased 4 or more times, the data output rate of the system (either 10- or 100-meter) will be low enough for direct transmission to earth. This, of course, degrades resolution by a factor of 4, but could be a valuable mode of operation if the recorder should fail.

5.4 IMPACT UPON A SPECIFIC BASELINE SPACECRAFT

To enable a more specific and objective analysis of the effects of using a given photo-imaging system in a given spacecraft, an impact analysis was performed, using as a baseline the Task D spacecraft described in Volume 2. In essence, the two television systems (both cameras and tape recorders) were removed, and then one of the possible twelve combinations of mapping/reconnaissance systems was added. The result is the net Planetary Vehicle weight change due to each combination candidate system. Four steps are necessary to derive this weight change:

a. The weight of that part of each photo-imaging system located on the scan platform is listed in Table 5-4. Using these values, it is then possible to read from Figure 5-1, the total science payload weight and the whole scan platform weight,

including additional structure, thermal control, gimbals, and motors. Table 5-5 shows the increase in scan platform total weight for each of the 12 combinations, assuming a baseline weight of 250 pounds.

b. Table 5-6 shows the increase in energy or steady-state power required by each of the combinations. Figure 5-2 is used to translate this into increased power subsystem weight (including array and batteries) at a rate of 1.65 lb/watt. Table 5-7 shows the increase in power subsystem weight due to each of the combinations of candidate systems.

c. The increase in total body weight (dry, less scan platform) is shown in Table 5-8. This figure includes weight of the body mounted portions of science payload, data storage (or lack of it) on body, increased power subsystem weight, array weight, etc. The increase in dry spacecraft body weight in Table 5-8 is added to the increase in scan platform weight from Table 5-5 to yield the total increase in Planetary Vehicle payload weight shown in Table 5-9.

d. The payload weight from Table 5-9 is used in Figure 5-3 to determine the propulsion subsystem weight increase. This includes casing, propellant, tankage, hardware, etc. The required propulsion subsystem weight increase is tabulated in Table 5-10.

The increases in payload weights and propulsion weights from Tables 5-9 and 5-10 are summed in Table 5-11 to give the total increase in Planetary Vehicle weight.

The heaviest systems with regard to increasing the weight of the Planetary Vehicle is any combination involving the heavy (f/4) photographic film system. These combinations weigh from 150 to 500 pounds more than the other systems. The weight increase is due to the extremely heavy f/4 optics.

The lightest system is the combination of optomechanical scan for 100-meter resolution and television for 10-meter resolution. The heaviest, (exclusive of the f/4 systems) is television for 100-meter resolution and the f/8 film for 10-meter resolution. It is of interest that any combination of film and television is heavier by at least 100 pounds than use of either film or television alone for both resolution missions.

In addition to the total weight impact, both the weight and volume of that part of the photo-imaging system mounted on the planet scan platform have a major effect on its design and performance. Added weight causes an increase in the structural weight, deployment and

actuator requirements, and also increases the difficulty of maintaining a small center of mass tolerance for the entire spacecraft. Added volume causes an increase in the difficulty of locating and mounting the platform on the spacecraft, and limits the fields of view of other spacecraft sensors. An analysis of these weights and volumes, shown in Tables 5-2, 5-3 and 5-4, indicates that the lightest combination is that of optomechanical scan and television, and that the smallest is the all-television system. All the remaining combinations are relatively equivalent, except for the 10-meter film system used with anything except itself for the 100-meter system. These combinations are roughly 100 pounds heavier.

Table 5-4. Weight of Photo-Imaging System on Scan Platform (Pounds)

10-METER SYSTEMS \ 100-METER SYSTEMS	Television	Photographic Film	Opto-mechanical Scan
Television	200	222	150
Photographic Film (f/8, light)	352	212	302
Photographic Film (f/4, heavy)	712	572	662
Optomechanical Scan	225	247	175

Table 5-5. Increase in Total Scan Platform Weight (Pounds)

10-METER SYSTEMS \ 100-METER SYSTEMS	Television	Photographic Film	Opto-mechanical Scan
Television	121	150	60
Photographic Film (f/8, light)	255	135	245
Photographic Film (f/4, heavy)	745	575	685
Optomechanical Scan	151	178	90

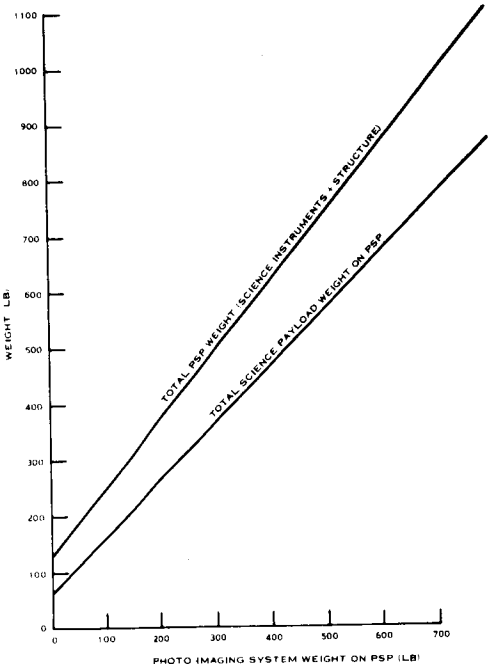

Figure 5-1. Photo-Imaging Weight on PSP vs Science Payload Weight on PSP and Total PSP Weight

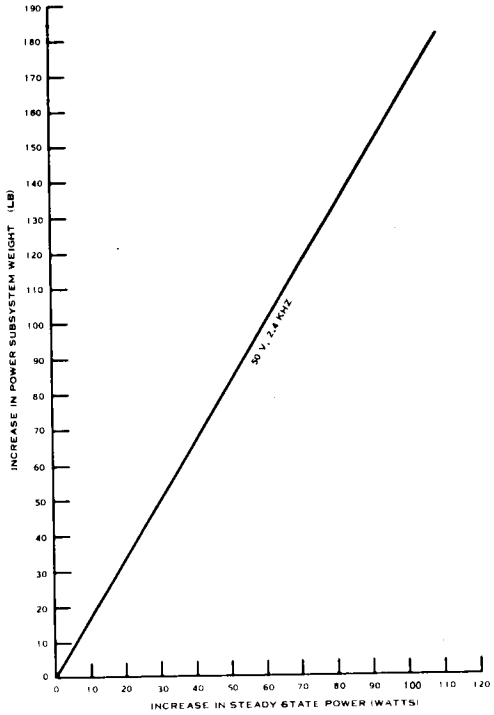

Figure 5-2. Power Subsystem Weight vs Science Subsystem Power Increase

Table 5-6. Increase in Steady State Power (Watts)

10-METER SYSTEMS \ 100-METER SYSTEMS	Television	Photographic Film	Opto-mechanical Scan
Television	0	90	0
Photographic Film (f/8, light)	90	105	90
Photographic Film (f/4, heavy)	100	115	100
Optomechanical Scan	0	90	0

Table 5-7. Increase in Power Subsystem Weight (Pounds)

10-METER SYSTEMS \ 100-METER SYSTEMS	Television	Photographic Film	Opto-mechanical Scan
Television	0	157	0
Photographic Film (f/8, light)	157	173	157
Photographic Film (f/4, heavy)	165	189	165
Optomechanical Scan	0	157	0

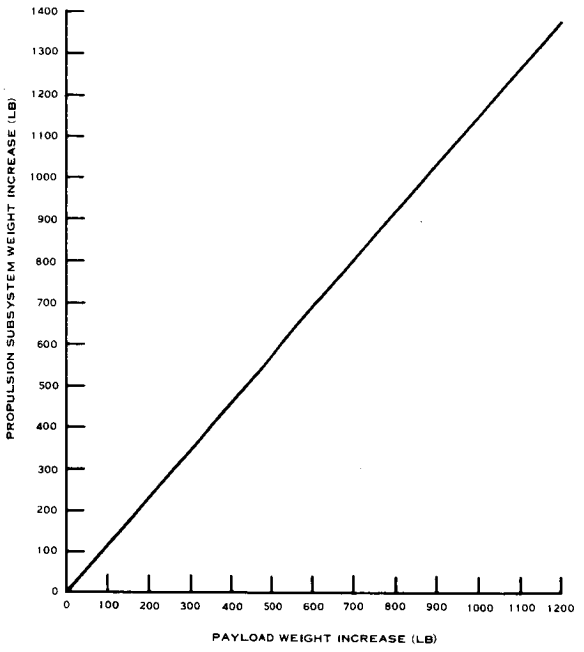

Figure 5-3. Propulsion Subsystem Weight Increase vs. Payload Weight Increase

Table 5-8. Increase in Dry Spacecraft Weight (Not Including Scan Platform Weight) (Pounds)

10-METER SYSTEMS / 100-METER SYSTEMS	Television	Photographic Film	Opto-mechanical Scan
Television	79	136	29
Photographic Film (f/8, light)	186	102	136
Photographic Film (f/4, heavy)	194	118	144
Optomechanical Scan	79	136	29

Table 5-9. Total Increase in Planetary Vehicle Payload Weight (Pounds)

10-METER SYSTEMS / 100-METER SYSTEMS	Television	Photographic Film	Opto-mechanical Scan
Television	200	286	89
Photographic Film (f/8, light)	441	237	381
Photographic Film (f/4, heavy)	939	693	829
Optomechanical Scan	230	314	119

Table 5-10. Propulsion Subsystem Weight Increase (Pounds)

10-METER SYSTEMS \ 100-METER SYSTEMS	Television	Photographic Film	Opto-mechanical Scan
Television	228	325	100
Photographic Film (f/8, light)	503	270	435
Photographic Film (f/4, heavy)	1075	795	950
Optomechanical Scan	261	358	134

Table 5-11. Total Planetary Vehicle Weight Increase (Pounds)

10-METER SYSTEMS \ 100-METER SYSTEMS	Television	Photographic Film	Opto-mechanical Scan
Television	428	611	189
Photographic Film (f/8, light)	944	507	816
Photographic Film (f/4, heavy)	2014	1488	1779
Optomechanical Scan	491	672	253

SECTION 6

CONCLUSIONS AND RECOMMENDATIONS

The following five items are the major conclusions of the photo-imaging study.

6.1 MISSION REQUIREMENTS

Mapping of most of the planet at 100 meter resolution and spot reconnaissance at 10 meter resolution seem to constitute a good compromise between what can be attained and what is required to satisfy topological, areological, biological, and landing site selection requirements. In addition, a small number of pictures at 1000 km resolution and a few frames of the entire planet would help determine cloud patterns and planet gross features. Although polar regions are of interest, most biologically attractive regions can be covered from a 40 degree inclined orbit. Topographic mapping will have to be performed under low contrast conditions i.e., intensity resolution of about 0.5 percent will be required. Long wavelengths, towards the red, are recommended for use.

6.2 MAPPING COVERAGE

For 100 meter resolution mapping, the data storage rates limit the field of view of the television and optomechanical scan systems to about 10 degrees. Furthermore, the data transmission rate limits the total area that each candidate photo-imaging system can map during one orbit.

The baseline orbit will permit medium resolution mapping of about 32 percent of the total Martian surface within one month's time if a 10 degree field of view sensor is used. The baseline orbit, however, is required to satisfy a whole series of orbit constraints including those designed to enhance capsule descent and landing conditions. Thus, it is not an optimum orbit for photo-imaging. However, orbit optimization for photo-imaging will not of itself significantly shorten mapping time. If mapping is to be completed within shorter time periods, the data rate must be increased.

6.3 CANDIDATE SYSTEMS

Based on performance, reliability, availability, and impact upon the spacecraft, the three candidate systems, Television, Photographic Film, and Optomechanical Scanning can perform useful photo-imaging experiments of the Martian surface from an orbiting spacecraft. The chief performance differences have been found to be in the sensing of very low contrast scenes, such as are expected on Mars. The lack of uniformity and potential radiation damage are major questions in the low contrast performance of film. Similarly, the design of the Optomechanical Scan System has a marginal signal output for the high resolution mission.

6.4 IMPACT UPON SPACECRAFT

Evaluating all impacts, such as weight, power, and attitude control accuracy, and expressing them in terms of the total planetary vehicle weight increase above the baseline design, the lightest system is the combination of a medium resolution Optomechanical Scanner and a high resolution Television System. This is due to the simplicity of the Scanner when it is used for a medium resolution application, and the low platform weight of the Television system.

Of the individual systems, the heaviest is television for 100 meter resolution and film for 10 meters. Any combination of film and television is heavier by at least 100 pounds than use of either for both resolution missions.

6.5 RELIABILITY

Reliability is the major problem of the candidate photo-imaging systems. Although each candidate design was based on work of a previous flight program (Mariner, Nimbus, Lunar Orbiter and ATS), potential unreliabilities are present in each. For example:

Television - tape recorder; Vidicon

Photographic Film - radiation effect on film; processor

Optomechanical Scanner - scanning mechanism

General - electromechanical devices; image motion compensation

An image motion compensation sensor for the low contrast Martian surface is the most complex and difficult development required.

The use of three television cameras and of three optomechanical scanners makes possible complete loss of one camera or scanner with only 33 percent reduction in the rate of mapping. On the other hand, if a tape recorder failure occurs, the television cameras and optomechanical scanners can scan slower to produce pictures of poorer resolution which can then be telemetered directly back to Earth. These degraded modes of operation could lead to a high degree of realization of mission objectives despite a major element failure.

The following studies, developments, and evaluations will assist in the definition of photo-imaging requirements and in the selection of systems with the best performance and reliability. Therefore, we recommend they be carried out in the near future.

6.6 MISSION STUDIES

These studies are required to provide a more detailed definition of the photo-imaging objectives and to determine suitable techniques to meet these objectives. Analytical and physical modeling of the Martian surface and atmosphere is needed to perform tradeoffs between spatial and intensity resolution, intensity and spectral (multicolor) resolution, and topographic mapping using stereographic as opposed to clinometric techniques. How should data bits be allocated between medium resolution, high resolution, color and stereo pictures? What information should be gathered during the early orbits to optimize operation during the remainder of the orbiting phase?

6.7 ORBIT AND COVERAGE STUDIES

Additional orbit studies are needed to determine not only the optimum orbits for photo-imaging, but the cost in propulsion and guidance accuracy in achieving these orbits. A comparison of the orbits selected for a Voyager with an orbiter and a soft lander, an orbiter and an atmospheric probe, and an orbiter only would be useful. What overlap is required between frames in the same ground trace and adjacent ground traces in order to be able to piece the frames together into a map? At high altitudes and latitudes or in

near-synchronous orbits the amount of overlap becomes excessive. How must the field of view, the time between frames, and the orbit period be varied and adjusted in order to control the amount of overlap?

6.8 OPTICS STUDIES

Advanced techniques should be studied to improve the design and decrease the large physical dimensions of the optics. Zoom lenses for resolution control at varying altitudes should be investigated.

6.9 DATA RATE STUDY

Methods of increasing the data transmission rate need definition to determine required development tasks. Feasibility of attaining higher data compression ratios needs to be investigated.

6.10 TAPE RECORDER DEVELOPMENT

This development should emphasize long-life reliability, higher record rate, and larger capacity. More sophisticated ways of combining analog recorders having high input rates and digital recorders having high amplitude accuracy should be studied in order to arrive at a storage system which gives 0.5 percent accuracy at record rates exceeding 100 kHz.

6.11 IMAGE MOTION COMPENSATION DEVELOPMENT

An image motion sensor that will reliably operate with the low contrast targets expected on Mars should be developed for all the candidate photo-imaging systems. This is the most difficult problem area encountered.

6.12 OPTOMECHANICAL SCANNER DEVELOPMENT

Since this is the newest concept and offers promise of simplicity and low weight, a development and feasibility study should be conducted. Direct telemetry of data in a degraded, lower resolution mode in case of tape recorder failure, makes this approach quite attractive.

6.13 FILM RADIATION EVALUATION

Evaluation of the fogging and other effects of particle radiation is required. This includes fogging experiments, and analysis to estimate shielding requirements for both natural and RTG radiation environments.

6.14 LOW CONTRAST FILM EVALUATION

Evaluation of the low contrast performance of film is needed, particularly with respect to intensity distortions and nonuniformities. Conclusive results of such evaluation could confirm or eliminate film as a contender for the Voyager mission.

6.15 FILM PROCESSOR EVALUATION

Long-life storage tests of candidate film processors are needed to ensure that Voyager life requirements can be met reliably.

APPENDIX A

OPTIMUM COVERAGE ORBITS

A.1 INTRODUCTION

In mapping the surface of the earth, moon, or a planet with an imaging system, the areas that are seen are determined by the path that the orbiting spacecraft follows. This path can be chosen such that the maximum amount of surface area will be overflown in minimum time with proper overlap between adjacent frames. Such a path is defined as an optimum coverage orbit, and a generalized solution for such an orbit is presented here. The development of the method is completely independent of any sensor hardware considerations, except for the imaging sensor angular field of view.

The method results in a closed form mathematical relationship between all the orbital parameters which describe the Flight Spacecraft's path about Mars, such that the maximum available planetary surface may be mapped in minimum time with a known and controlled amount of overlap between picture swaths. Such a method also defines the minimum field of view of the sensor in order to achieve full coverage.

A.2 METHOD

One can obtain full coverage by considering how a photographic or TV imaged swath is produced on the planetary surface. There are three independent motions which generate the ground track of the satellite over the planetary surface; these are the angular rotation of Mars, the motion of the Flight Spacecraft in its orbital plane, and the angular rotation of the orbit plane in inertial space or the so-called rotation of the line of nodes. The sensor is assumed to be aligned along the local vertical so that the center of the field of view coincides with the subsatellite point or the ground track. Figure A-1 shows the Flight Spacecraft at altitude h above the Martian surface with a sensor field of view of γ degrees producing a coverage swath of width, s. Now the object is to produce a combination of orbit parameters and a sensor field of view that yields perfectly interlacing swaths about the planet's surface in some selected nominal time period. We pick the minimum time in

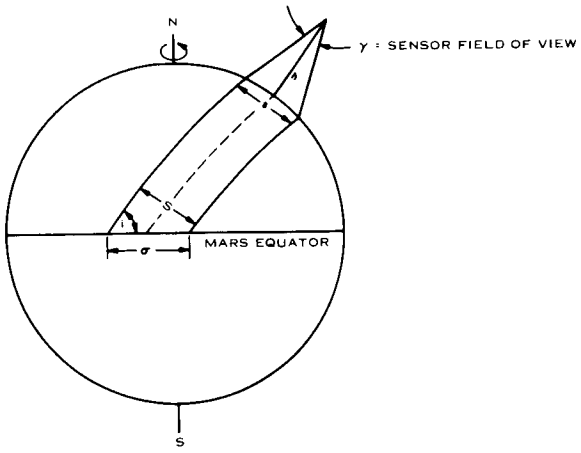

$$\sigma = 360^{\circ}/n$$

$$s = \frac{\pi R_M}{90}\left\{180 - \sin^{-1}\left[\left(\frac{h+R_M}{R_M}\right)\left(\sin\frac{\gamma}{2}\right)\right] - \frac{\gamma}{2}\right\}$$

$$S = \frac{\pi R_M}{180}\sin^{-1}\left\{\sin s \sin\sigma\right\}$$

Figure A-1. Mapping Coverage from an Orbiting Spacecraft

terms of an integer number of Martian planetary rotations, N, about its own axis in inertial space. One such inertial rotation takes a little more than 24 hours and 37 minutes and may loosely be considered the length of a Martian day. The importance of the integer N is that it defines the number of photo-imaging swaths that will be generated between any two successive ground tracks such as m and m + 1. Next we consider the Martian equator as a circle cut into an integral number of arc segments, n, corresponding to the number of Flight Spacecraft revolutions about the planet necessary to accomplish full coverage. Each cut on the equator simulates the point where the ground track will intersect the equator. (For reasons that will become clear later, the integer n is equal to (Nj-k), where j and k are also integers to be selected. A restriction on the selection of integer k is that the fraction k/N must be irreducible. For instance, the values k=15, N=30, which yield k/N = 15/30, are disallowed since they reduce to the fraction 1/2, representing the case k=1, N=2.) To insure coverage, the width of the swath S generated by the sensor must be equal to or greater than each of the n equatorial arc lengths. Each arc has an angular

"length" equal to $\sigma = 360^{o}/n$. When the orbit is purely polar, $i=90^{o}$, then S must be chosen equal to $\sigma\pi R_M/180$, where R_M = 3393 km is the equatorial radius of Mars. When the orbit is not polar, a smaller S may be chosen due to the forshortening effect of the inclination so that $S = (\pi R_M/180)\text{SIN}^{-1}$ (SIN i SIN σ). These relationships are listed in Figure A-1. Although it is not immediately obvious, the maximum coverage constraint must always be satisfied at the equator regardless of orbit eccentricity and periapsis location. Based upon the values of N, j, and k selected, orbit parameters are generated such that the Flight Spacecraft will experience a repeat cycle over the Martian landscape every n revolutions, and the center of each swath will be equally spaced from the center of each adjacent swath by exactly σ degrees of longitude.

All of the results are based upon the following considerations from the schematic of Figure A-2, which has been drawn for N=30. This represents a repeat cycle every 30 Martian days, or approximately 30 days, 18 1/2 hours in our time system. N may be selected as

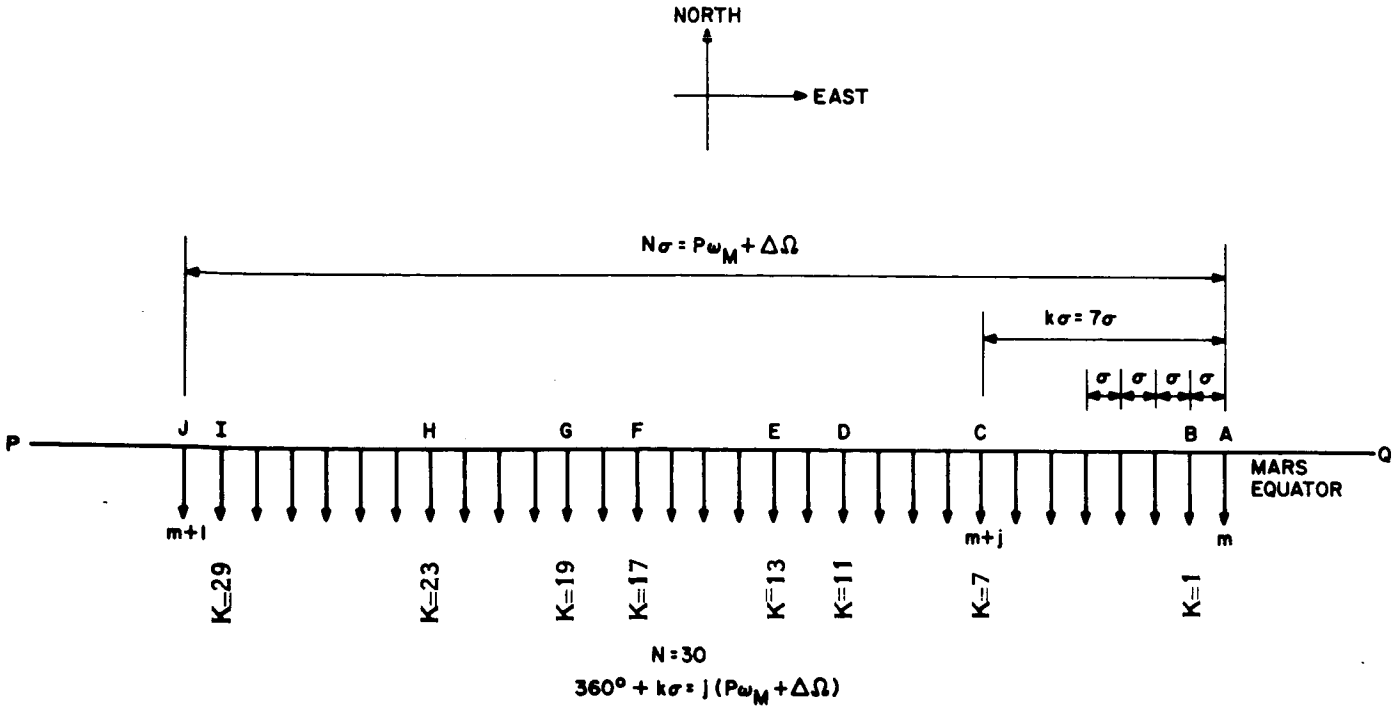

Figure A-2. Schematic of Optimum Mapping Coverage

any integer, depending upon the frequency of the repeat cycle desired. Line PQ represents any segment of the Martian equator and the arrows pointing downward represent the direction of the Flight Spacecraft's ground track as it passes downward through the equator. Nomenclature in the sketch is as follows:

N = nominal cycle in Martian days for which a repetitive uniform coverage pattern is desired. N may be any integer.

σ = the number of longitudinal degrees of spacing between neighboring ground tracks after n revolutions

n = total number of revolutions required for the coverage cycle. n is an integer.

ω_M = Mars angular rate of rotation in degrees per second = $0.40611886 \times 10^{-2}$

P = period of the Spacecraft from ascending node to ascending node in seconds

k = the skip parameter, a positive integer with a range of values from k=1 to k=N-1

j = a positive integer with a range of values from j=2 to j=14

$\Delta\Omega$ = the number of degrees of longitudinal precession of the orbital plane with respect to Mars per Spacecraft revolution about the planet

m = some generalized revolution number of the Spacecraft about Mars

In one revolution, the ground track moves about Mars from point A to point J. The longitudinal shift of the ground track after one revolution is equal to the number of degrees that Mars rotates during one revolution plus or minus the number of degrees that the orbital plane has precessed during one revolution. This is equal to $(P\omega_M \pm \Delta\Omega)$ degrees. Since we wish the ground track to exactly repeat after N Martian days and we wish the spacing between adjacent ground tracks to be equal to the constant σ degrees we set:

$$N\sigma = P\omega_M \pm \Delta\Omega \qquad \text{(A-1)}$$

or

$$\sigma = (P\omega_M \pm \Delta\Omega)/N \qquad \text{(A-2)}$$

The ground track of the $(m + j)^{th}$ revolution will lie somewhere between n and n+1. We can obtain uniform planetary coverage by forcing the $(m + j)^{th}$ revolution to pass through any of the N-1 equally spaced points. However, the point which is chosen for the $(m + j)^{th}$ ground track must correspond to a skip parameter, k, such that k/N is an irreducible fraction. Thus, for the 30-day case under consideration, the only permissible k's are 1, 7, 11, 13, 17, 19, 23, and 29 as shown in Figure A-2, and labeled as points B, C, D, E, F, G, H and I. After j revolutions of the Flight Spacecraft after leaving point A, we force the j^{th} ground track to shift to some acceptable k point such as point C where k=7. After j revolutions of the Flight Spacecraft, this shift is equal to the angular rotation of Mars plus or minus the orbital precession, $\Delta\Omega$. For $0^o \leq i \leq 90^o$, $\Delta\Omega$ is chosen negative and for $90^o \leq i \leq 180^o$, $\Delta\Omega$ is chosen positive.

Therefore, we can say:

$$360^o + k\sigma = jP\omega_M \pm j\Delta\Omega \tag{A-3}$$

or

$$360^o + k\sigma = j(P\omega_M \pm \Delta\Omega) \tag{A-4}$$

Substituting for σ in Equation (A-4) we obtain:

$$360^o + k/N\,(P\omega_M \pm \Delta\Omega) = j(P\omega_M \pm \Delta\Omega) \tag{A-5}$$

or

$$360^o = (P\omega_M \pm \Delta\Omega)(j - k/N) \tag{A-6}$$

After N planetary revolutions Mars will turn through an angle of $N \cdot 360$ degrees. Meanwhile, the ground track is indexing $P\omega_M + \Delta\Omega$ degrees every orbit revolution. Thus, the number of revolutions, n, required for any repeat cycle equals:

$$n = \frac{N360}{P\omega_M \pm \Delta\Omega} = N(j - \frac{k}{N}) = N_j - k \quad \text{revolutions} \tag{A-7}$$

Or, saying the same thing in another way, the Flight Spacecraft will appear over the same Martian subsatellite point every N_j-k revolutions. Factoring Equation A-5 and solving for the period P we obtain:

$$P = \frac{1}{\omega_M}\left\{\frac{360}{j - \frac{k}{N}} \pm \Delta\Omega\right\} \text{ seconds} \qquad \text{(A-8)}$$

For an oblate planet, the period may be expressed as:

$$P = 2\pi\sqrt{\frac{a^3}{\mu}}\left\{1 - J\left(\frac{R_M}{a(1 - e^2)}\right)^2\left(\frac{7\cos^2 i - 1}{4}\right)\right\} \text{ seconds} \qquad \text{(A-9)}$$

where a is the semi major axis in kilometers, μ is $(0.42830 \pm 0.00008) \times 10^5$ km^3/sec^2, J is the oblateness potential chosen to be 2.52×10^{-3}, e is the orbit eccentricity, and i is the orbit inclination in degrees.

Also, the angular rotation of the orbital plane during one revolution of the Spacecraft is given by:

$$\Delta\Omega = -360J\left\{\frac{R_M}{a(1 - e)^2}\right\}^2 \cos i \quad \frac{\text{degrees}}{\text{revolution}} \qquad \text{(A-10)}$$

Substituting Equations A-9 and A-10 into A-8 we obtain:

$$2\pi\sqrt{\frac{a^3}{\mu}}\left\{1-J\left(\frac{R_M}{a(1-e^2)}\right)^2\left(\frac{7\cos^2 i - 1}{4}\right) = \frac{1}{\omega_M}\left\{\frac{360^\circ}{j-\frac{k}{N}} - 360J\left(\frac{R_M}{a(1-e^2)}\cos i\right)\right\}\right. \qquad \text{(A-11)}$$

Note that the form of Equation A-11 causes the fraction k/N to be only significant in its most reduced form such as 1/3 rather than 2/6, 3/9, etc.

This equation is now solved for the semi major axis, a, by an interative technique for any desired inclination and eccentricity. If it is desired to hold the periapsis altitude, h_p, constant at the minimum permissable level, eccentricity may be inputted in the form:

$$e = (a - R_M - h_p)/a \tag{A-12}$$

In this manner one can obtain any desired set of orbits which are precisely Mars repetitive after N Martian days for all altitudes, inclinations and eccentricity. The duration of each repeat cycle or the mission life for complete coverage, T, is given by:

$$T = nP = n2\pi\sqrt{\frac{a^3}{\mu}}\left\{1 - J\left(\frac{R_M}{a(1 - e^2)}\right)^2\left(\frac{7\cos^2 i - 1}{4}\right)\right\}\text{seconds} \tag{A-13}$$

A.3 EXAMPLES

COP, or Coverage Optimization Program, is the name of the General Electric 605 Computer Program which has been written to solve the equations developed in the previous section. COP will be used to generate a set of optimum orbit parameters satisfying any given set of constraints. These orbit parameters are then used to run PASS, or the Planetary Area Seen by a Satellite program, which outputs planetary coverage as a time function for given lighting and altitude conditions.

COP was used to generate the set of orbits which yield uniform coverage over 30 days, holding periapsis at 1000 km and varying apoapsis from 6000 to 16,000 km. Results are shown in Figures A-3, A-4 and A-5 for inclinations between 20 and 160 degrees. Each curve is identified by the skip parameter, k, total revolutions required for coverage, n, and the longitudinal spacing between ground swaths, σ. In each figure there also appears a single curve representing the set of sun-synchronous orbits for a periapsis of 1000 km. Where the curves intersect, the double constraint of uniform coverage and sun-synchronism is satisfied.

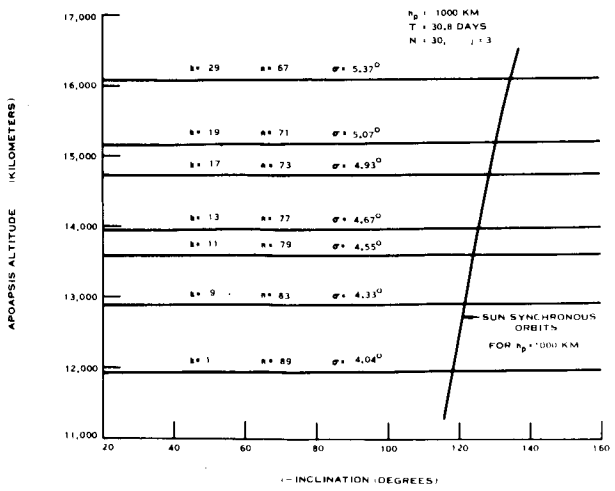

Figure A-3. Optimum Orbit Results (12,000 to 16,000 km Apoapsis)

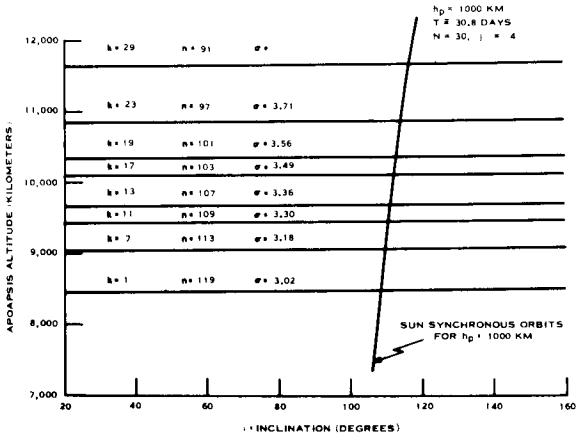

Figure A-4. Optimum Orbit Results (8,000 to 12,000 km Apoapsis)

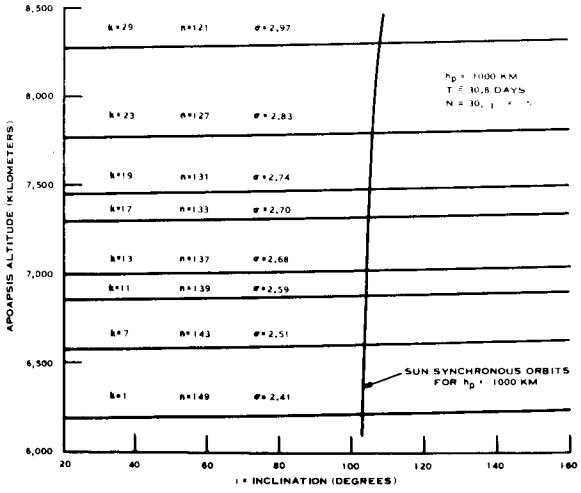

Figure A-5. Optimum Orbit Results (6,000 to 8,000 km Apoapsis)

A.3.1 NOMINAL ORBIT

An example of the use of these curves may be illustrated by considering the nominal orbit having the following parameters:

Inclination	= 40 degrees
Periapsis altitude	= 1000 km
Apoapsis altitude	$\cong$ 12,000 km
Argument of periapsis	= 336 degrees

From Figure A-3, it may be seen that 30-day uniform coverage may be achieved between 40^{o} south latitude and 40^{o} north latitude by selecting an apoapsis altitude of 11,950 km ($k = 1$, $n = 89$, $\sigma = 4.04^{o}$). Figure 3-11 shows that the periapsis point will shift approximately 0.22 degrees/rev. Since 89 revolutions of the Spacecraft are required before the 30-day coverage is complete, the total angular travel of periapsis within the orbit plane may easily be calculated as (89 rev) (0.22 deg/rev) = 19.6 degrees. Thus, only a relatively narrow Martian latitude band ($< 15^{o}$) is observable at the periapsis altitude over the 30 days. Next, we find the minimum value of the ground swath width that must be generated by the onboard sensor. Figure A-6 shows the relationships between orbit inclination, i, longitudinal ground swath spacing, σ, and the swath width, S. For an inclination of 40 degrees and $\sigma = 4.04$ degrees, the minimum required swath width, S, may be seen to be 155 km. From Figure A-7, which plots the relationship between field of view, γ, altitude, h, and swath width, s, we find that for s = 155 km and h = 1000 km that the required minimum field of view of the sensor must be 9 degrees. It must be emphasized that to insure coverage, the field of view must be sized for the minimum altitude that will occur at the equator. As the periapsis location varies with time, the altitude at the equator is constantly changing also. For this example, it was assumed that the minimum altitude at the equator would be 1000 km.

A.3.2 CIRCULAR POLAR ORBITS

For the purposes of illustrating the coverage advantages of circular polar orbits, COP was used to generate an orbit set for 30-day coverage for circular orbit altitudes ranging from 2800 km to 950 km as shown in Figures A-8, A-9, A-10 and A-11. Also shown in each

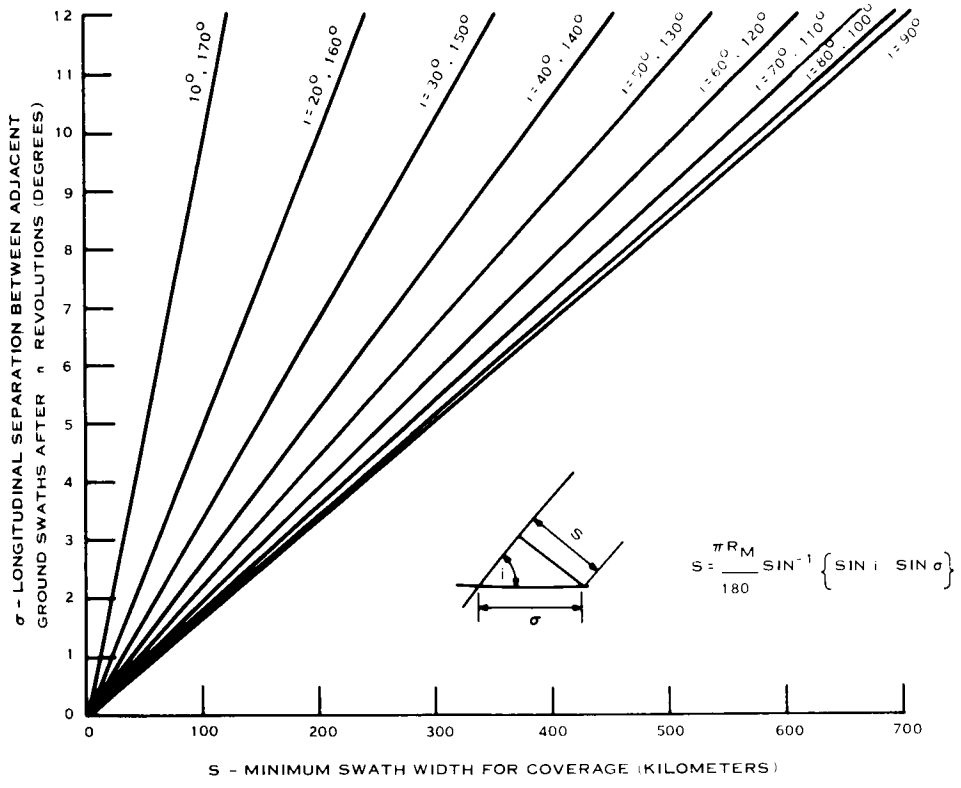

Figure A-6. Sensor Swath Width

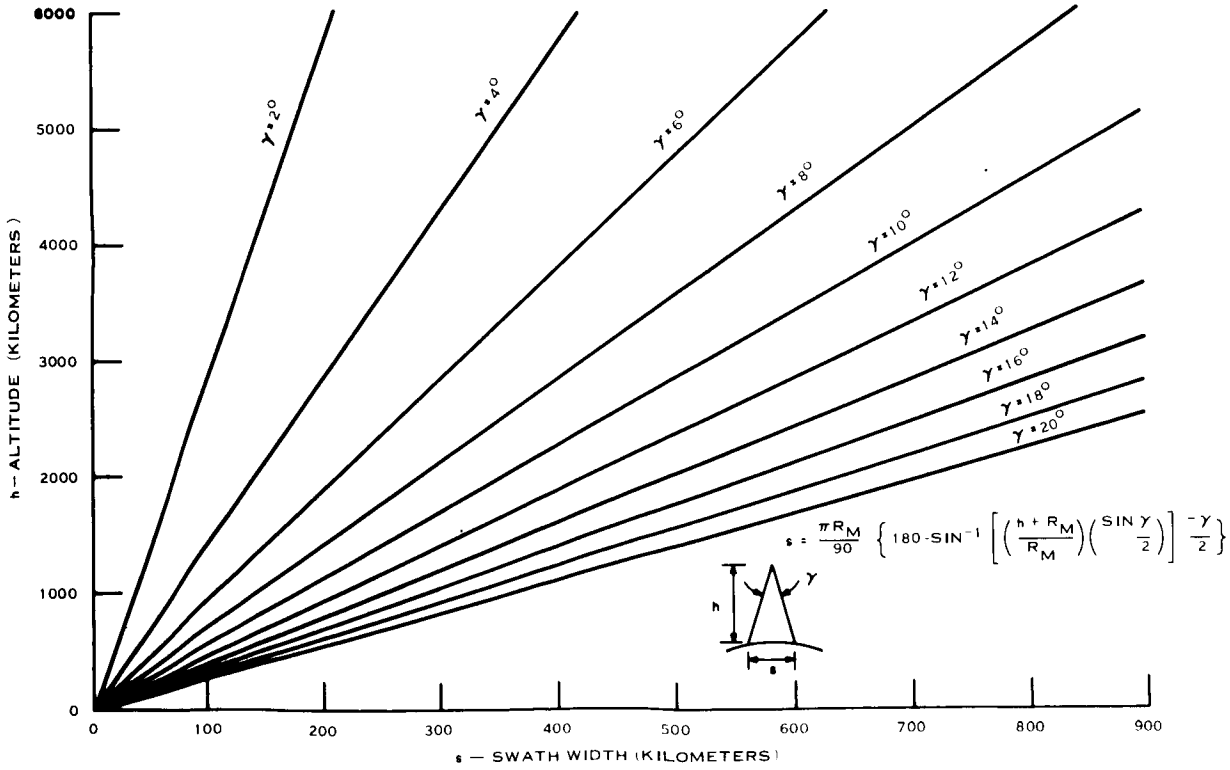

Figure A-7. Sensor Field of View

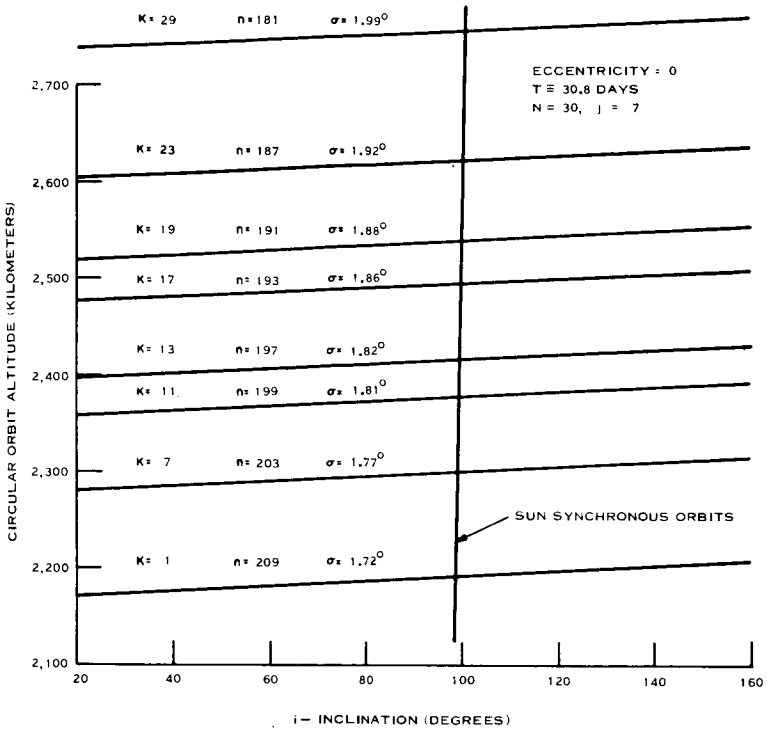

Figure A-8. Optimum Orbit Results (2200 to 2700 km Altitude)

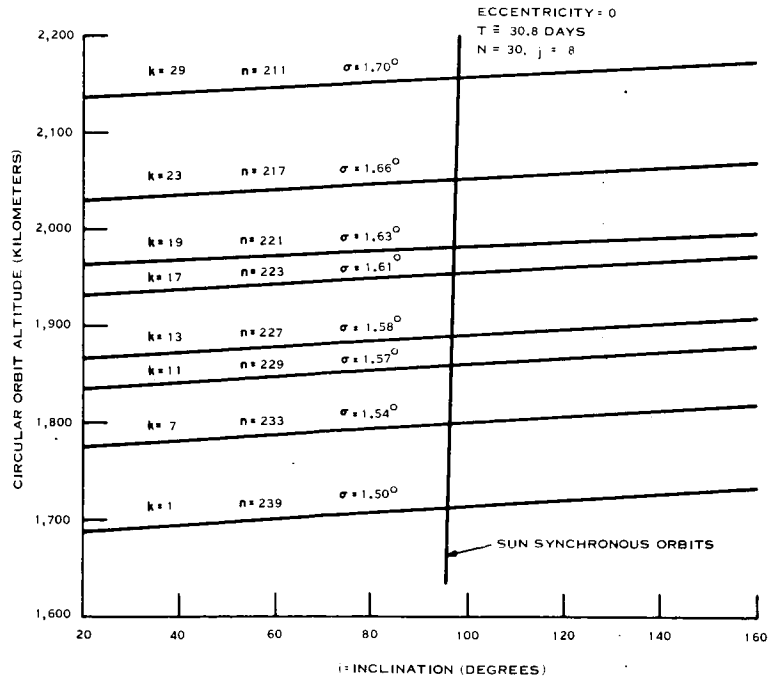

Figure A-9. Optimum Orbit Results (1700 to 2200 km Altitude)

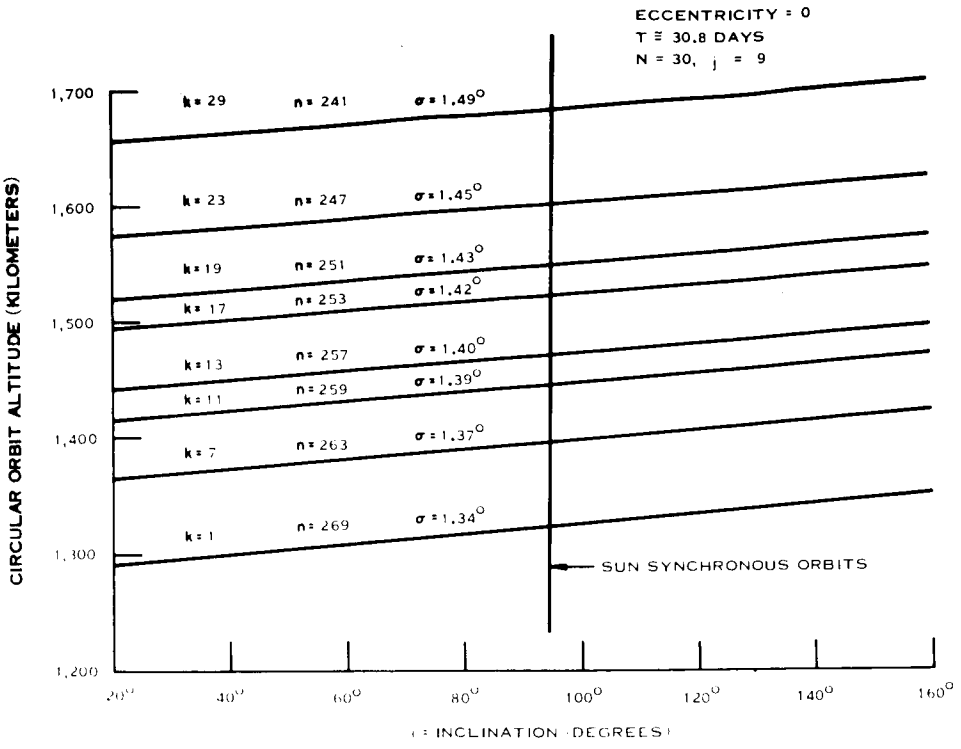

Figure A-10. Optimum Orbit Results (1300 to 1700 km Altitude)

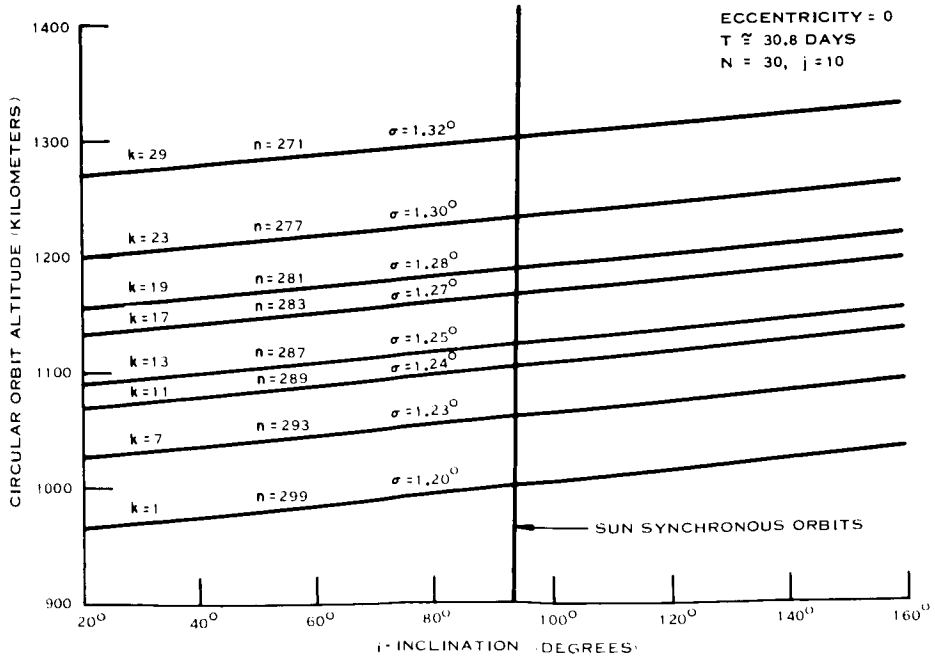

Figure A-11. Optimum Orbit Results (900 to 1300 km Altitude)

figure is the curve representing sun-synchronous circular orbits. Advantages of near circular polar orbits are (1) higher resolution, (2) constant frame size due to orbit circularity, (3) availability of entire planetary surface for mapping, and (4) option to select a sun-synchronous orbit, if constant surface illumination is seen to be advantageous.

As an example, consider the case of $k = 1$, $n = 299$, $\sigma = 1.20$ degrees and $h = 1002.5$ km, as shown in Figure A-11. By choosing an inclination of 93.5 degrees, we assure 100 percent coverage of the entire planetary surface within 30 days, as well as constant illumination conditions on the surface. From Figures A-6 and A-7 the minimum swath width required and minimum field of view are 70 km and 4 degrees, respectively.

APPENDIX B

EFFECT OF RADIATION IN SPACE ON PHOTOGRAPHIC FILM

B.1 INTRODUCTION

Photographic film is meant to be activated by electromagnetic radiation of approximately the wavelength range of visible light. The exposure to the radiation must be controlled to be useful. However, there are other types of radiation to which the film is sensitive, all of which are more energetic (per photon or particle) than light; in fact, their greater energy means that they may penetrate the normal film containers and activate the film before it is intended to be activated. Thus, a supply of film may be ruined before use by undesired irradiation.

Space contains radiations in the form of radio waves, infrared, visible light, ultraviolet, X rays, gamma rays, electrons, protons, alpha particles, and heavier atomic nuclei. All of these except radio waves may activate the film to decrease its light-responding characteristics. Each of these occurs with a different flux and a different penetrating ability. The flux is measured in particles/cm^2sec, ergs/cm^2sec, or even watts/cm^2, the energy is measured in Mev, million electron volts, and their energy deposition in a target material in rads, 100 ergs/gram. Thus, with a flux of 4×10^5 protons/cm^2 sec (as in the Van Allen belts) and, with each proton depositing energy in aluminum at 9 Mev/gram/cm^2 (50 Mev protons), the dose rate will be 0.06 rads/sec or 1.44 rads/hr. If the film-shielding limits the dose to 50 rads (see below), the film can only remain there for 35 hours without protection.

Radiations can be stopped by interposing material such as black paper for light or lead for X rays. The thickness can be measured in centimeters, but usually it is given in grams/sq cm. Aluminum is most convenient, for it may serve as part of the regular structure, although water, polyethylene, or liquid fuel could also be used. The shield is necessarily neither a single material nor continuous in depth. The important item is grams/cm^2 along the track or trajectory of the radiation. Therefore, all the parts of the spacecraft structure form a part of the shield and hence decrease the extra weight which should be added to the spacecraft to protect the film.

The added weight is the cost of safeguarding the unexposed film; of course, once the film is exposed and developed, there is no need for further protection. In this sense, an optimum shield weight may be found for each mission. The Voyager mission will be taken as 6.5 hours in the Van Allen belts, 6 months in traveling to Mars, and 6 months in orbit about Mars, all this taking place in 1973 and 1974.

These items (radiation effects, radiation environment, shielding considerations, weights required) and results will be discussed in the following sections.

B.2 GENERAL EFFECTS OF RADIATION OF FILM

B.2.1 FILM ACTIVATION AND DEVELOPMENT

A film consists of an emulsion laid down on a base. The base provides a stable carrier for the emulsion. It is commonly 2.5 or 4.5 mils thick, is made of a transparent plastic such as Estar, Cronar, or triacetate, and may be any width (in Voyager's case probably 70 millimeters wide) with or without sprocket holes.

The emulsion is a suspension of silver bromide crystals in a clear gelatin. These crystals are small, 10 microns or less, with the size being one criterion for resolution and speed. The majority of the grains to be used in the present film are between 0.3 and 0.5 μ in diameter. This provides high resolution but low speeds. When struck by a light photon, the silver bromide crystal has an electron knocked out of its normal location so that an atom has been ionized. Each crystal or grain now has an abnormal spot about which silver atoms may congregate. The number of spots depends upon the number of photons which strike the emulsion so that the blackening caused by the silver is a function of the flux of photons. In the same way, if several photons hit one grain, there will be more nucleating points on that grain and hence a darker negative. When the film is placed in a developing solution, the ionization and nucleating processes are continued being controlled by time and temperature. A fixing solution is added which stops the process so that the final degree of darkening is controlled by the developing as well as the activating stages. In one Voyager candidate system, the developing and fixing processes are accomplished by pressing a Bimat or Poromat strip against the exposed film. Thus, one is also concerned about maintaining a suitable environment for the second material.

B.2.2 FILM CHARACTERISTICS

The characteristics of the emulsion-developer-fixer process are generally given as the gamma, the granularity, the resolution, and the S/N ratio. The gamma is the slope of the straight portion of the line expressing the relation between the optical density and the logarithm of the exposure. A slope of 1 means that the scene lights and shadows will be reproduced accurately. If gamma is higher, the contrast is heightened. If gamma is smaller, the contrast is low or the photograph is flat.

The granularity refers to the standard deviation of the grain size in the developed photograph. Usually, the density of the negative is measured with a microdensitometer having an aperture of 48 microns in diameter. Variations in density are easily detected; from these variations, the standard deviation or granularity can be calculated. The data are taken at a density of 1.0 for standardization, for the granularity varies with the square root of the density. For photographs capable of showing fine detail, the granularity should be smaller than 0.01 optical density units (logarithm of the opacity).

The resolution of adjacent items on a film depends principally upon the grain size with small grains producing the highest resolution. Such items must be formed by groups of developed or darkened grains separated by undarkened spaces. Statistical fluctuations can thus be uniform to produce patterns or random to destroy them. Although this is described better by a signal-to-noise ratio (S/N), it is obvious that only with small grains can small image details be detected.

Noise in an image may be caused by lens aberrations, atmospheric turbidity, variation in film sensitivity to light, and actual light flux variations on a photon scale. These may be systematic or random, but, in either case, statistical treatments of the data are necessary. Usually, the RMS of these fluctuations is the measure of noise. The S/N then will depend upon the size of the signal. Therefore, radiation degradation will affect the S/N by limiting the range of signals or the contrast in the image. The extent to which the S/N can be degraded in the film by radiation will depend upon the other contributions to the final telemetered signal and the tolerance or specifications set down elsewhere.

B. 2. 3 RADIATION DOSAGE

The effects of radiations on the characteristics curve are shown in Figure B-1. Here the curves indicate that the gamma decreases with increasing absorption of energy for both SO226 and SO243 films. Since the SO226 film is activated at a smaller exposure (note negative logarithms), it is a faster film than the SO243, but it is also affected more strongly than the SO243. The film is darkened with radiation so that the total contrast is lowered.

Even though the gamma is raised by the radiation, the electronic circuits can correct for this, if the gamma is changed as little as shown in Figure B-1. The important feature is that the base fog is raised by the radiation, which means that the usable density range is decreased. For other reasons, the base fog point should not be raised above 0.6 density units. Thus the radiation dose should be kept below 100 rads for the SO-243 film.

The granularity is increased with irradiation. Table B-1 shows the percent of increase. This increase is caused in part by the density increase from radiation, since the granularity

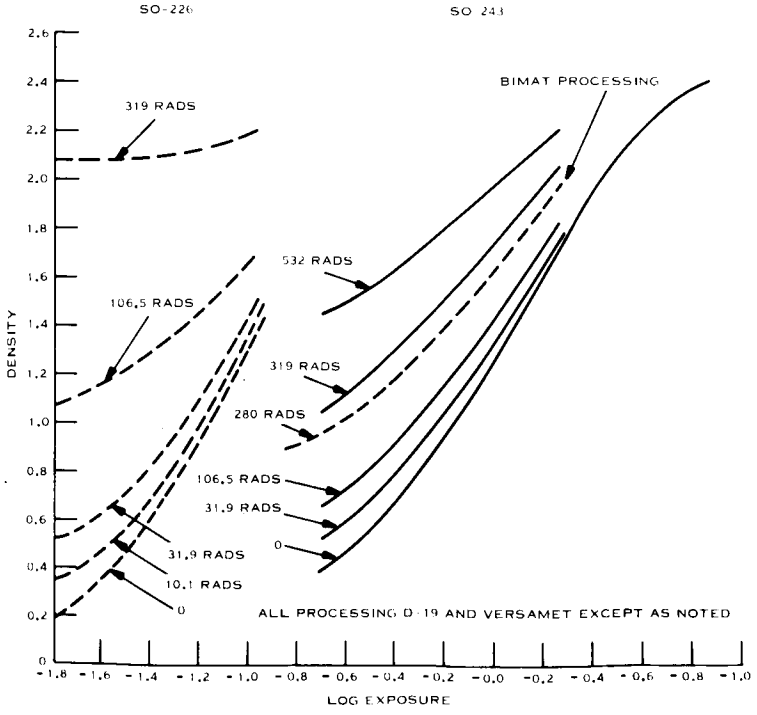

Figure B-1. Characteristic Curves After Proton Irradiation

Table B-1. Film Variation with Proton Irradiation for SO-243 Film

Radiation (rads)	Granularity Increase (percent)	S/N Change (db)
0	0	0
32	15	-1.3
106	30	-2.7
280	56	-5.8
319	61	-6.5
582	92	-10.5

is approximately proportional to the square root of the density according to Mees. It is expected that the granularity could be increased by 30 percent, which means the radiation should be kept below 100 rads.

Since the grain size is changed but little during irradiation, the resolution should not be affected. However, the background plays a large part in the resolution because the contrast is decreased. Therefore, an irradiated film with a higher base fog will have a lower resolution. Furthermore, the resolution is proportional to the granularity, so this increase in granularity will further degrade the resolution. A limit to the dosage will depend upon the other features.

The signal-to-noise ratio will be decreased by radiation because of the decrease in density range in the image. Table B-1 shows this effect with radiation. From other considerations (e.g., communication equipment) the S/N should not fall by more than 1.5 db or the dosage should be limited to 50 rads.

There is another serious problem caused by charged particle bombardment in the tracks formed in the emulsion. As is pointed out by Casanati, "The passage of a charged particle through the emulsion is represented by a track of metallic silver grains, visible after the development process, under the microscope. In this case, the track analysis is a more

suitable method than density measurements." The tracks produced by charged particles are a function of the path length of the particle, the particle velocity, charge, and energy. Solar protons traversing the film parallel to the film plane will have a large delta ray density (a delta ray is a track produced by electrons set in motion by the field of the charged particle.)

It is expected that these tracks could interfere with analysis of the image with respect to the limiting size of detectable ground features. The size of these tracks can vary with the particle energy and type. Furthermore, the effect upon the photograph interpretation will be intimately connected with the other portions of the equipment.

B.2-4 RECOMMENDED RADIATION LIMIT

From the above attributes, the limit should be kept below 100 rads with respect to gamma, base fog, granularity, and resolution. On the other hand, the S/N ratio degradation indicates that the radiation should be limited to 50 rads. It is expected that the latter is the more important case.

B.3 RADIATIONS IN SPACE

The film is sensitive to infrared, visible light, ultraviolet, X rays, gamma rays, electrons, protons, alpha particles, and heavier nuclei. The fluxes in space will be treated, and, where appropriate, the shielding indicated.

Infrared, visible light, and ultraviolet as present in sunlight will immediately expose the film. Therefore, the film will be encased in a "light-tight" container for handling before launching. This container is not expected to be removed during flight so that the film will be safely protected throughout the mission against such radiations.

X rays are present in emanations from the sun with the solar flares being the largest source. In fact, some X-ray flares have been detected behind the limb of the sun. W. A. White shows the flux measured from a small flare on March 8, 1962 as 0.225 ergs/cm^2 for X rays between 2 and 8A. This would be a dose of 2 millirads/flare. Few flares have been measured, but this should be representative.

Gamma rays are also emanated at the time of solar flares being emitted by the interaction of protons with subsequent π meson decay. Fazio shows that the energy is greater than 100 Mev, but the flux is only 10^{-2} photons/cm^{2}sec during a type 3 flare, and 3×10^{-3} photons/cm^{2}sec maximum from the quiet sun. The latter dose is roughly 0.1 rads/yr in 1 gram/cm^2 absorber while that during a flare would be 1 millirad if it lasted 24 hours (the time is probably less than 1 hour). Shielding required for this gamma ray is too high to consider, but fortunately the dose can be neglected.

Electrons can be stopped with a very thin shield (a 2-Mev electron has a range of 1 gm/cm^2); therefore, 150 mils of aluminum will be sufficient for the electrons in space. However, the Bremsstrahlung produced as the electrons are stopped could be important. On Voyager, the greatest flux of electrons will occur as it passes through the Van Allen belts. There have been numerous reports on these electrons but the one most apropos is shown in Figure B-2. This shows relative effects of protons, electrons, and Bremsstrahlung in the Van Allen belts. We note that at 2 gram/cm^2 (probably the absolute minimum shield weight) the dose rate of electrons is about two orders of magnitude less than that of protons, and the dose rate of Bremsstrahlung is three orders of magnitude less than that of protons.

Protons are by far the largest contributor to dose rates in spacecraft. Protons are present in the Van Allen belts, as a flux emanating from our sun, and as a flux traveling throughout our galaxy. These will be treated in that order.

As Voyager leaves Earth, it must pass through the Van Allen belts, unless it is launched from somewhere close to a magnetic pole. Time spent in passing through the belt will be short, say $\frac{1}{2}$ hour maximum. Although the parking orbit is expected to be below the belts, a more conservative approach was taken by assuming the orbit to be within the belts. At two hours per orbit and three orbits we have 6.5 hours. Madey has calculated a dose rate of 1.5 rads/hr behind 2 grams/cm^2 shield (protons < 40 Mev are stopped) which is a dose of 10 rads. At 10 grams/cm^2 the dose rate is 0.25 rad/hr or 1.6 rads. The electron and Bremsstrahlung rates behind a 2 gram/cm^2 shield would be 0.1 and 0.016 rads, respectively. With a 10 grams/cm^2 shield, the respective rates become 0.01 and 0.002 rads.

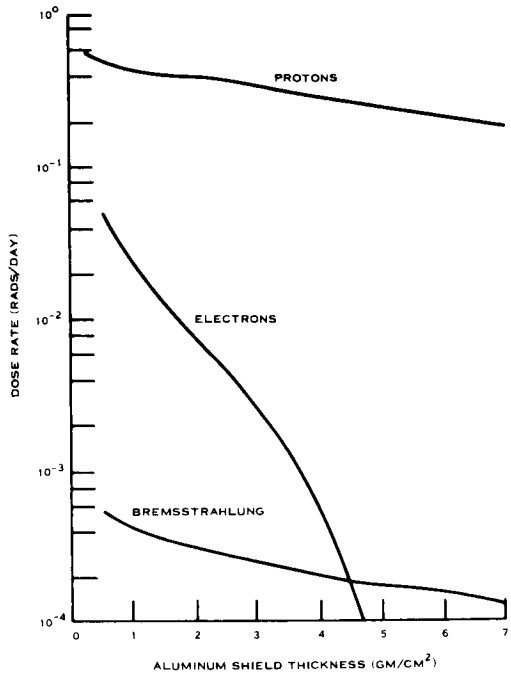

Figure B-2. Dose Rate in a Circular Orbit at 30-Degree Inclination and 240-Nautical-Mile Altitude

In the solar wind, the energy of the protons is in the kiloelectron volt range which will be screened out by a 2 gram/cm^2 shield.

Solar flares provide the source of high-energy protons with the largest fluxes. The number and size of flares are a function of the number and groupings of sunspots. The daily average of sunspots vary over a wide range (200 to 6) over a period of about 11 years. Longer periods such as 80, 150, 170, and 400 years have also been identified, but the 11-year cycle is by far the most important for Voyager. The last minimum occurred in July, 1964 so that 1973-75 will be a period with a minimum number of sunspots with its expected minimum number of flares.

There are large flares and small flares that are classified according to the area of the solar photosphere covered and the flux of particles emitted. The small flares are more

numerous, (2000 per year) than the large flares (4 to 10 per year) in maximum years to 0 to 1 per year in minimum years. Measurements have shown that the proton fluxes from large flares have produced dosages of 440 rads, May 10, 1959, to 0.5 rads, September 28, 1961, for protons >30 Mev. Table B-2 from the Solar Proton Manual shows a listing of flares during the last maximum period. Usually 2000 small flares do not produce a total dose of 1 rad from protons >30 Mev. Therefore, only the large flares are of possible concern. This is not to say that 1973 or 1975 would be a safe year, because the occurrence of flares is not predictable with respect to either their number or size. To be conservative, the average flux of protons should be factored into the shield design. The flux of protons by year are shown in Table B-3. The table shows the number of protons >30 Mev and >100 Mev dropping by a factor of 3 to 14. These energy levels are chosen because they correspond to 2 and 10 grams/cm^2 of aluminum, respectively, which represent two shielding levels apropos to the film. At 50 rads, the recommended shield will fall between these limits. The values are listed as well as the predicted years for cycle 20 according to Hess and Pounder. In calculating dose rates, the differential flux rather than the integrated flux is used and may be expressed as

$$\frac{d\phi}{dE} = 4\pi \ CE^{-b} \quad \text{protons/cm}^2 \text{ sec Mev} \qquad \text{(B-1)}$$

where C and b are constants peculiar to each flare. Figure B-3 shows some representative spectra with the parameters C and b given in Table 4 for four large flares. Note the wide variation.

The expected flare rate varies during the cycle as indicated above. The number of large flares as listed in Table B-2 indicates one aspect of the problem of predicting the occurrence of solar flares.

Galactic cosmic rays come from outside the solar system and are made up of many different particles. Protons occur in the largest number (84 percent); alpha particles (15 percent), light element nuclei (0.2 percent), medium element nuclei (0.5 percent), heavy nuclei (0.2 percent), and other nuclei make up the balance of the rays. The flux is 4 particles/cm^2 sec during sunspot minimum years and 1 particle/cm^2 sec during sunspot maximum

Table B-2. Schedule of Solar Flares

Year	Sunspot Number	Total No. of Flares	Individual Flares Date	Flux Particles/ cm^2 > 30 Mev	Galactic Cosmic Rays Particles/cm^2	Skin Dose > 30 Mev	> 100 Mev
1956			Feb 23	1×10^9		120	28
			Aug 31	3×10^7		10	--
Total	142	2576			1×10^8		
1957			Jan 20	3×10^8		60	1
			Aug 29	5×10^7		15	-
Total	190	3876			7×10^7		
1958			Mar 23	2×10^8		50	1
			July 7	3×10^8		80	1
			Aug 22	5×10^7		20	.1
			Aug 26	5×10^7		17	-
Total	185	3438			6×10^7		
1959			May 10	7×10^8		440	10
			July 10	9×10^8		148	11
			July 14	1×10^9		180	7
			July 16	8×10^8		125	19
Total	159	3805			6×10^7		
1960			Apr 28	3×10^7		6	0.1
			May 4	7×10^6		16	0.1
			May 6	5×10^6		2	-
			Nov 12	2×10^9		205	33
			Nov 15	6×10^8		100	12
			Nov 20	6×10^7		15	1
Total	112	2301			8×10^7		
1961			July 12	1×10^8		10	0.3
			July 18	2×10^8		27	3
			Sept 28	2×10^5		.01	0.05
Total	54	----			1×10^8		

Table B-3. Yearly Flux of Solar Flare Protons

Cycle 19	Year Number of Large Flares	Flux Protons/cm^2			Year Cycle 20
		E > 10 Mev	E > 30 Mev	E > 100 Mev	
1956	2	2.7×10^9	1.1×10^9	$37. \times 10^7$	1968
1957	5	10.	0.85	5.9	1969
1958	6	11.	1.3	9.6	1970
1959	4	22.	4.3	42.	1971
1960	8	7.0	2.1	39.	1972
1961	5	2.1	0.4	4.9	1973
1962		0.002	0.0003	0.003	1974
1963		0.10	0.019	0.20	1975

Table B-4. Solar Flare Parameters

Date	C	b	Proton Flux		α Particle Flux	
			> 30 Mev	> 100 Mev	> 30 Mev/Nucleon	> 100 Mev/Nucleon
Feb. 23, 1956	6.88×10^{20}	6.33	1.0×10^9	3.5×10^8	--	--
May 10, 1959	2.86×10^{10}	4.8	0.7	0.85	0.42×10^8	0.35×10^6
July 16, 1959	3.18×10^{11}	5.0	0.8	1.3	1.2	6.0
Nov 12, 1960	1.66×10^5	2.7	2.0	1.2	2.5	11.0

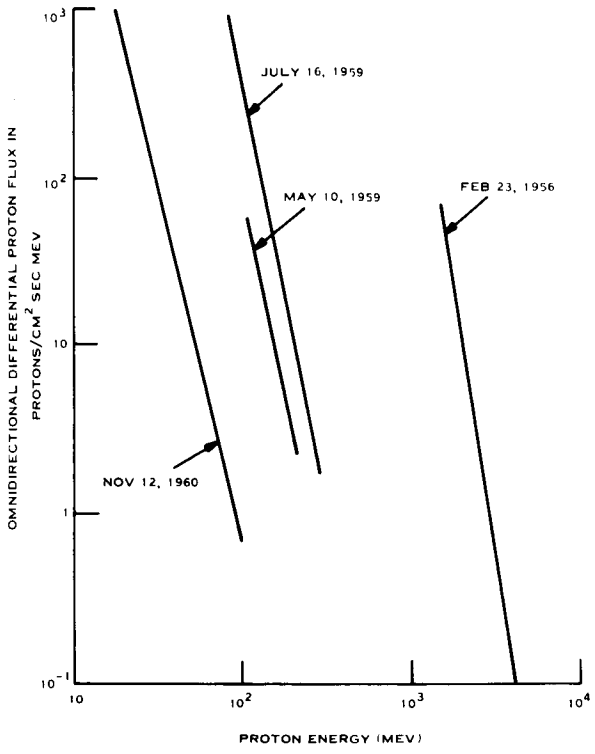

Figure B-3. Solar Flare Proton Energy Spectra

years. There is an anticorrelation, because of the variation in the interplanetary magnetic field. About 98 percent of the particles are higher energy than 1000 Mev so that they pass through most shields and deposit very little energy. In a thin sheet the dose rate has been estimated to be 2 millirads/hr by Haffner which makes the annual dose 17 to 18 rads.

Alpha particles in galactic cosmic rays will have enough energy/nucleon to pass through any plausible shield. Being four times as effective in ionizing the film, they will increase the dose by 60 percent over that of the protons. The total dose due to galactic rays will then be close to 28 rads/year.

Alpha particles occur in solar flare emanations having fluxes approximately 10 percent of that of the protons for energies > 30 Mev/nucleon. The dosage will be increased over the proton dose by 20 percent behind 2 grams/cm^2. Behind 10 grams/cm^2 the alpha particle dose will be negligible because the alpha particles are attenuated 10 times as fast as the protons.

Secondary particles are those which are ejected by primary particles during a collision within a target material. They may be protons, neutrons, mesons, or similar particles. The proton and neutron and heavy meson fluxes can be calculated with computing machines. The resulting fluxes within or leaving a target then are tabulated according to the energy of the impacting proton and the thickness of the target. Ordinary targets less than 20 grams/cm^2 thick do not produce many secondaries.

Figure B-4 from Scott shows the dose in rads/flare behind an aluminum slab.

The dose behind a spherical shield is larger because all protons pass through the same thickness of material. Furthermore, such a shield would represent the structure of the spacecraft. Figure B-5 shows the dose behind an aluminum spherical shield as computed by Alsmiller, et al, for the May 10, 1959 flare. This was one of the largest flares as shown on Table B-2. One would not expect to have such a large flare during the years of a solar minimum. The dose at 20 grams/cm^2 from all secondaries is 10 percent of that of the primaries and is a smaller percentage for thinner slabs.

B.4 SHIELDING CONSIDERATIONS

Stopping powers of shields are dependent upon a process of slowing down the protons by ionization or excitation, nuclear collisions, or photon emission. For solar flare protons, the first is the most important and is normally computed by the Bethe equation. This ionization process requires the equation to take into account the initial energy of the proton, the atomic number, atomic density, the ionization energy of the target atoms, and the additive effect of various atomic specii in the target. This may be summarized in an equation for the proton range of the type

$$X = KE^{\alpha} \quad \text{grams/cm}^2 \tag{B-2}$$

where K and α are constants of the material. For aluminum Sternheimer gives K as 2.9×10^{-3} and α as 1.77 when E is given in Mev. The stopping power given in Mev/cm or Mev/gm/cm^2 is a function of the range and the energy (dE/dX) which decreases as the energy increases.

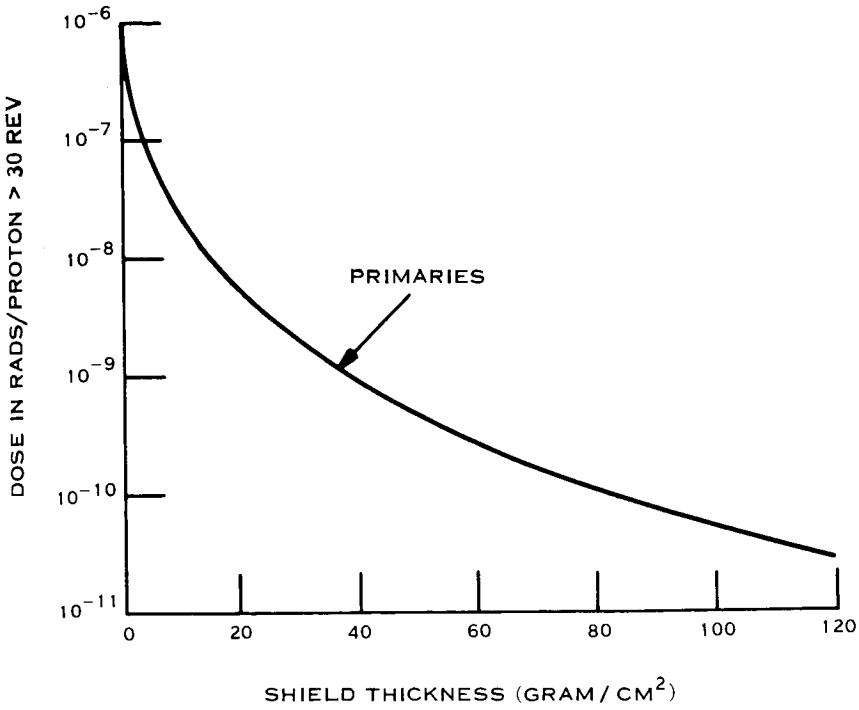

Figure B-4. Dose Behind an Aluminum Slab for a Solar Flare Spectrum ($d = 10^{-6}\ e^{-P/100\ mv}$)

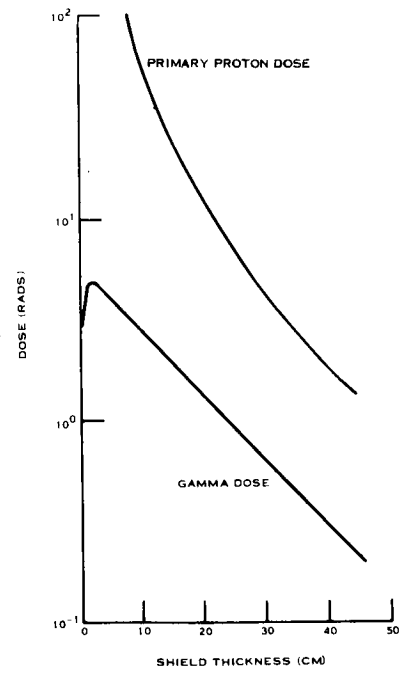

Figure B-5. Dose at Center of Aluminum Shell for Flare of May 10, 1959

Figure B-6, taken from Sheldon and deLoach, indicates that a greater flux of 130 Mev protons is needed to produce a given optical density in a film than of 10 Mev protons. Such relations show that the total dose due to a flux of protons having a spectrum of energies is not easily calculated. In fact, it means that some flares may have a large flux and deposit small doses whereas others may have 10 percent of that flux and produce a large dose. Such features may mean that a monitor could be added to determine the background on the film so that the exposure or the development times could be adjusted to account this condition of the film.

Figure B-7 shows the flux of secondaries made up of protons, neutrons, and mesons. The dose was seen to be small except for thick shields. There are also gamma rays generated as shown on Figure B-7 by Madey. Again the proportion of dose from γ rays to protons is about 1 to 100 for a 1 cm (2.7 gm/cm^2) thick aluminum shell. As shown on Table B-2, this flare was also a large one which is not expected to be repeated in a solar minimum year.

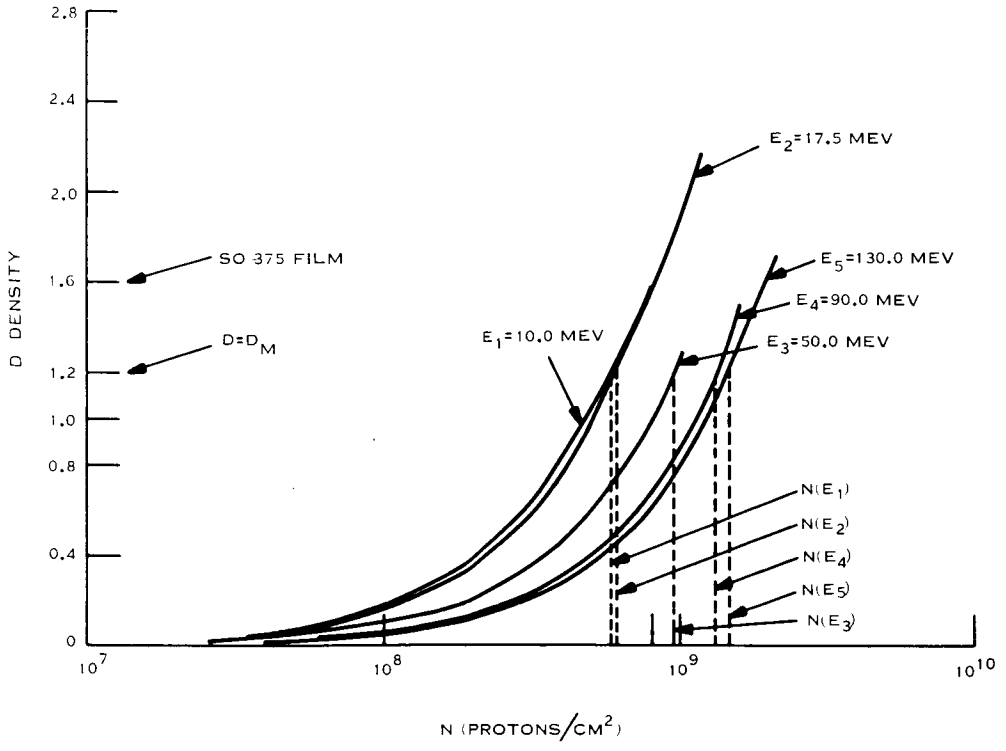

Figure B-6. Photographic Film Density as a Function of Proton Dose

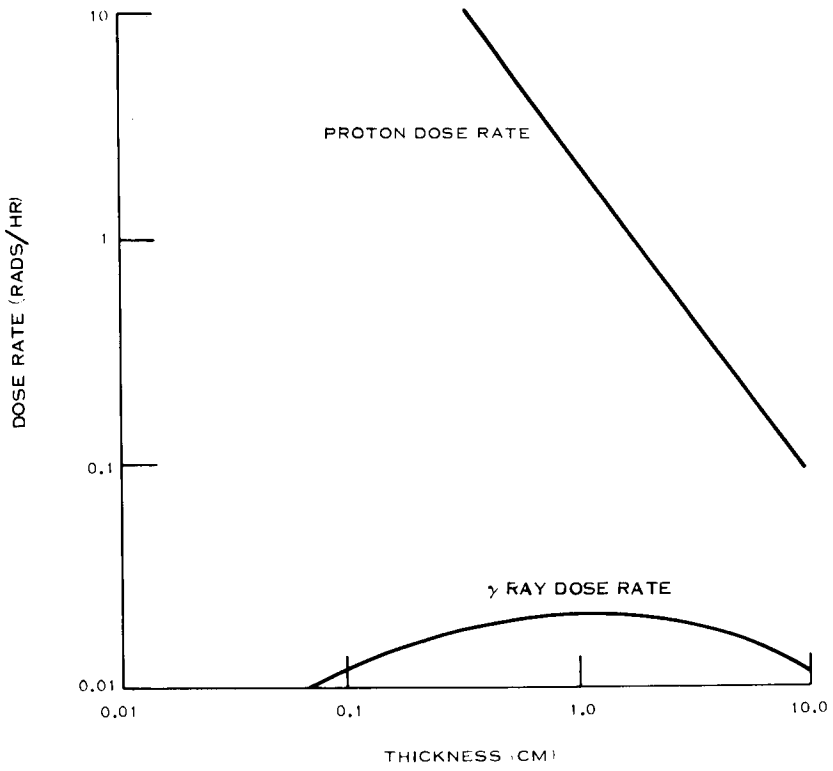

Figure B-7. Dose Rate at Center of Aluminum Shell for November 12, 1960 Solar Flare with Gamma Rays as Secondaries

Dosage calculations are done by numerically integrating the flux over the energy range, taking into account the various stopping powers at each time period during the flare. The dose from each period is then added to get the total. The calculation by Alsmiller used three different energy spectra to include the flux during the buildup, the flux during the maximum period, and the flux during the decline.

This process is repeated for each type of incident particle, e.g., protons and alpha particles. Each will have its own stopping power so that the effect of the energy spectrum will be different for each particle.

Secondary particles may be generated which are emitted during the intranuclear collisions in many directions. Each of these particles will then be slowed down according to the Bethe equation for energy loss, and, of course, these particles may generate secondary particles of their own. This process is called a cascade and has been studied for several years.

These computations must take into account the cross sections (probability) for each interaction so that the computing machine code quickly becomes quite complicated. Of course, many of these collisions do not take place unless the target is thick (> 40 gm/cm^2). For small shields such as one expects to use here, these computations are not as important because the dose due to the secondaries is 1 percent or so, which is well outside the accuracy of the estimation of the original flux.

B.5 SHIELD WEIGHTS

The dosages given above are tabulated in Table B-5. Considering the dose limit of 50 rads, one may compute the required shield thickness.

The total dose behind 2 grams/cm^2 with one large flare would be 210 rads per year using the average over all the solar flares and 63 rads per year using the average over the 4 years close to the solar minimum. Behind 10 grams/cm^2, the dose would be 40 or 41 rads per year, unless there would be a large flare such as on May 10, 1959 when the dose would be 100 rads per year.

It is apparent that the shield should be thicker than two but thinner than 10 grams/cm^2. The quantity chosen depends upon how much faith can be placed in the probability of flares occurring during the solar minimum. Because the galactic cosmic rays cannot be shielded, about 30 rads per year will be absorbed. If the period of photography were confined to the first month in orbit, this dose could be cut by 5/12 to 18 rads.

Shield thickness estimation then shows that for a 1-year mission 6.9 grams/cm^2 might be a good compromise and for a 7-month mission 6.1 grams/cm^2.

Shield weight as a function of thickness and film length or reel diameter is shown in Figure B-8. For a film length of 500 feet, the reel would be about 8 inches in diameter and the weight 6.8 lb/cm. Thus, at 6.9 grams/cm^2 the weight is 17 pounds and at 6.1 grams/cm^2 the weight is 15 pounds.

Table B-5. Dose Rates Behind 2 Grams/Cm^2

X rays	2×10^{-3}	rads/flare	
Gamma rays	1×10^{-3}	rads/flare	0.1×10^{-3} rads/yr
Electrons	1%	Proton dose/flare	
Bremsstrahlung	0.1%	Proton dose/flare	
Van Allen Belt			
Protons			10 rads
Electrons			0.1 rads
Bremsstrahlung			0.01 rads
Solar Flares			
Protons			
Average of all flux data		140 rads/flare	
Average of 4 minimum years		20 rads/flare	
Small flares			1 rad/yr
Alpha particles			
Average of all flux data		28 rads/flare	
Average of 4 minimum years		4 rads/flare	
Small flares			0.2 rads/yr
Galactic Cosmic Rays			
Protons			18 rads/yr
Alpha particles			10 rads/yr
Secondary Particles			
1% of above dose			

Dose Rates Behind 10 Grams/Cm^2

X rays, Gamma rays, Galactic rays - same as above			
Van Allen Belt			
Protons			1,600 millirads
Electrons			16 millirads
Bremsstrahlung			2 millirads
Solar Flares			
Protons	1.1 rads/flare		
Secondaries			
8% of above dose			
May 10, 1959 flare		60 rads/flare	

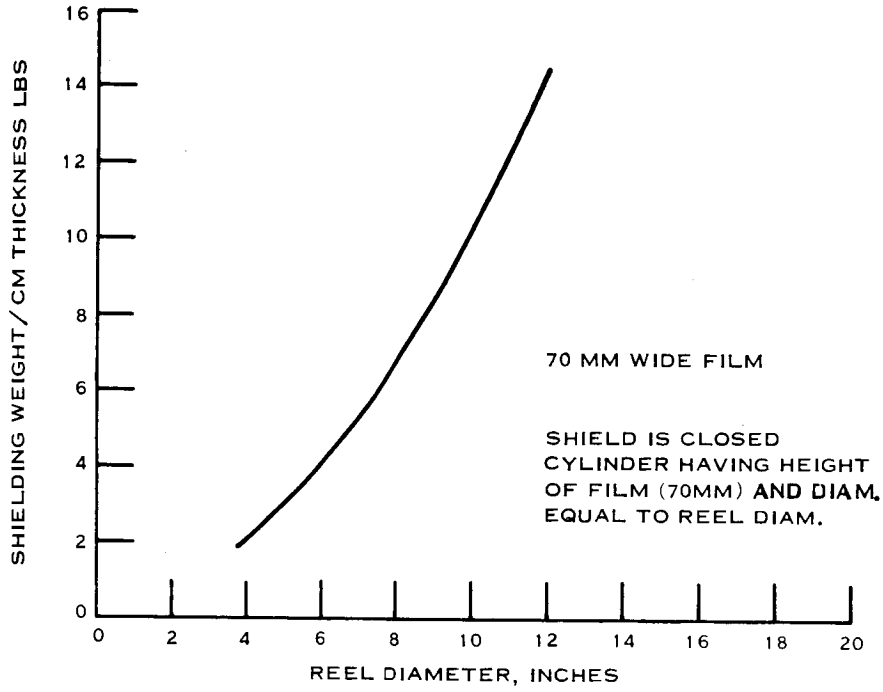

Figure B-8. Aluminum Shield Weight Per Cm of Thickness

There have been other estimates of the average flux from solar flares. Many reports have been concerned with the probability of experiencing a flare of a given size during any given time interval. The latest has been published by Snyder, who states that the probability of an astronaut receiving a given skin dose over a 1-year period is given in terms of the shield weight. By relating the sensitivity of the present film to that of skin (tissue) an estimate of the probability of irradiating the film can be obtained.

The above dose was held to a maximum of 50 rads; 28 rads are delivered by the galactic cosmic rays which were not considered by Snyder. Thus 22 is the new limit. If one takes an RBE of 1 for tissue, then the ordinates in Figure B-9 become rads. Haffner has shown that the RBE is 1 for protons having energies > 10 Mev and higher values for lower energetic protons. All protons of initial eneregy < 10 Mev will be screened out by the shield proposed, but some of those of higher energy will be slowed down to this range (0-10 Mev). To account for these let us take an RBE of 2 (the actual range in the RBE is from 1.0 to 20). Thus all ordinates on Figure B-9 would be divided by 2 to read in rads.

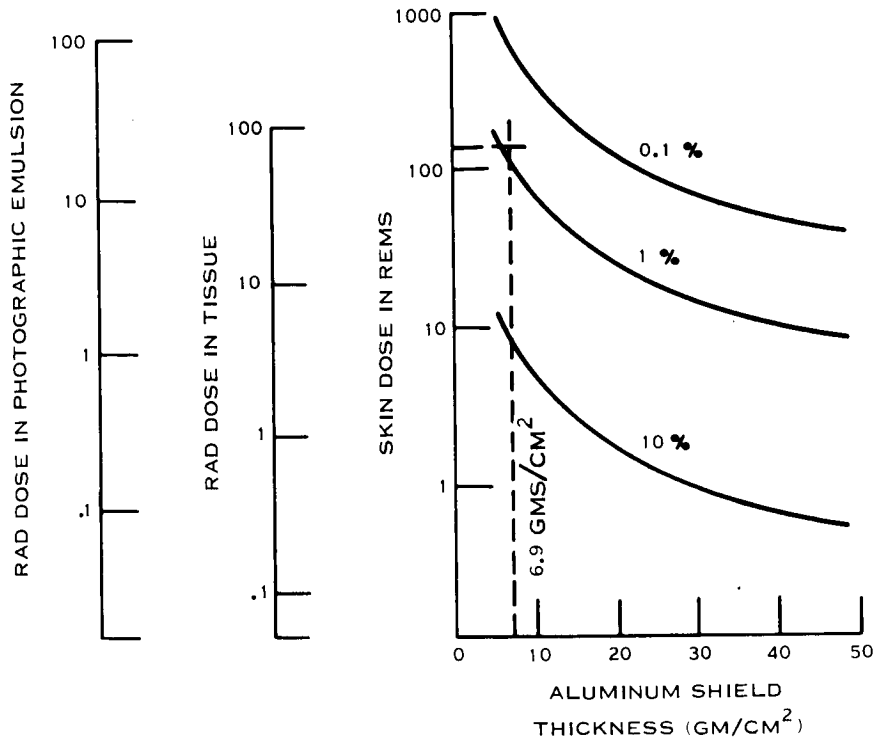

Figure B-9. Probability of Receiving Radiation Dosage from Solar Flares

Nuclear emulsions are 2.3 times as sensitive to protons as tissue according to a table by Janni. Nuclear emulsions are also twice as sensitive as high-speed films according to Mees. High-resolution films are 25 percent as sensitive as the high-speed films so that the S0-243 film should be 1/3 as sensitive to protons as tissue as shown on the ordinate scale in Figure B-9. Thus, at 22 rads and 6.9 grams/cm^2 there is a probability slightly under 1 percent of exceeding 50 rads dosage in the film.

B.6 RESULTS AND RECOMMENDATIONS

A mission was chosen as follows: launch, 6 hours in a parking orbit, 1/2 hour to leave the orbit and pass through the inner and outer Van Allen belts, 6 months of travel time to Mars, and 6 months in orbit. The last orbit time might be cut to 1 month, which represents the time to consume the film aboard.

The effects on film by protons have been cataloged, with the worst case being the general rise in base fog which decreases the signal-to-noise ratio. The limit was placed at a dose of 50 rads in the film.

Space radiations were studied to determine their fluxes and capabilities of depositing energy in the film. Shielding was discussed with two thicknesses, 2 and 10 grams/cm^2, chosen to bracket the range. The galactic particles, protons and alpha particles, were found to produce a dose of 28 rads per year regardless of the above shield thickness.

Solar flares provide the largest dosage but they are variable and highly unpredictable. Fortunately 1973 and 1975 are in the low part of the sunspot cycle, so that the probability of large flares is low. (Estimates of this probability have been made but have a low confidence level.) To be conservative, the flux of protons/cm^2 has been averaged over two intervals: the 8 years from 1956 to 1963, which covers the last maximum and the 4 years from 1961 to 1964, which covers the last minimum.

Information on shield weights for different thicknesses has been calculated by assuming film lengths and equipment dimensions.

Combinations of the above factors lead to the values given in Table B-6.

Table B-6. Dosage Results of Shield Calculations

Time of Photographic Mission	12 months		7 months	
	Shield thickness in grams/cm^2			
	2	10	2	10
A. Maximum expected dose	210	41	198	29 rads
B. Minimum expected dose	63	40	51	28 rads
C. Minimum plus the largest flare	403	100	391	78 rads
Shield thickness to get 50 rads	6.9		6.1 grams/cm^2	
Shield weight for 500 feet of film	17		15 lbs.	

The average shield thickness to obtain 50 rads was calculated by weighting the dosages as 9, 90, and 1 percent, respectively, for items A, B, and C in Table B-6.

The shield weights are 15 and 17 pounds for 7 and 12 months, respectively. Further calculations would be hard to justify in view of the uncertainties involved in possible solar flares.

Using data by Snyder, we find that the probability of exceeding this dose is 1 percent or less. These relations were calculated by using broad definitions of high-speed and high-resolution films. The exact relations can only be obtained by testing the films to be used.

A shield weight of 23 pounds was used for the Photographic Film System design in order to allow for a 50 percent additional length of film for the mission.

The question of tracks produced by the protons or other charged particles has been treated only as an increase in density of the film or a rise in the fog level. There will be tracks in the film that run parallel to the film plane, thereby possibly causing misinterpretation of features on the photograph. The extent of these tracks will depend upon the flux of particles passing through the film in the proper direction. Because this has not been investigated for photographic film, it is recommended that a study be started to follow along these lines: (1) Calculate the number of protons that have incidence angles smaller than those needed to produce the necessary minimum track length, (2) determine the track widths to obtain the additional number of grains activated, (3) estimate the fogging due to the total tracks on the film, and (4) determine the loss of resolution caused by the tracks. The net result will be to increase the shield weight to drop the fog level back to that corresponding to 50 rads.

B.7 BIBLIOGRAPHY

C. E. K. Mees, The Theory of the Photographic Process, Macmillan Co., New York, 1954.

W. A. White, Solar X rays: A Comparison with Microwave Radiation, AAS-NASA Symposium on the Physics of Solar Flares, Oct. 1963, NASA-SP-50, pg. 131-137.

G. C. Fazio, Comments on Gamma Rays, AAS-NASA Symposium on the Physics of Solar Flares, Oct. 1963, NASA-SP-50, pg. 145.

R. Madey, A. G. Duneer, & T. J. Krieger, Proton Dose Rates in Manned Space Vehicles, RAC 433 (SRS-TR-35), Sept. 1961, Republic Aviation Co., Farmingdale, New York.

J. W. Haffner, Space Radiation Dose Rates in the Earth's Atmosphere, AIAA Paper No. 65-511, July 1965.

W. W. Scott, Estimates of Primary and Secondary Particle Doses Behind Aluminum and Polyethylene Slabs Due to Incident Solar-flare and Van Allen Belt Protons, ORNL-RSIC-18, July 1967.

M. Livingston and H. A. Bethe, "Nuclear Dynamics, Experimental," Rev. Mod. Phys., Vol. 9, 1937, pg. 245.

R. M. Sternheimer, "Range-Energy Relations for Protons in Be, C, Al, Cu, Pb, and Air, "Phys. Rev., Vol. 115, 1959, pg. 137.

F. B. McDonald, Solar Proton Manual, NASA TR-R-169, Dec. 1963.

D. S. Hess & E. Pounder, Voyager Environmental Predictions Document, SE003BB001-1B28, File SE1DB-6J-003, Task 544-1DB00-1-2940, JPL, Oct. 1966.

F. S. Alsmiller, R. G. Alsmiller, Jr., & D. R. Trubey, "Comparison of Primary Proton Dose with the Dose from Gamma Rays Produced by Inelastic Scattering of Solar Flare Protons," Proc. Symp of Prot. Against Rad. Hazards in Space, Nov. 5, 1962, TID 7652 ORNL, pg. 718.

R. D. Shelton & A. C. deLoach, ATM Film Damage Analysis, NASA, MSFC, Memo, R-SSL-N, July 26, 1967.

J. W. Snyder, "Radiation Hazard to Man from Solar Proton Events," J. Spacecraft & Rockets, Vol. 4, No. 6, June 1967, pg. 826-8.

J. F. Janni, Calculations of Energy Loss, Range, Pathlength, Straggling, Multiple Scattering, and the Probability of Inelastic Nuclear Collisions for 0.1 to 1000 Mev Protons, AFWL-TR-65-150, Sept. 1966.

J. W. Haffner, RBE of Protons and Alpha Particles, Second Symp. on Prot. against Rad. in Space, NASA-SP-71, Oct. 1964, pg. 513-25.

E. Casanati, "Photographic Dosimetry," in Proceedings of International School of Physics, Enrico Fermi, Academic Press, N. Y. C. 1964, pg. 192-211.

APPENDIX C

DATA HANDLING AND STORAGE

C.1 INTRODUCTION

The following topics and their effect on photo-imaging are discussed in this appendix:

a. Transmission capability

b. Data processing

c. Data storage

Figure C-1 shows the alternates available for handling the data from the imaging sensor. In the upper path, the image signal can be stored directly on photographic or electrostatic film. If TV is used, the analog signal is recorded on an analog tape recorder. The output from the analog storage device is then converted to a digital signal by the analog-to-digital converter (ADC). Data compression is then performed, if it is used, and its output goes to the transmission channel. It will be shown that the limiting item in this path is the capability of the transmission link.

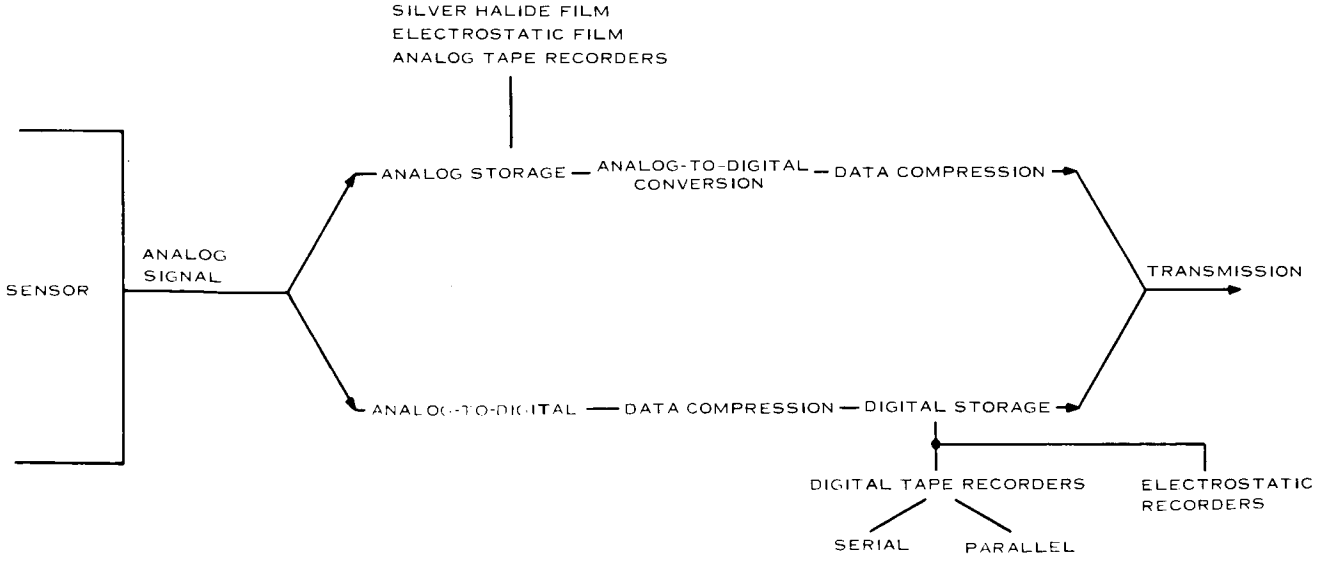

Figure C-1. Data Handling Decision Tree

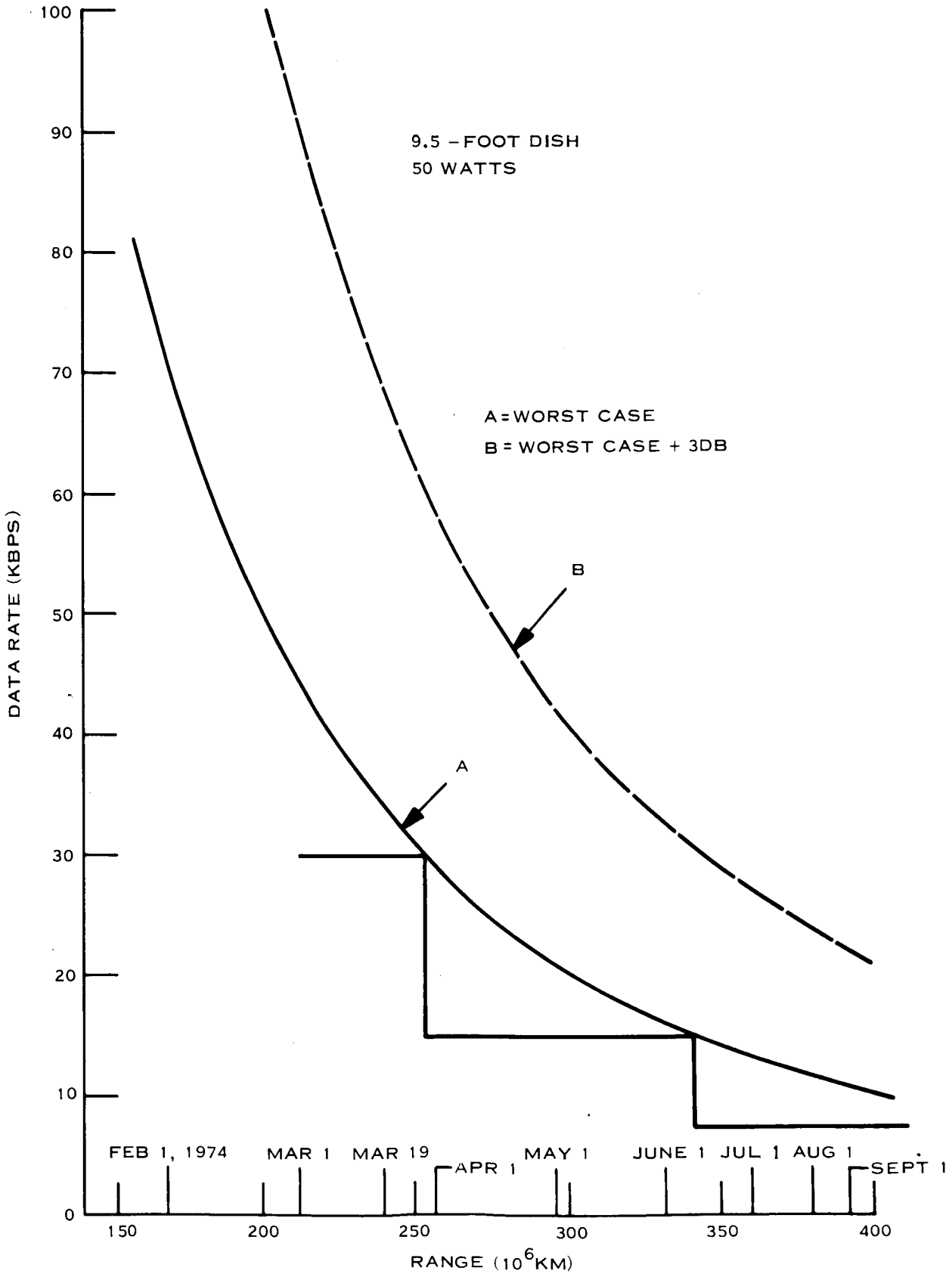

Figure C-2. Data Rate Versus Range

In the lower path of Figure C-1, the analog signal is immediately converted to a digital bit stream by the ADC. Data compression is then performed if it is used, which will reduce the input rate to the digital storage device as well as the capacity required. The output of the digital storage device goes to the transmission channel. It will be shown that the limiting item in this path is the digital tape recorder, or the transmission channel if the electrostatic digital recorder is used.

C.2 TRANSMISSION CAPABILITY

Since, the transmission rate times the time available for transmission determines the amount of data that can be collected from the photo-imaging sensor, it is imperative to obtain a realistic transmission rate in order to constrain the data collection from the photo-imaging device.

Figure C-2 shows the data rate capability versus range for the following assumptions:

a. 9.5-foot antenna (1-degree pointing error)

b. 50-watt power amplifier

c. 2.6-decibel coding gain

The solid line curve is based on worst-case tolerances, while the dotted line indicates a capability 3 decibels better than worst-case capability. For this study, the worst conditions of a March 1 encounter and a 30-kilobits-per-second (kbps) data rate have been selected. For the March 1 encounter, the 30-kbps transmission rate can be maintained for approximately 3 weeks under worst-case conditions. If the 3-db better-than-worst case capability exists once orbit is achieved, then 60 kbps can be maintained for approximately 3 weeks or 30 kbps for approximately 3 months. Given 30 to 60 kbps as the maximum realistic data rates that can be expected, the total bits transmitted per orbit can be determined and thus the capacity required of the storage devices. Table C-1 shows the capacity for various orbits.

Table C-1. Transmitted Bits Per Obit

Orbit Period (hrs)	Transmitted Bits @ 30 kbps	Transmitted Bits @ 60 kbps
8	8.4×10^8	16.8×10^8
10	1.1×10^9	2.1×10^9
12	1.3×10^9	2.6×10^9
14	1.5×10^9	3.0×10^9

Assuming continuous picture taking, the data collection period, as constrained by the transmission rate, is given by:

$$T_C = \frac{R_D \cdot C \cdot T_O}{K \cdot B_i + R_D \cdot C}$$

where R_D = data transmission rate

C = compression ratio

T_O = orbit period

K = conversions from hertz to bits per second

B_i = input bandwidth to storage device during collection period

which assumes no transmission during the collection time.

C. 3 DATA PROCESSING

C. 3.1 BACKGROUND SIGNAL REMOVAL

The signal from the imaging device can be represented as being composed of two components: the background level and the contrast signal. It is expected that the background level will occupy in excess of 75 percent of the total output voltage. The background level is essentially a dc component and, therefore, it is not desirable to transmit this information as often as the contrast signal. Also, considering the errors introduced by the data processing and data storage elements (required for the TV and optomechanical systems), it is desirable

to remove the dc component so that the contrast signal can occupy the complete dynamic range of the data processing and data storage elements. In this way the errors that occur will be with respect to just the contrast signal instead of the background level and the contrast signal. A number of schemes are possible for determining and removing the background level. The most obvious scheme is to average the signal over a line and use the average value found to remove the background level for the next line. This scheme is shown in Figure C-3. The background level can be inserted in the data stream along with sync and status data during retrace time.

C. 3. 2 DATA COMPRESSION

Through the use of data compression, the effective data transmission rate can be increased; and for the digital storage scheme, the input rate can be reduced as well as the storage capacity required.

Since displays of high-quality pictures are desired by the scientist, reduction schemes such as only transmitting signal statistics or the times at which a certain level is exceeded will

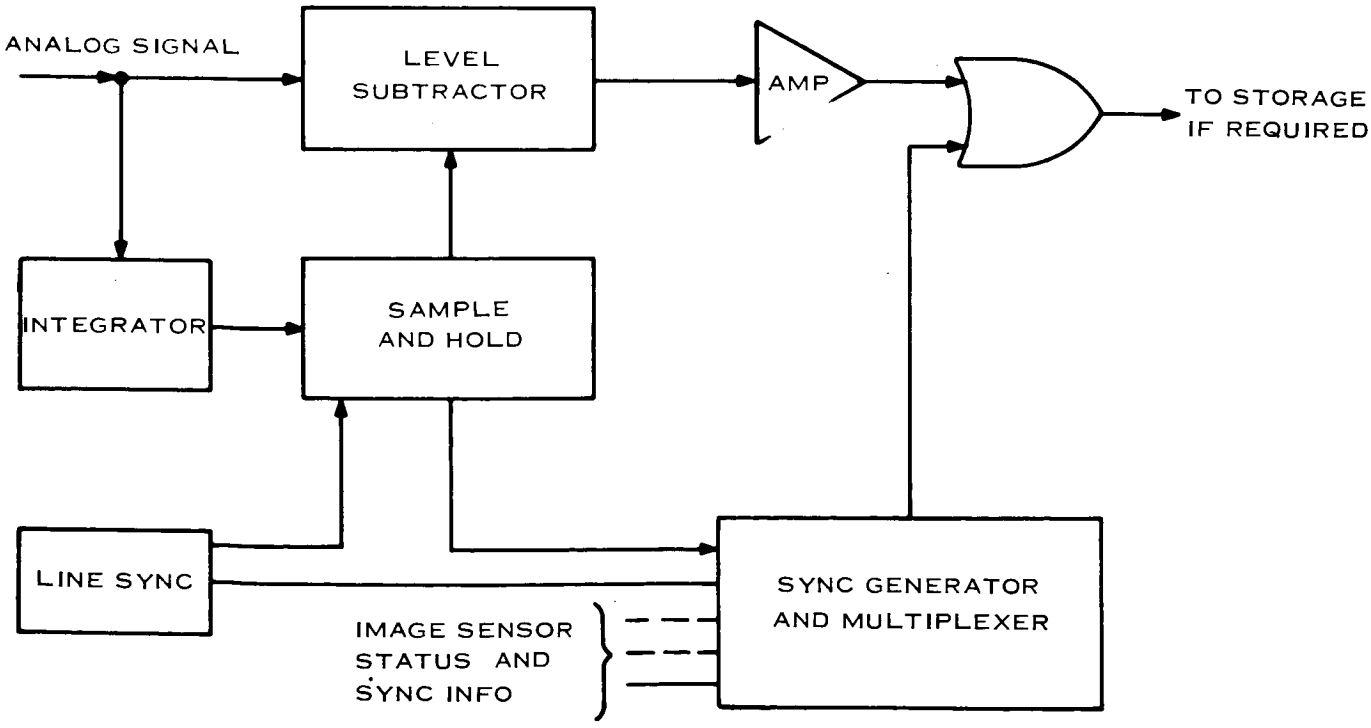

Figure C-3. Background Signal Removal

not be acceptable. The most promising method appears to be a form of redundancy removal that does not destroy the image. There are any number of ways to implement redundancy removal by fitting a polynomial to the data. As long as the data does not vary by more than a prescribed amount from the value of the polynomial, the data is considered redundant, and only the coefficients of the polynomial must be defined.

The order of the polynomial and the implementation of a redundancy removal technique that is most efficient and provides the most acceptable image upon re-creation is a direct function of the actual images and their statistics. In an application such as in Voyager where very little is known concerning the statistics of Mars images, the compressor, if included, should have provisions for bypassing it upon receipt of a command from the ground station. This would occur when the compression ratio is less than 1, which would be a result of high channel activity and the required addition of address bits. The result of data compression is straightforward: for a compression ratio of 2, twice the number of pictures can be obtained, and the digital storage input rate can be reduced by a factor of 2. In this study a compression ratio of 1.5 has been assumed.

C.4 DATA STORAGE

The types of high-capacity storage media considered were the "dielectric film" electrostatic type as well as the more conventional magnetic tape type employing recently developed wide-band and high-density recording techniques. Other bulk storage techniques previously studied and discarded in Task A,--such as magnetic discs and drums, thermoplastic recorders, and cryogenic storage systems--have not progressed sufficiently to merit reconsideration.

One of the most significant parameters affecting the data storage device is the bandwidth of the imaging sensor output, which must be passed by the storage device. For the case of magnetic tape recorders, the input bandwidth of the recorder is proportional to the head-to-tape velocity, which has limits imposed by design and reliability considerations.

An enlightening relationship can be derived between ground resolution, sensor field of view, and input bandwidth required.

Assume:

a. Continuous mapping and no overlap

b. 1000-km altitude (H) - constant

c. 3000 m/sec ground speed (V)

The area covered per sec (A/sec) is

$$A/sec = 2\,HV\tan(FOV/2)$$

where FOV is the sensor field of view.

The resolution cells/sec (C/sec) is

$$C/sec = \frac{A/sec}{R^2}$$

where R = resolution

Then the sensor output bandwidth is given by

$$BW = C/sec \times 0.5 \left\{2 \text{ cells per cycle}\right\} \times \frac{1}{\left\{0.7 \text{ Kell factor}\right\}}$$

$$\times \frac{1}{1-0.1\left\{\text{horizontal retrace time}\right\}}$$

$$= \frac{1.586\ HV\ \tan(FOV/2)}{R^2}$$

which for the assumed altitude and velocity yields

$$BW = \frac{4.76 \times 10^9 \tan(FOV/2)}{R^2}$$

Figure C-4 shows this relationship for fields of view of 5 and 10 degrees.

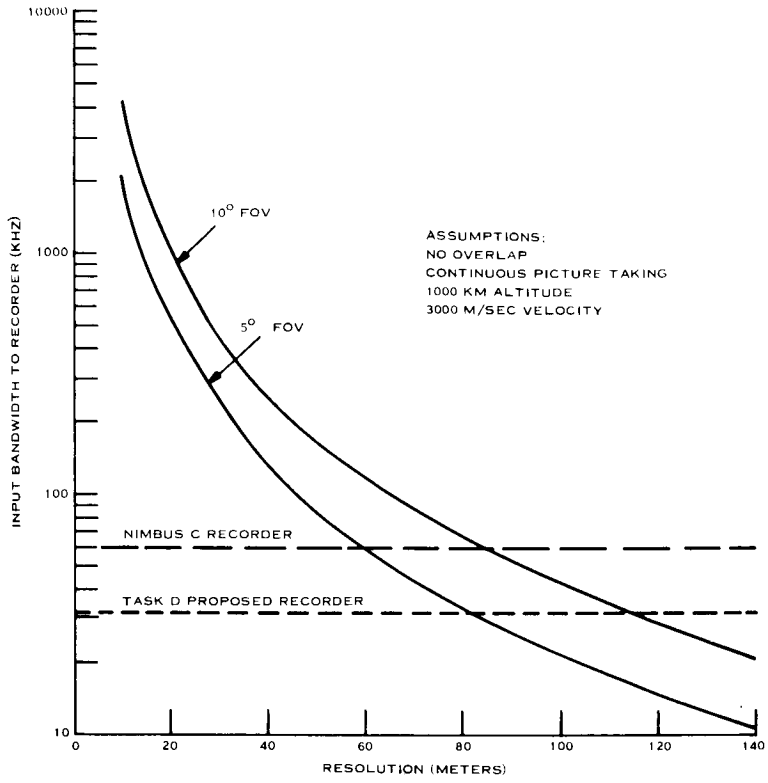

Figure C-4. Required Recorder Input Bandwidth Versus Resolution

On Figure C-4 are shown two magnetic tape recorders: The Nimbus C recorder and the recorder proposed in the Systems Update Task. The Task D proposed recorder satisfies the 100-meter resolution, 5.7-degree field of view, while the Nimbus C recorder is shown to satisfy the 100-meter resolution, 10-degree field of view chosen for the photo-imaging task.

C.4.1 MAGNETIC TAPE STORAGE

As part of the System Update Task, a vendor survey was conducted by a GE subcontractor, Texas Instruments. This survey consisted of both a literature search and direct contacts with vendors of the proposed storage components. A summary of the vendors contacted and their recent experience with space applications of high-density or wideband recording techniques is given in Table C-2.

Table C-2. Results of Vendor Survey

Vendor	Experience with High-Density Digital Recording	Experience with Wideband Recording
Ampex	None in space; 10 kbpi in ground applications	Built one for Dynasoar; no specifications available
Consolidated Electrodynamics	None	None
Kinelogic Corp.	Have done 6 kbpi in laboratory models; none flown	None
Leach Corp	Has flown 3 on classified system with 10 kbpi. Dropout rate $\sim 1 \times 10^{-6}$	None
Lockheed Electronics	Have breadboard at 8 to 10 kbpi	None
RCA	4 kbpi on Gemini model	Built prototype for AAP program NASA Houston. Has flown a rotating head recorder on a classified program. Has flown Nimbus recorder, dc to 60 kHz.
Raymond	None	None

C.4.1.1 Analog Tape Recorders

Because of the high bandwidths (40 kHz to 400 kHz) expected from the photo-imaging device, analog recording appears as the most likely candidate, unless the input bandwidth can be reduced. Calibration signals are assumed to be required to eliminate drifts and speed variation errors of analog recorders.

C.4.1.1.1 Logitudinal Scan

If the input bandwidth is on the order of 60 kHz to 100 kHz, the recorder built for the Nimbus satellite to record TV pictures of cloud cover appears to be applicable. The gross characteristics of this recorder, RCA model QRA-2, are given in Table C-3. This particular recorder relayed TV data for 1440 orbits before failure.

Table C-3. Analog Recorder (Longitudinal Scan) Specification Summary

Characteristic	Value
Data bandwidth	Dc to 60 kHz
Flutter	1.0% p-p dc to 60 kHz
Modulation	FM 96~kHz carrier
S/N	35 db
Number of tracks	4
Tape speed	30 ips
Tape length	1200 feet
Size	14-in. diameter, 7.5-in. height
Weight	16 lb
Power	11 watts

C.4.1.1.2 Rotating Head Recording[1]

The only vendor indicating recent experience with wideband (4 MHz) analog recording in a space environment was RCA, who has developed a prototype AAP recorder for MSC. This recorder, designated the DSU, employs a rotating head, helical scan system to provide 30 minutes of recording time with a signal bandwidth of 4 MHz, which is equivalent to storage of approximately 10^{11} binary bits, or a 4-hour record time with a signal bandwidth of 500 kHz.

The accuracy of reproduction obtained with this machine has not been determined, except that the time base stability meets FCC standard Section 3.3687 (a) for video recording.

The physical parameters of the DSU are summarized in Table C-4. The life figures reflect two inputs from different RCA sources and should be further investigated.

---

[1] Final Report for Wideband Television Recorder, prepared for NASA Manned Spacecraft Center, Houston, Texas, Contract NAS9-4629 by RCA.

Table C-4. Analog Recorder (Transverse Scan)

Parameter	Value
S/N	38 db p-p/rms
Bandwidth	
Dc to 4 mHz	1/2 hr at 10 ips
Dc to 0.5 mHz	4 hrs at 1.25 ips
Head-to-tape speed	1120 ips and 140 ips (headwheel runs at 38, 800 and 3600 rpm)
Start time	50 sec for 4 mHz BW; 5 sec for 0.5 mHz BW
Tape	1600 ft of 1-in. width
Life	150 to 1000 tape passes
Motors	2 hysteresis synchronous (capstan and headwheel)
Size	10 x 14 x 6.1 in. = 854 in.^{3}
Weight	28 lb
Power	53 watts max during high-speed record

It was reported that one DSU has flown on a classified satellite and that MSC will soon be testing the delivered prototype. This recorder uses the negator spring reeling system and coaxial reels proven on the Gemini program. A clock signal is recorded on a longitudinal track to provide synchronization information during playback. This servo is of the closed-loop type and, although nominally of rather straightforward design, the time stability of the rotating head mechanism and the output signal it generates depend on the head-servo stability. Overall, this recorder looks promising, if the number of tape passes can be substantially increased.

C.4.1.2 Digital Tape Recorder

The digital recorder does not suffer from the accuracy problem of the analog recorder. However, the read-in rates expected from the photo-imaging device present the major obstacle to their use. Assuming a 40 kHz to 400 kHz input bandwidth, two samples per

cycle and six bits per sample, the read-in rate to the recorder becomes 0.48 Mbps to 4.8 Mbps. An additional stringent requirement is the capacity required. From the transmission capability section, it is seen that capacities in the range of $1 - 3 \times 10^9$ bits are required.

C.4.1.2.1 High-Density Recording

This is a series recording technique of bit packing densities in the range of 10 kbpi.

Several vendors indicated laboratory experience with HDDR techniques (Table C-2), while Leach Corporation has one of their model 2000 satellite recorders configured for 10 kbpi, and reported that three of these have flown in classified earth satellite programs.

The approximately five-fold increase in packing densities for digital recording over bit packing densities achievable a few years ago has two basic causes. First, the recording techniques have been converted from NRZ saturation recording to split-phase recording below saturation levels. The detection process for this type of signal employes limiting and binary detection and can operate at significantly lower signal-to-noise levels than those permitted in NRZ saturation recording, which is much more sensitive to amplitude noise due to head-tape contact or tape consistency.

The second major factor permitting the use of higher densities is the availability of ferrite head structures to replace the usual laminated head type. Because of the physical characteristics of the ferrite playback head, a narrow gap (18 micro-inch) can be made and maintained for many more tape passes. The narrower gap and the low losses inherent in ferrites permit operation at higher frequencies.

The maximum input rate possible with HDDR is limited by the maximum allowable tape velocity; that is, the input rate is the product of the tape velocity and the packing density. Rates of 1 Mbps have been demonstrated with 100 ips tape speeds on space-type machines; but 30 to 50 kbps is probably a more desirable upper boundary because of reliability, wear, and power considerations. The start/stop time of the recorder also is proportional to the tape speed, which may be of importance if stops occur between video frames.

The estimated characteristics of two typical HDDR recorder implementations based on Leach model 2000 and the Mariner continuous loop machine are summarized in Table C-5.

Table C-5. Digital Recorder (High Density - Series)

Characteristic	Leach	Modified Mariner
Size (in^3)	450	575
Weight (lb)	15	21
Power (w)	15 rec/5 play	12 rec/10 play
Start time (sec)	5	2
Tape	1/4 in. - 3000 ft - 4 tracks	1/4 in. - 300 ft - 4 tracks
Life (passes)	10^4	2×10^3
Record rate (kbps)	500	150
Capacity	1.5×10^9	1.5×10^8

Multitrack recording (parallel) at 10 kbpi is not recommended due to the skew problem. This is discussed more in the next section.

A series machine can be used as a parallel machine during the record process, thus increasing the allowed read-in rate, if the readout process is performed in series. This scheme presents a significant ground data reconstruction problem of the image, when it is realized that interlacing lines of the image would be received by different DSIF stations.

C.4.1.2.2 Parallel Recorders

Parallel recording can be used to increase the read-in rate to within limits. High-density recording is presently not possible for parallel recording due to the interchannel time displacement (skew) problem.

There are two types of skew: static and dynamic. Static skew is caused by head gap scatter, head tilt, and tape motion other than 90 degrees.

Dynamic skew is caused by temperature distortion and nonuniform motion of the tape. Four possible solutions to static and dynamic skew are:

a. Packing-density adjustment

b. Close mechanical tolerances

c. Electrical storage

d. Servo-controlled mechanical adjustment

Considering the 10-kbpi packing density of the serial high-density recorder, in order to achieve this density and maintain alignment to within one-half bit across a 1/4-inch tape, the total skew error would have to be less than approximately 0.01 degree, and this would have to be maintained at high speeds, such as 30 ips. A typical gap scatter specification* is 100 μ inches, which corresponds to 0.02 degrees for a 1/4-inch tape. Misalignment to greater than one-half bit can be allowed at the expense of de-skewing buffers. Maintaining mechanical tolerances becomes extremely difficult especially with wear. The complexity of a servo-controlled mechanical adjustment rules out its use for spaceborne recorders. The remaining alternative is to reduce the packing density.

In summary, then, in order to achieve high input rates on a parallel machine, it is desirable to run at high speeds, have many tracks, and have a high bit-packing density. However, dynamic skew increases with speed, and static skew increases with the number of tracks, both requiring a reduction in bit-packing density. The result is that presently the read-in rate limitation is in the range of 500 kbps for a parallel recorder.

C.4.1.3 Summary

Table C-6 summarizes the discussion of the previous paragraphs. A tape speed of 30 ips has been assumed.

*Magnetic Tape Recording, Skipwith W. Athey, NASA Doc. SP-5038, January, 1966.

Table C-6. Summary of Recording Technique Characteristics

Characteristic	Direct	Analog AM	Extended Range FM	Wideband FM	Digital
Packing density/ max frequency response	Can provide the highest frequency capability for given tape speed: 125 kHz	Approximate max frequency response: 30 kHz	Approximate frequency response in kHz equal to 0.67 times tape speed: 20 kHz	Approximate frequency response equal to two times the tape speed in ips: 60 kHz	Frequency response approximately = (density/ 12) · speed for 6 bit/ sample, Nyquist rate sampling: 25 kHz (equivalent)
Low-frequency limitations	Low frequencies lost - cannot record dc	Can record dc, but errors greatest at low frequencies	Can record dc	Can record dc	Can record dc
Tape quality effects (including head/ tape contact)	Directly effect accuracy - typically 3% rms over spectrum	Same as direct	Unaffected by amplitude variations unless signal falls below threshold of detector system		Same as FM
Tape speed effects	Directly effect accuracy - errors concentrated at lower frequencies by flutter	Same as direct	Directly affect accuracy by shifting frequencies. Use of separate pre-recorded clock track can allow compensation		No effect except bit jitter which can be buffered if not too severe
Accuracy of data transfer	Frequency dependent worse at lower end. Total error typically 5 to 15%	Same as direct except error extends to dc.	Error at low frequency due to flutter; at high end due to frequency limitations and spectral foldover. Typical error: 1 to 5%		Easily achieve 1 bit in 10^6 error rate. No frequency dependence of errors.
Electronics required	Sampling and ADC plus filtering	Envelope detector or synchronized sampling - ADC	For the accuracies desired for Voyager, a phase-lock detector with flutter compensation would be required, plus limiter, filter, etc.		Comparator or digital with delay line, depending on modulation technique

C. 4. 2 ELECTROSTATIC DIGITAL RECORDERS

Only two companies were found to be presently studying the use of dielectric film systems for the electrostatic storage of data: RCA and Westinghouse. Contract with both these sources indicated that:

a. No flight systems have been built, although RCA did develop a prototype Nimbus imaging system for NASA 2 years ago.

b. Neither has used electrostatic storage for digital information, primarily because of the difficulty of recovering the information by precise electron beam positioning.

c. Westinghouse has built tubes with both electrical and optical input and electrical output, but none have yet been fully tested or incorporated into systems.

In summary, this storage technique holds promise for analog storage of image data, but its use in space has not been demonstrated. The probability is small that the concept will be applied to the storage of digital data in the near future.